STUDIA

UNIVERSITATIS BABEŞ-BOLYAI

Chemia

CLUJ-NAPOCA 2004

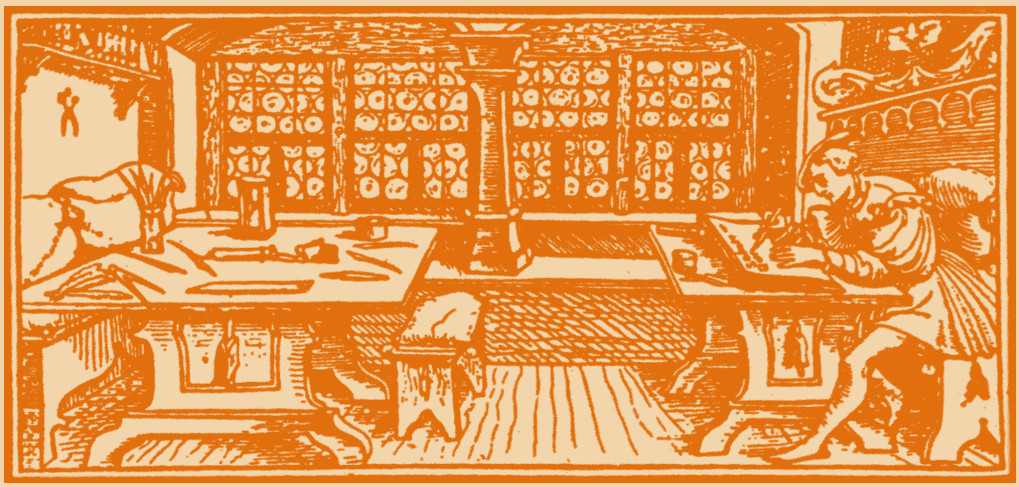

1

ANUL XLIX **2004**

S T U D I A
UNIVERSITATIS BABEŞ-BOLYAI
CHEMIA

1

EDITORIAL OFFICE: Republicii no. 24, 400015 Cluj-Napoca ♦ Phone 0264-40.53.52

SUMAR - CONTENTS - SOMMAIRE - INHALT

STUDIA UNIVERSITATIS BABEŞ-BOLYAI, CHEMIA, XLIX, 1, 2004

IN MEMORIAM

Zsakó Ioan (János) (1926 – 2001)

The brilliant scientist Professor Zsakó Ioan *(János)* was born on January 22, 1926, and died on August 7, 2001, in his natal town Cluj-Napoca.

He was educated at “Bolyai" University of Cluj-Napoca, Faculty of Sciences, Chemistry Department, where he graduated as a chemist in 1948. He studied for his Ph.D. with the famous scientist Academician Professor Raluca Ripan in the field of complex protolytic equilibria in aqueous solutions, particularly about physico-chemical investigations of phosphoric acids and his Ph.D. degree was awarded in 1956.

As well as being a world-class scientist, he was a great teacher. He was appointed assistent in 1950 and lecturer in 1955 at “Bolyai" University, where he taught students in Hungarian language. In 1959, when “Bolyai" University was united with “Babes" University (with Romanian language for the students instruction), he was nominated associated professor (*reader*) at the “Babes -Bolyai" University, where he taught in both Romanian and Hungarian languages. In l990 he was appointed full professor at the same university in Cluj-Napoca, physical chemistry department. Later, in 1991, he was retired and nominated as a consultant professor remaining active in research and teaching activities as well as being supervisor for Ph. D. students untill his death.

He taught general chemistry and physical chemistry, such as kinetics, electrochemistry, chemical structure, thermodynamics, and quantum chemistry both in Romanian and Hungarian languages. He also taught courses abroad, *e.g.*, chemical structure, quantum chemistry and quantum mechanics in French language at the University in Constantine, Alger (1972-1976). Then, in l992, he was invited professor at Politechnic Institute in Budapest, Hungary, for two months and had a special course of quantum chemistry.

As a recognition of his accomplishments, in l990, he received the honor to be a supervisor and lead students for Ph.D. degree in chemistry, specialty in physical chemistry. Many of his Ph.D. students or co-workers became leaders in their fields at the forefront of science and technology.

He was a world-renowned physico-chemist for his remarkable scientific achievements combined with his personal integrity. In this context, we would like to recall some of his major scientific interests.

A series of studies of n*on-isothermal kinetics in homogeneous and heterogeneous systems* was carried out and he developed kinetic theories, new calculation methods, and novel experimental methods for thermogravimetry, particularly, for the thermal decomposition of coordinative combinations with an emphasis on the kinetic effect of compensation. For outstanding achievements he was nominated in 1971 as a member in the Editorial Advisory Board for the Journal of Thermal Analysis, Budapest, Hungary. Then, he initiated and developed a scientific collaboration between "Babes-Bolyai" University of Cluj-Napoca and Technical

University of Budapest, Hungary. For outstanding work in science and for the Journal of Thermal Analysis, his 75th birthday was celebrated at the Hungarian Academy of Sciences, when a scientific meeting was dedicated for that event.

Important contributions also include: *kinetic studies of ligand-exchange reactions and of protolytic equilibria*, IR spectra of coordinative combinations and the calculation of force constants, UV-VIS spectra, protolytic equilibria in bulk solutions, acidity constants using potentiometric and spectro-photometric methods.

Further, an outline of his remarkable work with major importance in *physical chemistry of interfaces* and *surface science* will be given here.

He developed the surface thermodynamics and described phase equilibria, complex phase diagrams in mixed Langmuir monolayers, compression isotherms of Langmuir and Gibbs monolayers by using molecular models, molecular packing in the two-dimensional lattice, and molecular conformational transitions. A novel approach to the surface protolytic equilibria was developed and the interfacial pH was determined with large applications in membrane science.

A series of studies of molecular associations at interfaces with the formation of supramolecular functional associations was also carried out. The developed thermodynamic theory of supramolecular associations in interfacial solutions opens a new horizon to the modern physical and biophysical chemistry and explains the formation of complex supramolecular associations in monolayers at fluid interfaces, liquid/gas and liquid/liquid, with large applications in bio-medicine, cosmetics, pharmaceutics, material science and micro-electronics.

The work done on systems containing Langmuir bio-active monolayers and anesthetics, *such as* procaine, dibucaine and tetracaine, and Gerovital formula, is directly applicable to studies of some diseases of the nervous system, such as Alzheimer's and Parkinson's disease. The effects of procaine, in very specific formulations, on Langmuir monolayers can be substantially correlated with its interfacial effects on the neuronal membrane and they might play an important role in the molecular treatment of these diseases. This scientific research has generated effective therapeutic modalities to treat neurological and aging disorders and was developed in collaboration with well known scientists, Professor Petre T. Frangopol, Professor David A. Cadenhead from State University of New York State (SUNY) at Buffalo, USA, Professor Peter J. Quinn from University of London, UK, and Professor Traianos Yupsanis from Aristotle University of Thessaloniki, Greece. The kinetic models developed for the adsorption of various surfactants at fluid interfaces and for the collapse mechanisms and relaxation processes within Langmuir monolayers represent a key step to describe various industrial phenomena including emulsions, lubrication, drug delivery systems, pharmaceuticals, cosmetics, food industry, micro- and nano-technology and oil recovery. These accomplishments led to the development of new membrane models and selective methods in biophysics of membranes and thin films and in colloid chemistry.

We would like to mention that many outstanding contributions, in the field of *"physical chemistry of interfaces"*, were developed jointly with the eminent scientist Professor Emil Chifu (*In Memoriam*, ***Studia Universitatis Babes-Bolyai, Chem., XLIII, 1-2, 1998, pp. 3-17***). Their application to chemistry, physics and biology leads to the creation of new original theoretical tools in this inter- and multi-disciplinary

enterprise and represents major achievements in modern science. For exceptional original contributions in this field – in l983 - he received jointly with Professor Emil Chifu and other colleagues the prestigious *Gheorghe Spacu* award of the Romanian Academy of Sciences on *"The physical and chemical properties of thin films"* with important applications in the space technology of liquids and in the modeling of biological surfaces.

He published over 270 *scientific papers* in peer review journals (***the attached List of publications***) with a cumulative citation index greater than 1500. Many of them cited over 30 times, and another one cited more than 200 times, which is an unusual event for the citation of *original papers* in the field of physical chemistry. For major contributions to science and technology in 1993, he was elected vice-president of the Thermal Analysis and Calorimetry Section at the Romanian Academy of Sciences, Bucharest.

He was a member of the Romanian Academy of Sciences, the Hungarian Academy of Sciences and the Romanian Society of Colloids and Surface Science.

He elaborated single or in collaboration eight *scientific books*, in Romanian and in Hungarian languages. Two of them, namely, *Physical Chemistry: The structure of atoms and molecules,*1973, and *Symmetry and Molecular Structure,* 1998, (***the attached List of publications***), are used frequently by students not only in Cluj-Napoca but all over the country, at all university centres in Romania. He is also co-outhor at an Encyclopedia for Chemistry in Hungarian language.

He was also interested in phylosophical problems risen from natural sciences and he published papers in *Korunk* Review. He also published articles for the community science in newspapers. In 1990 he was nominated the editor in chief of *Firka* Review, for Section of physical chemistry and informatics, edited for high school level by the Hungarian Society for Science and Technology in Transylvania.

He was a private but generous person with consideration for others reflected in his research group as well as in his home.

We would like to thank his wife Magdolna Zsako, and to colleagues and friends Aurora Mocanu and Iosif Albu for valuable discussions during the preparation of this obituary.

Maria Tomoaia-Cotişel
"Babeş-Bolyai" University of Cluj-Napoca
Faculty of Chemistry and Chemical Engineering
Physical Chemistry Department
The Section of Thermodynamics, Biophysics and Colloid and Surface Chemistry
400028 Cluj-Napoca

LIST OF PUBLICATIONS

BOOKS

1. **J. Zsako**, M. Tomoaia-Cotişel
   Simetria şi structura moleculelor
   Presa Universitara Clujeană, Cluj-Napoca, (**1998**) 259 pag.
2. Z. Andrei, L. Zador, E. Gavrilă, **J. Zsako**, L. D. Boboş, C. Mureşan, I. Bugan
   Lucrări practice de termodinamică şi structură chimică
   Litografia Universității Babeş-Bolyai, Cluj-Napoca, (**1995**) 192 pag.
3. O. Felszeghy, S. Abraham, F. Makkay, K. Makkai, J. Vodnar, **J. Zsako**
   Kemiai kislexikon
   Kriterion, Bucureşti (**1980**), în 2 volume, 1038 pag.
4. **I. Zsako**
   Chimie fizică, Structura atomilor şi moleculelor
   Editura Didactică şi Pedagogică, Bucureşti (**1973**) 687 pag.
5. L. Oniciu, **I. Zsako**
   Chimie Fizică, Vol. 2. Stările de agregare şi termodinamică chimică
   Editura Tehnică, Bucureşti (**1968**) 420 pag.
6. **J. Zsako**
   Az elemek tortenete
   Editura ştiințifică, Bucureşti, **Ediția II *revizuită***, (**1964**) 295 pag.
7. **J.Zsako**, Cs.Varhelyi
   Az atomok es molekulak vilaga
   Editura ştiințifică, *Bucureşti (***1959**) 390 pag.
8. **J. Zsako**
   Az elemek tortenete
   Editura ştiințifică, Bucureşti, **Ediția I,** (**1959**) 254 pag.

PAPERS

1. **I.Zsakó**
   CALCULAREA CONCENTRAȚIEI IONILOR DE HIDROGEN ÎN SOLUȚIILE APOASE ALE ACIZILOR SLABI ŞI DE TĂRIE MIJLOCIE PE BAZA CONSTANTELOR DE DISOCIERE.
   Stud.Cercet.ştiințifice, Ser.I.(Cluj), 6(1955)121-130.
2. R.Ripan and **I.Zsakó**
   STUDIUL FIZICO-CHIMIC AL FORMĂRII MOLIBDATO-FOSFAȚILOR ÎN SOLUȚII APOASE.
   Stud.Cercet.Chimie(Cluj), 7(1956)23-43.
3. R.Ripan and **I.Zsakó**
   COMPORTAREA ACIDULUI PIROFOSFORIC ÎN SOLUȚII APOASE.
   Stud.Cercet.Chimie(Cluj), 7(1956)45-52.
4. **I.Zsakó**
   ACIZII CROMATO-FOSFORICI.
   Stud.Cercet.Chimie(Cluj), 7(1956)53-59.

5. R.Ripan and **I.Zsakó**
STUDIUL FIZICO-CHIMIC AL FORMĂRII MOLIBDATO-PIROFOSFAȚILOR ÎN SOLUȚII APOASE.
Stud.Cercet.Chimie(Cluj), 8(1957)7-19.
6. **I.Zsakó**
CALCULAREA CONCENTRAȚIEI IONILOR DE HIDROGEN ÎN SOLUȚII DE ELECTROLIȚI. 2.Soluții apoase care conțin mai mulți electroliți.
Stud.Cercet.Chimie(Cluj), 9(1958)67-77.
7. **J.Zsakó**
HIDROLIZA ACIZILOR POLIFOSFORICI şI PROBLEMA EXISTENȚEI ACIDULUI $H_7[PO_6]$.
Studia Univ.Babeş et Bolyai, Ser.I. 3(2)(1958)69-76.
8. **J. Zsakó** and E.Fülöp
KOLORIMETRIÁS FOSZFORMEGHATÁROZÁSI ELJÁRÁS.
Studia Univ.Babeş et Bolyai, Ser.I. 3(2)(1958)125-132.
9. **I.Zsakó,** G.Balogh and E.Bodor
STUDIUL COLORIMETRIC AL HETEROPOLIACIZILOR. I. Formarea şi stabilitatea acizilor molibdato-fosforici.
Stud.Cercet.Chimie(Cluj), 10(1959)67-77.
10. **I.Zsakó**
CALCULAREA CONCENTRAȚIEI IONILOR DE HIDROGEN ÎN SOLUȚII DE ELECTROLIȚI. III.Limitele de aplicabilitate a formulelor la soluțiile ideale ale acizilor monovalenți.
Stud.Cercet.Chimie(Cluj), 10(1959)79-96.
11. **I.Zsakó**
CALCULAREA CONCENTRAȚIEI IONILOR DE HIDROGEN ÎN SOLUȚII DE ELECTROLIȚI. IV Aplicabilitatea formulelor la soluțiile ideale ale acizilor bivalenți.
Stud.Cercet.Chimie(Cluj), 10(1959)97-111.
12. **I.Zsakó** and G.Balogh
STUDIUL COLORIMETRIC AL HETEROPOLIACIZILOR. II. Stabilitatea acizilor molibdato-fosforici.
Stud.Cercet.Chimie(Cluj), 10(1959)227-232**.**
13. **I.Zsakó**
STUDIUL COLORIMETRIC AL HETEROPOLIACIZILOR. III. Formarea hete-rotriacizilor fosfo-molibden-wolframici în soluții apoase.
Stud.Cercet.Chimie(Cluj), 10(1959)233-243.
14. **I. Zsakó**
CALCULAREA CONCENTRAȚIEI IONILOR DE HIDROGEN ÎN SOLUȚII DE ELECTROLIȚI. V. Ecuația generală pentru soluții neideale.
Studia Univ.Babeş-Bolyai,Chem., 5(2)(1960)13-21.
15. **I.Zsakó,** L.Almasi and A.Kelemen
INTERACȚIUNEA DERIVAȚILOR O,O-DIETILESTERULUI ACIDULUI ARILSULFO-NAMIDOTIOFOSFORIC CU AZOTAT DE ARGINT. I. Studiul potențiometric şi conductometric al O,O-dietilesterului acizilor p-metil-fenil şi p-clor-fenil-sulfonamidotiofosforici în mediu etanol-apă.
Stud.Cercet.Chimie(Cluj), 12(1961)269-283.
16. **I.Zsakó,** L.Almasi, M.Giurgiu and A.Hantz
CONSTANTA DE DISOCIERE ACIDĂ A O,O-DIETILESTERULUI ACIDULUI p-IOD-FENIL-SULFONAMIDOTIOFOSFORIC ÎN AMESTECURI ETANOL-APĂ.
Stud.Cercet.Chimie(Cluj), 14(1963)271-280.
17. **J.Zsakó** and E.Petri
ÜBER DIE STABILITÄT DER SILBERCYANOKOMPLEXE.
Rev.Roumaine Chim., 10(1965)571-580.

18. **J.Zsakó,** L.Almasi, M.Giurgiu, A.Hantz
ISSLEDOVANIE FIZIKO-KHIMICHESKIH SVOISTV O,O-DIALKILOVYH EFIROV ARIL-SULFONAMIDOFOSFORNYH I –TIOFOSFORNYH KISLOT. I. Konstanty kislotnosti nekotoryh O,O-dietilovyh efirov arilsulfonamidotiofosfor-nyh kislot v smesah etanol-voda i primenimost uravnenia Hammetta k etim soedi-neniam.
Zhur.Obshch.Khim., 35(1965)1866-1871.
19. **I.Zsakó,** Cs.Várhelyi and E.Kékedy
DATE CINETICE REFERITOARE LA PIROLIZA UNOR COMPLECşI DE TIPUL $[Co(DH)_2(AMIN)_2]$I PE BAZA ANALIZELOR TERMOGRAVIMETRICE. (I).
Studia Univ.Babeş-Bolyai,Chem., 10(2)(1965)7-15.
20. **J.Zsakó,** Cs.Várhelyi and E.Kékedy
CINETICA DESCOMPUNERII TERMICE A COMPLECŞILOR DE TIPUL $[Co(DH)_2(Amin)_2]$NCS ÎN CONDIȚIILE ANALIZEI TERMOGRAVIMETRICE (II).
Anal.Univ.Bucureşti, Chim. 14(2)(1965)15-24.
21. **J.Zsakó,** Cs.Várhelyi and E.Kékedy
APPLYING THERMOGRAVIMETRIC ANALYSIS TO THE STUDY OF KINETICS AND MECHANISM OF SUBSTITUTION REACTIONS IN COM-PLEXES. Pyrolysis of complexes of the type$[Co(DH)_2Am_2]X$.
Proc.Anal.Chem.Conf.Budapest, (1966)353-359.
22. **J.Zsakó**
BERECHNUNG VON BILDUNGSKONSTANTEN DER KOMPLEXE AUS SPEKTRO-PHOTOMETRISCHEN DATE. Eine Weiterentwicklung der Methode von Jazimirskij.
Rev.Roumaine Chim., 11(1966)315-320.
23. **J.Zsakó**, M.Giurgiu, L.Almasi and A.Hantz
ÉTUDE DES PROPRIÉTÉS PHYSICO-CHIMIQUES DES O,O-DIALCOYL-ESTERS DES ACIDES ARYLSULFONAMIDO PHOSPHORIQUES ET ARYLSULFONAMIDO THIOPHOSPHORIQUES. II. Les constants d'acidité des O,O-diéthylesters de certains acides arylsulfonamidophosphoriques dans des mélanges éthanol-eau.
Rev.Roumaine Chim., 11(1966)1019-1023.
24. **J.Zsakó,** Cs.Várhelyi and E.Kékedy
KINETICS AND MECHANISM OF SUBSTITUTION REACTIONS OF COMPLEXES. III. Thermal decomposition of complexes of the type $[Co(DH)_2Am_2]X$.
J.inorg.nucl.Chem., 28(1966)2637-2646.
25. **J.Zsakó,** Cs.Várhelyi and E.Kékedy
KINETICS AND MECHANISM OF SUBSTITUTION REACTIONS OF COMPLEXES. IV. Thermal decomposition of complexes of the type $[Co(Cy)_2(Amin)_2]X$.
Acta Chim.Acad.Sci.Hung., 51(1967)53-63.
26. **J.Zsakó** and E.Fekete
GHIDROKSO-TSIANO-KOMPLEKS SEREBRA.
Studia Univ.Babeş-Bolyai,Chem., 12(1)(1967)45-49.
27. A.Benkö, **J.Zsakó** and P.Nagy
THIAZOL VERBINDUNGEN. I. Synthese einiger 2-Aryl-4-carboxy-thiazole. Der Einfluss der Substituenten auf die Dissoziationskonstanten.
Chem.Ber., 100(1967)2178-2183.
28. **I.Zsakó,** Cs.Várhelyi and I.Mostis
CINETICA ŞI MECANISMUL REACȚIILOR DE SUBSTITUȚIE A COMPLECŞILOR. VI. Acvatizarea ionului $[Co\ en_2\ (\gamma\text{-pic})Cl]^{2+}$
Studia Univ.Babeş-Bolyai,Chem., 12(2)(1967)127-131.
29. O.Horowitz and **I.Zsakó**
MOLECULAR ORBITAL CALCULATION OF HAMMETT'S ρ CONSTANT FOR 2-X-PHENYL-THIAZOLE-CARBOXYLIC ACID.
Studia Univ.Babeş-Bolyai,Chem., 13(1)(1968)79-87

30. **J.Zsakó,** Cs.Várhelyi and I.Gănescu
KINETICS AND MECHANISM OF SUBSTITUTION REACTIONS OF COMPL. VII. Solvolysis of $[Cr(SCN)_4(ANILINE)_2]^-$ in ethanol-water mixtures.
Rev.Roumaine Chim., 13(1968)581-590.
31. **J.Zsakó**
KINETIC ANALYSIS OF THERMOGRAVIMETRIC DATA.
J.Phys.Chem., 72(1968)2406-2411.
32. **J.Zsakó**, M.Giurgiu, L.Almasi and A.Hantz
UNTERSUCHUNG DER PHYSIKALISCH-CHEMISCHEN EIGENSCHAF-TEN DER O,O-DIALKYLESTER DER ARYLSULFONYLAMIDO-PHOS-PHORSÄUREN BZW. – THIOPHOSPHORSÄUREN. III. Die Stabilität der Sil-berkomplexe der O,O-Diäthylester der Arylsulfonylamido-thiophosphorsäuren.
Z.anorg.allg.Chem., 359(1968)220-224.
33. **J.Zsakó,** I.Gănescu and Cs.Várhelyi
LA FORCE DE CERTAINS ACIDES COMPLEXES OCTAÉDRIQUES DES MÉTAUX TRIVALENTS.
Rev.Roumaine Chim., 13(1968)727-730.
34. **I.Zsakó,** Cs.Várhelyi and L.Banici
KINETICS AND MECHANISM OF SUBSTITUTION REACTIONS OF COMPLEXES. VIII. Synthesis of some $[Co(en)_2$ benzylamine $Cl]^{2+}$ salts and the hydrolysis kinetics of this complex ion.
Studia Univ.Babeş-Bolyai,Chem., 13(2)(1968)21-26.
35. C.Anghel, **I.Zsakó** and M.Knejev
SUR L'ISOMÉRIE SYN-ANTI DE LA 5-CHLORO-2,4'-DIAMINOBENZO-PHÉNONE-OXIME.
Studia Univ.Babeş-Bolyai,Chem., 13(2)(1968)53-58.
36. **J.Zsakó,** Cs.Várhelyi and M.Szécsi
KINETICS AND MECHANISM OF SUBSTITUTION REACTIONS OF COMPLEXES. IX. Thermal decomposition of some trisethylenediamine-chromium-(III)-complex salts.
Rev.Roumaine Chim., 13(1968)1335-1345.
37. **J.Zsakó**, L.Almasi and L.Paskucz
SILBERKOMLEXE DER O,O-DIÄTHYLAROYLAMIDO-THIOPHOSPHOR-SÄUREN.
Rev.Roumaine Chim., 13(1968)1483-1487.
38. **J.Zsakó**
GLEICHGEWICHTE IN LÖSUNGEN VON KOMPLEXVERBINDUNGEN VOM TYPUS AB_2. Nomogramme für die Ermittlung der Bildungskonstanten.
Rev.Roumaine Chim., 13(1968)1609-1616.
39. **J.Zsakó,** Cs.Várhelyi and E.Kékedy
TERMICHESKOE RAZLOZHENIE KOMPLEKSNYH SOEDINENII TIPA $[Co(NioxH)_2Am_2]X$.
Zh.Neorg.Khim., 13(1968)3279-3284.
40. **J.Zsakó,** Cs.Várhelyi, I.Gănescu and L.Zöldi
KINETIK UND MECHANISMUS DER SUBSTITUTIONSREAKZIONEN VON KOMPLEX-VERBINDUNGEN. 10. Mitt. Solvolyse des $[Cr(NCS)_4$(p-tolui-dine$)_2]$-Ions in Äthanol-Wasser Mishungen.
Monatsh., 99(1968)2235-2243.
41. **J.Zsakó,** Cs.Várhelyi, I.Gănescu and J.Turós
KINETICS AND MECHANISM OF SUBSTITUTION REACTIONS OF COMPLEXES. XI. New Reinecke-salt-like compounds containing para-phene-tidine and the solvolysis of $[Cr(NCS)_4$(p-phenetidine$)_2]^-$ in ethanol-water mix-tures.
Acta Chim.Acad.Sci.Hung., 61(1969)167-179.

42. **J.Zsakó,** Cs.Várhelyi and D.Dobocan
KINETICS AND MECHANISM OF SUBSTITUTION REACTIONS OF COMPLEXES. XII. Solvolytic aquation of some cis-chloro-amino-bis-ethylenedi-amino-Co(III)-complexes.
J.inorg.nucl.Chem., 31(1969)1459-1465.
43. **J.Zsakó**, O.Horowitz, L.Almasi and L.Paskucz
DIE SÄUREDISSOZIATIONSKONSTANTEN VON O,O-DIALKYL-ESTERN DER AROYLAMIDO-THIOPHOSPHORSÄUREN IN ÄTHANOL-WASSER MISCHUNGEN.
Monatsh., 100(1969)587-593.
44. **I.Zsakó**, Cs.Várhelyi and Z.Finta.
KINETICS AND MECHANISM OF SUBSTITUTION REACTIONS OF COMPLEXES. XIII. New derivatives of the dibromo-bis-dimethylglyoximato-co-baltous(III)-acid and the solvolysis of the ion $[Co(DH)_2Br_2]^-$ in water-dimethyl-formamide mixtures.
Studia Univ.Babeş-Bolyai,Chem., 14(1)(1969)51-59.
45. O.Horowitz and **I.Zsakó**
MO-STUDY OF HAMMETT'S REACTION CONSTANT FOR THE ACID DISSOCIATION OF SOME N-SUBSTITUTED BENZOYLAMIDES.
Studia Univ.Babeş-Bolyai,Chem., 14(1)(1969)61-67.
46. **J**.**Zsakó**
LA FORME THÉORIQUE DES COURBES THERMOGRAVIMÉTRIQUES.
J.Chim.Phys., 66(1969)1041-1047.
47. Cs.Várhelyi, Z.Finta and **J.Zsakó**
KINETICS AND MECHANISM OF SUBSTITUTION REACTIONS OF COMPLEXES. XIV. New derivatives of the dichloro-bis-dimethylglyoximato-co-baltous(III)-acid and the solvolysis of the ion $[Co(DH)_2Cl_2]^-$ in water-dimethyl-formamide mixtures.
Rev.Roumaine Chim., 14(1969)1133-1141.
48. **I.Zsakó,** E.Kékedy and Cs.Várhelyi
KINETICS AND MECHANISM OF SUBSTITUTION REACTIONS OF COMPLEXES. XVII. Thermal decomposition of the chorides and bromides of some bis-diphenylglyoximato-diamino-cobaltous(III)-complexes.
Studia Univ.Babeş-Bolyai,Chem., 14(2)(1969)117-124.
49. **I.Zsakó**, Z.Finta and Cs.Várhelyi
ÜBER α-DIOXIMIN-KOMPLEXE DER ÜBERGANGSMETALLE. XXVII. Struktur und Säure-Base Eigenschaften einiger Wasserstoff-diacido-bis-dimethyl-glyoximato-kobaltiate.
Studia Univ.Babeş-Bolyai,Chem., 14(2)(1969)145-150.
50. Z.Finta, **J.Zsakó** and Cs.Várhelyi
KINETIK UND MECHANISMUS DER SUBSTITUTIONSREAKZIONEN VON KOMPLEXVERBINDUNGEN. XV. Die Solvolyse des $[Co(DH)_2J_2]^-$Ions in Wasser-Dimethylformamid-Mischungen.
Z.phys.Chem., 242(1969)200-214.
51. **J.Zsakó,** E.Kékedy and Cs.Várhelyi
KINETICS AND MECHANISM OF SUBSTITUTION REACTIONS OF COMPLEXES. XX. Influence of heating rate on the thermal decomposition of $[Co(DH)_2(amine)_2]NCS$ type complexes as investigated by thermogravimetry.
J.Thermal Anal., 1(1969)339-348.
52. Cs.Várhelyi, **I.Zsakó** and Z.Finta
KINETICS AND MECHANISM OF SUBSTITUTION REACTIONS OF COMPLEXES. XXIV. The hydrogen-bis-1,2-cyclopentenedion-dioximato-di-se-lenocyanato-cobalt(III) acid and the aquation kinetics of the $[Co(CpdoxH)_2(NCSe)_2]^-$ ion.
Studia Univ.Babeş-Bolyai,Chem., 15(1)(1970)81-86.

53. **I.Zsakó**
KINETICS AND MECHANISM OF SUBSTITUTION REACTIONS OF COMPLEXES. XXV. Solvation of $[Cr(NCS)_4(p\text{-toluidine})_2]^-$ and $[Cr(NCS)_4(p\text{-phenetidine})_2]^-$ complex ions in ethanol-water mixtures.
Studia Univ.Babeş-Bolyai,Chem., 15(1)(1970)93-103.

54. Cs.Várhelyi, Z.Finta and **J.Zsakó**
KINETIK UND MECHANISMUS DER SUBSTITUTIONSREAKZIONEN VON KOMPLEX-VERBINDUNGEN. XXIII. Die Wasserstoff-bis-nyoximato-di-selenocyanatokobaltiat(III)-Säure und die Kinetik der Aquotisierung des $[Co(NioxH)_2(NCSe)_2]$-Ions.
Z.anorg.allg.Chem., 374(1970)326-336.

55. **J.Zsakó**
KINETIC ANALYSIS OF THERMOGRAVIMETRIC DATA. II. Improvement of T. Ozawa's integral method.
Rev.Roumaine Chim., 15(1970)693-704.

56. **J.Zsakó,** Cs.Várhelyi and M.Agoşescu
THERMAL DECOMPOSITION OF $[Co(DH)_2Am_2]X$ TYPE COMPLEXES UN-DER ISOTHERMAL CONDITIONS.
Proc.3rd Analyt.Conf.Budapest, (1970)279-283.

57. **J.Zsakó,** Z.Finta and Cs.Várhelyi
KINETICS AND MECHANISM OF SUBSTITUTION REACTIONS OF COMPLEXES. XXXI. Aquation kinetics of the complexes $[Co(DH)_2(NO_2)_2]^-$ and $[Co(DH)_2(H_2O)(NO_2)]$.
Proc.3rd Symp.Coord.Chem.Debrecen, vol.I.(1970)333-345.

58. **J.Zsakó,** Cs.Várhelyi and E.Kékedy
KINETICS AND MECHANISM OF SUBSTITUTION REACTIONS OF COMPLEXES. XVIII. Thermal decomposition of bis-α-diphenylglyoximato dia-mino-cobalt(III) complexes.
J.inorg.nucl.Chem., 32(1970)2999-3011.

59. Z.Finta, Cs.Várhelyi and **J.Zsakó**
KINETICS AND MECHANISM OF SUBSTITUTION REACTIONS OF COMPLEXES. XXI. New derivatives of the dithiocyanato-bis-dimethylglyoxima-to-cobalt(III)-acid and the aquation of the $[Co(DH)_2(NCS)_2]^-$ ion.
J.inorg.nucl.Chem., 32(1970)3013-3024.

60. **J.Zsakó**
HOMOGENEOUS KINETICS WITH PROGRAMMED TEMPERATURE VARIATIONS. I. Basic principles and basic relations.
J.Thermal Anal., 2(1970)141-144.

61. **J.Zsakó**
KINETIC ANALYSIS OF THERMOGRAVIMETRIC DATA. II. Improvement of Doyle's integral method.
J.Thermal Anal., 2(1970)145-149.

62. **J.Zsakó,** E.Kékedy and Cs.Várhelyi
KINETICS AND MECHANISM OF SUBSTITUTION REACTIONS OF COMPLEXES. XIX. Influence of heating rate on the thermal decomposition of $[Co(DH)_2(amine)_2]$I type complexes in the conditions of thermogravimetric analysis.
Rev.Roumaine Chim., 15(1970)865-872.

63. Cs.Várhelyi, **J.Zsakó** and Z.Finta
KINETIK UND MECHANISMUS DER SUBSTITUTIONSREAKZIONEN VON KOMPLEX-VERBINDUNGEN. 22. Mitt. Neue Derivate der Bis-dimethyl-glyoximato-diselenocyanato-kobalt(III)-säure und die Kinetik der Aquotisierung des Komplexes.
*Monatsh.,*101(1970)1013-1024.

64. **J.Zsakó**, I.Gănescu**,** Cs.Várhelyi and A.Popescu
CINÉTIQUE ET MÉCANISME DES RÉACTIONS DE SUBSTITUTION DES COMPLEXES. XXVII. Solvolyse de l'ion $[Cr(NCS)_4(p\text{-éthylaniline})_2]^-$ dans des mélanges éthanol-eau.
Rev.Chim.min., 7(1970)927-939.

65. Cs.Várhelyi, **I.Zsakó** and Z.Finta
KINETICS AND MECHANISM OF SUBSTITUTION REACTIONS OF COMPLEXES. XXX. New bis-dimethylglyoximato-dinitro-cobalt(III) derivatives and aquation kinetics of the $[Co(DH)_2(NO_2)_2]^-$ ion.
Studia Univ.Babeş-Bolyai,Chem., 15(2)(1970)27-32.

66. **I.Zsakó,** Cs.Várhelyi and M.Agoşescu
KINETICS AND MECHANISM OF SUBSTITUTION REACTIONS OF COMPLEXES. XXXIII. Thermal decomposition of $[Co(DH)_2\ Am_2]X$ type complexes in isothermal conditions.
Studia Univ.Babeş-Bolyai,Chem., 15(2)(1970)33-39.

67. **I.Zsakó**
KINETICS AND MECHANISM OF SUBSTITUTION REACTIONS OF COMPLEXES. XXXVII. Thermal decomposition of bis-α-dioximato-diamino-cobalt(III)-complexes.
Studia Univ.Babeş-Bolyai,Chem., 15(2)(1970)113-118.

68. **J.Zsakó**
HYPERBOLIC TEMPERATURE VARIATION PROGRAM IN KINETIC INVESTIGATION.
J.Thermal Anal., 2(1970)459-460.

69. **J.Zsakó**, O.Horowitz, L.Almasi and A.Hantz
DIE SÄUREDISSOZIATIONSKONSTANTEN VON O,O-DIÄTHYLDITHIO-PHOSPHO-RYLARYLSULPHONYLAMIDEN IN ÄTHANOL-WASSER MI-SCHUNGEN.
Rev.Roumaine Chim., 16(1971)51-54.

70. **I.Zsakó,** C.Anghel and R.Cohn
ACID-BASE EQUILIBRIUM OF THE PHENYLCYANOMETHYLENE-P-QUINONE-OXIME.
Studia Univ.Babeş-Bolyai,Chem., 16(1)(1971)5-8.

71. **J.Zsakó** and Z.Finta
HOMOGENEOUS KINETICS WITH PROGRAMMED TEMPERATURE VARIATIONS. II. Integral method for simple reactions with linear temperature vari-ation program..
Rev.Roumaine Chim., 16(1971)483-494.

72. **J.Zsakó**, I.Gănescu**,** Cs.Várhelyi and A.Popescu
KINETIK UND MECHANISMUS DER SUBSTITUTIONSREAKZIONEN VON KOMPLEX-VERBINDUNGEN. XXVI. Solvatation des $[Cr(NCS)_4$(p-Ani-sidin$)_2]$-Ions in Äthanol-Wasser-Mischungen.
Z.anorg.allg.Chem., 380(1971)216-230.

73. **J.Zsakó,** Cs.Várhelyi and F.Kormos
KINETICS AND MECHANISM OF SUBSTITUTION REACTIONS OF COMPLEXES. XXXIV. Ligand exchange reaction of *trans*-dichloro-bis-ethy-lene-diamino-cobalt(III) ion with 1,2-cyclohexanedionedioxime.
Rev.Roumaine Chim., 16(1971)1045-1051.

74. **J.Zsakó,** Cs.Várhelyi and R.Pop
AKVATSIA SOLI ERDMANNA $NH_4[Co(NH_3)_2(NO_2)_4].H_2O$ V KISLYH RASTVORAH.
Zh.Neorg.Khim., 16(1971)1614-1619.

75. Cs.Várhelyi and **J.Zsakó**
KINETICS AND MECHANISM OF SUBSTITUTION REACTIONS OF COMPLEXES. XXXV. Formation of the 1,2-$[Co(en)_2$ Br pyridine$]^{2+}$ complex ion and its aquation kinetics in acid solutions.
Rev.Roumaine Chim., 16(1971)1185-1192.

76. **J.Zsakó,** Cs.Várhelyi and S.Bleoca
KINETICS AND MECHANISM OF SUBSTITUTION REACTIONS OF COMPLEXES. XXXVI. Formation of the *cis*-$[CoBr(en)_2$(**ϒ**-picoline$)]^{2+}$ and *cis*-$[CoBr(en)_2$(**ϒ**-picoline$)]^{2+}$ complex ions and their aquation in acid solutions.
Acta Chim.Acad.Sci.Hung., 70(1971)175-184.

77. Z.Finta, **J.Zsakó** and Cs.Várhelyi
KINETICS AND MECHANISM OF SUBSTITUTION REACTIONS OF COMPLEXES. XXXVIII. Aquation kinetics of the hydrogen-dinitro-bis-nyoxi-mato-cobalt (III) complex acid.
Rev.Roumaine Chim., 16(1971)1731-1736.

78. Cs.Várhelyi**, I.Zsakó** and M.Zsigmond
KINETIK UND MECHANISMUS DER SUBSTITUTIONSREAKZIONEN VON KOMPLEX-VERBINDUNGEN. XXXIX. Einige Probleme der Solvation von Komplexverbindungen in alkalischem Medium und die Aquation des $[Co(DH)_2(NO_2)_2]^-$-Ions.
Studia Univ.Babeş-Bolyai,Chem., 16(2)(1971)53-60.

79. **J.Zsakó**, Z.Finta and Cs.Várhelyi
KINETIKA I MEHANIZM REAKTSII ZAMESHCHENIA V KOMPLEKSAH. XVI. Akvatsia kompleksa neelektrolita $[Co(DH)_2NH_3Cl]$.
Teoria rastvorov, Alma-Ata, (1971)315-322.

80. Cs.Várhelyi, **J.Zsakó** and Z.Finta
KINETICS AND MECHANISM OF SUBSTITUTION REACTIONS OF COMPLEXES. XL. The hydrogen-dinitro-bis-1,2-cyclopentanedion-dioximato-cobalt(III) complex acid and its aquation in acid solutions.
J.inorg.nucl.Chem., 34(1972)2583-2593.

81. **J.Zsakó**, Z.Finta and Cs.Várhelyi
KINETICS AND MECHANISM OF SUBSTITUTION REACTIONS OF COMPLEXES. XLI. Aquation of the complexes $Na[Co(DH)_2(NO_2)_2]$ and $[Co(DH)_2(NO_2)(H_2O)]$ in basic solutions.
J.inorg.nucl.Chem., 34(1972)2887-2894.

82. **J.Zsakó** and F.Makkay
LINEARISATION DER POTENZIOMETRISCHEN TITRATIONSKURVEN.
I. Fällungstitrationen.
Rev.Roumaine Chim., 17(1972)1071-1081.

83. **J.Zsakó,** E.Kékedy and Cs.Várhelyi
KINETIC ANALYSIS OF THERMOGRAVIMETRIC DATA. IV. Influence of heatig rate and of sample weight on thermal decomposition of $[CoBr_2(m\text{-tolui-dine})_2]$.
Thermal Anal., vol.2, Proc.3rd ICTA, Davos, (1971)487-499.

84. **J.Zsakó**, V.Voiculescu, I.Gănescu and A.Popescu
KINETICS AND MECHANISM OF SUBSTITUTION REACTIONS OF COMPLEXES. XLV. Solvation of the $[Cr(NCS)_4(m\text{-xylidine})_2]^-$ ion in etanol-water mixtures.
Rev.Roumaine Chim., 17(1972)1977-1984.

85. **J.Zsakó**, D.Oprescu, Cs.Várhelyi and I.Gănescu
KINETIKA SOLVATSII KOMPLEKSNOVO IONA $[Cr(NCS)_4(Py)_2]^-$ V SME-SAH ATSETON-VODA.
Zh.Neorg.Khim., 17(1972)3242-3249.

86. Cs.Várhelyi**, J.Zsakó** and Z.Finta
KINETIK UND MECHANISMUS DER SUBSTITUTIONSREAKZIONEN VON KOMPLEXVERBINDUNGEN. XLII. Nichtelektrolyte des Typs $[Co(DH)_2(NH_3)X]$ und ihre Aquotisierungskinetik.
Z.anorg.allg.Chem., 397(1973)83-90.

87. Z.Finta, Cs.Várhelyi and **J.Zsakó**
KINETICS AND MECHANISM OF SUBSTITUTION REACTIONS OF COMPLEXES. XLIII. Basic hydrolysis of $[Co(DH)_2(H_2O)(NCS)]$.
Rev.Roumaine Chim., 18(1973)417-424.

88. **J.Zsakó,** Z.Finta and Cs.Várhelyi
KINETICS AND MECHANISM OF SUBSTITUTION REACTIONS OF COMPLEXES. XLIV. Basic hydrolysis of the selenocyanato-bis-dimethylglyoxi-mato-aquo-cobalt(III) nonelectrolytic complex.
J.inorg.nucl.Chem., 35(1973)2839-2847.

89. **J.Zsakó**, Cs.Várhelyi and E.J.Maxim
CINÉTIQUE ET MÉCANISME DES RÉACTIONS DE SUBSTITUTION DES COMPLEXES. XLVI. Aquation acide de l'ion $[Co(en)_2Cl$ aniline$]^{2+}$.
Rev.Chim.min., 10(1973)681-688.
90. L.Almasi, N.Popovici and **I.Zsakó**
ÜBER HETEROORGANISCHE VERBINDUNGEN. XLIV. O-Alkylester der (Arylsulfonamido) benzolthiophosphonsäuren.
Chem.Ber., 106(1973)1384-1388.
91. Cs.Várhelyi**, J.Zsakó** and A.Ionuţ
KINETIK UND MECHANISMUS DER SUBSTITUTIONSREAKZIONEN VON KOMPLEX-VERBINDUNGEN. 47. Mitt. Aquationskinetik des *cis*-$[Co(en)_2Cl($*m*-Toluidin$)]^{2+}$ in sauren Lösungen.
Monatsh., 104(1973)1231-1239.
92. **J.Zsakó**, J.Sata and Cs.Várhelyi
ELECTRONIC SPECTRA OF TRANSITION METAL COMPLEXES. I. Ligand field parameters of some dimethylglyoximato-diamino-cobalt(III) complexes.
Rev.Roumaine Chim., 18(1973)1759-1767.
93. **I.Zsakó**, J.Sata and Cs.Várhelyi
ELECTRONIC SPECTRA OF TRANSITION METAL COMPLEXES. II. Li-gand field parameters of some bis-α-benzyldioximato-diamino-cobalt(III) com-plexes.
Studia Univ.Babeş-Bolyai,Chem., 18(1)(1973)37-45.
94. Cs.Várhelyi, **I.Zsakó** and G.Simó
KINETICS AND MECHANISM OF SUBSTITUTION REACTIONS OF COMPLEXES. LI. Aquation of chromium(III) complexes. Aquation of the trans-$[Cr(en)_2(NCS)_2]^+$ in acid solutions.
Studia Univ.Babeş-Bolyai,Chem., 18(1)(1973)123-131.
95. **J.Zsakó,** Cs.Várhelyi and F.Mánok
KINETICS AND MECHANISM OF SUBSTITUTION REACTIONS OF COMPLEXES. LII. Basic hydrolysis of *trans*-di-isothiocyanato-bis-ethylene-diamine-chromium(III) ions.
Rev.Roumaine Chim., 18(1973)1897-1902.
96. **J.Zsakó** and M.Lungu
KINETIC ANALYSIS OF THERMOGRAVIMETRIC DATA. V. Compensation effect in the thermal decomposition of bisdioximatocobalt(III) complexes.
J.Thermal Anal., 5(1973)77-82.
97. **J.Zsakó**
KINETIC ANALYSIS OF THERMOGRAVIMETRIC DATA. VI. Some prob-lems of deriving kinetic parameters from TG curves.
J.Thermal Anal., 5(1973)239-251.
98. **J.Zsakó**, J.Sata and Cs.Várhelyi
ELECTRONIC SPECTRA OF TRANSITION METAL COMPLEXES. III. Ligand field parameters of some Reinecke salt-type complexes.
Acta Chim.Acad.Sci.Hung., 78(1973)387-392.
99. **J.Zsakó**, Cs.Várhelyi, I.Gănescu and D.Oprescu
KINETICS AND MECHANISM OF SUBSTITUTION REACTIONS OF COMPLEXES. XXVIII. New derivatives of the type $M[Cr(NCS)_4($benzyl-amine$)_2]$ and the solvation of this complex ion in ethanol-water mixtures.
Roczniki Chem., 48(1974)1141-1150.
100. Cs.Várhelyi, **J.Zsakó** and I.Gergely-Kis
VLIANIE KISLOTNOSTI SREDI NA KINETIKU AKVATSII KOMPLEKS-NOVO IONA *cis*-$[Co(en)_2Br($*m*-toluidin$)]^{2+}$.
Zh.Neorg.Khim., 19(1974)1842-1847.

101. **J.Zsakó**, Cs.Várhelyi and K.Szász-Sata
KINETICS AND MECHANISM OF SUBSTITUTION REACTIONS OF COMPLEXES. LIV. Aquation of tetranitro-diamine-cobaltiate(III) in buffered solutions.
Acta Chim.Acad.Sci.Hung., 80(1974)177-182.

102. **J.Zsakó** and H.E.Arz
KINETIC ANALYSIS OF THERMOGRAVIMETRIC DATA. VII. Thermal de-composition of calcium carbonate.
J.Thermal Anal., 6(1974)651-656.

103. **J.Zsakó** and F.Makkay.
SPRIAMLENIE KRIVYH POTENTSIOMETRICHESKOVO TITROVANIA. Titrovanie odnoosnovnyh kislot I osnovanii.
Zh.Anal.Khim., 29(1974)1894-1899.

104. **J.Zsakó** and Cs.Várhelyi
KINETIC ANALYSIS OF THERMOGRAVIMETRIC DATA. IX. Thermal decomposition of some $[CoX_2(amine)_2]$ type complexes under isothermal condi-tions.
J.Thermal Anal., 7(1975)33-40.

105. **J.Zsakó,** Cs.Várhelyi, G.Liptay and K.Szilágyi
KINETIC ANALYSIS OF THERMOGRAVIMETRIC DATA. X. Thermal de-composition of some tris-ethylenediamine-cobalt(III) and chromium(III) comp-lexes.
J.Thermal Anal., 7(1975)41-51.

106. **J.Zsakó,** Cs.Várhelyi and E.Kékedy
THERMAL DEAMINATION OF $[Me(amine)_nX_2]$ TYPE COMPLEXES.
Thermal Anal., Proc.4th ICTA, Budapest, vol.1.(1974)177-183.

107. **J.Zsakó,** Cs.Várhelyi and G.Liptay
THERMAL DECOMPOSITION OF $[Co(Diox.H)_2(amine)_2]X$ TYPE COM-PLEXES.
Thermal Anal., Proc.4th ICTA, Budapest, vol.1.(1974)825-830.

108. **J.Zsakó,** Cs.Várhelyi**,** Z.Finta und J.Kiss-Jakab
KINETIK UND MECHANISMUS DER SUBSTITUTIONSREAKZIONEN VON KOMPLEX-VERBINDUNGEN. XLVIII. Eifluss der Wasserstoffionenkon-zentration auf die Aquotisierungskinetik des Nitro-aquo-bis-dimethylglyoximato-kobalt(III)-Nichtelektrolytes.
Z.Naturforsch., 30 b(1975)393-398.

109. **J.Zsakó**
EMPIRICAL FORMULA FOR THE EXPONENTIAL INTEGRAL IN NON-ISOTHERMAL KINETICS.
J.Thermal Anal., 8(1975)593-596.

110. Cs.Várhelyi, **J.Zsakó** and M.Boáriu-Farkas
KINETIC ANALYSIS OF THERMOGRAVIMETRIC DATA. VIII. Thermal de-composition kinetics of some $[Co(II)X_2(amine)_2]$ type complexes.
Rev.Roumaine Chim., 20(1975)657-663.

111. **J. Zsakó**
THE KINETIC COMPENSATION EFFECT.
J.Thermal Anal., 9(1976)101-108.

112. E.Gavrilă, **J.Zsakó** and I.Cădariu
ÜBER TRIAZINE. LV. Die Molekulardiagramme und die physiko-chemischen Eigenschaften einiger Triazine, wie sie sich aus der MO-Methode (Hückel) erge-ben.
Studia Univ.Babeş-Bolyai,Chem., 22(1)(1977)47-52.

113. **J.Zsakó**, E.Brandt-Petrik, G.Liptay and Cs.Várhelyi
KINETIC ANALYSIS OF THERMOGRAVIMETRIC DATA. XI. Thermal de-composition of some metal dithionates.
J.Thermal Anal., 12(1977)421-428.

114. **J.Zsakó**, Cs.Várhelyi, D.Oprescu and I.Gănescu
KINETICS AND MECHANISM OF SUBSTITUTION REACTIONS OF COMPLEXES. LV. Solvation of $[Cr(NCS)_4(benzylamine)_2]^-$ in acetone-water mixtures.
Acta Chim.Acad.Sci.Hung., 97(1978)159-166.

115. Cs.Várhelyi**, J.Zsakó** and B.Gagyi
KINETIK UND MECHANISMUS DER SUBSTITUTIONSREAKZIONEN VON KOMPLEX-VERBINDUNGEN. LIII. Aquotisierung des *cis*-Di-isothio-cyanato-bis-äthylendiaminchrom(III)-Ions in sauren Lösungen.
Monatsh., 109(1978)1321-1328.

116. **J.Zsakó**
SHAPE AND POSITION OF THE ANALYTICAL RESPONSE IN FLAME-LESS ATOMIC ABSORBTION SPECTROMETRY.
Anal.Chem., 50(1978)1105-1107.
Exchange of comments. Factors controlling the shape and position of the absorp-tion curves at the electrothermal rod atomizer.
Anal.Chem., 51(1979)2039-2041.

117. **J.Zsakó**, S.Jitian, Cs.Várhelyi and M.Lungu
CINÉTIQUE ET MÉCANISME DES RÉACTIONS DE SUBSTITUTION DES COMPLEXES. LVI. Olation de l'ion *trans*-$[Co(en)_2(NCS)_2]^+$.
Rev.Roumaine Chim., 24(1979)257-264.

118. **J.Zsakó**
KINETIC ANALYSIS OF THERMOGRAVIMETRIC DATA. XII. A nomogram method of deriving kinetic parameters.
J.Thermal Anal., 15(1979)369-377.

119. **J.Zsakó**, J.Horák, Z.Finta, Cs.Várhelyi and I.Mitrache
ACIDITY CONSTANTS OF 1,2-CYCLOHEPTANE- AND 1,2-CYCLOOC-TANE DIOXIMES.
Mikrochim. Acta, (1979)405-413.

120. **J.Zsakó**
CORRELATION DIAGRAM FOR HOMONUCLEAR DIATOMIC MOLE-CULES AND THE NON-CROSSING RULE.
Rev.Roumaine Chim., 24(1979)523-530.

121. **J.Zsakó**, M.Várhelyi and Cs.Várhelyi
KINETIC ANALYSIS OF THERMOGRAVIMETRIC DATA. XI. Thermal de-composition of complexes of type $[Co(en)_2(pyridine)Cl]X_2$.
J.Thermal Anal., 17(1979)123-131.

122. **J.Zsakó**, E.Chifu and M.Tomoaia-Cotişel
ROTATING RIGID-PLATE MODEL OF CAROTENOID MOLECULES AND THE BEHAVIOUR OF THEIR MONOLAYERS AT THE AIR-WATER IN-TERFACE.
Gazz.Chim.Ital., 109(1979)663-668.

123. **J.Zsakó**, A.Benk**ő**, J.Horák and Cs.Várhelyi
ACIDITY CONSTANTS OF 1,2,3-CYCLOHEXANE TRIONE DIOXIME(1,3) AND OF 1,2,3-CYCLOHEXANE TRIONE TRIOXIME.
Acta Chim.Acad.Sci.Hung., 103(1980)51-58.

124. I.Ceteanu and **J.Zsakó**
DÉTERMINATION DE LA CONSTANTE DE STABILITÉ DU COMPLEXE 1:1 DE TUNGSTATE DE SODIUM-PYROCATÉCHINE PAR VOIE PHOTO-COLORI-MÉTRIQUE.
Studia Univ.Babeş-Bolyai,Chem., 25(1)(1980)10-13.

125. **J.Zsakó** and I.Feneşan
TRANSITION METAL COMPLEXES OF SOME DERIVATIVES OF THE AMIDO-THIOPHOSPHONIC ACID.
Studia Univ.Babeş-Bolyai,Chem., 25(1)(1980)37-40.

126. **J.Zsakó** and F.Makkay
LINÉARISATION DES COURBES DE TITRAGE POTENTIOMÉTRIQUE. III. Titrage d'un acid bivalent avec une base forte.
Chem.Analityczna, 25(1980)95-106.

127. **J.Zsakó,** C.Anghel, S.Molia and D.Iuga
ÉTUDE SPECTROPHOTOMÉTRIQUE SUR LA STABILITÉ DES COM-PLEXES DE CUIVRE(II) DE L'ESTER MÉTHYLIQUE ET DE L'HYDRA-ZIDE DE 4-CARBOXY-8-HYDROXY-2-MÉTHYL-QUINOLINE.
Studia Univ.Babeş-Bolyai,Chem., 25(2)(1980)11-16.

128. **J.Zsakó** and J.Zsakó jr.
KINETIC ANALYSIS OF THERMOGRAVIMETRIC DATA. XIV. Three integral methods and their computer program.
J.Thermal Anal., 19(1980)333-345.

129. **J.Zsakó**
SOME PROBLEMS OF DERIVING STABILITY CONSTANTS OF ML_2 TYPE COMPLEXES FROM SPECTROPHOTOMETRIC DATA.
Rev.Roumaine Chim., 25(1980)1499-1504.

130. **J.Zsakó,** Cs.Várhelyi and S.Magyarósi
KINETIC ANALYSIS OF THERMOGRAVIMETRIC DATA. XVII. Thermal deamination of $[Co(en)_2(aniline)Br]Br_2$ and $[Co(en)_2(\beta\text{-picoline})Cl]I_2$.
Studia Univ.Babeş-Bolyai,Chem., 26(1)(1981)52-57.

131. J.Horák, **J.Zsakó** and Cs.Várhelyi
ON THE α-DIOXIMINE COMPLEXES OF TRANSITION METALS. LVIII. Spectrophotometric study of some tris-dione-dioximine-nickel(IV) type complexes.
Studia Univ.Babeş-Bolyai,Chem., 26(1)(1981)65-70.

132. **J.Zsakó,** Cs.Várhelyi, B.Csegedi and J.Zsakó jr.
KINETIC ANALYSIS OF THERMOGRAVIMETRIC DATA. XVIII. Thermal Decomposition of some $[Co(amine)_2(NCS)_2]$ type complexes.
Thermochim.Acta, 45(1981)11-21.

133. M.Tomoaia-Cotişel**, J.Zsakó** and E.Chifu
DIPALMITOYL LECITHIN AND EGG LECITHIN MONOLAYERS AT AN AIR/WATER INTERFACE.
Ann.Chim.(Rome), 71(1981)189-200.

134. **J.Zsakó** and T.László
COMPLEX COMPOUNDS OF SOME DIOSPHENOLIC TYPE CAROTENOIDS. Astacene complexes. Spectrophotometric study of the system Fe(III)-astacene.
Rev.Roumaine Chim., 26(1981)237-243.

135. **J.Zsakó,** J.Horák and Cs.Várhelyi.
KINETIC ANALYSIS OF THERMOGRAVIMETRIC DATA. XVI. Thermal decomposition of some complexes of the type $[Co(Niox.H)_2(amine)_2]X$.
J.Thermal Anal., 20(1981)435-445.

136. **J.Zsakó**, J.Horák, Cs.Várhelyi and A.Benkő
ON THE α-DIOXIMINE COMPLEXES OF TRANSITION METALS. LXIV. Thermal deamination of some complexes of the type $[Co(Diox.H)_2(amine)_2]X$.
Monatsh., 112(1981)945-957.

137. **J.Zsakó**, J.Horák and Cs.Várhelyi
ON THE α-DIOXIMINE COMPLEXES OF TRANSITION METALS. LXIII. Spectro-photometric study on the stability of Fe(II) and Co(II) complexes of 1,2-cycloheptane- and 1,2-cyclooctanedione dioxime.
Rev.Roumaine Chim., 26(1981)1271-1277.

138. M.A.S.El Absy, Gh.Marcu, **J.Zsakó** and Cs.Várhelyi
STUDIES ON SOME NITRO-bis-ACETYLACETONATO-COBALT(III) COMPOUNDS.
Rev.Roumaine Chim., 26(1981)1245-1254.
139. G.Liptay**,** Cs.Várhelyi, E.Brandt-Petrik and **J.Zsakó**
KINETIC ANALYSIS OF THERMOGRAVIMETRIC DATA. XIX. Study of the thermal decomposition of some hexathiocyanatochromates.
J.Thermal Anal., 22(1981)205-211.
140. **J.Zsakó,** M**.**Várhelyi and Cs.Várhelyi.
KINETIC ANALYSIS OF THERMOGRAVIMETRIC DATA. XXI. Derivato-graphic study on the thermal decomposition of some $[Co(en)_2X_2]Y$ and $[Co(en)_2X\ (amine)]Y_2$ type complexes.
Thermochim.Acta, 51(1981)277-286.
141. **J.Zsakó**, G.Liptay, Cs.Várhelyi and E.Brandt-Petrik
KINETIC ANALYSIS OF THERMOGRAVIMETRIC DATA. XX. Study of the thermal decomposition of some tetrathiocyanato-diamino-chromate complexes with derivatograph.
J.Thermal Anal., 23(1982)123-133.
142. **J.Zsakó**, Gh.Marcu and M.Várhelyi
KINETIC ANALYSIS OF THERMOGRAVIMETRIC DATA. XV. Thermal de-composition of $[Co(en)_2(pyridine)Br]X_2$ type complexes.
Rev.Roumaine Chim., 27(1982)815-821.
143. M.A.S.El Absy, Gh.Marcu, **J.Zsakó** and Cs.Várhelyi
SPECTROPHOTOMETRIC AND DERIVATOGRAPHIC STUDY ON SOME NEW TETRA-DENTATE MIXED CHELATES OF COBALT(III) WITH ACETYLACETONE DERIVATIVES.
Rev.Roumaine Chim., 27(1982)917-925.
144. **J.Zsakó,** Cs.Várhelyi, M.J.Tóth and É.Péter
KINETIC ANALYSIS OF THERMOGRAVIMETRIC DATA. XXII. Dehydration of calcium oxalate monohydrate.
Studia Univ.Babeş-Bolyai,Chem., 27(1982)38-44.
145. **J.Zsakó**, M.Várhelyi and Gh.Marcu
ELECTRONIC SPECTRA OF SOME *cis*-$[Co(en)_2AX]^{2+}$ TYPE COMPLEXES.
Rev.Roumaine Chim., 28(1983)107-114.
146. M.Tomoaia-Cotişel**, J.Zsakó**, E.Chifu and P.J.Quinn
INFLUENCE OF ELECTROLYTES ON THE MONOLAYER PROPERTIES OF SATURATED GALACTOLIPIDS AT THE AIR-WATER INTERFACE.
Chem.Phys.Lipids, 34(1983)55-64.
147. E.Chifu**, J.Zsakó** and M.Tomoaia-Cotişel
XANTHOPHYLL FILMS. I. Single component monolayers at the air/water interface.
J.Colloid Interface Sci., 95(1983)346-354.
148. M.Tomoaia-Cotişel**, J.Zsakó**, E.Chifu and P.J.Quinn
FILME MONOMOLECULARE DE GALACTOLIPIDE – MODELE DE MEMBRANĂ – ŞI HISTEREZA ÎN CICLURILE COMPRESIUNE-EXPANSIUNE.
Probl.act.biofiz.,XVI-lea Simp.Naţ.Biofiz.Iaşi, (1983)45-49.
149. M.Tomoaia-Cotişel, M.Sălăjan, I.Albu, E.Chifu and **J.Zsakó**
MONOMOLECULAR FILMS OF CAROTENOIDS – MEMBRANE MODELS – AND MECHANISM OF COLLAPSE.
2nd Nat.Symp.Meth.Models,Techn.Phys.Cluj-Napoca, (1984)175-179.
150. M.Tomoaia-Cotişel**, J.Zsakó**, E.Chifu and P.J.Quinn
STRUCTURE OF GALACTOLIPID MONOLAYERS.
2nd Nat.Symp.Meth.Models,Techn.Phys.Cluj-Napoca, (1984)190-194.
151. **J.Zsakó**, M.Tomoaia-Cotişel and E.Chifu
INSOLUBLE MIXED MONOLAYERS. I. Phase equilibria at the collapse of binary monolayers at gas/liquid interfaces.
J.Colloid Interface Sci., 102(1984)186-205.

152. **J.Zsakó**, J.Máthé, E.Kästner-Marian and Cs.Várhelyi
ON THE α-DIOXIMINE COMPLEXES OF TRANSITION METALS. LXXV. Vibration bands of the NO_2-group in some nitro-bis-(dimethylglyoximato)-cobalt (III) complexes.
Acta Chim.Hung., 117(1984)323-333.

153. **J.Zsakó**, I.Gănescu, Cs.Várhelyi and Gh.Brînzan
KINETICS AND MECHANISM OF SUBSTITUTION REACTIONS OF COMPLEXES. LVII. Solvation of the $[Cr(NCS)_4(Morpholine)_2]^-$ anion in ethanol-water mixtures.
Z.phys.Chem., 265(1984)1001-1008.

154. M.Tomoaia-Cotişel**, J.Zsakó**, E.Chifu and P.J.Quinn
MIXED MONOLAYERS OF 1,2-DISTEAROYL DIGALACTOSYL GLYCEROL AND ASTAXANTHIN.
Struct.Funct.Metab.Plant Lipids, Elsevier, (1984) p.421-424.

155. **J.Zsakó**
KINETIC ANALYSIS OF THERMOGRAVIMETRIC DATA.
Thermal Analysis, Ed. Ž.D.Živkovič, Bor, (1984) p.167-237.

156. **J.Zsakó,** Cs.Várhelyi, B.Csegedi and E.Kékedy
KINETIC ANALYSIS OF THERMOGRAVIMETRIC DATA. XXIII. Thermal decomposition of some $[Co(pyridine)_4(NCX)_2]$ type complexes.
Thermochim.Acta, 83(1985)181-191.

157. M.Tomoaia-Cotişel**,** E.Chifu and **J.Zsakó**
THE STRUCTURE OF SOME LECITHIN MONOLAYERS AT THE AIR/WATER INTERFACE.
Water and Ions in Biol. Syst., Proc.2nd Internat.Conf., Bucharest l982. Ple-num Press, (1985)243-250.

158. M.Tomoaia-Cotişel, E.Chifu and **J.Zsakó**
MIXED MONOLAYERS OF EGG-LECITHIN AND CAROTENOIDS.
Colloids and Surfaces, 14(1985)239-246

159. E.Chifu, **J.Zsakó,** M.Tomoaia-Cotişel, A.Mocanu, M.Sălăjan, I.Demeter-Vodnár and I.Albu
FILME INTERFACIALE DE INTERES BIOLOGIC.
A III-a Conf.Naţion.Biofizică, Iaşi, (1985)16-23.

160. **J.Zsakó,** M.Tomoaia-Cotişel, I.Stan, V.Coman, V.Tămaş and E.Chifu
COLAPSUL UNOR MONOSTRATURI DE CAROTENOIDE LA INTERFAŢA AER/APĂ.
A III-a Conf.Naţion.Biofizică, Iaşi, (1985)63-68.

161. **J.Zsakó**
INFLUENCE OF SUBPHASE LIQUID ACTIVITY ON THE EQUILIBRIUM COLLAPSE CURVES OF INSOLUBLE MONOLAYERS.
J.Colloid Interface Sci., 106(1985)51-57.

162. Cs.Várhelyi **J.Zsakó**, G.Liptay and M.Somay
ON THE DIOXIMINE COMPLEXES OF TRANSITION METALS. LXVII. New sulfito-bis-dimethylglyoximato-cobalt(III) complexes and their thermal decomposition.
Rev.Roumaine Chim., 30(1985)695-702.

163. **J.Zsakó**, E.Kästner-Marian and Cs.Várhelyi
DIOXIMINE COMPLEXES OF TRANSITION METALS. LXXVI. Vibration bands of the NO_2-group in some dinitro chelates of cobalt (III) with bidentate ligands..
Polish J.Chem., 59(1985)247-253.

164. M.Tomoaia-Cotişel, **J.Zsakó,** M.Sălăjan and E.Chifu
INTERACTION OF UNIMOLECULAR FILMS OF SOME CAROTENOIDS WITH ELECTROLYTES AT THE AIR/WATER INTERFACE.
Water and Ions in Biol. Syst., Proc.3rd Internat.Conf., Bucharest l982. Plenum Press, (1985)371-381.

165. **J.Zsakó**, Cs.Várhelyi, G.Liptay and A.Borbély-Kuszman
ON THE DIOXIMINE COMPLEXES OF TRANSITION METALS. LXXVII. Formation and thermal decomposition of some complexes $NH_4[Co(DH)_2(SO_3)$ (amine)].tH_2O.
J.Thermal Anal., 31(1986)285-295.

166. **J.Zsakó,** J.Demeter-Vodnár, I.Bâldea and Cs.Várhelyi
KINETICS AND MECHANISM OF SUBSTITUTION REACTIONS OF COMPLEXES. LVIII. Hg(II) assisted aquation of *cis*-$[Co(en)_2Br(\Upsilon\text{-picoline})]^{2+}$.
Rev.Roumaine Chim., 31(1986)443-449.

167. **J.Zsakó**, M.Tomoaia-Cotişel, A.Mocanu and E.Chifu
INSOLUBLE MIXED MONOLAYERS. II. Protolytic equilibria and the in-fluence of pH on the collapse pressure.
J.Colloid Interface Sci., 110(1986)317-334.

168. E.Chifu, **J.Zsakó,** M.Tomoaia-Cotişel, M.Sălăjan and I.Albu
XANTHOPHYLL FILMS. IV. Interaction of zeaxanthin and astaxanthin with electrolytes at the air/water interface.
J.Colloid Interface Sci., 112(1986)241-251.

169. E.Chifu, M.Tomoaia-Cotişel, A.Mocanu, L.Andrei and **J.Zsakó**
PROTOLYTIC EQUILIBRIA IN MONOLAYERS OF BIOLOGICAL SIGNIFICANCE.
Studia Univ.Babeş-Bolyai,Chem., 31(1)(1986)74-79.

170. **J.Zsakó**, G.Liptay and. Cs.Várhelyi
KINETIC ANALYSIS OF THERMOGRAVIMETRIC DATA. XXV. Derivato-graphic study of some $[Co(NCS)_2(amine)_2]$ type complexes.
J.Thermal Anal., 31(1986)1027-1036.

171. **J.Zsakó** and M.Fekete
ISO-K_x AND ISO-CONVERSION DIAGRAMS FOR THE HYDROGENATION OF CARBON MONOXYDE.
Studia Univ.Babeş-Bolyai,Chem., 31(2)(1986)54-60.

172. M.Tomoaia-Cotişel, E.Chifu and **J.Zsakó**
XANTHOPHYLL FILMS. III. Two-component monolayers of some xantho-phylls and L-α-dipalmitoyl lecithin at the air/water interface.
Studia Univ.Babeş-Bolyai,Chem., 31(2)(1986)80-89.

173. E.Chifu, **J.Zsakó**. and M.Tomoaia-Cotişel
INSOLUBLE MIXED MONOLAYERS. IV. Ejection curves of β-cryptoxanthin palmitate – egg lecithin films at the air/water interface.
Studia Univ.Babeş-Bolyai,Chem., 31(2)(1986)90-96.

174. **J.Zsakó**, G.Liptay**,** Cs.Várhelyi and E.Brandt-Petrik
KINETIC ANALYSIS OF THERMOGRAVIMETRIC DATA. XXIV. Derivato-graphic study on the thermal deamination of some $CoX_2(amine)_2$ type comple-xes.
Polish J.Chem., 60(1986)369-377.

175. I.Gănescu, Cs.Várhelyi**, J.Zsakó** and I.Papa
NEW BIS-OXALATO-DIAMINE-CHROMATES(III) WITH HETEROCYCLIC AMINES.
Polish J.Chem., 60(1986)679-687.

176. M.Tomoaia-Cotişel, **J.Zsakó,** E.Chifu, D.A.Cadenhead and H.E.Ries, Jr.
COLLAPSE MECHANISM OF SOME CAROTENOID MONOMOLECULAR FILMS – MEMBRANE MODEL.
*Progr.Photosynth.Res.,Ed.J.Biggins,M.Nijhoff Publ.v.*II.4(1987)333-337.

177. **J.Zsakó**, J.Sztatisz, Á.Czégeni, G.Liptay and Cs.Várhelyi
KINETIC ANALYSIS OF THERMOGRAVIMETRIC DATA. XXVI. DSC stu-dy on the thermal decomposition of some metal and ammonium salts of the acid hydrogen hexachlororhenate(IV).
J.Thermal Anal., 32(1987)463-470.

178. M.Tomoaia-Cotişel, **J.Zsakó,** A.Mocanu, M.Lupea and E.Chifu
INSOLUBLE MIXED MONOLAYERS. III. The ionization characteristics of some fatty acids at the air/water interface.
J.Colloid Interface Sci., 117(1987)464-470.

179. M.Tomoaia-Cotişel, **J.Zsakó,** E.Chifu and P.J.Quinn
MOLECULAR ASSOCIATIONS IN LIPID-CAROTENOID MONOLAYERS
Metab.Struct.Func.Plant Lipids,Ed.P.K.Strumpf et al.Plenum Press,(1987) 131-133.

180. Cs.Várhelyi,**J.Zsakó**, G.Liptay and Z.Finta
ON THE DIOXIMINE COMPLEXES OF TRANSITION METALS. LXXVIII. TG and DTA study on the thermal decomposition of some complexes $M[Co(DH)_2XY]$ and $[Co(DH)_2(H_2O)X]$..
J.Thermal Anal., 32(1987)785-795.

181. E.Chifu, A.Chifu, M.Tomoaia-Cotişel and **J.Zsakó**
SPECIFIC INTERACTIONS IN MONOMOLECULAR MEMBRANES OF BIOLOGICAL INTEREST.
Rev.Roumaine Chim., 32(1987)627-636.

182. M.Tomoaia-Cotişel, **J.Zsakó** and E.Chifu
EJECTION CURVES AND MISCIBILITY OF EGG LECITHIN WITH SOME CAROTENOID DERIVATIVES.
Rev.Roumaine Chim., 32(1987)663-670.

183. **J.Zsakó,** V.Neagu, M.Tomoaia-Cotişel and E.Chifu
MOLECULAR STRUCTURE AND MONOLAYER PROPERTIES.
Rev.Roumaine Chim., 32(1987)739-748.

184. **J.Zsakó** and K.N.Somasekharan
CRITICAL REMARKS ON “ON THE COMPENSATION EFFECT".
J.Thermal Anal., 32(1987)1277-1281.

185. M.Tomoaia-Cotişel, **J.Zsakó,** E.Chifu and P.J.Quinn
MONOMOLECULAR FILMS AND COLLAPSE STRUCTURES AS BIOMEMBRANE MODELS.
Studia Univ.Babeş-Bolyai,Chem., 32(1)(1987)35-49.

186. E.Chifu, M.Sălăjan, M.Tomoaia-Cotişel, J.Demeter-Vodnár and **J.Zsakó**
INTERACTIONS OF SOME BIOLOGICALLY ACTIVE COMPOUND MONOLAYERS WITH ELECTROLYTES AT THE AIR/WATER INTERFACE.
Studia Univ.Babeş-Bolyai,Chem., 32(1)(1987)50-57.

187. M.Tomoaia-Cotişel, **J.Zsakó,** A.Mocanu, I.Albu and E.Chifu
RELAXATION PHENOMENA IN FATTY ACID MONOLAYERS.
Studia Univ.Babeş-Bolyai,Chem., 32(1)(1987)58-67.

188. J.Demeter-Vodnár, M.Sălăjan, M.Tomoaia-Cotişel, **J.Zsakó** and E.Chifu
COMPLEX FORMATION AT THE BENZENE/WATER INTERFACE.
Studia Univ.Babeş-Bolyai,Chem., 32(1)(1987)92-98.

189. **J.Zsakó,** M.Tomoaia-Cotişel, V.Tămaş, V.Coman and E.Chifu
MONOMOLECULAR FILMS OF SOME APOCAROTENOID DERIVATIVES.
Rev.Roumaine Chim., 32(1987)1193-1202.

190. M.Tomoaia-Cotişel**, J.Zsakó,** E.Chifu and P.J.Quinn
INTERMOLECULAR INTERACTIONS IN LIPID/CAROTENOID MONOLAYERS.
Biochem.J., 248(1987)877-882.

191. E.Chifu, **J.Zsakó**, M.Tomoaia-Cotişel, M.Sălăjan, J.Demeter-Vodnár and Cs.Várhelyi
ADSORBED FILMS AT THE BENZENE/WATER INTERFACE.
Studia Univ.Babeş-Bolyai,Chem., 32(2)(1987)90-97.

192. Z.Finta, **J.Zsakó** and Cs.Várhelyi
KINETICS AND MECHANISM OF SUBSTITUTION REACTIONS OF COMPLEXES. LIX. Influence of pH upon the aquation kinetics of iodo-aquo-bis-dimethylglyoximato-cobalt(III).
Rev.Roumaine Chim., 33(1988)263-269.

193. M.Tomoaia-Cotişel, **J.Zsakó,** A.Mocanu, E.Chifu and P.J.Quinn
MONOLAYER PROPERTIES OF MEMBRANE LIPIDS OF THE EXTREME HALOPHILE *Halobacterium cutirubrum,* AT THE AIR/WATER INTERFACE.
Biochim.Biophys.Acta, 942(1988)295-304.
194. **J.Zsakó** and F.Makkay
LINEARIZATION OF POTENTIOMETRIC TITRATION CURVES. IV. Redox titrations.
Studia Univ.Babeş-Bolyai,Chem., 33(1)(1988)85-92.
195. M.Tomoaia-Cotişel, E.Chifu, A.Mocanu, **J.Zsakó,** M.Sălăjan and P.T.Frangopol
STEARIC ACID MONOLAYERS ON PROCAIN CONTAINING SUBPHASES.
Rev.roum.Biochim., 25(1988)227-237.
196. M.Tomoaia-Cotişel, **J.Zsakó** and E.Chifu
STATE EQUATIONS OF FATTY ACID MONOLAYERS.
Studia Univ.Babeş-Bolyai,Chem., 33(2)(1988)54-60.
197. **J**.**Zsakó**
REMARKS ON “A NEW EQUATION FOR MODELLING NONISOTHERMAL REACTIONS".
J.Thermal Anal., 34(1988)1489-1494.
198. I.Gănescu**, J.Zsakó**, Cs.Várhelyi and E.Páll
STUDY ON THE TETRANITRO-PLATINITES(II) AND HEXANITRO-PLATINATES(IV).
Rev.Roumaine Chim., 34(1989)771-777.
199. M.Tomoaia-Cotişel, **J.Zsakó,** E.Chifu and P.J.Quinn
HYSTERESIS IN COMPRESSION-EXPANSION CYCLES OF DISTEAROYL-MONO-GALACTOSYL GLYCEROL MONOLAYERS.
Chem.phys.Lipids, 50(1989)127-133.
200. M.Tomoaia-Cotişel, **J.Zsakó,** E.Chifu, P.T.Frangopol, W.A.P.Luck and E.Osawa
INTERACTION OF PROCAIN WITH UNCHARGED STEARIC ACID MONOLAYER AT THE AIR/WATER INTERFACE.
Rev.roum.Biochim., 26(1989)305-313.
201. **J.Zsakó,** M.Tomoaia-Cotişel and E.Chifu
DISCUSSION OF COMPRESSION ISOTHERMS OF SOME CAROTENOID MONOLAYERS ON THE BASIS OF HMO CALCULATIONS.
Surfactants in Solution, Ed.K.L.Mittal, Plenum Press, vol.9(1989)311-324.
202. E.Chifu, **J.Zsakó,** M.Tomoaia-Cotişel and A.Mocanu
A COMPARATIVE STUDY OF SOME FATTY ACID MONOLAYERS AT THE AIR/WATER INTERFACE.
Studia Univ.Babeş-Bolyai,Chem., 34(2)(1989)3-9.
203. **J.Zsakó**, Cs.Várhelyi and T.Sárvári
ON THE DIOXIMINE COMPLEXES OF TRANSITION METALS. LXXIX. Some new chelates of iron with nioxime and trioxime.
Studia Univ.Babeş-Bolyai,Chem., 34(2)(1989)10-15.
204. E.Chifu, M.Tomoaia-Cotişel, M.Sălăjan, A.Chifu and **J**.**Zsakó**
XANTHOPHYLLS. V. Dynamics of xanthophyll monolayers at the liquid/air in-terface.
Studia Univ.Babeş-Bolyai,Chem., 34(2)(1989)28-34.
205. **J.Zsakó**, Cs.Várhelyi and M.Máté
INFRARED SPECTROSCOPICAL STUDY ON SOME SALTS OF THE HE-XATHIOCYANATO-CHROMIUM(III) COMPLEX ANION.
Studia Univ.Babeş-Bolyai,Chem., 34(2)(1989)74-79.
206. M.Tomoaia-Cotişel, **J.Zsakó**, M.Sălăjan and E.Chifu
SURFACE COMPLEXES OF XANTHOPHYLL FILMS WITH TRANSITION METAL IONS.
Rev.Roum.Morph.Émbryol.Physiol.,Physiologie, 26(1989)341-347.
207. M.Tomoaia-Cotişel, **J.Zsakó,** E.Chifu and D.A.Cadenhead
RELAXATION PHENOMENA IN APOCAROTENOID MONOLAYERS.
Langmuir, 6(1990)191-197.

208. E.Chifu, M.Tomoaia-Cotişel, **J.Zsakó,** A.Mocanu, M.Sălăjan, M.Neag and P.T. Frangopol
PROCAIN PENETRATION INTO UNCHARGED STEARIC ACID MONOLA-YERS IN TERMS OF GIBBS' ADSORPTION EQUATION.
Seminars in Biophysics, vol.6.(1990)117-128.

209. I.Gănescu, Cs.Várhelyi**, J.Zsakó** and M.Preda
NEUE TETRATHIOCYANATO-DIAMINCHROMIATE MIT IMIDAZOL UND BENZIMIDAZOL.
Rev.Roumaine Chim., 35(1990)767-775.

210. E.Chifu, **J.Zsakó**, M.Tomoaia-Cotişel and I.Albu
INTERFACIAL TENSION EXTREMA AT THE ADSORPTION FROM POLY-COMPONENT SYSTEMS.
Rev.Roumaine Chim., 35(1990)767-775.

211. **J.Zsakó**, M.Tomoaia-Cotişel, E.Chifu, I.Albu, A.Mocanu and P.T.Frangopol
PROTOLYTIC EQUILIBRIA IN SURFACE SOLUTIONS OF STEARIC ACID, PROCAIN AND BENZOIC ACID AT THE AIR/WATER INTERFACE.
Rev.Roumaine Chim., 35(1990)867-877.

212. E.Chifu, M.Tomoaia-Cotişel, **J.Zsakó**, I.Albu, A.Mocanu and P.T.Frangopol
PENETRATION OF PROCAIN HYDROCHLORIDE INTO STEARIC ACID MONOLAYERS FROM UNDERLYING AQUEOUS SOLUTIONS.
Rev.Roumaine Chim., 35(1990)879-889.

213. **J.Zsakó**, M.Tomoaia-Cotişel, E.Chifu, A.Mocanu and P.T.Frangopol
INFLUENCE OF STEARIC ACID MONOLAYERS UPON THE PROCAINE ADSORPTION FROM UNDERLYING ALKALINE AQUEOUS SOLUTIONS.
Biochim.Biophys.Acta, 1024(1990)227-232.

214. Cs.Várhelyi**, J.Zsakó,** F.Mánok and A.Brutler
NEW MIXED SCHIFF'S BASE COMPLEXES OF Co(III) WITH ETHYLENE-DIIMINO-BIS-BENZOYLACETONE AND PYRIDINE DERIVATIVES.
Polish J.Chem., 64(1990)305-316.

215. **J.Zsakó**, Cs.Várhelyi and E.Grünwald
NEW MIXED TETRADENTATE CHELATES OF Co(III) WITH ETHYLENE-DIIMINO-BIS-BENZOYLACETONE
Acta Chim.Hung., 127(1990)819-828.

216. **J.Zsakó**, M.Tomoaia-Cotişel, A.Mocanu and E.Chifu
SURFACE EQUATIONS OF STATE FOR OLEIC ACID MONOLAYERS ON ACIDIC AQUEOUS SOLUTIONS.
Studia Univ.Babeş-Bolyai,Chem., 35(1)(1990)74-84.

217. **J.Zsakó,** M.Tomoaia-Cotişel, I.Albu, A.Mocanu, E.Chifu and P.T.Frangopol
ACID-BASE PROPERTIES OF SOME LOCAL ANESTHETICS.
Rev.roum.Biochim., 28(1991)33-40.

218. **J.Zsakó**, M.Tomoaia-Cotişel and E.Chifu
INSOLUBLE MIXED MONOLAYERS.V. Molecular associations in binary films. The regular association approach.
J.Colloid Interface Sci., 146(1991)353-362.

219. **J.Zsakó**, Cs.Várhelyi and I.Gănescu
ON THE DIOXIMINE COMPLEXES OF TRANSITION METALS. LXXXII. Study on some isoselenocyanato mixed chelates of cobalt(III) with dimethylglyoxime.
Rev.Roumaine Chim., 36(1991)1269-1273.

220. **J.Zsakó**, G.Liptay, Cs.Várhelyi, Cs.Novák and I.Gănescu
KINETIC ANALYSIS OF THERMOGRAVIMETRIC DATA. XXVII. Thermal decomposition of some metal and ammonium salts of hexachloroplatinic acid.
J.Thermal Anal., 37(1991)2681-2691.

221. Cs.Várhelyi, **J.Zsakó**, M.Máté and E.Grünwald
ON THE DIOXIMINE COMPLEXES OF TRANSITION METALS. LXXXV. New isothiocyanato-amine-bis-dimethylglyoximato cobalt(III) nonelectrolytes.
Studia Univ.Babeş-Bolyai,Chem., 36(1991)22-27.

222. **J.Zsakó**, Cs.Várhelyi and G.Liptay
THERMAL DECOMPOSITION OF SOME SALTS OF HEXATHIOCYANATO-PLATINIC ACID.
Thermochim.Acta, 203(1992)297-305.

223. **J.Zsakó**, Cs.Várhelyi, I.Gănescu and M.Máté
INFRARED SPECTRA OF SOME REINACKE-SALT ANALOGOUS COMPOUNDS: $M[Cr(NCS)_4(AMINE)_2]$.
Rev.Roumaine Chim., 37(1992)187-195.

224. O.Cozar, V.Znamirovschi, L.David, L.Giurgiu and **J.Zsakó**
ESR INVESTIGATION OF SOME COPPER(II)-DIOXIME-DICHLORIDE COMPOUNDS.
Appl.Magn.Res., 3(1992)849-857.

225. Cs.Várhelyi, **J.Zsakó**, Cs.Várhelyi jr. and G.Liptay
ON THE DIOXIMINE COMPLEXES OF TRANSITION METALS. LXXXVIII. New mixed nitro-complexes of cobalt(III) with 1,2-cyclohexanedione dioxime.
Periodica Polytechnica,Ser.Chem.Eng., 36(1992)43-56.

226. G.Liptay, **J.Zsakó**, Cs.Várhelyi and Cs.Novák
KINETIC ANALYSIS OF THERMOGRAVIMETRIC DATA. XXVIII. Thermal decomposition of some metal and ammonium salts of hexabromoplatinic acid.
J.Thermal Anal., 38(1992)2301-2310.

227. M.Tomoaia-Cotişel, E.Chifu, **J.Zsakó,** A.Mocanu, P.J.Quinn and M.Kates
MONOLAYER PROPERTIES OF ARCHEOL AND CALDARCHEOL POLAR LIPIDS OF A METHANOGENIC ARCHAEBACTERIUM, *Methanospirillum hungatei,* AT THE AIR/WATER INTERFACE.
Chem.phys.Lipids, 63(1992)131-138.

228. **J.Zsakó**, Cs.Várhelyi, J.Demeter-Vodnár and G.Liptay
ON THE DIOXIMINE COMPLEXES OF TRANSITION METALS. XCV. New iodo-amino-bis-dimethylglyoximato-cobalt(III)-nonelectrolytes.
Periodica Polytechnica,Ser.Chem.Eng., 36(1992)271-278.

229. **Zsakó J**.
ANALÓGIÁK ÉS KÜLÖNBSÉGEK A KÉT- ÉS HÁROMDIMENZIÓS REND-SZEREK TERMODINAMIKÁJÁBAN.
Múzeumi Füzetek, I(1992)27-43.

230. I.Gănescu, Cs.Várhelyi**, J.Zsakó** and L.Chirigiu
NEW MIXED COMPLEX ACIDS AND NONELECTROLYTES OF COBALT(III) WITH GLYOXIME.
Polish J.Chem., 67(1993)15-23.

231. M.Tomoaia-Cotişel, E.Chifu, **J.Zsakó,** P.T.Frangopol, P.J.Quinn and A.Mocanu
INTERACTION OF SOME DRUGS WITH MONOMOLECULAR MEMBRANES AT THE FLUID INTERFACES.
Studia Univ.Babeş-Bolyai,Chem., 38(1993)81-85.

232. F.Makkay, Cs.Várhelyi**, J.Zsakó** and Zs.Szász
ON THE DIOXIMINE COMPLEXES OF TRANSITION METALS. XCII. Spec-trophotometric study on the formation of copper(II) chelates with some α-substituted alycyclic oximes.
Studia Univ.Babeş-Bolyai,Chem., 38(1993)99-106.

233. **J.Zsakó,** M.Tomoaia-Cotişel, E.Chifu, A.Mocanu and P.T.Frangopol
PROCAIN INTERACTIONS WITH PHOSPHOLIPID MONOLAYERS AT THE AIR/WATER INTERFACE.
Gazz.Chim.Ital., 124(1994)5-9.

234. **Zsakó J.** and Várhelyi Cs.
AZ ÁTMENETI FÉMEK DIOXIMIN-KOMPLEXEI. 100. A $[Co(en)_2AX]^{n+}$ és $[Co(Diox.H)_2XY]^{n-}$ típusú halogenokomplexek akválódási kinetikája. Összefog-laló közlemény.
Magyar Kém.Folyóirat, 100(1994)257-264.

235. **J.Zsakó,** E.Chifu, M.Tomoaia-Cotişel, A.Mocanu and P.T.Frangopol
PROCAIN PENETRATION INTO MIXED MONOMOLECULAR FILMS OF CHOLESTEROL AND DIPALMITOYLPHOSPHATIDYLCHOLINE.
Rev.Roumaine Chim., 39(1994)777-786.

236. Cs.Várhelyi, F.Makkay, **J.Zsakó**, G.Liptay and K.Kovács-Ludescher
ON THE DIOXIMINE COMPLEXES OF TRANSITION METALS. XCVII. α-Substituted oxime derivatives in the spectrophotometric determination of co-balt.
Periodica Polytechnica,Ser.Chem.Eng., 38(1994)165-181.

237. **J.Zsakó**, Cs.Várhelyi, F.Makkay and K.Kovács-Ludescher
ON THE DIOXIMINE COMPLEXES OF TRANSITION METALS. XCVI. Spectrophotometric study on the deprotonation of some $[Co(DH)_2XY]^n$ type com-plexes.
Studia Univ.Babeş-Bolyai,Chem., 39(1994)85-89.

238. J.Bódis, **J.Zsakó**, Cs.Németh and J.Mink
FOURIER TRANSFORM INFRARED SPECTROSCOPIC STUDY ON THE MECHANISM OF HETEROGENEOUS RHODIUM-CATALYZED METHANOL CARBONYLATION.
Vibr.Spectroscopy, 9(1995)197-202.

239. **J.Zsakó**, E.Bódis, E.Cîmpian, Á.Imre and N.Palibroda
KINETIC STUDY OF THE HOMOGENEOUS Rh-CATALYZED CARBONYLATION OF SOME BENZYL ALCOHOL DERIVATIVES.
Progr.Catal.Bucharest, 4(1995)1-14.

240. Cs.Várhelyi . J.**Zsakó ,** Gy**.**Liptay and M.Somay.
AZ ÁTMENETI FÉMEK DIOXIMIN-KOMPLEXEIRŐL. IC. Új szulfito-bisz-dimetilglioximin-kobalt(III)-komplexek képződése és reakciói.
Múzeumi Füzetek, 4(1995)27-32.

241. **J.Zsakó**
KINETIC ANALYSIS OF THERMOGRAVIMETRIC DATA. XXIX. Remarks on the “many curves" methods.
J.Thermal Anal., 46(1996)1845-1864.

242. **Zsakó J.** and Várhelyi Cs.
AZ ÁTMENETI FÉMEK DIOXIMIN-KOMPLEXEI. CI. Halogeno-bisz-dioxi-mino-kobalt(III)-komplexek akvatálódási kinetikája..
Múzeumi Füzetek, 5(1996)19-23.

243. **J.Zsakó**
COMPENSATION EFFECT IN HETEROGENEOUS NON-ISOTHERMAL KINETICS.
J.Thermal Anal., 47(1996)1679-1690.

244. **J.Zsakó,** I.Gănescu, Cs.Várhelyi and L.Chirigiu
KINETIC ANALYSIS OF THERMOGRAVIMETRIC DATA. XXX. Thermal decomposition of some Reinecke salt like complexes.
J.Thermal Anal., 48(1997)367-371.

245. M.Tomoaia-Cotişel, **J.Zsakó,** E.Chifu, A.Mocanu, P.T.Frangopol and P.J.Quinn
PROCAIN BINDING TO STEARIC ACID MONOLAYERS SPREAD AT THE AIR/BUFFER INTERFACE. Influence of pH and surface pressures.
J.Romanian Coll.Surf.Chem.Ass., 2(3-4)(1997)30-36.

246. **J.Zsakó,** M.Tomoaia-Cotişel, A.Mocanu, Cs.Rácz and E.Chifu
THERMODYNAMICS OF ADSORPTION AND MICELLE FORMATION OF SODIUM CHOLATE IN TWO-PHASE SYSTEMS.
J.Romanian Coll.Surf.Chem.Ass., 2(3-4)(1997)37-40.

247. **J.Zsakó,** A.Mocanu, Cs.Rácz, K.Rácz and E.Chifu
CRITICAL MICELLE CONCENTRATION OF SODIUM CHOLATE SOLUTIONS.
Studia Univ.Babeş-Bolyai,Chem., 42(1997)67-72.
248. E.Chifu, **J.Zsakó,** M.Tomoaia-Cotişel, A.Mocanu and A.Voina
INTERACTION OF CHOLESTEROL WITH BILE SALTS AT THE CCl_4/WATER INTERFACE.
Studia Univ.Babeş-Bolyai,Chem., 42(1997)177-182.
249. Cs.Várhelyi , J. **Zsakó** and Cs..Várhelyi.
A NITRITO-KOBALT-OXIMIN-KOMPLEXEK ÉS A NITRIT KOORDINÁ-CIÓJÁNAK KÉRDÉSEI.
Magyar Kém.Folyóirat, 104(1998)177-187.
250. **J.Zsakó** and Cs.Várhelyi .
A KOBALT(III)-NITRO-DIOXIMIN-KOMPLEXEK NITRO-AQUA LIGAN-DUMCSERÉJÉNEK KINETIKÁJA VIZES OLDATOKBAN.
Magyar Kém.Folyóirat, 104(1998)188-194.
251. **J.Zsakó** and M.Hints
USE OF THERMAL ANALYSIS IN THE STUDY OF SODIUM CARBONATE CAUSTICIZATION BY MEANS OF DOLOMITIC LIME.
J.Thermal Anal., 53(1998)323-331.
252. **J.Zsakó**, L.Nagy, Cs.Várhelyi, Cs.Novák and E.Lovász
ON THE DIOXIMINE COMPLEXES OF TRANSITION METALS. 106. Spectroscopic and DSC study of some complexes of the types $[Cu(DioxH)_2]$ and $[CuX_2.DioxH_2]$.
J.Thermal Anal., 53(1998)421-429.
253. **J.Zsakó**
KINETIC ANALYSIS OF THERMOGRAVIMETRIC DATA. XXXI. Derivation of a non-linear kinetic compensation law.
J.Thermal Anal., 54(1998)921-929.
254. **J.Zsakó,** Cs.Várhelyi, Gy.Liptay and K.Majdik
MX_2L_n TÍPUSÚ KOMPLEXEK KÉPZŐDÉSE ÉS TERMIKUS BOMLÁSA.
Múzeumi Füzetek, 7(1998)20-27.
255. **J.Zsakó**, Cs.Várhelyi jr., Gh.Marcu and G.Liptay
KINETIC ANALYSIS OF THERMOGRAVIMETRIC DATA. XXXII. DSC study of some $[Co(Diox.H)_2(amine)_2]X$ and $H[Co(Diox.H)_2(N_3)_2]$ type complexes with alicyclic α-dioximes.
*J.Thermal Anal.Cal.,*55(1999)311-320.
256. M.Tomoaia-Cotişel, L.C.Stewart, M.Kates, **J.Zsakó,** E.Chifu, A. Mocanu, P.T.Frangopol, L.J.Noe and P.J.Quinn
ACID DISSOCIATION CONSTANTS OF DIPHYTANYLGLYCEROLPHOS-PHORYLGLY-CEROL METHYLPHOSPHATE AND DIPHYTANYLGLYCE- ROLPHOSPHORYL-GLYCEROPHOSPHATE AND ITS DEOXY ANALOG.
Chem.Phys.Lipids, 100(1999)41-54.
257. **J.Zsakó**, **Cs.**Várhelyi . and G.Nagy .
AZ ÁTMENETIFÉMEK OXIMIN KOMPLEXEIRŐL. 109. Sav-bázis egyensú-lyok a kobalt(III) vegyes bisz-dioximin-komplexek vizes oldataiban.
Múzeumi Füzetek, 8(1999)34-40.
258. L.Nagy, **J.Zsakó**, Cs.Novák, Cs.Várhelyi, Gy.Vankó and G.Liptay
ON THE OXIMINE COMPLEXES OF TRANSITION METALS. Part 110.
Spectroscopic and DSC study on some $[Fe(Diox.H)_2L_2]$ and $[Fe(Diox)_3(BOR)_2]$ type chelates and clathrochelates.
J.Thermal Anal.Cal., 57(1999)433-445.
259. M.Tomoaia-Cotişel, A.Mocanu, **J.Zsakó,** T.Oproiu, A.Aldea and P.J.Quinn
NUMERICAL ANALYSIS OF PHASE DIAGRAM OF DISTEAROYL DIGALACTOSYL GLYCEROL SPREAD AT THE AIR-WATER INTERFACE.
J.Romanian Coll.Surf.Chem.Assoc., 3(2)(1999)5-11.

260. M.Tomoaia-Cotişel, **J.Zsakó,** A.Mocanu, E.Chifu, M.Sălăjan and S.Bran
ADSORPTION KINETICS OF ANAESTHETICS AT THE BENZENE/WATER INTERFACE
J.Romanian Coll.Surf.Chem.Assoc., 3(2)(1999)32-40.
261. **J**.**Zsakó** and G. Szabo
POLAROGRAPHIC STUDY ON THE KINETICS AND MECHANISM OF THE HYDROLYSIS OF 1,2,3,- CYCLOHEXANETRIONE 1,3-DIOXIME
*Periodica Polytechnica Ser.Chem.Eng.,*43(1)(1999) 35-40
262. Cs.Varhelyi, **J**.**Zsakó,** T.J. Megyes, K. Majdik and G.Liptay
ON THE OXIME COMPLEXES OF TRANSITION METALS, PART CXIII. PROTOLYTIC EQUILIBRIA IN THE SOLUTIONS OF SOME COMPLEXES OF THE TYPE $[Co(Diox.H)_2AB]$ WITH α-BENZYLDIOXIME AND α-FURYLDIOXIME
*Periodica Polytechnica Ser.Chem.Eng.,*43(1) (1999) 41-49
263. Cs.Varhelyi, **J**.**Zsakó, I.** Gănescu
TIOCIANÁTO-KRÓM(III)-KOMPLEXEK KÉPZŐDÉSE ÉS SZERKEZETE.
Magyar Kém.Folyóirat, 106(2000)1-6.
264. F.C.Buciuman, F.Pătcaş and **J.Zsakó**
TPR-STUDY OF SUBSTITUTION EFFECTS ON REDUCIBILITY AND OXIDATIVE NON-STOICHIOMETRY OF $La_{0.8}A_{0.2}'MnO_{3+\delta}$ PEROVSKITES.
J.Thermal Anal.Cal., 61(2000)819-825.
265. F.Pătcaş, F.C.Buciuman and J.Zsakó
OXYGEN NON-STOICHIMETRY AND REDUCIBILITY OF B-SITE SUBSTITUTED LANTHANUM MANGANITES.
Thermochim.Acta, 360(2000)71-76.
266. M. Tomoaia-Cotişel, T. Oproiu, **J. Zsako**, A. Mocanu, P. T. Frangopol and P. J. Quinn,
NUMERICAL ANALYSIS OF COMPRESSION ISOTHERMS OF DISTEAROYL MONOGALACTOSYL GLYCEROL MONOLAYERS,
Rev. Roumaine Chim., 45(9)(2000)851-861.
267. **J**.**Zsakó,** G. Pokol, Cs.Varhelyi , A.Dobo and G.Liptay
KINETIC ANALYSIS OF TG DATA XXXV. Spectroscopic and thermal studies of some cobalt (III) chelates with ethylenediamine
*J.Thermal Anal.Cal,*64 (2001) 843-856.
268. **J. Zsakó J** , Cs. Várhelyi , and I. Gănescu
TIOCIANÁTO-KRÓM(III)-KOMPLEXEK SZOLVATÁCIÓJA.
Magyar Kém.Folyóirat, 107(2001)139-149.
269. M. Tomoaia-Cotişel, G.Tomoaia, **J.Zsako**, A. Mocanu and I.Albu
THE INFLUENCE OF THE LOCAL ANESTHETIC PROCAINE ON PHOSPHOLIPID MEMBRANES, SOME IMPLICATIONS IN ANESTHESIA
J. Colloid Surf. Chem., 4 (1) (2001)13-25.
270. M. Tomoaia-Cotişel, A. Mocanu, G.Tomoaia, **J.Zsako** and T.Yupsanis
SUPRAMOLECULAR COMPLEXES OF STEARIC ACID AND DESFERAL IN MONOLAYER MEMBRANES
J. Colloid Surf. Chem., 4 (1) (2001)5-12.
271. **J. Zsako**, M.Tomoaia-Cotisel, I.Albu, A. Mocanu and A.Aldea
ACID-BASE PROPERTIES OF DESFERRIOXAMINE MESYLATE
Rev. Roumaine Chim., 47(8-9)(2002)869-879.
272. **J**. **Zsakó,** I.Szilagyi**,** A. Simay, Cs.Varhelyi and K. Kerekes
KINETIC ANALYSIS OF TG DATA XXXVI. Influence of procedural variables upon the apparent kinetic parameters of the thermal deamination
*J.Thermal Anal.Cal.,*69 (2002) 125-133

273. M. Tomoaia-Cotisel**, J. Zsako**, A. Mocanu, M. Salajan, Cs. Racz, S. Bran and E. Chifu
ADSORPTION KINETICS OF DIBUCAINE AND TETRACAINE AT THE BENZENE-WATER INTERFACE STUDIED BY PENDANT DROP METHOD
Studia Univ.Babeş-Bolyai,Chem., 48(1)(2003)201-218.
274. M.Tomoaia-Cotisel**, J. Zsako,** G. Tomoaia, A. Mocanu, V-D. Pop and E.Chifu
ADSORPTION DYNAMICS OF SOME BIOSURFACTANTS AT THE BENZENE/WATER INTERFACE
Rev.Roumaine Chim. (in press 2003)
275. A.Mocanu, G. Tomoaia, M. Tomoaia-Cotisel**,** Cs. Racz, C. R. Ispas and **J. Zsako**
SPECIFIC MOLECULAR INTERACTIONS BETWEEN BOVINE SERUM ALBUMIN AND MELATONIN. SIMULATIONS OF SOME BIOMEMBRANE INTERFACIAL PHENOMENA
SQAtudia
Univ.Babeş-Bolyai,Chem., 48(2)(2003); this issue.

STUDIA UNIVERSITATIS BABEŞ-BOLYAI, CHEMIA, XLIX, 1, 2004

SIMULATIONS OF SOME BIOMEMBRANE INTERFACIAL PHENOMENA. I. SPECIFIC MOLECULAR INTERACTIONS BETWEEN BOVINE SERUM ALBUMIN AND MELATONIN

AURORA MOCANU[a], GHEORGHE TOMOAIA[b], MARIA TOMOAIA-COTIŞEL[a], CSABA RACZ[a], CRISTINA RAMONA ISPAS[a] and JANOS ZSAKO[a,&]

[a] *"Babeş-Bolyai" University, Faculty of Chemistry and Chemical Engineering, Physical Chemistry Department, 400028 Cluj-Napoca, Roumania*
[b] *"Iuliu Haţieganu" University of Medicine, Orthopaedic Surgery, 400015 Cluj-Napoca, Romania*
[&] *Deceased August 2001*

ABSTRACT. This study was designed to investigate the effect of melatonin on the bovine serum albumin (BSA) at the air/aqueous solutions interfaces. Melatonin is a known secretory hormone of the pineal gland with multiple actions "in vitro" and "in vivo", namely, it clearly protects macromolecules from oxidative damage. This hypothesis is supported by our experimental data which show that melatonin specifically interact with bovine serum albumin (BSA). Our findings indicate that melatonin increases the surface pressure of BSA adsorbed films exerting a substantial stabilizing effect on BSA interfacial self-assembled films at the air/water interface. This effect suggests that melatonin might act as a protective agent of macromolecules "in vitro" and "in vivo" through physicochemical specific interactions with bio-molecules, such as BSA, and/or with their biologically active assemblies. As a consequence, melatonin may facilitate the inhibition of the peroxidation damage of bio-molecules by increasing their supramolecular assemblies stability. Our results confirm both the involvement of melatonin in specific interactions with BSA and its remarkable effect on the stabilization of biological compounds at fluid interfaces.

Key words: adsorption at liquid interfaces, melatonin, bovine serum albumin, interfacial pressure, ring du Noüy method.

INTRODUCTION

Melatonin (N-acetyl-5-methoxy-tryptamine; Fig. 1), the main secretory hormone of the pineal gland of vertebrates including the humans, it is also produced by extrapineal tissues and edible plants and it has multiple actions "in vivo". Recently, melatonin was reported to efficiently protect biomolecules against oxidative damage and, consequently, against carcinogenesis [1,2]. Melatonin's function is substantially consistent with a general protection action, upon fatty acids [3,4] lipids, proteins and DNA. It is evaluated as being an effective hydroxyl free radical scavenger and an efficient antioxidant [5,6]. This non-receptor related action might shed light on several of melatonin activities on cell membrane function, that is largely committed to cellular membrane integrity. The multiple actions make melatonin a potentially useful compound in the treatment of various diseases generated by the oxidative damage "in vivo" [7-9].

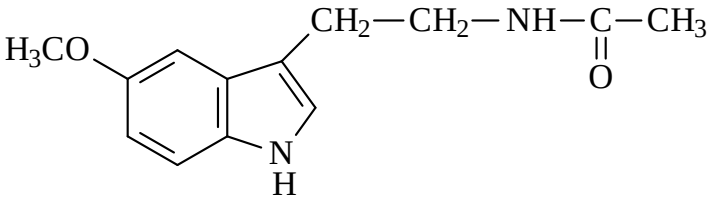

Fig. 1 Molecular structure of melatonin

To our knowledge, no data are available about the effects of melatonin on proteins at fluid interfaces. The goal of this study was to determine the effects of melatonin on the bovine serum albumin (BSA) self-assembled films adsorbed at the air/aqueous solution interface, near the physiological pH. Our results indicate that melatonin interacts with BSA and stabilizes the supramolecular structure of BSA self-assemblies formed at fluid interfaces. Consequently, melatonin might modulate some biological phenomena by having its ability to stabilize macromolecules from oxidative stress both "in vitro" and "in vivo".

EXPERIMENTAL

Melatonin was purchased from Sigma Chemical Co. and used without further purification. Bovine serum albumin (BSA) was obtained from Merck and used also without further purification. All other chemicals were of the highest grade available commercially. Other chemicals used were of analytical grade and obtained from commercial sources. Twice distilled water was used in all experiments. In order to ensure identical working conditions, all BSA solutions were prepared in phosphate buffer (pH 7), made up from phosphate salts (6.6×10^{-2}M) in twice distilled water.

Surface tension σ (dyn/cm) measurements were performed at the interface between the air and phosphate buffer solutions, in the presence of melatonin (ranging from 10^{-4} M to 10^{-2} M) both in the absence of BSA and in the presence of the constant concentration of BSA of 0.4% w/v, at 20^0 C, by using the ring du Noüy method, with an accuracy of ± 0.1 dyn/cm. The experimental details have already been given in one of our previous work [10].

RESULTS AND DISCUSSION

The equilibrium adsorption of melatonin at the air/aqueous phosphate buffer interface, in terms of surface tension as a function of time, was reached in about 60 minutes, in the absence of bovine serum albumin (BSA), and in 40 minutes in the presence of BSA at a constant concentration in BSA of 0.4 % w/v. The more rapid attainment of the adsorption equilibrium for melatonin at the air/water interface in the presence of BSA is probably the result of the interaction of melatonin with BSA within the interfacial self-assembled films.

These results clearly show that both melatonin and BSA are surface active bio-molecules and both act by lowering the surface tension of the pure air/water interface. The simultaneous adsorption of melatonin and BSA at the air/water interface is a complex phenomenon difficult to be fully analyzed.

However, the two compounds show a synergistic effect when adsorbed together from water phase to the fluid interfaces being incorporated into interfacial mixed self-assemblies. The molecular association of melatonin and BSA in the interfacial self-assembled films or adsorbed membranes at fluid interfaces is particularly noteworthy and might explain some biomembrane phenomena.

Further, the equilibrium values of the surface tension were given versus logarithm of the melatonin concentrations in Fig. 2, both in the absence and in the presence of BSA. By analyzing these isotherms a linear dependence of $\sigma = \sigma(\log c)$ is found in the range of large concentrations of melatonin.

The maximum adsorption coefficient (Γ_{max}) and molecular area (a_o) for melatonin in adsorbed films at the air/water (pH 7) interfaces, both in the absence and in the presence of bovine serum albumin (0.4% w/v) in aqueous phase, were determined from the slope of the linear portions of the isotherms (Fig. 2) by using the Gibbs adsorption equation. These values are given in Table 1.

Table 1

Maximum adsorption coefficient (Γ_{max}) and molecular area (a_o) for melatonin in adsorbed films at the air/water (pH 7) interfaces, both in the absence and in the presence of bovine serum albumin (0.4% w/v) in aqueous phase.

Interface	Aqueous solution of melatonin (pH=7)/air	Aqueous solutions of melatonin and bovine serum albumin (BSA: 0.4% w/v; pH 7)/air
Γ_{max} , moles/cm^2	2.6×10^{-10}	1.02×10^{-10}
a_o , Å^2/molecule	63.85	162.78

From the data given in Table 1 we can observe that the melatonin film is more expanded in the presence of BSA due to the penetration of biopolymer into the melatonin film, in a similar case with the drug penetration from water phase into the model membranes at the air/water interface [11-14].

In order to obtain an image of the possible interactions in the interfacial mixed film of melatonin and BSA, in Table 2, are listed the data related to the variation of the equilibrium interfacial tension with the melatonin concentration (column I), both in the absence (column II) and in the presence of BSA (column III), respectively. By comparing column II with column III, it can be seen that the presence of BSA lead to a supplementary decrease of the interfacial tension, respectively to an increase of the pressure in the adsorbed melatonin film.

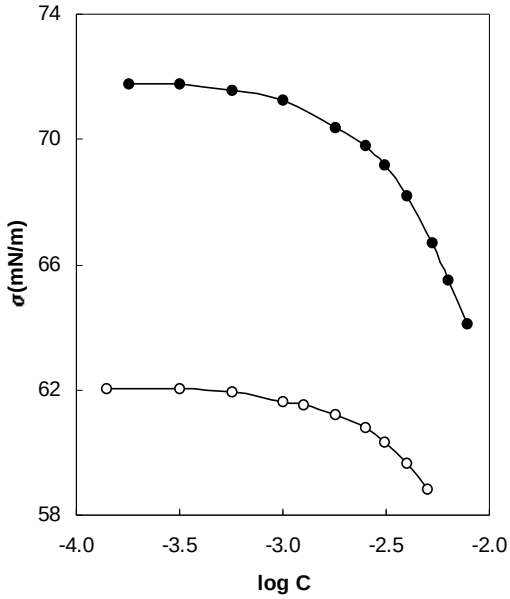

Fig. 2. *Dependence of static (equilibrium) interfacial tension, as a function of logarithm of melatonin concentration in aqueous buffer phosphate pH 7, both in the absence of bovine serum albumin (BSA) (•) or in the presence of BSA (o), at the air/water interfaces.*

Column IV contains the interfacial pressures of pure melatonin film. In colum V of the Table 2, the contributions of the BSA to the interfacial pressure of the mixed melatonin- BSA film are given, in considering the melatonin contribution (column IV) as constants. The BSA contribution was evaluated from the difference between the values in columns II and III for each melatonin concentration. It can be seen that the interfacial pressure due to BSA (column (V) is lowered as the melatonin concentration increases. In other words, the contribution of each component to the interfacial pressure of the melatonin-BSA film is not independent. This fact also suggests that the interaction between melatonin and BSA is a strong and specific one.

Furthermore, one considers the adsorption of BSA as being constant at the air/water interface with the value of σ = 62.50 dyn/cm for the interfacial tension (see column III). The last column VI of Table 2 indicates the interfacial pressure increment ($\Delta\ \pi$, dyn/cm) due to the melatonin adsorption and it is calculated with the values in column III. The increase of interfacial pressure is more pronounced as the concentration in melatonin is increased. The interaction between melatonin and BSA is thus evidenced by the decrease of the interfacial tension, respectively, by the increase of the interfacial pressure at the air/water interface.

Table 2

The effect of melatonin and of bovine serum albumin (BSA) on the surface tension and the surface pressure at the air/aqueous buffer (pH 7) interface.

Melatonin Conc. [M] 10^4	σ dyn/cm (without BSA)	σ dyn/cm (with BSA 0.4 % w/v)	π dyn/cm (for pure melatonin films)	π dyn/cm (BSA: 0.4 % w/v)	$\Delta\ \pi$ dyn/cm (melatonin and BSA)
I	II	III	IV	V	VI
0.00	72.75	62.50	0.00	10.25	0.00
1.00	71.85	62.05	0.90	9.80	0.45
3.10	71.76	62.03	0.99	9.73	0.47
5.60	71.57	61.96	1.18	9.61	0.54

Melatonin Conc. [M] 10^4	σ dyn/cm (without BSA)	σ dyn/cm (with BSA 0.4 % w/v)	π dyn/cm (for pure melatonin films)	π dyn/cm (BSA: 0.4 % w/v)	$\Delta\ \pi$ dyn/cm (melatonin and BSA)
10.00	71.28	61.64	1.47	9.64	0.86
17.70	70.58	61.21	2.17	9.37	1.29
31.00	69.20	60.31	3.55	8.89	2.19
39.00	68.22	59.67	4.53	8.55	2.83
50.00	66.72	58.85	6.03	7.87	3.65

Consistent with our data are the findings on the interaction of bovine serum albumin with various soluble surfactants [15–17] showing a good stability of molecular associations of surfactants to BSA.

The mechanism of specific interaction between melatonin and BSA is unknown. Melatonin probably interact with the hydrophobic regions of the protein and also with the hydrophilic groups of the protein, taking into account its hydrophilic and hydrophobic structure (Fig.1). Consequently, the melatonin molecules might be covalently attached to proteins. These experimental findings should bring insights on the binding of soluble compounds to biomembranes and might simulate and explain some biomembrane phenomena [18].

Taking into account that melatonin decreases significantly the surface tension of BSA adsorbed films at fluid interfaces, our data are, certainly, an important contribution to the knowledge of the interfacial action of melatonin on bio-macromolecules stabilizing their interfacial supramolecular structures. This binding of melatonin with macromolecules is likely to be of a physiological significance, but future studies will be design to systematically evaluate the melatonin capacity to stabilize the cellular membranes.

CONCLUSIONS

Melatonin has a hydrophilic and a hydrophobic character, possessing a methoxy group in the 5-position and an acetyl side chain that can orient the molecule at the air/water interfaces. Our findings show that melatonin associates with and increases the stability of BSA interfacial adsorbed layers. These results confirm the involvement of melatonin in specific interactions with soluble proteins.

Melatonin effect on the stabilization of biopolymers might provide a general protection of biological compounds against oxidative damage "in vitro" and "in vivo". The detailed mechanism of melatonin action on BSA interfacial self-assemblies and for its stabilizing effect is not clear at the present time and it is a research subject of future interest in our laboratories.

REFERENCES

1. M. Karbownik, E. Gitto, A. Lewinski and R. J. Reiter, *J. Cellular Biochemistry*, **81**, 693 (2000).
2. A. G. Turjanski, R. E. Rosenstein and D. A. Estrin, *J. Med. Chem.,* **41**, 3684 (1998).
3. M. L. Pita, M. Hoyos, I. Martin-Lacave, C. Osuna, J. M. Fernandez-Santos and J.M. Guerrero, *J. Pineal Res.*, **32**, 179 (2002).
4. P. Leaden, J. Barrionuevo and A. Catala, *J. Pineal Res.,* **32**, 129 (2002).
5. M. A. Livrea, L.Tesoriere, D. D'Arpa and M. Morreale, *Free Radical Biology and Medicine,* **23** (5), 706 (1997).
6. R. J. Reiter, D. Acuna-Castroviejo, D. X. Tan and S. Burkhardt, *Ann. NY Acad. Sci*., **939**, 200 (2001).
7. M. F. Xu, S. Ho, Z.M. Qian and P. L. Tang, *J. Pineal Res.*, **31**, 301 (2001).
8. B. J. Lee, J.S. Choe and C. K. Kim, *J. Microencapsul*., **15** (6), 775 (1998).
9. H. S. Gwak., S.U. Kim and I. K. Chun, *Arch. Pharm. Res*., **25** (3), 392 (2002).
10. E. Chifu and M. Tomoaia-Cotişel, *Studia, Univ."Babeş-Bolyai", Chemia,* **26** (2), 3 (1981).
11. M. Tomoaia-Cotişel, *Progr. Colloid Polym. Sci*., **83**, 155 (1990).
12. M. Tomoaia-Cotişel and D.A. Cadenhead, *Langmuir*, **7**, 964 (1991).
13. B. Asgharian, D.A. Cadenhead and M. Tomoaia-Cotişel, *Langmuir*, **9**, 228 (1993).
14. M. Tomoaia-Cotişel and P. J. Quinn, "Biophysical Properties of Carotenoids", *Subcellular Biochemistry, Volume **30**: Fat-Soluble Vitamins,* Quinn and Kagan, *Eds.,* Plenum Press, New York, *Chapter 10,* pp. 219- 242, (1998).
15. N. Nishikido, T. Takahara, H. Kobayashi and M. Tanaka, *Bull. Chem. Soc. Jpn.,* 1982, **55**, 3085.
16. M. Tribout, S. Paredes, J.M. Gonzalez-Manas and F.M. Goni, *J. Biochem. and Biophys. Methods.*, **22**, 129 (1991).
17. E. Tlissi, E. Abuin, M. E. Lanio and C. Alvarez, *J. Biochem. Biophys. Methods.*, **50**, 261 (2002).
18. M. Messner, R. Hardeland, A. Rodenbeck and G. Huether, *Adv. Exp. Med. Biol*., **467**, 303 (1999).

STUDIA UNIVERSITATIS BABEŞ-BOLYAI, CHEMIA, XLIX, 1, 2004

RELAXATIONPHENOMENAINCAROTENOIDFILMS ATTHEOIL/WATERINTERFACE

MARIA TOMOAIA-COTISEL[a] and PAUL JOOS[b]

[a] *"Babeş-Bolyai" University, Faculty of Chemistry and Chemical Engineering, Physical Chemistry Department, 400028 Cluj-Napoca, Romania*
[b] *University of Antwerp, Department of Chemistry, B-2610 Wilrijk,Belgium*

ABSTRACT. The kinetic analysis of the relaxation phenomena in carotenoid films adsorbed at the oil/water interface is presented for several carotenoid concentrations in the oil phase. A new kinetic approach is applied and it addresses the diffusion adsorption associated with a reversible interfacial reaction of reorientation of carotenoid molecules between two conformations The new model contains two characteristic times, i.e., *diffusion relaxation* and *kinetic relaxation times* and it describes with high accuracy the experimental data of dynamic interfacial tensions for the adsorption of two carotenoids: ethyl ester of β – apo – 8' – carotenoic acid and β-carotene, both all-*trans* isomers, from n-hexane phase to the n-hexane/water interface. The calculations give the two characteristic times for the relaxation phenomena in carotenoid adsorbed films at the oil/water interface. The data are in substantial agreement with the molecular structure of these carotenoids.

Keywords*:* relaxation kinetics; dynamic interfacial tensions; ethyl ester ofββ– apo - 8' – carotenoic acid; β -carotene; hexane/ water interface; diffusion relaxation time; kinetic relaxation time

INTRODUCTION

Carotenoids are important biological pigments that play vital role in cell membrane stability, cellular differentiation, growth control, photooxidative protection, vision process, photosynthesis and nutrition [1-4]. It clearly appears that the varied biological activities of carotenoids in living organisms are determined by the biophysical and chemical properties of these molecules [1-7]. Among them, the adsorption properties of carotenoids seem to be defined by their molecular structure and their molecular geometry [1, 5]. In addition, specific conformations of carotenoid derivatives and their correct orientation [5] at various biological interfaces [6, 7] will determine their proper function within cellular and subcellular structures [1].

Generally, a surfactant solution is characterized by the adsorption of surfactant molecules in monolayers at the fluid interface [8-26]. The adsorption kinetics can be controlled by surfactant molecular diffusion from the bulk to the subsurface [11-14, 19-22] and/or by an energy barrier, which controls the transfer of the surfactant molecules from the subsurface to the interface [9, 19].

In the present study, we focus on the relaxation kinetics in carotenoids films adsorbed from oil solutions at the oil/water interface, by using interfacial tension measurements as an experimental tool. For our systems containing carotenoids, the dynamic interfacial tensions versus time show long time effects which cannot be understood by diffusion from the bulk to the subsurface and the transfer from the subsurface to the interface.

These time effects can be described by a surface reaction of reorientation of surfactant molecules. This type of behavior is also found with some sulfosuccinates [20] at the air/water interface and with proteins [26] at the oil/water interface.

The kinetic analysis of the interfacial tension relaxation becomes more complex when the surfactant molecules participate in an interfacial reaction of molecular reorientation [8, 26- 29] or when they form aggregations or clusters in the bulk phase or in the interfacial adsorbed layer [30, 31]. Although relevant for many important applications in various fields, like, pharmaceutical formulations, food processing, and emulsification processes, the relaxation kinetics in carotenoid films at fluid interfaces has received so far only a marginal attention [29].

The major goal of this study is to describe the long time effects recorded for the dynamic interfacial tensions of carotenoid systems at the oil/water interface. To reach this goal, a new kinetic theoretical model is applied to allow for a diffusion process to be associated with a surface reaction of reorientation.

KINETIC MODEL OF RELAXATION PHENOMENA

The kinetic model applied in this study, consists of a bulk diffusion process, given by the diffusion penetration theory [12-14, 20, 32], which is associated with a first order reversible interfacial reaction of surface reorientation.

The surfactant molecules are adsorbed at the liquid/liquid interface as conformation 1, soluble in oil phase, and at the interface they undergo a transformation to the conformation 2. The conformation 1 is exchangeable with the bulk oil phase, but the conformation 2 is not, being stable only at the interface. Both conformations are assumed practically insoluble in the aqueous phase.

To model the relaxation phenomena in adsorbed films at the liquid/liquid interface, we start from the mass balance at the interface for conformation 1 written as:

$$\frac{d\,\Gamma_1}{d\,t} = D\,\frac{c_0 - c_s}{\sqrt{\pi D t}} - k\left(\Gamma_1 - \Gamma_1^e\right) \tag{1}$$

or written in an equivalent form:

and for conformation 2, given by:

$$\frac{d\Gamma_1}{dt} = \left(\frac{D}{\pi t}\right)^{\frac{1}{2}}\left(c_0 - c_s\right) - k\left(\Gamma_1 - \Gamma_1^e\right) \tag{2}$$

$$\frac{d\,\Gamma_2}{d\,t} = k\left(\Gamma_2^e - \Gamma_2\right) \tag{3}$$

where, c_0 and c_s are the surfactant bulk and subsurface concentrations, respectively, at the time t: π is 3.1415; D value is the diffusion coefficient of the surfactant molecules in the bulk solution; Γ_1 and Γ_2 are the adsorption of conformation 1 and of conformation 2, respectively, at the time t; Γ_1^e and Γ_2^e represent the adsorption of conformation 1 and of conformation 2, respectively, at the equilibrium; k is the rate

constant for the surface reaction of molecular transformation or reorientation. The subsurface layer is situated only a few angstroms away from the interface and still belonging to the oil bulk solution.

Eq. (3) is readily integrated, taking in to account that at t =0, Γ_2 =0, whence:

$$\Gamma_2 = \Gamma_2^e - \Gamma_2^e e^{-k t} \tag{4}$$

The subsurface concentration (noted c_s or simply c) in equilibrium with the composition at the liquid/liquid interface depends on $\Gamma_1$and Γ_2, as follows:

$$dc = \left(\frac{\partial c}{\partial \Gamma_1}\right)_{\Gamma_2} d\Gamma_1 + \left(\frac{\partial c}{\partial \Gamma_2}\right)_{\Gamma_1} d\Gamma_2 \tag{5}$$

or

$$c_0 - c_s = \left(\frac{\partial c}{\partial \Gamma_1}\right)_{\Gamma_2} \left(\Gamma_1^e - \Gamma_1\right) + \left(\frac{\partial c}{\partial \Gamma_2}\right)_{\Gamma_1} \left(\Gamma_2^e - \Gamma_2\right) \tag{6}$$

The Eq. (6) can be further written in another equivalent form:

$$c_0 - c_s = \left(\frac{\partial c}{\partial \Gamma_1}\right)_{\Gamma_2} \left[\left(\Gamma_1^e - \Gamma_1\right) + \frac{\left(\partial c / \partial \Gamma_2\right)_{\Gamma_1}}{\left(\partial c / \partial \Gamma_1\right)_{\Gamma_2}} \left(\Gamma_2^e - \Gamma_2\right)\right] \tag{7}$$

We note by ν:

$$\nu = -\frac{\left(\partial c / \partial \ln \Gamma_2\right)_{\Gamma_1}}{\left(\partial c / \partial \ln \Gamma_1\right)_{\Gamma_2}} = -\frac{\left(\partial c / \partial \Gamma_2\right)_{\Gamma_1} \Gamma_2^e}{\left(\partial c / \partial \Gamma_1\right)_{\Gamma_2} \Gamma_1^e} \tag{8}$$

and it obtains

$$\frac{\left(\partial c / \partial \Gamma_2\right)_{\Gamma_1}}{\left(\partial c / \partial \Gamma_1\right)_{\Gamma_2}} = -\nu \frac{\Gamma_1^e}{\Gamma_2^e} \tag{9}$$

With Eq. (9), Eq.(7) becomes:

$$c_0 - c_s = \left(\frac{\partial c}{\partial \Gamma_1}\right)_{\Gamma_2} \left[\left(\Gamma_1^e - \Gamma_1\right) - \nu \frac{\Gamma_1^e}{\Gamma_2^e} \left(\Gamma_2^e - \Gamma_2\right)\right] \tag{10}$$

Further, with Eqs.(4) and (10), Eq. (2) becomes:

$$\frac{d\,\Gamma_1}{dt} = \left(\frac{D}{\pi t}\right)^{\frac{1}{2}} \left(\frac{\partial c}{\partial \Gamma_1}\right)_{\Gamma_2} \left[\left(\Gamma_1^e - \Gamma_1\right) - \nu\,\Gamma_1^e\, e^{-kt}\right] - k\left(\Gamma_1 - \Gamma_1^e\right) \quad (11)$$

We introduce the *diffusion relaxation time* [32-34], noted τ_D or τ, defined as:

$$\frac{1}{(\tau)^{1/2}} = D^{1/2}\left(\frac{\partial c}{\partial \Gamma_1}\right)_{\Gamma_2} \quad (12)$$

and in this way Eq.(11) is written as:

$$\frac{d\left(\Gamma_1^e - \Gamma_1\right)}{dt} + \left[\left(\frac{1}{\pi\tau t}\right)^{1/2} + k\right]\left(\Gamma_1^e - \Gamma_1\right) = \frac{\nu\,\Gamma_1^e\, e^{-kt}}{(\pi\tau t)^{1/2}} \quad (13)$$

The Eq. (13) is a linear differential equation and its integral is:

$$\Gamma_1^e - \Gamma_1 = e^{-\left(\frac{4t}{\pi\tau}\right)^{1/2}} e^{-kt}\left[K + \nu\,\Gamma_1^e\, e^{\left(\frac{4t}{\pi\tau}\right)^{1/2}}\right] = K\, e^{-\left(\frac{4t}{\pi\tau}\right)^{1/2}} e^{-kt} + \nu\,\Gamma_1^e\, e^{-kt} \quad (14)$$

From the initial conditions, t=0 and Γ_1=0, the integration constant K is obtained:

$$K = \Gamma_1^e(1-\nu) \quad (15)$$

Finally:

$$\Gamma_1^e - \Gamma_1 = \Gamma_1^e\,(1-\nu)\, e^{-\left(\frac{4t}{\pi\tau}\right)^{\frac{1}{2}}} e^{-kt} + \nu\,\Gamma_1^e\, e^{-kt} \quad (16)$$

Further, since the surface tension depends on Γ_1 and Γ_2, it results:

$$\sigma - \sigma_e = \left(\frac{\partial \sigma}{\partial \Gamma_1}\right)_{\Gamma_2}\left(\Gamma_1 - \Gamma_1^e\right) + \left(\frac{\partial \sigma}{\partial \Gamma_2}\right)_{\Gamma_1}\left(\Gamma_2 - \Gamma_2^e\right) \quad (17)$$

By using Eqs.(4) and (16), the Eq. (17) gives:

$$\sigma - \sigma_e = \left\{-\left(\frac{\partial \sigma}{\partial \ln \Gamma_1}\right)_{\Gamma_2}\left[(1-\nu)\, e^{-\left(\frac{4t}{\pi\tau}\right)^{1/2}} + \nu\right] - \left(\frac{\partial \sigma}{\partial \ln \Gamma_2}\right)_{\Gamma_1}\right\} e^{-kt} \quad (18)$$

By noting:

$$-\left(\frac{\partial\sigma}{\partial\ln\Gamma_1}\right)_{\Gamma_2} = \varepsilon_{01}$$

$$-\left(\frac{\partial\sigma}{\partial\ln\Gamma_2}\right)_{\Gamma_1} = \varepsilon_{02} \tag{19}$$

the Eq. (18) becomes:

$$\sigma-\sigma_e = \left[\varepsilon_{01}(1-\nu)e^{-\left(\frac{4t}{\pi\tau}\right)^{1/2}} + (\nu\varepsilon_{01}+\varepsilon_{02})\right]e^{-kt} \tag{20}$$

By making the notations:

$$\begin{aligned}&\varepsilon_{01}(1-\nu)=\Delta\sigma_{01}\\&\nu\varepsilon_{01}+\varepsilon_{02}=\Delta\sigma_{02}\\&(\sigma-\sigma_e=\Delta\sigma)\end{aligned} \tag{21}$$

the Eq. (20) becomes:

$$\sigma = \sigma_e + \left[\Delta\sigma_{01}\,e^{-\left(\frac{4t}{\pi\tau}\right)^{1/2}} + \Delta\sigma_{02}\right]e^{-kt} \tag{22}$$

where, for t=0, it results:

$$\Delta\sigma_{01}+\Delta\sigma_{02}=\Delta\sigma_0=\sigma_0-\sigma_e \tag{23}$$

σ_0 being the surface tension of the pure interface without surfactant. It should be remarked that we have linearized the mathematical problem, i.e., $\left(\frac{\partial c}{\partial\ln\Gamma_1}\right)_{\Gamma_2}$; $\left(\frac{\partial c}{\partial\ln\Gamma_2}\right)_{\Gamma_1}$; $\left(\frac{\partial\sigma}{\partial\Gamma_1}\right)_{\Gamma_2}$ and $\left(\frac{\partial\sigma}{\partial\Gamma_2}\right)_{\Gamma_1}$ are considered as constants. In practice, however, Eq. (22) describes the experiments quite well, as it will be detailed in this investigation. It is also noteworthy here that the dynamic interfacial tension, σ(t), appears to be determined mainly by the two characteristic times, *namely*, τ the diffusion relaxation timeand τ_k the reaction relaxation (k^{-1}) time, k being the rate constant of the interfacial reaction.

In Eq. (22), the term $\exp-\left(\frac{4t}{\pi\tau}\right)^{1/2}$ accounts for diffusion relaxation with τ (noted also as τ_D) the diffusion relaxation time and e^{-kt} accounts for the surface reaction of reorientation at the oil/water interfacewith τ_k the reaction relaxation (k^{-1}) time.

The Eq. (22) describes the dynamic surface tension with time. For k = 0 (no surface reaction) and $\Delta\sigma_{02} = 0$, $\Delta\sigma_{01} = \Delta\sigma_0$, and Eq. (22) becomes:

$$\sigma - \sigma_e = \Delta\sigma = \Delta\sigma_0 \; e^{-\left(\frac{4t}{\pi\tau}\right)^{1/2}} \tag{24}$$

The Eq. (24) is the equation for a pure diffusion controlled process.

Further Eq. (22) can be used to derive simple analytical expressions describing the relaxation behavior in the short and long time limits of the relaxation diffusion time. For some situations it may happen that diffusion equilibration is so fast $\tau_D \langle\langle \tau_k$, that we only observe the transformation step and the Eq. (22) becomes:

$$\sigma = \sigma_e + \Delta\sigma_{02} \; e^{-kt} \tag{25}$$

The Eq. (25) shows an exponential decrease of $\Delta\sigma$ with time. The extrapolation of Eq. (25) at t=0 do not yield σ_0 value, but the following relation results:

$$\sigma(t \to 0) = \sigma_e + \Delta\sigma_{02} \tag{26}$$

If diffusion is slow $\tau_D \rangle\rangle \tau_k$, Eq. (22) gives:

$$\Delta\sigma = \Delta\sigma_0 \exp\left(-\frac{t}{\tau_k}\right) \tag{27}$$

and the diffusion is the rate controlling step and, for $\tau_D \to \infty$, Eq. (22) extrapolates to an equivalent form of Eq. (27) given by:

$$\Delta\sigma(t) = (\Delta\sigma_{01} + \Delta\sigma_{02}) e^{-kt} = \Delta\sigma_0 e^{-kt} \tag{28}$$

and the$\Delta\Delta\sigma$ shows an exponential decrease with time, which for $t \to 0$ extrapolates to the σ_0 value. The decay is again exponential but the interfacial tension for $t \to 0$ extrapolates to σ_0 = 50 mN m^{-1}. Between these two limiting cases, the adsorption relaxation is affected by both diffusion and surface reorientation processes at liquid/liquid interfaces.

To describe the relaxation phenomena in adsorbed films at the oil/water interface we apply our new kinetic approach to the dynamic interfacial tension data for two carotenoids at the hexane/water interface and the characteristics time τ_D and τ_k are determined.

EXPERIMENTAL

The compounds used, *namely* ethyl ester of β - apo – 8'-carotenoic acid and β - carotene, were synthetic commercial products of analytical grade. They were purchased from Hoffmann La Roche. Both carotenoids are all-*trans* isomers and they are insoluble in the water phase. Therefore, their transfer through the interface towards aqueous phase can be neglected. The n-hexane was purchased from Merck. All chemicals were used without additional purification. Two distilled water was used as aqueous phase.

The equilibrium (σ_e) and the dynamic interfacial tensions, σ(t), were measured by Du Nouy ring method and Wilhelmy plate method as described elsewhere [1, 20, 34-36]. The agreement between the two methods is excellent and the deviations do not exceed the error of the individual method. The accuracy of interfacial tension measurements was ± 0.1 mN/m, in agreement with literature data on different systems [20, 34-36]. All measurements were carried out at constant temperature of 25 ± 0.1 °C.

RESULTS AND DISCUSSION

Dynamic interfacial tensions

The dynamic interfacial tension, σ(t), as a function of time for several concentrations of the ethyl ester of β - apo - 8' - carotenoic acid in n-hexane solutions at the hexane/water interface are presented in Figs. 1 and 2.

The results of measurements for different β - carotene concentrations in hexane phase at the hexane/water interface are presented in Figs. 3 and 4. As can be seen, in Figs. 1-4, both carotenoids possess a high surface activity as indicated by the equilibrium interfacial tensions(σ_e), values considered at the time of 120 minutes.

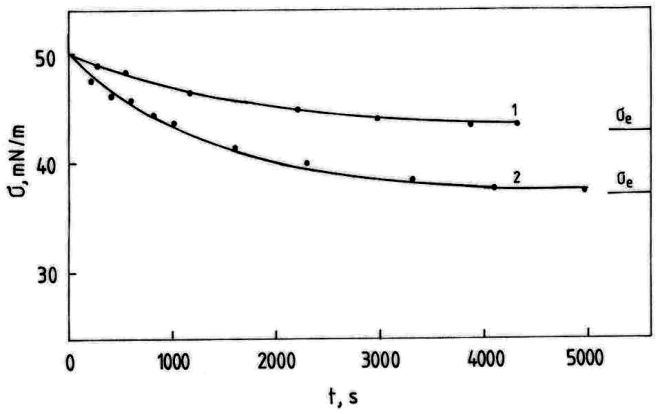

Fig. 1. *Dynamic interfacial tensions, σ (t), as a function of time, for hexane solutions of ethyl ester of β - apo-8'- carotenoic acid at the interface with water, for two ester concentrations. Curve (1) for c_0=3$10^{-8}$ mole cm^{-3} and (2) c_0 =7.9 10^{-8} mole cm^{-3}. Full line calculated by Eq. (22) using constant parameters given in Table 1. Horizontal line indicates σ_e value for each ester concentration.*

Figs. 1-4 show that the relaxation process illustrated by the dynamic interfacial tension measurements is long time dependent for the two selected carotenoids. To investigate the relaxation process in adsorbed films at the hexane/water interface for the two carotenoids we use our new kinetic model developed in this paper.

Kinetic analysis of dynamic interfacial tensions

The dynamic interfacial tensions, shown in Figs. 1-4, are analyzed applying our new kinetic approach, which considers diffusion relaxation associated with surface reorientation relaxation in carotenoid films at the oil/water interface, by using Eq. (22). The total jump in interfacial tension is $\Delta\sigma_0$ defined as $\Delta\sigma_0 = \sigma_0 - \sigma_e$ (σ_0 is the interfacial tension of the pure hexane/water interface of 50 mN m^{-1}), and $\Delta\sigma_0 = \Delta\sigma_{01} + \Delta\sigma_{02}$, where $\Delta\sigma_{01}$ and $\Delta\sigma_{02}$ are the amplitudes of the interfacial tension.

If τ is *very small*, the interfacial tensions with time seem to extrapolate for $t \to 0$ to $\sigma \to \sigma_e + \Delta\sigma_{02}$, given by Eq. (26). Here the diffusion equilibrium is established, *i.e.,* the equilibrium between the initial surface configuration and the bulk concentration is established, but the surface reaction did not start.

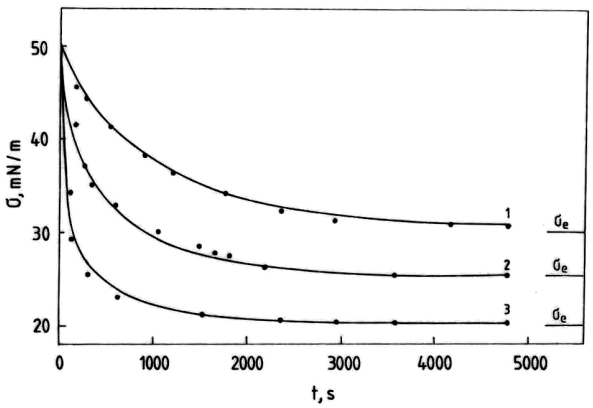

Fig. 2. *Dynamic interfacial tensions (σ versus t) at the hexane/water interface, for several concentrations of ethyl ester of β - apo-8'-carotenoic acid in hexane solution. Curve (1) for $c_0 = 1.76\ 10^{-7}$ mole cm^{-3}; (2): $c_0 = 2.97\ 10^{-7}$ mole cm^{-3} and (3): $c_0 = 5.07\ 10^{-7}$ mole cm^{-3}. The full line calculated with Eq. (22) using constant parameters given in Table 1. Symbols as in Fig. 1.*

The decay of the interfacial tension with time is exponential and it is given by Eq. (25). If τ is *very large*, diffusion is the rate controlling step and, for $\tau \to \infty$, Eq. (22) extrapolates to Eq. (28).

The decay is again exponential but the interfacial tension for $t \to 0$ extrapolates to σ_0 = 50 mN m^{-1}. We have analyzed the dynamic interfacial tensions for both carotenoids and the data are well fitted by the Eq. (22) and the standard deviation of experimental data from the calculated ones is within the experimental errors. The parameters of Eq. (22) that fit the experimental data for ethyl ester of β-apo-8'-carotenoic acidare given in Table 1 and for β-carotene in Table 2.

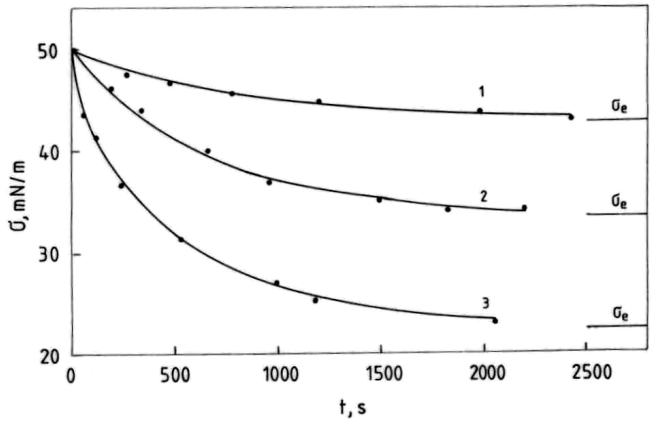

Fig. 3. *Dynamic interfacial tensions for hexane solutions of β- carotene at the interface with water, for different β- carotene concentrations. Curve (1): c_0=6.7 10^{-8} mole cm^{-3}; (2): 1.34 10^{-7} mole cm^{-3}; (3): 3.43 10^{-7} mole cm^{-3}. Full lines calculated with Eq. (22) using constant parameters given in Table 2. Horizontal line indicates σ_e value for each β- carotene concentration.*

From Tables 1 and 2, it is seen that for $\tau \to \infty$, $\Delta\sigma_{01}$ =0. In these cases and for $t \to 0$, Eq. (28) extrapolates to Eq. (26) and again $\sigma \to \sigma_e + \Delta\sigma_{02}$. Therefore, it is evident that the ($\sigma_e + \Delta\sigma_{02}$) values represent the interfacial tensions when the diffusion equilibrium is established, but the interfacial reaction did not start. The reaction rate constant k is nearly concentration independent for each of the two carotenoids. For the adsorption behavior of ethyl ester of β-apo-8'-carotenoic acid, the mean value of k is $\langle k \rangle = 8.2\ 10^{-4} s^{-1}$ (Table 1) and corresponds to a kinetic relaxation timeof $\tau_k = k^{-1} \sim 1.2\ 10^3$s (approx. 20 minutes). For β-carotene, the reaction rate constant k is again nearly independent on concentration and the mean value is $\langle k \rangle = 1.310^{-3} s^{-1}$ (see Table 2) and τ_k~760 s (approx. 13 minutes). The τ_k for the ethyl ester of β-apo-8'-carotenoic acid is higher than its value for β-carotene. This result is in substantial agreement with the molecular structure of these carotenoids and reflects the flexibility of the terminal group of the ethyl ester with possibilities of both the interfacial conformational changes and the polar group hydration against the terminal hydrocarbon β-ionone rigid ring from β-carotene molecule.

Both carotenoid compounds possess the same type of conjugated polyene hydrocarbon moiety, carrying the lateral methyl groups [37]. The β-carotene molecule has a symmetric structure with a long hydrocarbon chain with a terminal β-ionone ring at each end. The ethyl ester of β-apo-8'-carotenoic acid is an asymmetric molecule with a shorter hydrocarbon chain with only one terminal β-ionone ring and at the other extremity with an ethyl ester group.

The *diffusion relaxation time* for β-carotene (Table 2) is higher than its value for ethyl ester of β-apo-8'-carotenoic acid (Table 1) for a comparable carotenoid bulk concentration. This is plausible because the β-carotene molecule is longer than the molecule of ethyl ester of β-apo-8'-carotenoic acid.

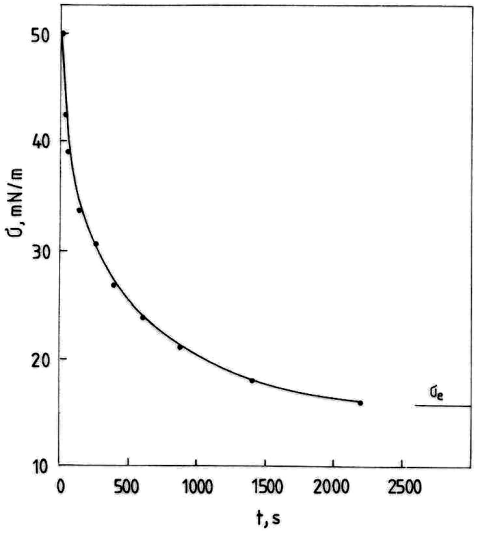

Fig. 4. *Dynamic interfacial tensions for hexane solutions of β- carotene at the interface with water, for the β - carotene bulk concentration c_0=5.99 10^{-7} mole cm^{-3}. Full lines calculated with Eq. (22) using constant parameters given in Table 2.*

Horizontal line indicates σ_e *value.*

Table 1

The parameters for the relaxation kinetics of dynamic interfacial tensions caused by the diffusion adsorption with surface reorientation of the ethyl ester of β-apo- 8'-carotenoic acid from hexane solutions to the hexane/water interface at 25 °C, calculated by Eq. (22).

c_0 mole cm^{-3}	σ_e mN m^{-1}	$\Delta\sigma_{01}$ mN m^{-1}	$\Delta\sigma_{02}$ mN m^{-1}	τ_D s	k s^{-1}	$\sigma_e+\Delta\sigma_{02}$ mN m^{-1}
5.07 10^{-7}	20.0	26	4.0	120	8.9 10^{-4}	24
2.97 10^{-7}	25.3	9	15.7	60	1.1 10^{-3}	41
1.76 10^{-7}	30.0	2	18.0	30	8.0 10^{-4}	48
7.90 10^{-8}	37.0	0	13.0	∞	7.2 10^{-4}	50
3.00 10^{-8}	43.0	0	7.0	∞	6.0 10^{-4}	50

Similar long time effects are also observed for other surfactants, soluble in the oil phase only, *such as*, lauric acid and palmitic acid at the oil/water interface [19]. Due to a few fatty acid concentrations reported it is not possible to evaluate the relaxation times by using our kinetic model. Sometimes, long time effects are also observed for adsorbed surfactants at the air/water interface [20, 21].

Table 2.

The parameters for the relaxation kinetics of the dynamic interfacial tensions generated by the diffusion adsorption of β-carotene from hexane solutions to the hexane/water interface associated with surface reorientation of β-carotene molecules at 25 ^{o}C, calculated by Eq. (22).

c_0 mole cm^{-3}	σ_e mN m^{-1}	$\Delta\sigma_{01}$ mN m^{-1}	$\Delta\sigma_{02}$ mN m^{-1}	τ_D s	K s^{-1}	$\sigma_e+\Delta\sigma_{02}$ mN m^{-1}
$5.99\ 10^{-7}$	15.6	27.0	7.7	450	$1.10\ 10^{-3}$	23.3
$3.43\ 10^{-7}$	22.5	8.6	18.9	160	$1.50\ 10^{-3}$	41.4
$1.34\ 10^{-7}$	33.8	0	16.2	∞	$1.55\ 10^{-3}$	50.0
$6.70\ 10^{-8}$	42.5	0	7.5	∞	$1.10\ 10^{-3}$	50.0

In the foreseen future we intend to deepen the description of the relaxation phenomena in adsorbed films at fluid interfaces and to extend this investigation on a large variety of biosurfactants.

Molecular mechanism of the surface relaxation

Among other factors, the hydrophobic effect [17, 38] seems to have an important role in the relaxation process of the dynamic interfacial tensions due to the adsorption of carotenoid molecules from oil phase at the oil/water interface and due to the molecular reorientation of carotenoids at the interface. It is important to mention that according to the hydrophobic effect, the hydrocarbon chains anchored in aqueous solutions are surrounded with structured water. We further suggest that the interfacial water is also structured around the polar groups (*e.g.*, ethyl ester group in the ethyl ester of β-apo-8'-carotenoic acid) and around the hydrocarbon β-ionone ring (in β-carotene), these moieties being oriented towards the water phase at the hexane/water interface or somehow the molecular chains are penetrating into the aqueous phase [5, 39].

Consequently, the two states of adsorption related to the conformer 1 and conformer 2 give different molecular interfacial areas, which can be evidenced thermodynamically (unpublished results). The molecular area at the initial states of the diffusion equilibrium is almost identical for both carotenoids and corresponds to the value of the cross section area of the hydrocarbon moiety existing in both carotenoid molecules. The cross section area determined by X-ray analysis [37] is around 15 Å^2/molecule and it almost equals the collapse molecular area for β-carotene spread at the air/water interface [39]. This indicates that the carotenoid molecules are vertically orientated in the adsorbed monolayer at the hexane/water interface at the initial states of the diffusion equilibrium.

We also suggest, as an alternative, that the conformation 1 corresponds to the non – hydrated molecules oriented vertically at the hexane/water interface and the conformation 2 corresponds to the carotenoid molecules vertically oriented at the interface having the structured water around their polar groups and around their hydrocarbon extremity anchored in the water phase. It is evident that in the

conformation 2, the carotenoid molecule with its anchoring terminal group in the aqueous phase and with structured water around it, is irreversibly adsorbed at the interface being insoluble in hexane phase or in water phase.

At the final state of the equilibrium of adsorption with surface reorientation probably the predominant molecular species are the hydrated forms of carotenoid molecules vertically oriented at the oil/water interface. It is evident that the mean molecular area of conformation 2 is higher than its value for the conformation 1. Thus, it seems that the carotenoid molecules are initially adsorbed from n-hexane in a very compact film at the interface with water, and then, they relax at the interface into an equilibrium interfacial film having their molecular terminal groups surrounded with structured interfacial water.

This new kinetic model sheds light on the relaxation phenomena of carotenoid films at the oil/water interface and it leads to the *diffusion relaxation times* and the *reaction relaxation times* in substantial agreement with their molecular structure. The understanding of the interfacial behavior may contribute to the design of new carotenoid derivatives with high surface activity that will determine an increased stability of multi-phases systems with a remarkable impact on the designing of new carotenoid delivery systems for therapeutic purposes.

CONCLUSIONS

In this paper, we present a new kinetic approach applied to the dynamic interfacial tensions, which are generated by the adsorption of two carotenoids (*e.g.*, ethyl ester of β-apo-8'-carotenoic acid and β-carotene, all *trans*-isomers) at the oil/ water interface for several carotenoid concentrations in the n-hexane solutions. For these systems it is found that the relaxation of the dynamic interfacial tensions is basically governed by two processes, *namely*, the diffusion process and the interfacial reaction of surfactant re-orientation and hydration.

In the theoretical description of this new kinetic model are included two characteristic relaxation times, *namely,* the relaxation diffusion time and the relaxation reaction time. The relaxation phenomena of the dynamic interfacial tensions are very well described by the new Eq. (22) within the limits of the experimental errors. The two specific relaxation times, *i.e.,* diffusion and surface reaction relaxation times are determined and they are in substantial agreement with the molecular structure of these biosurfactants.

Thus, it seems that the carotenoid molecules are initially adsorbed from hexane phase in a very compact film at the interface with water. Then, they seem to relax at interfaceintoan equilibrium interfacial film having their terminalgroups oriented towards water phase and finally surrounded with structured water molecules. This is also related to the hydrophobic effect or hydrophobic bonds. At the equilibrium, it is plausible that the interaction of carotenoid molecules with the interfacial water molecules leads to an expended interfacial lattice in adsorbed films at the hexane/water interface.

REFERENCES

1. M. Tomoaia-Cotisel and P. J. Quinn, in: P.J. Quinn and V. E. Kagan (Eds.), Subcellular Biochemistry, Volume 30: Fat-Soluble Vitamins, Chapter 10, Plenum Press, New York, 1998, pp. 219- 242
2. S. Adhikari, S. Kapoor, S. Chattopadhyay and T. Mukherjee, *Biophys. Chem*., **88**, 111–117 (2000)
3. N. I. Krinsky and K.-J. Yeum, *Biochem. Biophys. Res. Commun.,* **305**, 754 – 760 (2003)
4. T. A. Konovalova, Y. Gao, L. D. Kispert, J. van Tol and L.-C. Brunel, *J. Phys. Chem. B*, **107,** 1006 - 1011 (2003)
5. J. Zsako, E. Chifu and M. Tomoaia-Cotisel, *Gazz. Chim. Ital*., **109**, 663-668. (1979)
6. M. Tomoaia-Cotisel, J. Zsako, E. Chifu and P. J. Quinn,*Biochem. J.,* **248**,877 – 882. (1987)
7. J. Zsako, M. Tomoaia-Cotisel and E. Chifu, *J. Colloid Interface Sci*., **146**, 353-362. **(**1991)
8. F. Ravera, M. Ferrari and L. Liggieri, *Adv. Colloid Interface Sci.*, **88,** 129 – 177 (2000)
9. L. Liggieri, F. Ravera and A. Passerone, *Colloids Surfaces A: Physicochem. Eng. Aspects*, **114,** 351 –359 (1996)
10. C. -H. Chang and E. I. Franses, *Colloids Surfaces A: Physicochem. Eng. Aspects,* **100,** 1 - 45 (1995)
11. P. Joos and G. Serrien,*J. Colloid Interface Sci*., **127,** 97- 103, (1989)
12. R. Van den Bogaert and P. Joos, *J. Phys. Chem*., **83,**2244 –2248 (1979)
13. R. S. Hansen*, J. Phys. Chem*., **68,** 2012 –2014 (1964)
14. R. S. Hansen, *J. Phys. Chem*., **64,**637-641 (1960)
15. M. Tomoaia-Cotisel andD. A. Cadenhead,*Langmuir*, **7,** 964 – 974 (1991)
16. M. Tomoaia-Cotisel,*Progr. Colloid Polym. Sci.,* **83,** 155-166 (1990)
17. G. Bleys and P. Joos,*, J. Phys. Chem*., **89,** 1027-1032. (1985)
18. V.B.Fainermanan, S.A.Zholob, R.Miller and P.Joos, *Colloids Surfaces A: Physicochem. Eng. Aspects,* **143,**243-249 (1998)
19. J. Van Hunsel, G. Bleys and P. Joos, *J. Colloid Interface Sci.*, **114** ,432 –441 (1986)
20. G. Serrien and P. Joos, *J. Colloid Interface Sci.,* **139,**149 – 159 (1990)
21. P. Joos, J. P. Fang and G. Serrien, *J. Colloid Interface Sci*., **151,** 144 – 149 (1992)
22. F. Ravera, L. Liggieri and A. Steinchen,*J. Colloid Interface Sci*., **156,** 109 –116 (1993)
23. J. Van Hunsel and P. Joos, *Langmuir,* **3**, 1069 – 1074. (1987)
24. V. B. Fainerman and R. Miller, *J. Phys. Chem. B*, **104,** 8471-8476, (2000)
25. M. Tomoaia-Cotisel and I. W. Levin, *J. Phys. Chem. B,***101,** 8477-8485 (1997)
26. C. J. Beverung, C. J. Radke and H. W. Blanch, *Biophys. Chem*., **81,** 59 – 80 (1999)
27. R. Miller, E. V. Aksenenko, L. Liggieri, F. Ravera, M. Ferrari and V.B. Fainerman, *Langmuir*, **15,** 1328 – 1336 (1999)
28. V. B. Fainerman, S. A. Zholob, E. H. Lucassen-Reynders and R. Miller, *J.ColloidInterface Sci*., **261,** 180 – 183 (2003)

29. M. Tomoaia-Cotisel, J. Zsako, E. Chifu and D.A. Cadenhead, *Langmuir,* **6,**191 –197 (1990)
30. S. -Y. Lin, K. McKeigue and C. Maldarelli,*Langmuir,* **10,** 3442 – 3448 (1994)
31. V. B. Fainerman andR. Miller,*Langmui*r, **12,** 6011 –6014 (1996)
32. P. Joos and P. Petrov, *Colloids Surfaces A: Physicochem. Eng.Aspects*, **143,** 273 – 282 (1998)
33. K. D. Danov, D. S. Valkovska and P. A. Kralchevsky, *J. Colloid Interface Sci.*, **251,** 18-25 (2002)
34. J.-P. Fang, K.-D. Wantke and K. Lunkenheimer, *J. Phys. Chem*., **99,** 4632-4638 (1995)
35. E. Chifu, J. Zsakó and M. Tomoaia-Cotisel, *J. Colloid Interface Sci*., **95,** 346-354 (1983)
36. J. Wang and J. McGuire, *J. Colloid Interface Sci.,* **185,** 317 – 323 (1997)
37. O. Isler, *Carotenoids*, Birkhauser Verlag, Basel, 1971
38. C.Tanford, *The Hydrophobic Effect: Formation of Micelles and Biological Membranes*, Wiley, New York, 1973.
39. R. M. Leblanc and B. H. Orger, *Biochim. Biophys. Acta*, **275,** 102-104 (1972)

STUDIA UNIVERSITATIS BABEŞ-BOLYAI, CHEMIA, XLIX, 1, 2004

FLAME ATOMIC EMISSION QUANTIFICATION OF LITHIUM IN NATURAL WATERS USING THE METHANE–AIR FLAME AS AN ALTERNATIVE EXCITATION SOURCE

LADISLAU KÉKEDY-NAGY

Universitatea "Babeş-Bolyai" Facultatea de Chimie şi Inginerie Chimică
400028 Cluj-Napoca, Arany J. 11, România, e-mail: lkekedy@chem.ubbcluj.ro

ABSTRACT. The lithium content of some natural waters has been determined by flame atomic emission spectroscopy using the methane-air flame. It was studied the effect of Na, K, Rb, Cs, Mg, Ca, Sr and Ba on the emission of lithium in the conditions of earlier optimized flame and instrumental parameters. The lithium content of some mineral -, well - and seawaters has been quantified using the standard calibration and the standard addition method. The results agree between these two methods.

INTRODUCTION

Lithium is a physiologically important trace element for human, animal and plant life. It is the 27th in the rank of the element-abundance in the Earth crust, the mean Li-content of the soils being of 32 mg kg^{-1}, that of surface waters of tens of μg L^{-1}, respectively [1]. The peat, moorland and alluvial soils have low lithium content, whereas the calcareous soils as well as the soils in contact with high-salinity mineralized waters could contain with one order of magnitude higher quantities of Li, exhibiting phytotoxic effects. Lithium has a large mobility in the environment being retained by soils and by biosorption, primarily by plants (the mean Li-content of plants being between 20 – 200 mg kg^{-1}, species dependent). Usually, for most plant-species there is a direct relationship between the soil and the built in Li-content [2]. For human and animal life lithium is considered at present as an essential element, with multiple physiological effects: the lithium deficiency can cause for domestic animals and pets loss of gain in weight, increase of juvenile and dam mortality, decrease of milk production of goats [3]. These symptoms can occur for the humans too. In human medicine Li-salts are used in the therapy of psychic depression, its overdoses can produce different side effects, as: decrease of insulin and zinc [4], the vanadium and manganese [5] concentration in the blood plasma with the increase of the aluminum content in the same time, renal insufficiency [6]. The daily human lithium intake is attained with vegetables, diary products and drinking water. The knowledge of lithium content of different natural waters is important regarding to health protection aspect as well as to hydro-geochemical one concerning his origin.

Flame atomic emission spectrometry (FAES) is the standard method for the quantification of lithium in natural waters of different origin [7, 8, 9 and 10]. As excitation sources the use of C_2H_2-air, propane-butane-air (PB-A) flames are recommended, the optimal flame, instrumental and experimental conditions for the

quantification of lithium in waters are well known. The methane-air flame (M-A) has similar properties with the PB-A and natural gas-air (NG-A) flames, exhibiting lower temperature and burning velocity than the C_2H_2 ones. To our best knowledge the quantification of lithium in natural waters using the M-A flame was not reported. The aim of this work is to study the effect of different elements, existing in waters (as possible interferents) on the emission of lithium in the M-A flame and the quantification of lithium in natural waters of different origin, respectively.

EXPERIMENTAL

INSTRUMENTATION

The instrumental setup and operation conditions were the same as described earlier [11].

REAGENTS

Stock standard solutions of 1000 mg L^{-1} were prepared by dissolving the appropriate amounts of metals (Mg (Specpure, Johson Matthey Chemicals Limited, England)) and compounds (Li_2CO_3, $CaCO_3$, $SrCO_3$ (Specpure, Johnson Matthey Chemicals Limited, England) in corresponding acid. KCl, NaCl (analytical grade, Reactivul, Bucureşti, Romania), CsCl, RbCl (used as ionization suppressors), HCl (analytical grade, Merck, Darmstadt, Germany)) were dissolved and diluted with double distilled water, respectively. For further dilutions double distilled water was used in all cases. The diluted solutions were prepared just before measurements. The natural water samples of 350 ml were conserved with 1 ml of conc. HCl (analytical grade, Merck, Darmstadt, Germany).

SAMPLING AND SAMPLE HANDLING

The well water samples were collected in village Săvădisla (county Cluj), located 24 km far north-west from Cluj-Napoca city. The sea water sample arose from the Black Sea coast, Constanța zone. All waters were sampled and handled in accordance with the EPA-recommendations [7]. The mineral waters (commercial available, "Izvorul Minunilor", "Anavie", "Borsec", "Perla Harghitei", "Bona Aqua") were analyzed after the sealed bottles were opened and degassed by shaking and acidified with 2 ml of conc. HCl (analytical grade, Merck, Darmstadt, Germany). The determinations were carried out within 72 hours after sampling, the water samples were diluted properly before measurements.

PROCEDURE

The determinations have been carried out in the M-A flame at μ = 670.78 nm, at observation height over the burner head of 7 mm in fuel rich conditions, established earlier [12]. Six replicate measurements were made in each case. The mean, the standard deviation were calculated, it was tested the homogeneity of the means (at a significance level of 0.05) too [13,14]. The burner was held parallel to the optical axis of the spectrophotometer. The slit width of the monochromator was of 0.1 mm, the sensitivity of the strip chart recorder was different, considering the size of the measured signal intensity. For a given set of determinations the sensitivity was kept constant.

RESULTS AND DISCUSSION

First the effect of Na, K, Mg, Ca, Sr and Ba on the emission signal of lithium of 1 mg L^{-1} was investigated, till to five hundred-fold concentration excesses, as possible inorganic interferents in the samples. The effect of Rb, Cs was tested too, as ionization suppressors. The analytical signal, intensity (I, in a.u.), was measured at 670.78 nm and the background intensity (in the presence of interferent), at the base of the atomic emission, at 672 nm. The variation of the emission signal of lithium versus the concentration of the interferents is represented in Fig. 1 (The experimental data series for different elements are slightly shifted for better visibility).

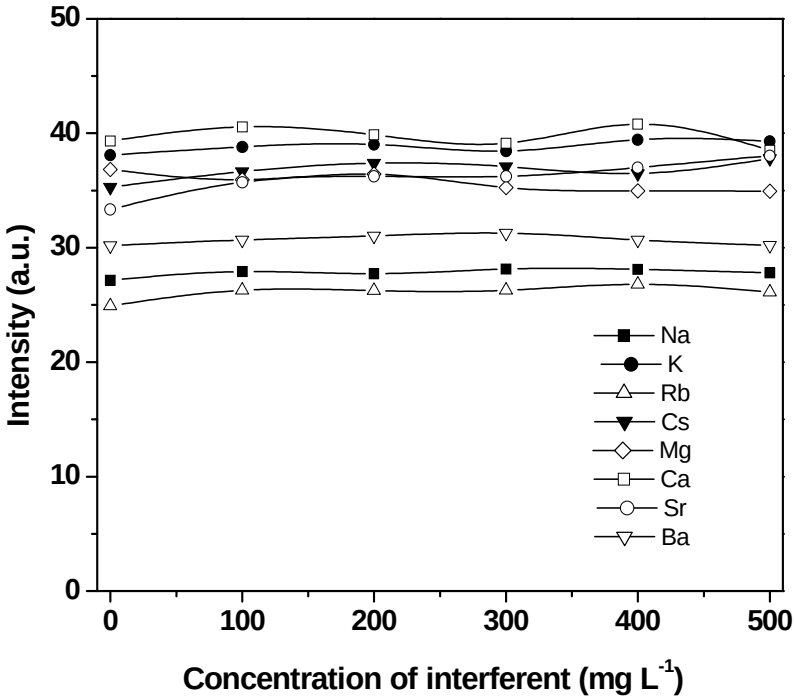

Fig. 1. *Influence of Na, K, Rb, Cs, Mg, Ca, Sr and Ba on the emission of lithium of 1 mg L^{-1}*

As expected, Rb, Cs acts as ionization suppressors due to slight ionization of lithium in the M-A flame. Sr and Ca enhances the analyte signal too, acting as releasing agent by binding the free OH radicals of the flame and hindering the formation of the low stability LiOH. Sr increases the flame background emission too by superimposing the SrOH molecular band over the flame spectrum. Na and Ba have no influence. Mg decreases gradually the lithium emission signal.

QUANTIFICATION OF LITHIUM IN WATER SAMPLES

The standard calibration and the standard addition method were carried out for the lithium quantification in natural waters, the later being used as reference one (absence of certified reference material) for validation. The determinations were performed with optimal instrumental parameters. Four parallel measurements (n=4) were made everywhere. To minimise the effect of the interferences the samples were diluted 1:1 before measurements. The linear regression calibration curve was established using six standards in the 0,1 – 1 μg L^{-1} concentration domain (I = 1.7037 + 45.647C and r^2 = 0.998). In case of standard addition method 100 μL of concentrated lithium standard was added (three additions in 1-mg L^{-1} concentration steps) to the 25 ml of diluted sample. The analyte content was determined from the intercept of the regression line. Comparing the calibration curves, the slope of calibration curves corresponding to the standard additions are close to that obtained by calibration, which suggests the absence of any interference. The results of the two methods (Table 1) agree within the error of determinations for the given water (except of mineral water "Borsec"), so the calibration method could be used for lithium quantification.

Table 1

Results of analysis of water samples (n = 4)

Sample		Concentration (μg L^{-1}, calibration)	Concentration (μg L^{-1}, standard addition)
Sea water		78 ± 6.6	76 ± 10.1
Mineral water	"Anavie"	636 ± 27	620 ± 45
	"Bona Aqua"	6.2 ± 3.8	8.1 ± 4.2
	"Izvorul Minunilor"	5.6 ± 3.8	6.1 ± 4.2
	"Perla Harghitei"	185 ± 7.6	164 ± 12.6
	"Borsec"	256 ± 6.6	218 ± 14.4
Well water	Nr. 1	60 ± 3.8	63 ± 4.2
	Nr. 2	43 ± 3.8	43 ± 4.2
	Nr. 3	82 ± 3.8	93 ± 4.2
	Nr. 4	60 ± 3.8	58 ± 4.2
	Nr. 5	54 ± 3.8	50 ± 4.2
	Nr.6	35 ± 3.8	32 ± 4.2
	Nr.7	13 ± 3.8	13 ± 4.2
	Nr.8	13 ± 3.8	13 ± 4.2
	Nr.9	15 ± 4.1	15 ± 4.2

The Li content of the seawater obtained with both methods is very close to each other although it exhibits high salinity, the highest of all waters studied. The mineral waters "Anavie", "Perla Harghitei" and "Borsec" have high lithium content suggesting (among the other dissolved alkaline- and earth metal ions) a deep groundwater origin, while "Bona Aqua" and "Izvorul Minunilor" could be considered mostly as surface spring waters. The well waters (samples Nr.1 – Nr.5) collected from the center area of the village has significantly higher Li-concentration as those ones collected from the side area (samples Nr.6 – Nr.9). This suggests the different origin of the ground waters feeding the wells and dissimilar geochemical composition of the rocks through the ground waters flow.

In conclusion we can consider that both methods give acceptable results, the lithium content of sea-, mineral- and well waters can be quantified with acceptable precision using atomic emission spectrometry with the M-A flame and the standard calibration. For the corroboration of the results the standard addition method is recommended.

CONCLUSIONS

Lithium exhibits slight ionization in the M-A flame, the phenomenon could be overcome by use Rb, Cs or K in 200 mg L^{-1} concentration, adding to the sample. The Ca and Sr salts act as releasing agents, increasing the emission of lithium, while Mg exhibits adverse effect. The lithium content of sea-, mineral- and well waters can be determined precisely with the standard calibration or the standard addition method. The former method is faster and easier, but for the corroboration of the results the standard addition method is recommended.

REFERENCES

[1] M. Anke, L.Angelow, *Proc. VI. Internat. Tr.El.Symp.*, (Ed.I.Pais), Budapest, (1994)

[2] Szentmihányi, S., et al., *Proc.I. Internat. Tr., El.Symp.,* (Ed. I. Pais), Budapest, (1985), 173

[3] M. Anke, et al, *Proc.IV. Internat. Tr., El.Symp.,* (Ed. M. Anke at al), Jena (1983), 58-65

[4] A. Seven, et al., *Med.Sci.Res.*, 1993, **21**, 279

[5] G.N. Schrauzer, et al., *Biol.Tr.El.Res.,* 1992, **34**, 161

[6] P. Plenge., *Li-Symp*, Jena (1983), 343

[7] *Standard Methods for examination of water and wastewater*, 17th Edition, Ed. L.S.Clesceri, A.E.Greenberg, , R.R Trussel, 1-30, 1989 APHA – AWWA – WPCF

[8] H. Huang, Y. Liu,, *Spectrochim Acta, Part B*, 1984, **39B**, 493

[9] G. Schwedt, *LaborPraxis*, 1990, **14**, 620

[10] Y. Ozdemir, A.E. Karagozler, S. Gucer, *J.Anal.At.Spectrom*., 1994, **9**, 797

[11] L. Kékedy-Nagy, E.A. Cordoş, *Talanta*, 2000, **52**, 645

[12] L. Kékedy-Nagy, E.A. Cordoş, *Rev.Roum.de Chimie*, 1998, **43**, 111-116

[13] C. Liteanu, I. Rîcã, *Statistical Theory and Methodology of Trace Analysis,* John Wiley, New York, 1980.

[14] D.L. Massart, B.G.M. Vandeginste, S.N. Deming, Y. Michotte, L. Kaufman, *Chemometrics: a textbook,* Elsevier, New York, 1988.

STUDIA UNIVERSITATIS BABEŞ-BOLYAI, CHEMIA, XLIX, 1, 2004

KINETICS OF THIOLACTIC ACID OXIDATION BY DECAVANADATE AND VO_2^+ IN ACIDIC MEDIA

DANA-MARIA SABOU and IOAN BÂLDEA

Department of Physical Chemistry, Faculty of Chemistry and Chemical Engineering, 'Babeş-Bolyai" University of Cluj-Napoca, 11 Arany Janos Str., Cluj-Napoca, 400028 Romania. E-mail: dsabou@chem.ubbcluj.ro

ABSTRACT. The oxidation of thiolactic acid by decavanadate and VO_2^+ in aqueous acidic media, using perchloric acid, has been followed spectrophotometrically. A first-order dependence on decavanadate has been found for both the hydrolysis and the oxidation process as well as a first-order dependence on the substrate. The activation energy has been obtained. The oxidation by VO_2^+ under the conditions of comparable concentration with the substrate, has been approached by a stopped-flow technique. The reaction obeys an 1.5 order dependence on VO_2^+ ion, first-order in thiolactic acid and a complex (negative order) dependence on hydrogen ion concentration. The V(IV) intermediate valence state has been identified by ESR spectroscopy. Some suggestions on the mechanism were put on.

Keywords*:* decavanadate, thiolactic acid, kinetics, oxidation

INTRODUCTION

In acidic medium, V(V) plays a role of an oxidizing agent relative to numerous inorganic or organic substances, and its ultimate valence state is V(III). Oxidation studies have been carried out on various compounds such as formic and malonic acids[1] glycollic acid[2], oxalic acid[3], mandelic acid[4], tartaric acid[5] and pinacol[6]. The oxidation of thiomalic acid (2-mercaptosuccinic acid)[7] has been approached using fast reaction techniques. In these oxidation reactions the mechanism postulated has involved the formation of a transient complex between the vanadium(V) and the organic substrate. No physical evidence for such complex was presented, with the exception of thiomalic acid oxidation where the spectrum of a purplish-brown colored intermediate has been recorded.

The difficulties arising in the oxidation with V(V) consist of the existence of numerous hydrolytic and acid-base equilibria involving this valence state, strongly depending on the solution pH, total V(V) concentration and ionic strength.

Monomeric species $VO_4^{3-}, HVO_4^{2-}, H_2VO_4^-, H_3VO_4$, and VO_2^+ or isopoly-vanadates $V_2O_7^{2-}, V_3O_9^{3-}, V_4O_{12}^{4-}, V_{10}O_{28}^{6-}, HV_{10}O_{28}^{5-}, H_2V_{10}O_{28}^{4-}$ are involved[8-14]. The decomposition and dissociation of decavanadate have been studied by spectrophotometrical means in basic[15,16], neutral and weakly basic[17] or acidic solutions[18-20], even from the kinetic point of view.

The purpose of this paper is to study the oxidation of thiolactic acid within the conditions where the main species is dacavanadate and/or vanadyl ion respectively and search for some reaction intermediates.

EXPERIMENTAL

The chemicals used in this study were of reagent grade purity, purchased from commercial sources (Reanal Budapest, Merck, Fluka and Aldrich) and employed without further purification.

The preparation of the decavanadate stock solution has been made in the following manner: 0.0117 g of NH_4VO_3 were weighted and introduced to a 50 mL volumetric flask. It was dissolved into 10 mL NaOH 0.1 mol/L. Perchloric acid 0.24 mol/L was added to neutralize the solution and get to a pH value around 5.5, when made up to the mark. This solution contains $HV_{10}O_{28}^{5-}$ ion[10] in a concentration of $2x10^{-3}$ mol/L, expressed in monomer. The solution has an intense yellow colour and is stable up to 3 hr. The solution stability has been checked, by recording the UV/VIS spectra.

A similar procedure has been followed to prepare the VO_2^+ solution, but adding enough $HClO_4$ until a pH value in the range of 1.5 – 1.7 was reached. The solutions were used after the accomplishment of hydrolysis (1-2 hrs), when they become stable.

Thiolactic solution was prepared from a concentrated one of this acid and standardized by acid-base titration. It has been freshly prepared before each set of runs and used within a period of at most 3 hr.

Stock solution of $HClO_4$ 0.24 mol/L was obtained by dilution of a concentrated perchloric acid 70% (density 1.664 g/mL) and standardized by acid-base titration. $NaClO_4$ solution used for the adjustment of ionic strength was prepared from crystalline $NaClO_4 \cdot H_2O$ and standardized by acid-base titration after passing a known volume through a column with Vionit ionic resin in H-form.

Classic spectrophotometry was employed when the oxidant was $HV_{10}O_{28}^{5-}$. Kinetic measurements were performed, always under the conditions of pseudo-first-order using substrate excess, by means of an ABLE JASCO V-530 spectrophotometer, provided with a temperature jacket surrounding the cell holder. The cuvette jacket was connected to a LAUDA M-20 recirculatory water bath. Reaction mixtures were prepared directly in the quartz cell of the spectrophotometer with 5 cm path length. A rapid injecting of a measured amount of oxidant solution over the reaction mixture containing $HClO_4$, $NaClO_4$, and thiolactic acid in de-ionized tetra-distilled water at desired concentration started the reaction.

Either $HV_{10}O_{28}^{5-}$ or VO_2^+ exhibits an absorption peak around 280 nm, the first having a larger molar absorptivity. To avoid interference of thiolactic acid absorbing in the same range of spectrum at the concentration around 50 fold excess, the reaction was monitored at 340 nm.

When VO_2^+ was the oxidant, stopped-flow measurements were performed with a custom built multi-channel apparatus with photomultiplier detection. They used comparable concentrations of VO_2^+ and thiolactic acid, but excess of H^+.

To search for paramagnetic intermediate species, some ESR measurements were performed on a JEOL X-band type PE-3X ESR spectrometer, connected to 8-inch AEG-magnet at 100 kHz field modulation. Field measurements were achieved by an NMR-Gaussmeter, Drusch MNR-2. The spectrometer was set up with a flow system composed of two solution containers of approximately one liter each, connected to a quartz mixing cell, assuring the mixing of the reactants to occur immediately upon entrance to the microwave resonator.

RESULTS AND DISCUSSIONS

The stoichiometry of the reaction has been considered 2 $CH_3CH(SH)COOH$: 1 V(V), as Pickering and McAuley[7] determined for the oxidation of mercaptosuccinic acid. The products were disulphide and V(III). It was confirmed by an experimental spectrophotometrical titration.

The oxidation by decavanadate. Under the condition of a large excess of thiolactic acid (noted as RSH in the paper) the evolution of absorbance presents an exponential shape. Such a dependence is shown in figure 1. It should be mentioned that, at the acidity employed in the measurements, the acid hydrolysis of decavanadate takes pace along with the oxidation process. This is also shown in figure 1. As seen, the hydrolysis proceeds slower as compared to the oxidation. The acid hydrolysis obeys a first-order dependence on the coloured species (decavanadate) concentration.

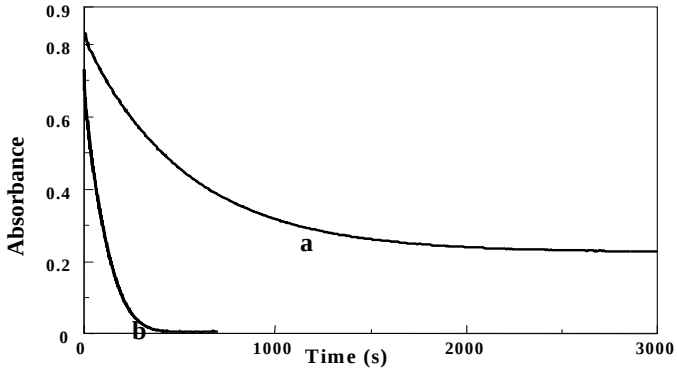

Fig. 1. *Absorbance against time dependence for the acid hydrolysis (curve a) and combined redox + hydrolysis (curve b). Conditions: $[HV_{10}O_{28}^{5-}] = 2.22x10^{-5}$ mol/L, [RSH] = $2.22x10^{-2}$ mol/L, $[HClO_4] = 3.16x10^{-2}$ mol/L, μ = 0.5 mol/L and T = 293 K.*

The semilogarithmic plots

$$\ln(A - A_\infty) = \ln(A_0 - A_\infty) - k^h_{obsd} t \quad (1)$$

were linear to more than 90 % of hydrolysis reaction. A, A_0 and A_∞ stands for absorbance at the time t, at the beginning and at the end of the process respectively, and k^h_{obsd} for the observed first-order rate constant of hydrolysis. It is in agreement with the data obtained by Clare and co-workers[18]. The same type of linear equation has been used for the sum hydrolysis + reduction by RSH process. It should be mentioned that the linear parts of such plots were only for at most 1-1,2 units of natural logarithm (about 40-50 % of reaction). Within this range of V(V) conversion, the correlation coefficients were in the range 0.9966 - 0.9998.

The reason for such a behaviour consists in the higher reactivity towards reduction of the smaller poly-oxovanadates or monomeric forms. Both hydrolysis and redox processes release fragments of higher reactivity, resulting a reaction rate increase. This work shows that the VO_2^+ ion reacts quite fast, requiring a stopped-flow device to monitor the reaction. In the same time this ion does not contribute significantly to the solution absorbance, due to its slow formation by hydrolysis and rapid consumption in redox reaction. By using the early part of the reaction it is to expect that decavanadate species $HV_{10}O_{28}^{5-}$ is the one involved. The fact the V(V) consumption by both hydrolysis and reduction by thiolactic acid proceeds faster that the hydrolysis itself indicates that polymeric vanadates accepts electrons, not only the monomeric V(V) species, generated by hydrolysis. Because the oxidation and hydrolysis take place simultaneously and obey first-order kinetics, one can distinguish them by making the differences between apparent first-order rate constants of the overall process and the hydrolysis one.

$$k_{obsd} = k_{overall} - k^h_{obsd} \quad (2)$$

k_{obsd} represents the first-order rate constant for redox process only. Table 1 contains values of first-order rate constants under several experimental conditions.

As seen from the data presented in Table 1, the acid hydrolysis exhibits a linear dependence on the acidity. The same order has been determined previously by Clare and co-workers[18] at higher H^+ concentrations using nitric acid. Our results, when using $HClO_4$ as the hydrogen ion source, extend the first-order range towards lower acid concentrations.

Concerning the redox process, a first-order dependence on the thiolactic acid concentration has been noted as shown in figure 2a, while the effect of the acidity on the rate is more complex, as depicted in figure 2b.

Table 1

First order rate constants* for overall, hydrolysis and redox processes at various excesses of thiolactic acid and various perchloric acid concentration at ionic strength μ = 0.5 mol/L and T = 293 K, when $[HV_{10}O_{28}^{5-}] = 2.22 \times 10^{-5}$ mol/L.

$10^2[HClO_4]$ mol/L	10^2[RSH] mol/L	$10^3 k_{overall}$ (s^{-1})	$10^3 k^h_{obsd}$ (s^{-1})	$10^3 k_{obsd}$ (s^{-1})
1.00	-	-	0.475	-
1.59	-	-	0.854	-
2.51	-	-	1.42	-
3.16	-	-	1.80	-
5.01	-	-	3.06	-
7.94	-	-	5.04	-
10.00	-	-	6.63	-
1.59	2.22	12.23		11.38
2.51	2.22	8.55		7.13
3.16	2.22	7.96		6.16
5.01	2.22	6.50		3.44
7.94	2.22	7.70		2.66
10.00	2.22	9.17		2.54
3.16	0.556	2.80		0.997
3.16	1.11	4.43		2.63
3.16	3.33	12.23		10.42
3.16	4.44	14.83		13.02
3.16	5.56	18.28		16.47

* The values in the table are means of at least 3 to 4 kinetic runs.

The equation of the line at constant acidity is:

$$k_{obsd} = -(0.0007 \pm 0.0003) + (0.312 \pm 0.009)[RSH] \quad (3)$$

confirming first-order dependence on RSH. The fig. 2b indicates a negative (–1) order with respect to hydrogen ion concentration. A plot of $1/k_{obsd}$ is quite linear. Therefore, the real rate constant (s^{-1}) can be computed as $k_{obsd}[H+]/[RSH]$. If some intermediate complex V-thiolactic acid is involved, through a V-S bond, as proved by McAuley[7], then the thiol function is involved and it should be acid dissociated before bonding or simultaneously with bonding, which is in accordance with a negative order on H^+.

Further experiments are needed to suggest a well argued reaction mechanism. It is obvious that some consecutive one-equivalent electron transfer steps are involved. The mixture change its colour to a pale-blue one, characteristic to V(IV) compounds. As presented in this paper, V(IV) has been identified by ESR studies.

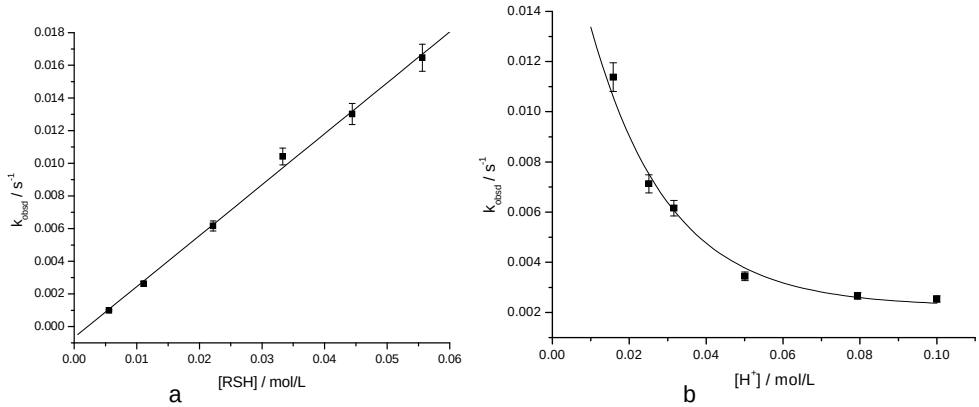

Fig. 2. *The effect of thiolactic acid (a), ([H^+]= 3.16x10^{-2} mol/L) and H^+ (b) ([RSH] = 2.22x10^{-2} mol/L) on the reaction rate at T = 293 K.*

An attempt to determine activation parameters has also been made. Measurements at three different temperatures (293, 303 and 313 K) have been carried out, studying both the hydrolysis and the redox processes, when the experimental activation energies E_a^h = 61.0 kJ/mol and respectively E_a^{redox} = 34.0 kJ/mol for the two reactions have been computed. Even if few, these measurements are quite reliable, as the value obtained for E_a^h is similar to the one given by Clare at al[18] in nitric acid (75 kJ/mol) and other pH range (other prevalent equilibria).

Oxidation by VO_2^+. Oscillograph traces, obtained by means of a stopped-flow device, showing the disappearance of VO_2^+ ion, were recorded under various concentration of VO_2^+, RSH and H^+, the last in the concentration range where vanadium VO_2^+ was the predominant species. The reaction has accomplished within 1- 1.5 seconds.

Reaction orders were determined combining the isolation and the initial rate methods, by varying one after the other the concentration of one reactant while keeping the concentration of the other constant, as well as solution pH (1.5) and ionic strength (0.1 mol/L). By calculation of the initial reaction rate, the reaction order with respect to the species whose concentration was varied, has been determined from the classic double logarithmic plot. Such plots are exemplified in figure 3, for the two main reactants.

For VO_2^+ concentration ranging from 5x10^{-4} mol/L to 3.5x10^{-3} mol/L at constant concentration of thiolactic acid (1.13x10^{-2} mol/L) the method leads to an order of 1.5. Analogously a first-order dependence was found for thiolactic acid (2.5x10^{-3} - 2.25x10^{-2} mol/L) at constant concentration of VO_2^+ (2.5x10^{-3} mol/L).

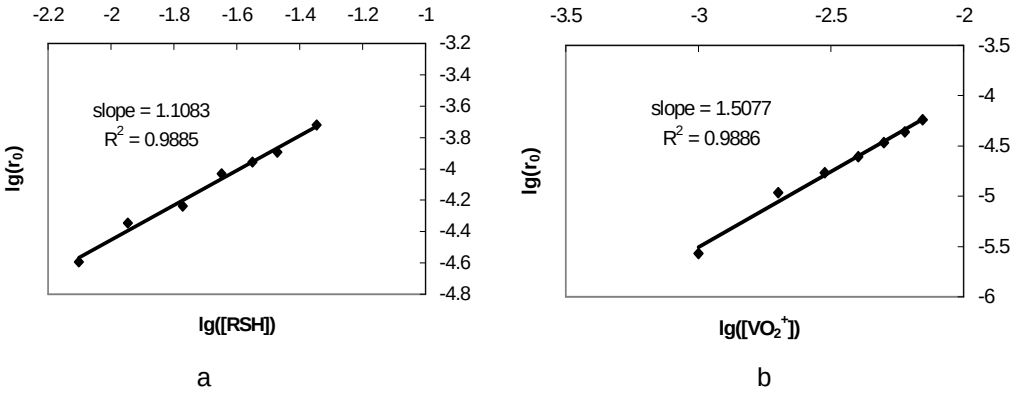

Fig. 3. *Double logarithmic plots giving the reaction orders on RSH (a) and VO_2^+ (b).*

Investigating the effect of H^+ upon the reaction rate proved more troublesome, which owes to the very narrow range of pH's usable in the investigations: 1.5-1.7. This limitation has two causes, the lower limit being that the construction of the stopped-flow apparatus does not allow for more acidic solutions, while the incomplete hydrolysis of the polymeric structure of the oxovanadate compound at higher pH's provided the upper limit. Nevertheless a clear trend towards decreasing rates with increasing pH was seen, allowing to estimate the reaction order on H^+ as being -1. The value is the same as in the case of decavanadate oxidation.

The influence of the ionic strength of the solution upon the reaction was also investigated, using constant concentrations of the reactants at pH 1.5, while varying ionic strength between 0.1 and 1 mol/L. It was found that the redox process suffers no effect of the ionic strength at pH 1.5, as the classical plot lg k_{obs} versus $\mu^{1/2}$ shows no trend.

It should be mentioned, at this point, that the information so far achieved was found not satisfactory to describe the full mechanism of the reaction. That is because one or more further steps are known from the presence of some intermediates, which have been investigated by other means.

ESR investigations on the VO_2^+/thiolactic acid system. The first ESR measurements were performed in continuous flow, when the attempts to identify paramagnetic species in the reaction of VO_2^+ (2.5×10^{-3} mol/L) with thiolactic acid (7.5×10^{-3} mol/L), at pH 1.5 and ionic strength 0.1 showed the presence of free V(IV), in moderate concentrations, at some stage of the reaction. This complies with results reported in literature[22,23]. Figure 4 shows the intensity of ESR signal of V(IV) at different elapsed-time.

The idea of comparing the results with those obtained for the oxidation of thiolactic acid by Cr(VI) urged us to search for organic radicals in the studied reaction[24]. However, no such species could be observed, due to either experimental limitations - such as the incapability of setting a sufficiently slow flow - or to reaction it self – the radical is formed in very low "teady-state" concentrations (has a too short life time).

With identical experimental setup - only differing by the application of stopped-flow in contrast to the previous continuos one - kinetic curves were obtained, directly from the plotter of the spectrometer console. That was achieved by positioning at a constant magnetic field corresponding to that found in the field sweep experiments, and monitoring the evolution of the signal in time (in the units of ”mm per second”). The curves obtained this way were then scanned and digitized, in order to be transferred to simple ASCII format for later use in computer simulations. Good, reproducible kinetic curves were produced, but this part of the study is still in its early stages.

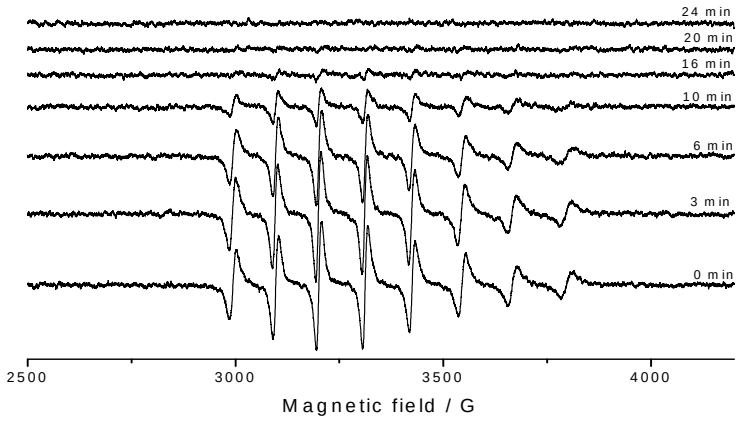

Fig. 4. ESR spectrum of free V(IV) and its evolution in time.

CONCLUSIONS

Although more data are needed to infer a certain and complete reaction scheme, there are several obvious findings as the rate law, the electron transfer with polyoxo-vanadate (before a more reactive monomer is separated), the involvement of V(IV) that reacts not too fast, small or lack of any effect of ionic strength. They argued the supposition that successive and parallel steps are involved: the formation of a 1:1 complex with a S-V bond along with a binuclear 1:2 RSH:V(V) complex, where the substrate is a bridge, the formation of V(IV) in one-equivalent electron transfer that

needs the formation of a thiyl radical, further oxidation by V(IV). The assumption of the binuclear intermediate also finds support in the work of Kiss at al.[25] who concluded that bidentate mercaptocarboxylates were formed COO^--V or S^--V coordinated mono or bis complexes.

On the base of these findings, the following mechanism can be assumed when having VO_2^+ as oxidizing agent:

$$VO_2^+ + RSH \underset{}{\overset{K_{a1}}{\rightleftharpoons}} VO_2 - SR + H^+ \quad (4)$$

$$VO_2 - SR \xrightarrow{k_1} V(IV) + RS\bullet \quad (5)$$

$$2\,VO_2^+ + RSH \overset{K_{a2}}{\rightleftharpoons} VO_2 - SR'COO - VO_2 + 2\,H^+ \quad (6)$$

$$VO_2 - SR'COO - VO_2 \xrightarrow{k_2} V(IV) + RS\bullet \quad (7)$$

$$V(IV) + RSH \xrightarrow{k_3} V(III) + RS\bullet + H^+ \quad (8)$$

$$2\,RS\bullet \xrightarrow{fast} RSSR \quad (9)$$

Further ESR studies will bring information on k_3.

When the oxidant is $HV_{10}O_{28}^{5-}$, a similar mechanism can be assumed. In the first step an adduct is formed, which reacts further to yield V(IV), thiyl free radical and a cluster having one vanadium unit less. Here, the volume of the V(V) species should make difficult the formation of the 1:2 intermediate complex. However, the fact that only first-order in polyoxo-vanadate has been found, does not rule out the binding of the substrate by thiol and carboxylic function to two neighboring VO_4 units in the cluster.

ACKNOWLEDGMENT

The authors would like to thank Prof. Guenter Grampp and Cand. Scient. Kenneth Rasmussen, Institute of Physical and Theoretical Chemistry, Technical University Graz, Austria for providing the stopped-flow and ESR equipment, as well as for their assistance with the ESR measurements.

REFERENCES

1. T. J. K e m p, W. A. W a t e r s, *J. Chem. Soc*., **1964**, 1610.
2. G. V. B a k o r e, R. S h a n k e r, *Can. J. Chem*., **1966**, *44*, 1717.
3. N. C. B h a r g a v a, R. S h a n k e r, G. V.B a k o r e, *Z. Phys.Chem. (Leipzig)*, **1965**, *229*, 238.
4. J. R. J o n e s, W. A. W a t e r s, J. S. L i t t l e r, *J. Chem.Soc.*, **1961**, 630.
5. G. V. B a k o r e, N. C. B h a r g a v a, *Z. Phys. Chem. (Leipzig),* **1966**, *232*, 120.
6. J. S. L i t t l e r, W. A. W a t e r s, *J. Chem. Soc*., **1959**, 1299.
7. W. F. P i c k e r i n g, A. M c A u l e y, *J. Chem. Soc. (A),* **1968**, 1173.
8. G. S c h w a r z e n b a c h, G. G e i e r, *Helv. Chim. Acta*, **1963**, *95*, 8762.
9. O. W. H o w a r t h, R. E. R i c h a r d s, *J.Chem. Soc*., **1965**, 864.
10. M. T. P o p e, B. W. D a l e, *Quart Rev. Chem. Soc*. **1968**, *22*, 527.
11. R. K. M u r m a n n, *J. Am. Chem. Soc*., **1974,** *96*, 7836.
12. S. E. O′ D o n n e l l, M. T. P o p e, *J. Chem. Soc. Dalton Trans*, **1976**, 2290.
13. R. K. M u r m a n n, K. C. G i e s e, *Inorg. Chem*., **1978**, *17*, 1160.
14. M. T. P o p e, "*Heteropoly and Isopoly Oxometalates"*, Springer Verlag, Berlin, Heidelberg, New York, Tokio, **1983**.
15. J. B. G o d d a r t, A. M. G o n a s, *Inorg. Chem*, **1973**, *12*, 587.
16. D. M. D r u s k o v i c h, D. L. Kepert*, J. Chem. Soc. Dalton Trans*, **1975**, 947.
17. F. C a r i g l i a n o, S. D i P a s q u a l e, *J. Chem. Soc. Dalton Trans*, **1978**, 1329.
18. B. W. C l a r e, D. L. K e p e r t, D. W. W a t t s, *J. Chem. Soc. Dalton Trans*, **1973**, 2479.
19. B. W. C l a r e, D. L. K e p e r t, D. W. W a t t s, *J. Chem. Soc. Dalton Trans*, **1973**, 2481.
20. B. V i o s s a t*, Bull. Soc. Chim. France*, **1975,** 1111.

A. M c A u l e y, *Coordin. Chem. Rev*., **1970** *(5)*, 245.

21. E. E. K r i s s, K. B. Y a t s i m i r s k i i, G. T. K u r b a t o v a, A. S. G r i g o r e v a, *Russ J. Inorg. Chem*., **1975**, *20,(1)*, 55.
22. E. E. K r i s s, G. T. K u r b a t o v a, K. B. Y a t s i m i r s k i i, *Russ J. Inorg. Chem*., **1975**, *20*, 59.
23. D.-M. S a b o u, I. B a l d e a, communications at "*The 27th National Conference of Chemistry*", Calimanesti-Caciulata, 23-25 Oct. **2002**; "*11th Physical Chemistry Conference (ROMPHYSCHEM 11)*", Timişoara, 2-5 Sept. **2003**.
24. T. K i s s, P. B u g l y o, G. M i c e r a, A. D e s s i, D. S a n n a, *J. Chem. Soc. Dalton Trans.*, **1993**, *12*, 1849.

STUDIA UNIVERSITAS BABEŞ-BOLYAI, CHEMIA, XLIX, 1, 2004

ELECTROCHEMICAL AND ELECTROGRAVIMETRICAL INVESTIGATION OF ZnS THIN FILM ELECTRODEPOSITION

ADRIAN NICOARA

"Babeş-Bolyai" University, Faculty of Chemistry and Chemical Engineering, 11 Arany Janos, RO-400028 Cluj-Napoca, Romania

ABSTRACT. Electrodeposition mechanism of ZnS thin film from acidic thiosulphate solutions was studied by cyclic voltammetry and electrochemical quartz crystal microbalance. For that, investigation of thiosulphate ions reduction was performed both in presence and in the absence of zinc ions. The formation of the electrodeposited film was confirmed and composition was evaluated by electrogravimetry.

INTRODUCTION

Materials in which charge carrier motion is restricted by physical size, such as quantum dots, quantum wells and multiple quantum wells, possess interesting optical, electronic and transport properties, that have broad technological applications as well as being of fundamental interest. Devices based on these nanomaterials require obtaining of thin films, usually by the means of vacuum deposition techniques (such as molecular beam epitaxy, vapor phase epitaxy or metal-organic chemical vapor deposition). Increasingly, however, electrochemical depositions are attractive alternatives to the vacuum-based methods mainly due to their cost and ability of working at ambient temperature and pressure.

Electrodeposition of semiconductor films is a field which has been driven, to a large extent, by the need for large-area thin films for photovoltaic and photoelectrochemical solar cells [1]. Although not commonly used, ZnS has the advantage of the low toxicity of its components, replacing other toxic compounds as those containing As, Sb, Se, Te or Cd.

The electrochemical quartz crystal microbalace (EQCM) is a powerful, versatile electroanalytical tool which has been used in the study of many semiconductor compounds electrodeposition such as CdSe [2], CdTe [3,4], PbSe [5], PbTe [6], CuSe [7,8] and $CuInS_2$ [9]. The operation of the EQCM is based on the converse piezoelectric effect which means that an oscillating electric field causes a mechanical oscillation in the quartz crystal. The resonant frequency of the mechanical oscillation depends on the mass of the crystal, which allows its use in the determination of very small mass changes. If the deposit is rigid, the change in the resonant frequency, Δf, is proportional to the change in mass of the deposit on the crystal according, Δm, to the Sauerbrey equation (Eq. 2, see below) [10].

For characterizing the electrochemical processes at the electrode surface, the primary Δf vs. potential (E) EQCM data can be treated in different ways. In this paper a straight-to-forward method, based on ΔQ - Δm correlation, was used. Using Faraday's law it is possible to calculate the parametre $\Delta M/n$:

$$\Delta M / n = -F\ \Delta m / \Delta Q \quad (1)$$

where ΔM is the stoechiometric molecular (or atomic) mass variation of the solid phase species involved in reaction, n the number of exchanged electrons, ΔQ the charge consumed by the reaction and F the Faraday constant (96,485.31 C mol^{-1}). The minus sign is a result of used current convention (negative current indicates a cathodic process).

Usually, the $\Delta M/n$ parametre is specific for a given reaction. The theoretical values are listed in the text after each redox reaction. By comparing these values with the experimental found ones, it is possible to identify the reactions taking place at the electrode.

There are more alternatives to electrodeposit ZnS films [11-13]. Beside the codeposition of metallic zinc and elementary sulphur, followed by generation of ZnS by a solid-state chemical reaction, in this paper another alternative is investigated. It involves the precipitation of zinc ions with sulphide (ions or acid) electrogenerated by reduction of thiosulphate. If the experimental conditions ensure total reduction of thiosulphate without reduction of zinc ions to metal, it is possible to obtain a film with an ideal Zn:S stoechiometric ratio.

The elementary equilibriums involved in this procedure of ZnS formation are as follow:

- sequential reduction of thiosulphate ions, at first to elementary sulphur: [3]

$$S_2O_3^{2-} + 6H^+ + 4e^- \Leftrightarrow 2S_{(s)} + 3H_2O \qquad E^o_{S_2O_3^{2-},H^+/S} = +0.47\ V$$

$$\Delta M / n = 16.03\ g\ mol^{-1} \quad (R1)$$

and secondly (at low pH value) to hydrogen sulphide:

$$S_{(s)} + 2H^+ + 2e^- \Leftrightarrow H_2S \qquad E^o_{S,H^+/H_2S} = +0.14\ V$$

$$\Delta M / n = -16.03\ g\ mol^{-1} \quad (R2)$$

or globally:

$$S_2O_3^{2-} + 10H^+ + 8e^- \Leftrightarrow 2H_2S + 3H_2O \quad E^o_{S_2O_3^{2-},H^+/H_2S} = +0.305\ V$$

$$\Delta M / n = 0\ g\ mol^{-1} \quad (R3)$$

It should be mentioned that the electrochemical sulphur formation step (R1) is potentially in competition with a homogenous chemical step, i.e. the decomposition of thiosulphidric acid generated in acidic media:

$$S_2O_3^{2-} + 2H^+ \Leftrightarrow H_2S_2O_3 \Rightarrow S_{(s)} + SO_2 + H_2O \quad (R4)$$

- formation of the ZnS film by precipitation:

$$H_2S + Zn^{2+} \Leftrightarrow ZnS_{(s)} + 2H^+ \qquad P_{s\ ZnS\ (\alpha)} = 1.6\ 10^{-24} \quad (R5)$$

leading to the global reaction:

$$S_2O_3^{2-} + 6H^+ + 2Zn^{2+} + 8e^- \Leftrightarrow 2ZnS_{(s)} + 3H_2O$$

$$E^o_{S_2O_3^{2-},H^+,Zn^{2+}/ZnS} = +0.362V\ ,\ \Delta M / n = 24.36\ g\ mol^{-1} \quad (R6)$$

The presence of the zinc ion can lead also to an undesired reduction to metallic zinc, as follows:

$$Zn^{2+} + 2e^- \Leftrightarrow Zn_{(s)} \qquad E^o_{Zn^{2+}/Zn} = -0.763\ V$$

$$\Delta M / n = 32.69\ g\ mol^{-1} \qquad (R7)$$

In order to stimulate the total reduction of thiosulphate, it must take place on experimental conditions (i.e. concentrations, pH) where the redox potential of (R1) is more positive than this of (R3). As indicated by the values of standard redox potentials, listed after each reaction [14], in standard conditions the total reduction is thermodynamically favoured by a margin of app. 0.17 V. Clearly, high concentration of thiosulphate and low pH value will favor (R1) in the competition with (R3). But these requirements cannot be simultaneously accomplished due to the homogenous reaction (R4), which leads to the obtaining of colloidal (mainly electrochemical inactive) sulphur. Although the presence of zinc ions impede on sulfur formation, a too high concentration would favor its reduction on metallic zinc as well.

In this study were examined some aspects of the ZnS thin film electrodeposition mechanism. Identification of the slow steps of the process and the reaction pathway were among the aims. For that, cyclic voltammetry and electrochemical quartz crystal microbalance were used in order to obtain qualitative and semi-quantitative information.

EXPERIMENTAL

The voltammetric measurements were performed using a Computer controlled (via an AT-MIO-16F-5, National Instruments, USA, data acquisition board) analogical potentiostat (PS3, Meinsberg, Germany). A data acquisition software package (developed in LabVIEW™, National Instruments, USA) ensures multi-channel input, including the frequency measurement via a high-speed digital timer/counter.

A standard three-electrode configuration was employed for the measurements. The reference electrode was a double-junction saturated calomel electrode and the counter electrode was a spiraled Pt wire.

Voltammetric measurements were performed using a Al (refined, 99.5% purity) disk electrode (A=0.032 cm^2), polished prior to use with a 1200 grade emery paper.

Planar AT-cut quartz crystals, with an Au film (A=0.503 cm^2) on a Cr adhesion layer, were used as a working electrode for EQCM measurements. The unpolished crystals were mounted vertically on a Teflon® holder, being operated at the fundamental mode (10 MHz). This EQCM cell (type EQCM-1, made at Department of Physical Chemistry, Eötvös Univesity, Budapest, Hungary) was a gift of Professor G. Inzelt.

All electrochemical measurements were performed at $20 \pm 2\ ^oC$.

The electrolyte used in this study contained 10 mM $Na_2S_2O_3$, desired pH value of 3.2 being adjusted using dilute H_2SO_4 (p.a., Panreac, Spain). When present, the $ZnSO_4$ concentration was 0.15 or 0.5 mM. 0.2 M Na_2SO_4 (p.a. Riedel-de Haen) was used as supporting electrolyte. All the solutions were prepared using bidistillated water.

High purity, with metallic impurities of 10^{-5} % m/m or less, $Na_2S_2O_3$ and $ZnSO_4$ were used as received from Dr. E. -J. Popovici ("Raluca Ripan" Institute of Chemistry, Cluj-Napoca).

The EQCM allows simultaneous measurement of the electrode potential dependence of current and frequency oscillation change, Δf, of the quartz crystal. While integration of the electric current gives the charge consumed, ΔQ, during an electrode process, the quartz oscillation frequency change, Δf, can be correlated with the electrode mass modification, Δm, using Sauerbrey equation:

$$\Delta f = -2\,\Delta m\, f_o^2 / \sqrt{\mu\rho} = -C_S\,\Delta m \qquad (2)$$

where f_o is the fundamental frequency of the crystal, μ the shear modulus (2,947 10^{11} g $cm^{-1}s^{-2}$) and ρ the density (2,648 g/cm^3) of quartz. All the constants of the equation can be included into a single constant (Sauerbrey constant, C_S) which was determined experimentally by copper electrodeposition, from a suplhate acidic bath, assuming ideal faradaic efficiency. A C_S value of 649.7±0.7 Hz μg^{-1} was obtained, in good agreement with the theoretical value of 653.7 Hz μg^{-1}, calculated with Eq. 2. This corresponds to a remarkable sensibility of 1.54 $\mu g\ Hz^{-1}$. As indicated, a mass increase causes a decrease in the resonant frequency and a mass decrease results in a higher frequency.

RESULTS AND DISCUSSION

At the beginning, the case of ZnS electrodeposition on the Al electrode is considered. In order to obtain information about the occurring mechanism, electrodeposition was considered under sweeping potential conditions, cyclic voltammetry being the chosen technique.

Fig. 1 shows the cyclic voltammograms in a solution containing 10 mM $Na_2S_2O_3$ and Na_2SO_4 0.2 M at pH 3.2 recorded with the Al electrode. Since no relevant electrode processes are occurring at higher potentials, the starting potential used here is –1.0 V vs. SCE.

The most important feature of this voltammogram is the presence of a single chemical irreversible reduction peak. This is consistent with the reduction of thiosuplhate ions, leading to formation of sulphur as an intermediate species, only if the sulphur reduction step (R2) occurs easier than its generation (R1). At least thermodynamically, this is in good agreement with the presented standard potentials.

Another experimental evidence of the sulphur formation is the important evolution of the voltammogram shape and parametres during successive scanning. This occurs only if at the electrode interface are taking place important changes, like those generated by the obtaining of sulphur, either as adsorbed or as distinct solid-phase. It can be mentioned that, during successive scanning, the peak definition

increases on initial cycles. After several cycles, however, the definition gradually decreases. For a better illustration of the different effects on the voltamograms, both first and second cycles will be taken into account.

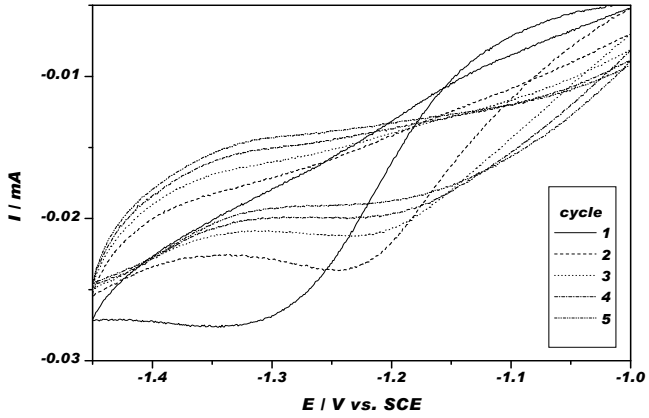

Fig. 1. *Multiple scan cyclic voltammograms recorded during reduction of 10 mM $Na_2S_2O_3$ and 0.2 M Na_2SO_4 at pH 3.2. Al electrode (A=0.032 cm^2). Scan rate: 10 mV s^{-1}.*

The scan rate influence on the voltammetric response can provide further information about investigated process, being presented in Fig. 2. The shift towards negative values of the peak potential, specific for an electrochemical irreversible system, reveals a slow charge transfer. Moreover, since it is indicated that the peak current is roughly proportional with the square root of the scan rate, specific for the systems with soluble reacting species, this peak can be related either to (R1) or (R3), totally excluding (R2).

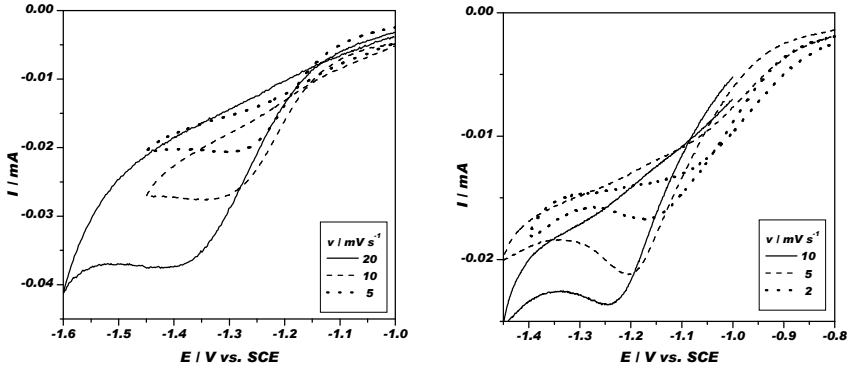

(a) **(b)**

Fig. 2. *Influence of scan rate on the voltammograms obtained during the first (a) or the second (b) scan. Conditions as in Fig. 1.*

Unfortunately, the chemical irreversible nature of occurring peak prevents the obtaining of further thermodynamic or kinetic information. Commonly, the influence of pH on the peak potential (or, better, on the formal standard potential) allows the evaluation of the stoechiometric ratio between the number of exchanged protons and electrons, see for instance [15]. But all three possible reactions have close values of the mentioned stoechiometric ratio, i.e. 1.5, 1 and 1.33, which together with the inaccessibility of the formal standard potential values prevents the identification of the electrode process based on pH influence.

The addition of zinc ions into the electrolyte solution allows not only the obtaining of ZnS films, but also provides supplementary information on the thiosulphate reduction. The common shape of the voltammograms in presence of zinc ions is depicted on Fig. 3.

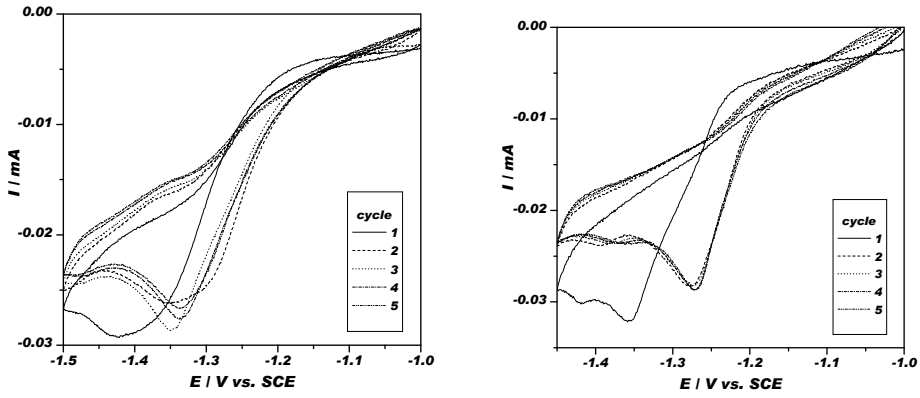

Fig. 3. *Multiple scan cyclic voltammograms recorded during reduction of 10 mM $Na_2S_2O_3$ and 0.2 M Na_2SO_4 at pH 3.2, after 0.15 mM, in (a), or 0.5 mM, in (b), addition of $ZnSO_4$. Al electrode (A=0.032 cm^2). Scan rate: 10 mV s^{-1}.*

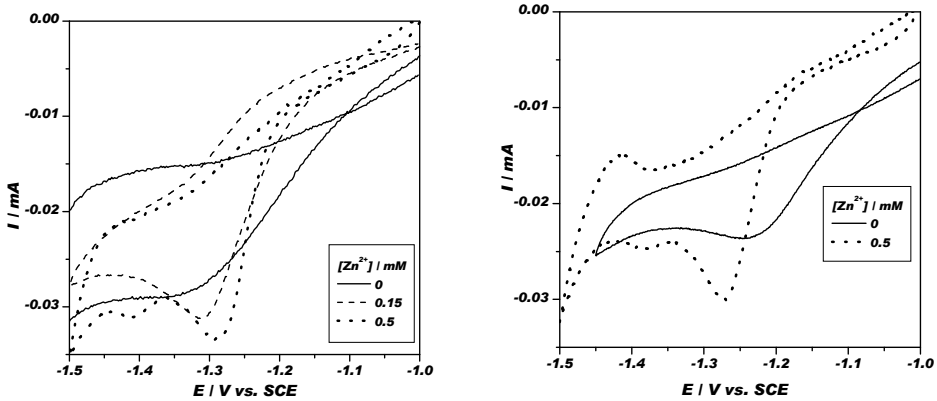

Fig. 4. *Influence of the $ZnSO_4$ concentration on the voltammograms obtained during the second scan. Scan rate 10 mV s^{-1}, in (a), or 20 mV s^{-1}, in (b). Other conditions, as in Fig. 1.*

The most important feature is the presence of a new reduction peak (at ≈ -1.4 V vs. SCE), with the current roughly proportional to the zinc ions concentration. For this reason it was attributed to reaction (R7) leading to metallic zinc. This is in agreement to the calculated equilibrium potential (of ≈ -1.1 V vs. SCE). Furthermore, the enhancement of hydrogen evolution, on very negative potentials, proves also the metallic zinc formation, since on zinc the hydrogen evolution occur slower than on aluminum (e.g., compare Fig. 1 with Fig. 3b) [14]. Another feature is a faster stabilization of the voltammogram during successive scanning. This can be related to the obtaining of an electrochemical inactive (at least for the used potential window) film with both composition and thickness homogeneity.

But, more important, is the effect of zinc ions concentration on the reduction peak of thiosulphate, as presented in Fig. 4. Regardless of scan rate, it can be evidenced an increase of peak intensity and a decrease of peak width while the peak area remains, roughly, constant. Starting from peak current (I_p) and width at half-height (W_p) relations, for an electrochemical irreversible system: [16]

$$I_p = 2.99\,10^5\, n(n_a\alpha)^{1/2} A C^* D^{1/2} v^{1/2} \tag{3}$$

$$W_p = \frac{152}{n_a\alpha} \qquad [mV] \tag{4}$$

some correlation can be established between the electrochemical response and the process chemistry. Here, n is the (total) number of exchanged electrons, n_a the number of electrons involved in the rate determining step, α the transfer coefficient, A the surface, v the scan rate, C^* the concentration and D the diffusion coefficient of the reacting species.

The above mentioned effects of the zinc ions addition can be explained by the increasing of the $n_a\alpha$ term. Very likely, during addition of zinc ions, the increasing of n_a parametre is the direct result of the activation of the slow electron transfer step. In this way, increasing the rate of the slower step up to the rate of other relatively slow elementary steps, the presence of zinc ions enhances the overall process. Since it does not involve additional reactions, the number of exchanged electrons remaining constant, the peak area (quantifying the electric charge involved) must be invariant, as experimentally evidenced. Because zinc ions presence influences only the sulphur reduction (R2), by shifting the equilibrium potential towards positive values caused by the precipitation process (R5), it can be assumed that the slow step is, or is contained by, reaction (R2). This is consistent to discussed single-peak exhibited by the voltammograms, only if kinetics of sulphur formation overcomes the thermodynamical limitations.

Fig. 5 reveals the influence of the scan rate on the voltammogram. Once again, both occurred peaks are electrochemically irreversible, due to the shift of the peak potential. Also, due to the dependence on the peak current it seems that are diffusion controlled as well.

Another parametre with potential relevance to the behaviour of the system is the starting potential. Fig. 6 shows this dependence. If a more positive starting potential was used (i.e. -0.8 V vs. SCE) an additional oxidation peak occurs at ≈ -0.95 V

vs. SCE. Since this peak is not present in the absence of the zinc ions (corresponding voltammogram not presented here), it can be attributed to the oxidation of metallic zinc. Also the complex shape of this peak is common to a metal dissolution process, see for instance [17]. Even if present, the oxidation of ZnS (in fact of the sulphide at some soluble products) is unimportant, since the charge used for reduction largely exceeds that used for oxidation.

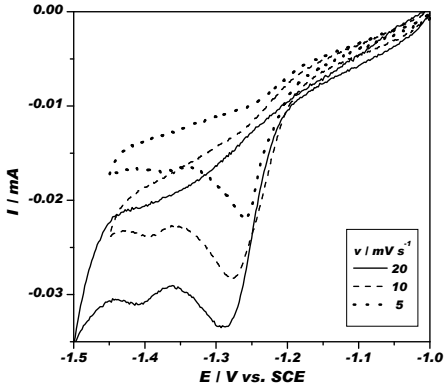

Fig. 5. *Influence of the scan rate on the voltammograms obtained during the second scan. Conditions as in Fig. 3 (b).*

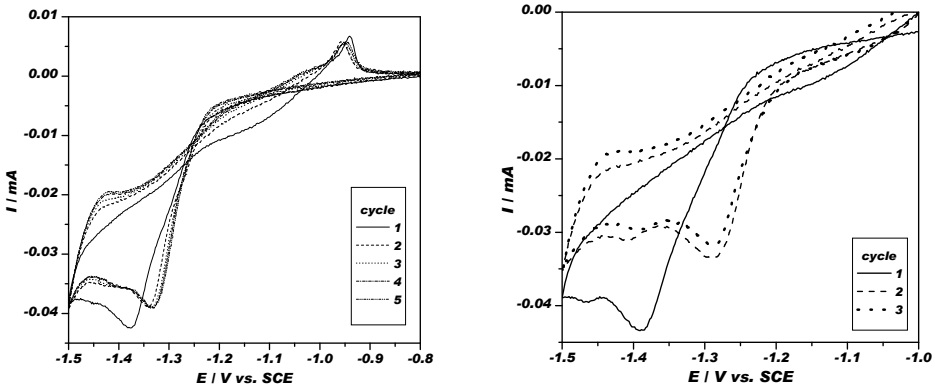

(a) **(b)**

Fig. 6. *Influence of initial potential on the voltammograms obtained during multiple scan. Scan rate: 20 mV s^{-1}. Other conditions, as in Fig. 3 (b).*

Concluding the voltammetric investigation, it was revealed that, for the Al electrode, is possible to electrodeposit ZnS by zinc ions precipitation with sulphide electrochemically-generated from reduction of thiosulphate. Using a potential value in between -1.2 and -1.3 V vs. SCE (for investigated electrolyte solution), the formation of metallic zinc can be avoided. The only difficulty is the generation of sulphur, which potentially can be obtained not only as intermediate in the ZnS formation, but also as the reduction product. Unfortunately, for the investigated system, no evidence about the presence or absence of sulphur incorporation into

the film was possible using cyclic voltammetry. Since it involves important mass changes at the electrode interface, EQCM measurements are much more appropriate for this kind of experiments.

EQCM measurements consist in simultaneous recording of current and mass deposited (via the resonance frequency of the quartz crystal) on the electrode during the potential shift. Thus, the results consist in a couple of representations: the current vs. potential (voltammogram) and mass vs. potential (often called voltamassogram) representations. Although the use of Au instead of Al for the electrode substrate changes somehow the reduction processes, the novel information provided surpasses this inconvenient.

Fig. 7 presents the EQCM measurements of thiosulphate reduction. Some difference can be noted: a small pre-peak wave is present (at ≈ -0.4 V vs. SCE) and the main peak is shifted towards positive potentials. Attempting the identification of occurred processes, the scanned range was divided into several potential windows. For each of these characteristic zones, the used charge (ΔQ) was calculated by integration of current intensity. Aiming the calculation of the $\Delta M/n$ parametre, the deposited mass (Δm) was determined using the voltamassogram. All these electrogravimetric parametres are presented in Tab. 1.

It was found that, during the initial cathodic scan (zone **Ia**), the reduction to sulphur (R1) prevails, since the determined $\Delta M/n$ parametre is close to the theoretic value of 16.03 g mol^{-1}. The lower founded value seems to indicate a slow sulphur desorption, leading to colloidal sulphur formation. At more negative potentials (zone **Ib**), the main reduction takes place. The -0.9 g mol^{-1} value indicates that the main process is the total reduction (R3), with a small contribution of sulphur reduction (R2) or desorption. At lowest potentials (zone **Ic**), in addition to (R3) a mass increasing process is present; it may well be the inclusion of hydrogen into the already deposited sulphur. During the anodic scan, the reduction process (R3) still prevails. Only at the highest potentials (zone **Ie**) the mass decreases; the slow release of the incorporated hydrogen can well be the explanation. After a complete cycle, little changes of the electrode surface can be evidenced.

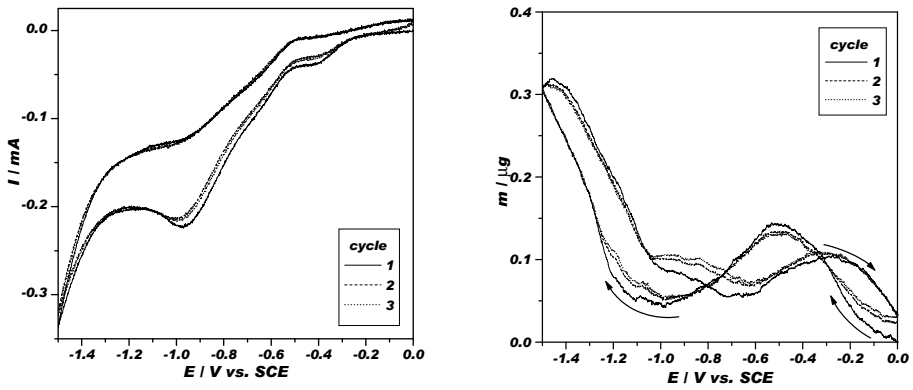

Fig. 7. *EQCM measurements of thiosulphate reduction. Electrolyte: 10 mM $Na_2S_2O_3$ and 0.2 M Na_2SO_4 at pH 3.2. Au electrode (A=0.503 cm^2). Scan rate: 10 mV s^{-1}.*

Table 1

Electrogravimetric parametres for thiosulphate reduction

Zone	Potential window	ΔQ / mC	Δm / μg	ΔM/n / g mol^{-1}
Ia	0 to -0.5 V	-0.91	0.14	15.2
Ib	-0.5 to -1.12 V	-10.33	-0.09	-0.9
Ic	-1.12 to -1.5 V	-9.77	0.26	2.6
Id	-1.5 to -0.5 V	-13.86	-0.25	-1.7
Ie	-0.5 to 0 V	-0.36	-0.03	-8.1

Overall, the total reduction to hydrogen sulphide is the predominant process. This explains the nature of chemical irreversibility of the voltammetric peak. Since the solubility of hydrogen sulphide in acidic media is limited, too small amount are available towards oxidation during anodic scan.

A similar procedure was used for the electrodeposition of ZnS, as it can be seen in Fig. 8 and Tab. 2. While the presence of the zinc ions causes little effects on the voltammograms, a striking difference is evidenced for voltamassograms. Not only that a tenfold mass change is exhibited, but after a complete cycle, the electrode mass has an important increase.

Once more, reduction to sulphur (R1) prevails on initial cathodic scan (zone **IIa**). But the charge used here is small enough (≈ 5%) to conclude that suplhur incorporation into the film cannot exceed 10% (in molar units). Compared to the cited Zn:S stoechiometric ratios, that usually are close to 1:2 [18,19], the described procedure of one-step electrodeposition of ZnS films gives much better results.

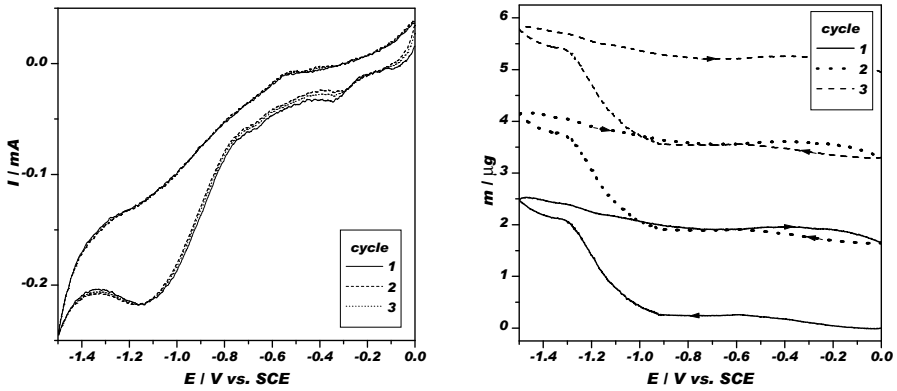

Fig. 8. *EQCM measurements of ZnS electrodeposition. Electrolyte: 10 mM $Na_2S_2O_3$, 0.5 mM $ZnSO_4$ and 0.2 M Na_2SO_4 at pH 3.2. Au electrode (A=0.503 cm^2).Scan rate: 10 mV s^{-1}.*

Table 2

Electrogravimetric parametres for ZnS electrodeposition

Zone	Potential window	ΔQ / mC	Δm / μg	ΔM/n / g mol^{-1}
IIa	0 to -0.6 V	-1.43	0.26	17.2
IIb	-0.6 to -0.9 V	-2.63	0	0
IIc	-0.9 to -1.3 V	-8.73	1.81	18.2
IId	-1.3 to -1.4 V	-2.29	0.47	15.7
IIe	-1.4 to -0.5 V	-15.07	-0.58	-3.7

After a depositless zone **IIb**, where the charge is unimportant, the main electrodeposition process takes place in zone **IIc** and **IId**. The obtained values of determined ΔM/n parametre and the absence of a zinc reduction peak indicate that here the ZnS formation (R6) is the main process. The absence of an oxidation voltammetric peak, accompanied with a mass decrease, also argues the metallic zinc deposition (R7). Zone **IIe** corresponds to a dissolution reduction; this can be explained either by sulphur reduction (R2) or by erosion of the ZnS film.

CONCLUSIONS

One-step electrodeposition of ZnS films from an acidified thiosulphate solution was investigated. The film formation is based on precipitation of zinc ions with sulphide electrogenerated by thiosulphate reduction. In this way, the film can be obtained with a close to ideal Zn:S stoechiometric ratio, which is extremely difficult to obtain with a co-deposition technique.

Cyclic voltammetry and electrochemical quartz crystal microbalance were used in order to obtain information about the electrodeposition mechanism. It was found that, under the investigated experimental conditions, the slow charge transfer step of thiosulphate reduction is, or is contained in, the sulphur reduction. Since sulphur is produced mostly at low overpotentials, a much different transfer coefficient favours the consumption (R2) in comparison to the production (R1) of sulphur.

Based on the unique gravimetric ability of EQCM, an evaluation of film composition is possible. While no evidence of metallic zinc was observed, only limited amounts of sulphur incorporated into the film was detected. A better than 1:1.1 value of Zn:S stoechiometric ratio was therefore estimated.

Acknowledgement. The Romanian Education and Research Ministry supported this work, under grant PNCDI CERES (Contract 28/2002). High purity $Na_2S_2O_3$ and $ZnSO_4$ (purified in the frame of above mentioned grant) were received by courtesy of Dr. Elisabeth-Janne Popovici ("Raluca Ripan" Institute of Chemistry, Cluj-Napoca).

The author would like to thank Professor György Inzelt (Department of Physical Chemistry, Eötvös Univesity, Budapest, Hungary) for his generous donation of the employed EQCM cell.

REFERENCES

1. Partain L.D., *Solar Cells and Their Applications*, John Wiley & Sons, New York, 1995.
2. Wei, C., Bose, C.S.C., Rajeshwar, K., J. Electroanal. Chem., **1992**, 327, 331.
3. Wei, C., Myung, N., Rajeshwar, K., J. Electroanal. Chem., **1993**, 347, 223.
4. Matias, J.G.N., Juliao, J.F., Soares, D.M., Gorestein, A., J. Electroanal. Chem., **1997**, 451, 163.
5. Saloniemi, H. Kemell, M., Ritala, M., Leskela, M., J. Mater. Chem., **2000** 10, 519.
6. Saloniemi, H. Kemell, M., Ritala, M., Leskela, M., J. Electroanal. Chem., **2000**, 482, 139.
7. Kemell, M., Saloniemi, H., Ritala, M., Leskela, M., Electrochim. Acta, **2000** 45, 3737.
8. Marlot, A., Vedel, J., J. Electrochem. Soc., **1999**, 146, 177.
9. Kemell, M., Saloniemi, H., Ritala, M., Leskela, M., J. Electrochem. Soc., **2001**, 148, C110.
10. Buttry, D.A., Ward, M.D., Chem. Rev., **1992**, 92, 1355.
11. Gal, D., Hodes, G., J. Electrochem. Soc., **2000**, 147, 1825.
12. Innocenti, M., Pezzatini, G., Forni, F., Foresti, M.L., J. Electrochem. Soc., **2001**, 148, C357.
13. Gichuhi, A., Boone, B.E., Shannon, C., J. Electroanal. Chem., **2002**, 522, 21.
14. Niac, G., Voiculescu, V., Baldea, I., Preda, M., *Physical Chemical Formulae, Tables and Problems* (in Romanian), Ed. Dacia, Cluj-Napoca, 1984.
15. Nicoara, A., Patrut, A., Margineanu, D., Mueller, A., Electrochem. Commun., **2003**, 5, 511.
16. Bard, A. J., Faulkner, L. R., *Electrochemical Methods: Fundamenatals and Applications*, Wiley, New York, 1980.
17. Macdonald, D.D., *Transients Techniques in Electrochemistry*, Plenum Press, New York, 1977.
18. Nishino, J., Chatani, S., Uotani, Y., Nosaka, Y., J. Electroanal. Chem., **1999**, 473, 217.
19. Fatas, E., Herrasti, P., Arjona, F., Parker, A.J., J. Electrochem. Soc., **1987** 134, 2799.

STUDIA UNIVERSITATIS BABEŞ-BOLYAI, CHEMIA, XLIX, 1, 2004

STUDY OF ANTIOXIDANT CAPACITY OF FLAVONOIDIC COMPOUNDS FROM *TILIA PLATYPHYLLOS* EXTRACT

ANAMARIA HOSU, VASILE MICLĂUŞ, CLAUDIA CIMPOIU and TEODOR HODIŞAN*

Faculty of Chemistry and Chemical Engineering, "Babes-Bolyai" University, 400028 Cluj-Napoca, Romania

ABSTRACT. Identification of compounds from medicinal plants is one of the oldest fields for the application of thin-layer chromatography (TLC). The past few years have seen tremendous growth in the use of herbal medicines worldwide.

The flavonoids are one of the most numerous and important group of natural compounds and they have many biological properties.

This paper is concerning to test the antioxidant capacity of flavonoids from Tilia Platyphyllos by treated the methanolic extract of plant with nitroxidic radical and analyzed of these samples by TLC in situ coupled with UV spectroscopy.

INTRODUCTION

Natural compounds offer without doubt the richest resources of chemical diversity. They can be found not even in medicinal plants. The term medicinal and aromatic plants (MAP) include not only the plants used for medicinal purposes, but also aromatic plants and spices [1]. Interest in research concerning the constituents and biological activities of MAP has significantly increased in recent year [2].

The principal aim of MAP researched development is to produce new or more efficient phytopfarmacons. This can be basically divided into four categories: pulverized MAP in which all the compounds occurring in the plant are presented; raw extracts of the MAP which contain only substances soluble in the extraction solvent used (e.g. aqueous extracts of different plants, tea, are the common raw extracts); purified extracts which occurring as a result of selective purification. They contain only certain types of biologically active compounds. The fourth category – used very often in conventional therapy, but rarely in phytotherapy - is that of isolated active substances, with purity greater than 99%.

Most of these categories are biological complex matrices; therefore planar chromatography is the first choice and, generally, the most useful analytical method in the research and development of MAP, because the widely used silica can be applied as the only stationary phase. Because of the usefulness of thin layer chromatography (TLC) when cost-effectiveness is essential, TLC or HPTLC is widely used as a standard technique for rapid and accurate identification of plant materials [3] or finished product, and for purity testing of raw materials and formulations in different pharmacopeial prescriptions. A disadvantage of planar chromatography is the skill and experience required because of relatively large number of factors influencing the result [4].

* *Corresponding author*

One of the most important and most widespread groups of natural compounds present in the composition of MAP with a lot of therapeutic properties is the flavonoid class [5]. Flavonoids occur in a variety of structural forms and they are phenolic compounds with a basic C_6-C_3-C_6 skeleton. First of all, they are remarkable because of their antioxidant capacity. Conveniently, the 5000 different flavonoids are divided into 12 classes according to the oxidation level of the central C_3 unit [6]. Paper chromatography, TLC, HPTLC, high performance liquid chromatography (HPLC), column chromatography (ion-exchange resins, polyamide powder, gel material), and countercurrent chromatography have been the most commonly used methods for the separation and purification of flavonoids [7]. TLC and HPTLC is a technique that is applicable to all classes of flavonoids and is especially useful for rapid analysis of partly purified mixtures derived from paper or column chromatography and various TLC or HPTLC systems have been described in the literature [8-12].

The aim of this study is to confirm the presence of flavonoids in *Tilia Platyphyllos* methanolic extract and to illustrate the antioxidant capacity of these compounds. *Tilia Platyphyllos* can be included in MAP category. *Tilia Platyphyllos* has been used traditionally as a calming agent in treatment of anxiety, indigestion, and common cold and as a remedy for ear infection and fever, but medical studies demonstrated its antispasmodic and diuretic actions.

EXPERIMENTAL

All the solvents were of analytical grade. The solution of tempol (Fluka, purity > 97%) was prepared by dissolving 0.0195g tempol in methanol.

The spectrophotometric measurements were performed using Spekol 20 (Carl - Zeiss Jena) spectrophotometer.

The chromatographic experiments was realized on silicagel plates Sil G F_{254} (Merck).The samples (50μL) were applied on plates as belts. The mixtures ethyl acetate – methyl-ethyl-ketone – formic acid – water (50 : 30 : 10 : 10, v/v) were used as mobile phase. The plates were developed on a 12cm distance, in saturated N-chambers at room temperature and then they were dried and the detection was performed in UV light either at 254nm or at 365nm after spraying the plates with diphenyl-borate-amino-buthylic alcohol (NTS).

The densitogram and the *in situ* UV spectra were recorded at 254nm using a Desaga CD60 densitometer.

RESULTS AND DISCUSSION

This research followed the next steps:

1) Establishing the total quantity of flavonoids contained in extract;
2) Testing the assumption that flavonoides react with the nitroxydic radical;
3) Qualitative analysis of simple extract in comparison with the extract treated with the radical for confirming the antioxidant capacity of flavonoides.

The extract of *Tilia Platyphyllos* is made by extraction of dry plant (flowers) in methanol and then the solution was concentrated by evaporation [13].

The total quantity of flavonoids from extract was determined spectrophotometrically at 430nm, using a calibration curve. Different concentration solutions, prepared from rutozid standard according to Pharmacopoeia [14] were used for

plotting the curve. The calibration curve is presented in Figure 1. The total quantity of flavonoidic compounds was expressed in rutozid units. In the *Tilia Platyphyllos* extract the total quantity of flavonoidic compounds, determined from calibration curve, was 17.74 mg/100mL (A = 0.480).

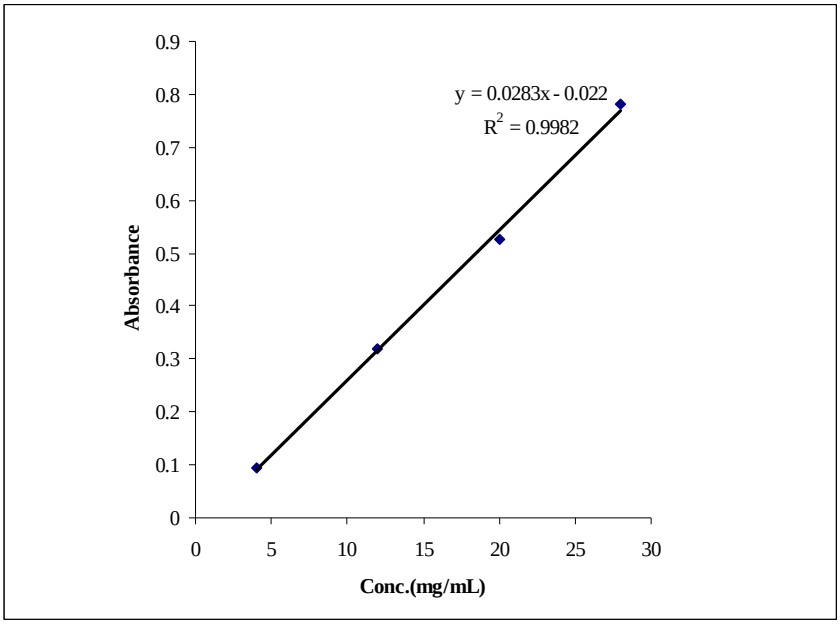

Fig. 1. *The calibration curve for spectrophotometric determinations of flavonoids.*

For testing the assumption that flavonoids act as antioxidant, the *Tilia Platyphyllos* extract was treated with methanolic solution of tempol. Tempol, 4-hidroxy-2,2,6,6-tetramethyl-piperidin-N-oxyl, is a free stable nitroxidic radical. Using different molar ratio extract: radical (1 : 1, 1 : 5) and the same spectrophotometric measurements it came out that absorbance, measured at 430nm decreased and this is the first proof that flavonoidic compounds react with nitroxidic radical and they have antioxidant capacity.

Qualitative analysis of samples – simple *Tilia Platyphyllos* extract and extract treated with tempol – was made by TLC coupled with UV spectroscopy.

The densitogram (Figure 2) shows that *Tilia Platyphyllos* extract contains four flavonoides. Comparing the densitograms of samples (Figure 2) it can be observed that the suitable spots of each flavonoidic compound decreased in intensity and this is another proof of antioxidant capacity.

There are also compared the *in situ* UV spectra of each flavonoidic compounds from *Tilia Platyphyllos* and from treated extract (Figure 3 – 6). From these figures it came out that the absorbance of flavonoidic compounds decreased in intensity or the place of the absorbency maximum is changed.

In conclusion, these researches confirm the fact that flavonoidic compounds act like antioxidant agents. As a remark we can say that these researches prove the advantages of TLC *in situ* coupled with UV spectroscopy.

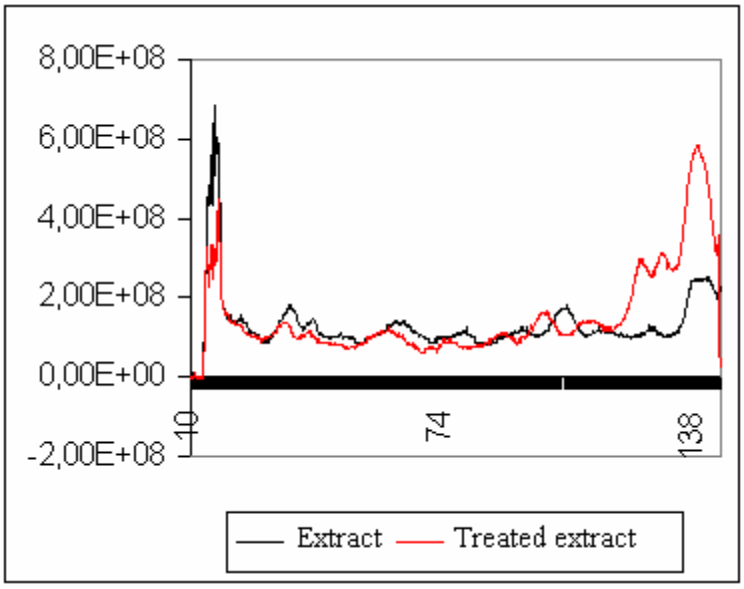

Fig. 2. *The densitograms of extract and treated extract with tempol*.

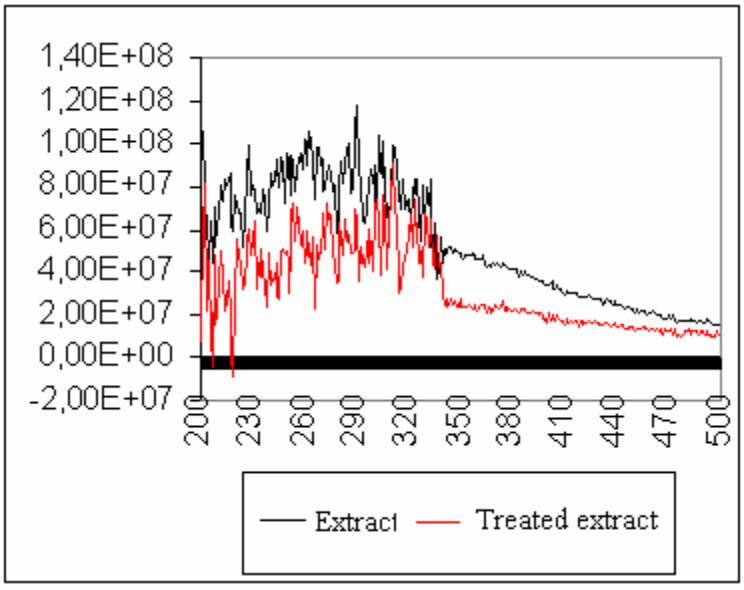

Fig. 3. *The UV spectra of flavonoidic compound I*.

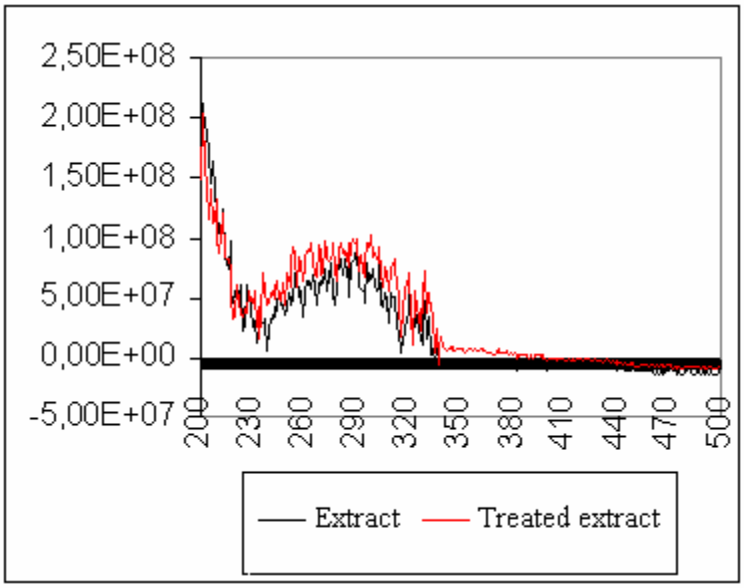

Fig. 4. *The UV spectra of flavonoidic compound II.*

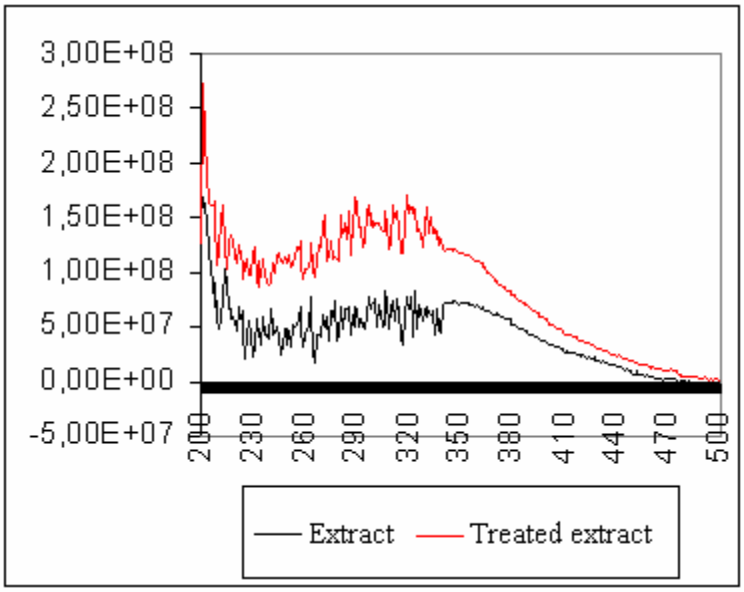

Fig. 5. *The UV spectra of flavonoidic compound III.*

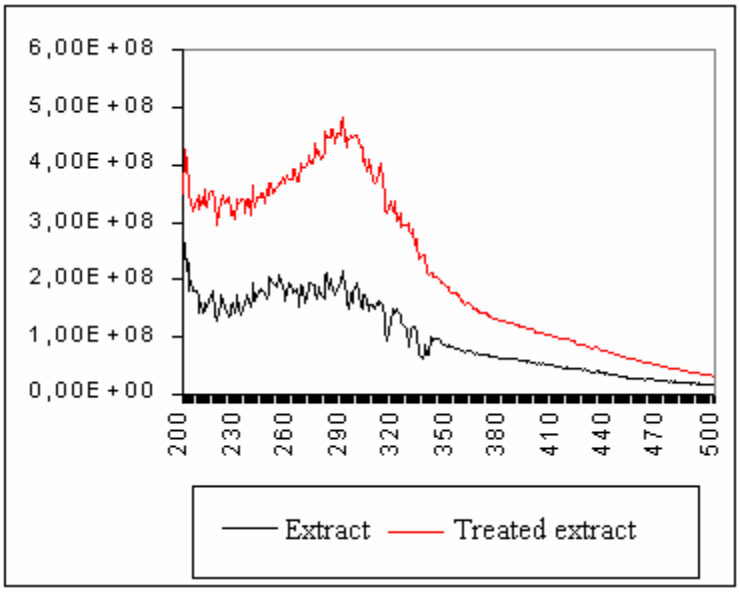

Fig. 6. *The UV spectra of flavonoidic compound IV.*

REFERENCES

1. Sz. Nyiredy, K. Glowniak, *Planar Chromatography in Medicinal Plant Research*, in: Sz. Nyiredy (Ed.) *Planar Chromatography*, Springer, Budapest, 2001, p. 550-568.
2. E. Reich, A. Blatter, *Herbal Drugs, Herbal Drug Preparations, and Herbal Medicinal Products*, in: J. Sherma and B. Fried (Eds.) *Handbook of Thin Layer Chromatography*, Marcel Dekker, New York, 2003, p. 535-564.
3. B. Renger, *J. AOAC Int*., **81** (1998) 333-339.
4. Sz. Nyiredy, *Planar Chromatography*, in: E. Heftmann (Ed.), *Chromatography*, Elsevier, Amsterdam, 1992, p. A109-A150.
5. G.W. Francis, O.M. Andersen, *Natural Pigments*, in: J. Sherma and B. Fried (Eds.) *Handbook of Thin Layer Chromatography*, Marcel Dekker, New York, 2003, p. 697-732.
6. J.B. Harborne, C.A. Williams, *Phytochemistry*, **55** (2000) 481-504.
7. A. Degenhardt, H. Knapp, P. Winterhalter, *J. Agric. Food Chem*., **48** (2000) 338-343.
8. A. Betti, G. Lodi, N. Fuzzati, *J. Planar Chromatogr.-Mod. TLC*, **6** (1993) 232-237.
9. T. Kartnig, I. Goebel, *J. Chromatogr. A*, **740** (1996) 99-107.
10. M.L. Bieganowska, *J. Liq. Chromatogr. Relat. Technol*., **20** (1997) 2089-2098.

11. E. Soczewinski, M.A. Hawryl, A. Hawryl, *Chromatographia*, **54** (2001) 789-794.
12. M. Medic-Saric, G. Stanic, I. Bosnjak, *Pharmazie*, **56** (2001) 156-159.
13. V. Hodisan, M. Tamas, *Clujul Medical*, **LV** (1982) 204-207.
14. * * * Farmacopeea Română, ed. VIII-a, Ed. Medicală, Bucureşti, 1965.

STUDIA UNIVERSITATIS BABEŞ-BOLYAI, CHEMIA, XLIX, 1, 2004

OPTIMIZATION OF THE TERNARY MOBILE PHASE USED IN THIN-LAYER CHROMATOGRAPHY BY THE "WINDOW DIAGRAMS" METHOD

DORINA CASONI[1], CLAUDIA CIMPOIU[1,*], VASILE MICLĂUŞ[1], TEODOR HODIŞAN[1] and COSTINELA GASPAR[2]

[1] *Faculty of Chemistry and Chemical Engineering, "Babeş-Bolyai" University, Cluj-Napoca, Romania*
[2] *Centrul de cercetări Oltchim Rîmnicu-Vîlcea, Romania*

ABSTRACT. The most important problem of planar chromatography is the theoretical and experimental elaboration of methods for predicting mixture separation conditions that would eliminate the arduous choice of the optimum parameters of a chromatographic process.

In this paper "window diagrams" method is used for optimizing the solvent system used in separating of eight dyes by thin-layer chromatography. Kowalska retention model is used to determine the separation selectivity.

Among the interpretative methods for optimizing separation quality, those that employ window diagrams play a specific role, mostly because of the compulsory implementation of this approach with a reliable theoretical model of solute retention as an unavoidable precondition.

An advantage of this optimization procedure is that the optimum composition can be easily obtained even for multicomponent mobile phase.

INTRODUCTION

In analytical TLC, as in any other chromatographic method, the greatest effort is devoted to the purpose of obtaining the largest separation of the compounds of a mixture. Optimization of the quality of separation can be considered as one of the major practical tasks of the theory of chromatography.

Because separated mixtures usually contain compounds of very similar chemical and electronic structure, their separation is not simple. Interaction of such chromatographied substances with the surface of stationary phases and components of the mobile phase are similar and separation of mixtures with mono or binary mobile phases is practically impossible. Multi-component mobile phases are very often used in modern chromatographic analysis. Because of the many different compositions possible for ternary and quaternary mobile phases, determining the optimum composition of mobile phases with more than two components is rather complicated.

The several techniques used for optimization of separation selectivity can be grouped under three major strategies: *simultaneous methods*, *sequential methods* and *interpretative methods*.

* *Corresponding author*

Among the interpretative methods for optimizing separation quality, those that employ window diagrams [1, 2] play a specific role.

Laub and Purnell [1, 2] in order to optimize the separation selectivity in gas chromatography first used the "window diagrams" method, which is an interpretative one. Ever since, the method has been widely used in gas chromatography (GC) and high performance liquid chromatography (HPLC).

In the case of direct phase liquid chromatography, is used the simplest variant of "window diagrams" method, where the efficiency of the chromatographic separation can be quantified by use of ΔR_f, which is responsible against the solvent composition. For any given pair of compounds, the value ΔR_f is given by relationship:

$$\Delta R_f = \frac{k_2 - k_1}{(1 + k_1)(1 + k_2)} \quad (1)$$

The k_1 and k_2 values can be calculated as a function of a binary solvent's composition:

$$\log k = a \log X_S \quad (2)$$

where X_S represents the molar fraction of the strongest solvent.

If all the pairs of solutes contained in a mixture are being considered, the maximum of ΔR_f values were arranged around a specific molar fraction of binary solvent system.

The advantage of this method resides in the fact that global optimum can be easily traced, either visually or by computer.

Same articles [3, 4] had compared optimization power of three different retention models suitable for liquid chromatography systems by aid of relationship proposed by Snyder [5], Schoenmakers [6] and Kowalska [7]. The direct optimization procedure was performed with aid of window diagrams method [3, 4]. The research studies concluded that Kowalska model is the most relevant model for obtaining the optimum results. According to this model, nonlinear relationship, which links the solute R_f coefficient with composition of binary mobile phase, is given below [8]:

$$R_f = A(X_1)^{1/2} + B(X_2)^{1/2} + C \quad (3)$$

where X_1, X_2 are the volume fractions of solvents and A, B, and C are, in the first instance, the constants of equation.

The separation selectivity α, offers the possibility of simple quantification of separation quality and for this practically reason the magnitude of α has very often been employed in procedures aimed at optimization of solute separation. The physico-chemical interpretation of α is given by the relationship:

$$\alpha = \frac{K_1}{K_2} = \frac{k_1}{k_2} \quad (4)$$

where K_1 and K_2 are the distribution coefficient of solutes 1 respectively 2 between the stationary and mobile phases, and k_1 and k_2 are the respectively capacity factors ($K_1 > K_2$ or $k_1 > k_2$).

Adaptation of eq.3 for determination of separation selectivity α results in formula [9]:

$$\alpha = \frac{\left[1-\left(A_1\sqrt{x_1}+B_1\sqrt{x_2}+C_1\right)\right]\left(A_2\sqrt{x_1}+B_2\sqrt{x_2}+C_2\right)}{\left(A_1\sqrt{x_1}+B_1\sqrt{x_2}+C_1\right)\left[1-\left(A_2\sqrt{x_1}+B_2\sqrt{x_2}+C_2\right)\right]} \quad (5)$$

where A_i, B_i and C_i are the constants of eq. 3 for solute i.

This research is concerning to the optimization of separation quality of some dyes.

EXPERIMENTAL

All the solvents were of analytical grade.

The silicagel plates with normal phase $60F_{254}$ (Merck) were used for the chromatographic experiment.

The mixtures of methanol, petroleum ether and acetone were used as mobile phases. These solvents were selected according to Snyder classification.

The solutions of dyes (0.1%) were prepared in methanol and the compounds (0,2µl) were applied on plates as spots. The plates were developed on a 9 cm distance at room temperature. After developing, the plates were dried and detection was performed in 254nm UV light.

RESULTS AND DISCUSSION

In the present paper "window diagrams" method is used for the optimizing the composition of solvent system used in separation of eight dyes by thin-layer chromatography. The dyes were recently synthesized with intend to create a new set of dyes. The structural formulas of dyes are presented in Figure 1.

Until now, the "window diagrams" method has been used for the optimization of binary mobile phase only. For this reason, in the first step of optimization procedure there are used mixture of methanol (strong solvent $\varepsilon^0 = 5,1$) and petroleum ether (week solvent $\varepsilon^0 = 0$) as mobile phase. Three chromatographic experiments were performed with methanol-petroleum ether in various proportions (Table 1). The experimental values of R_f (Table 1) were put in the eq.3 in order to determine the coefficients A, B and C for each solute. The values of these coefficients are presented in Table 1.

The plots of α against X_1 (Figure 2) and the plots ΔR_f against X_1 (Figure 3) (X_1 represent the molar fraction of methanol) for each solute represent the "window diagram" showing relationship between α and X_1 respectively ΔR_f and X_1.

Table 1.

The R_f values and the coefficients A, B and C of eq.3 for each solute.

Nr. crt.	R_f			Coefficients		
	Mobile Phase (methanol - petroleum ether, v/v)			A	B	C
	40 : 60	80 : 20	50 : 50			
1	0.084	0.070	0.064	-1.821	-1.157	1.930
2	0.241	0.270	0.258	0.929	0.536	-0.669
3	0.325	0.353	0.333	0.110	0.002	0.254
4	0.482	0.482	0.441	4.524	-2.963	5.127
5	0.494	0.506	0.538	4.524	2.933	-4.127
6	0.506	0.482	0.516	1.765	1.216	-1.340
7	0.542	0.541	0.581	4.331	2.839	-3.900
8	0.807	0.812	0.871	0.144	0.286	0.626

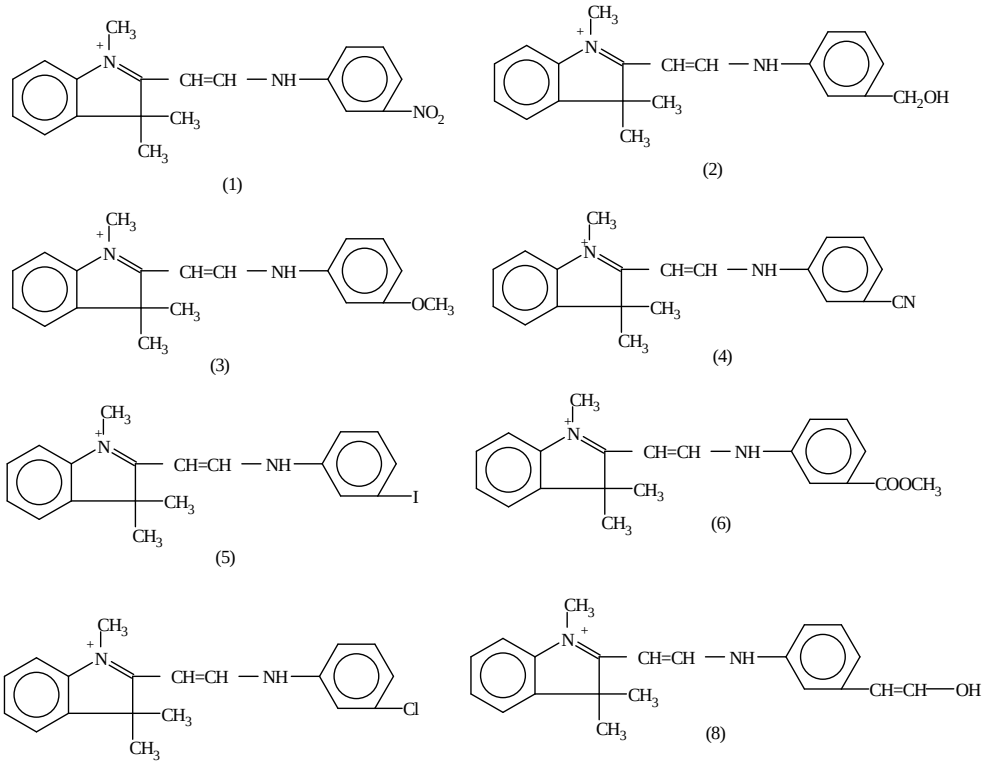

Fig. 1. *The chemical structures of dyes.*

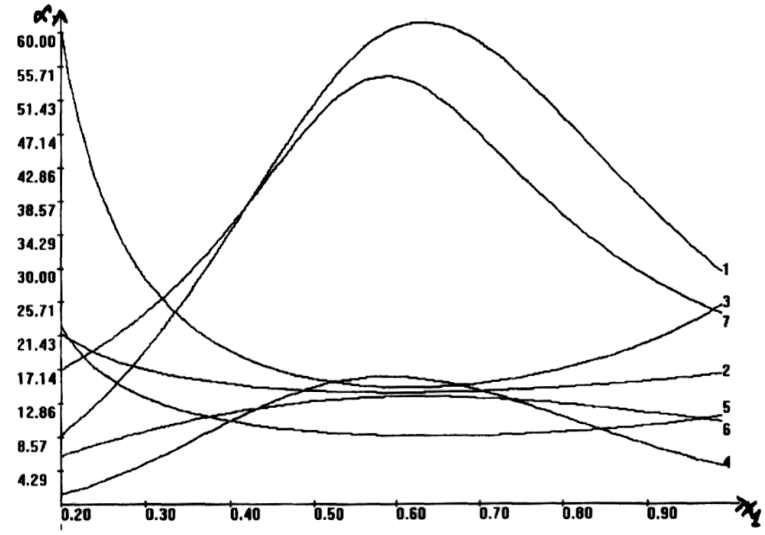

Fig. 2. *Window diagrams showing relationship between α and X_1 obtained by using methanol - petroleum ether mixture as mobile phase.*

From Figure 2, it can be observed that the greatest difference as a sum of differences between the values lies around the methanol fraction of 0.9 ± 0.02. This fact can also be proved by watching the plots ΔR_f of against X_1 (Figure 3).

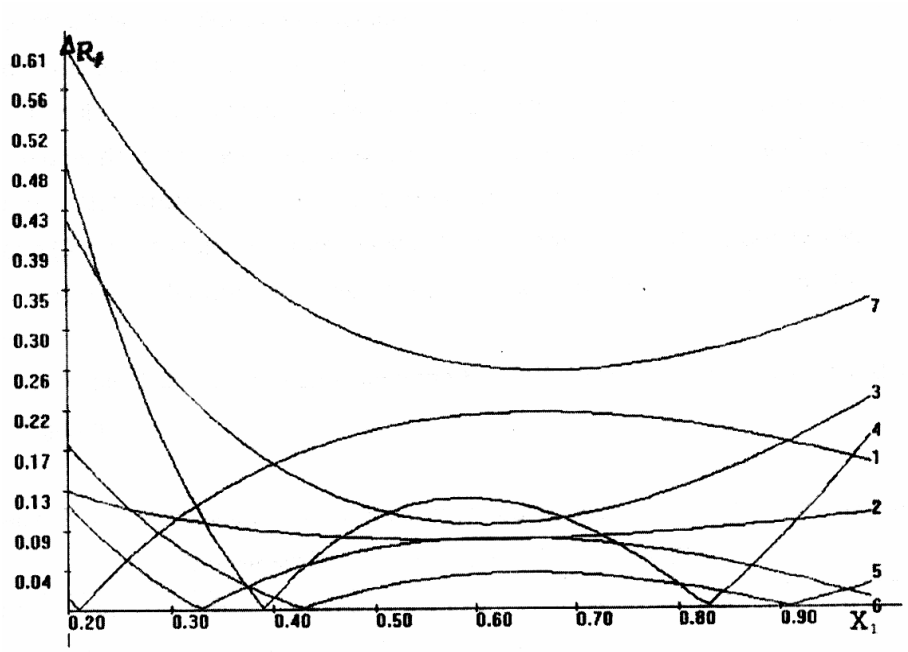

Fig. 3. *Window diagrams showing relationship between ΔR_f and X_1 obtained by using methanol - petroleum ether mixture as mobile phase*.

In accord with these models, the optimum composition is methanol - petroleum ether 9 : 1 (v/v).

With a mixture of more than two solutes it is again necessary to use the "window diagrams" approach in order to select the most suitable separation conditions. Therefore, in the second step the composition of ternary mobile phase was optimized in order to obtain a good separation of compounds. The procedure are similar with that used in first step but the strong solvent (I) is acetone (ε^0 = 5,1) and the mixture methanol-petroleum ether (9 : 1 v/v) represents the week solvent (II) (ε^0 = 4,6). The results are given in Table 2.

From Table 2, it can be observe that the R_f values increase with increasing of solvent I molar fraction.

In order to find out which proportion of methanol - petroleum ether - acetone mixture provides the optimum results, there are plotted again α and ΔR_f against X_1 (X_1 is molar fraction of acetone) for each solute.

Table 2.

The R_f values and the coefficients A, B and C (from eq.3) of each solute.

Nr. crt.	R_f			Coefficients		
	Mobile Phase (I – II, v/v)			A	B	C
	50 : 50	30 : 30	70 : 30			
1	0.077	0.055	0.072	0.903	0.610	-0.867
2	0.344	0.244	0.333	3.344	2.276	-3.092
3	0.411	0.333	0.389	3.344	2.276	-3.092
4	0.566	0.511	0.544	2.575	1.776	-2.144
5	0.589	0.522	0.567	2.977	2.037	-2.534
6	0.600	0.533	0.589	2.609	1.744	-2.117
7	0.622	0.578	0.628	1.280	0.793	-0.673
8	0.844	0.850	0.818	0.669	0.563	0.089

The plots of ΔR_f against X_1 (Figure 5) show that the greatest difference, as a sum of differences between the ΔR_f values, lies around the acetone fraction of 0.35. Same thing can be ascertained by watching the plots of α against X_1 (Figure 4). Thus, it was established that the optimum composition of solvents mixture I - II is 35 : 65.

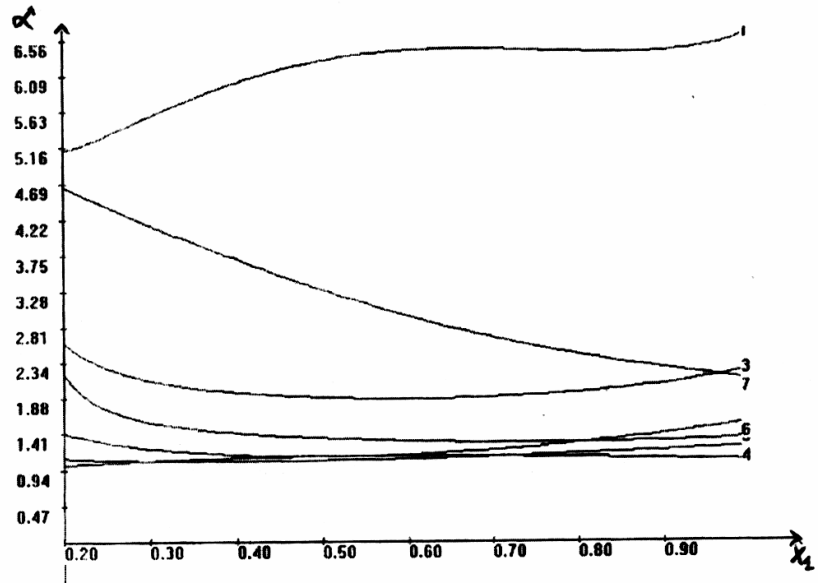

Fig. 4. *Window diagram showing the relationship between α and X_1 in case of ternary mobile phase (methanol - petroleum ether - acetone).*

Therefore, considering the fact that the optimum composition of solvent II is 9:1, it can conclude that in the case of the ternary mobile phase, the optimum composition acetone - methanol - petroleum ether is 35 : 58.5 : 6.5.

The mixture was further used to separate the eight dyes. As a result of chromatographic experiment, it was establish that this mobile phase mixture, acetone : methanol : petroleum ether in a volumetric proportion of 35 : 58.5 : 6.5 provides the best separation of the studied compounds.

In conclusion, for the first time the composition of ternary mobile phase was optimized using "window diagrams" method and retention model. The advantage of this method is that that optimum composition of mobile phase can be easily obtained.

Introduction of a physico-chemical logical to the optimization procedure is an ultimate goal of chromatography theory, and particularly of all efforts that aim to model solute retention.

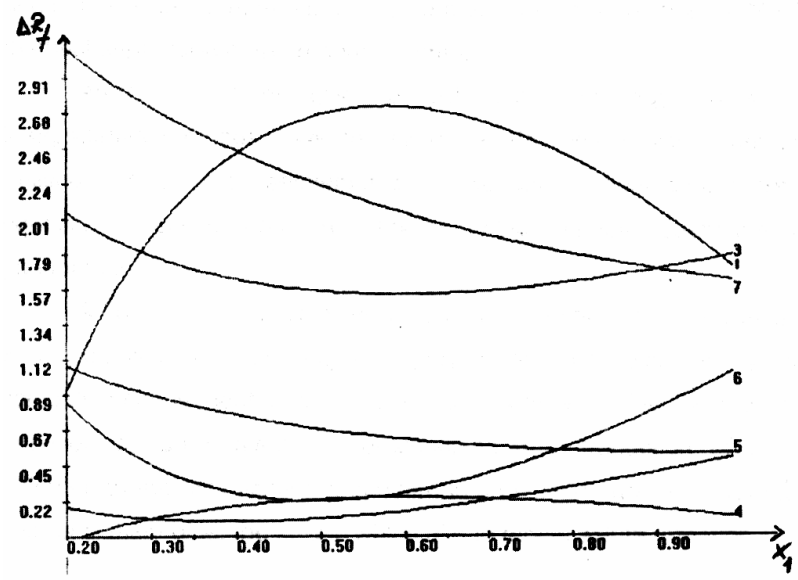

Fig. 5. *Window diagram showing the relationship between ΔR_f and X_1 in case of ternary mobile phases (methanol - petroleum ether - acetone).*

REFERENCES

1. R.J. Laub and J. H. Purnell, *J. Chromatogr.* 1975, **112**, 71-79.
2. J. Laub, J.H. Purnell, and P. S. Williams, *Anal. Chem. Acta*., 1977, **95**, 135-143.
3. W. Prus, T. Kowalska, *J. Planar Chromatogr.-Mod.TLC*, 1995, **8**, 288-291.
4. W.Prus, T. Kowalska, *J.Planar Chromatogr.-Mod.TLC*, 1995, **8**, 205-215.

5. L. R. Snyder, J. R. Gant, *J. Chromatogr*., 1979, **165**, 3-21.
6. P. J. Schoenmakers, H.A.H Billet, L. de Galan, *J. Chromatogr*., 1979, **185**, 179-192.
7. T. Kowalska, *Chromatographia*, 1989, **27**, 628-630.
8. T. Kowalska, B. Klama, J. Sliwiok, *J.Planar Chromatogr*.-*Mod.TLC*, 1992, **5**, 452-457.
9. T. Kowalska, B. Klama, *J.Planar Chromatogr*.-*Mod.TLC*, 1994, **7**, 63-69.

STUDIA UNIVERSITATIS BABEŞ-BOLYAI, CHEMIA, XLIX, 1, 2004

THIRD GENERATION AMPEROMETRIC BIOSENSOR BASED ON MEDIATED ELECTRON TRANSFER BETWEEN ALCOHOL DEHYDROGENASE AND 1,1,2,2,3,3,4,6,7,8,9-UNDECACHLORO-1,2-DIHYDRO-PHENOTHIAZINE

DELIA M. GLIGOR, GRAZIELLA L. TURDEAN, LIANA M. MURESAN and IONEL CATALIN POPESCU

Faculty of Chemistry and Chemical Engineering, Babeş-Bolyai University of Cluj, 11 Arany Janos Str. Cluj-Napoca 400028 Romania. E-mail:ddicu@chem.ubbcluj.ro

ABSTRACT. A new amperometric biosensor for ethanol was obtained using a graphite electrode modified with 1,1,2,2,3,3,4,6,7,8,9-undecachloro-1,2-dihydro-phenothiazine as transducer, and alcohol dehydrogenase (ADH) cross-linked with glutaraldehyde, as NAD^+/NADH dependent detecting enzyme. The ethanol amperometric detection is based on the oxidation of NADH generated in the enzymatic reaction between ethanol and NAD^+ in the presence of ADH. The biosensor response increases linearly with ethanol concentration up to 2 M and the detection limit was 1.5 mM. The biosensor activity remains relatively stable for about 2 days.

Keywords: amperometric biosensors, alcohol dehydrogenase, nicotinamide adenine dinucleotide, phenothiazine derivative, modified electrodes.

INTRODUCTION

The majority of redox enzymes widely used in amperometric biosensor research are NAD^+/NADH-dependent dehydrogenases [1,2]. Their electrical connection with electrodes reveals several fundamental limitations that prevent their broad use for biosensor applications. Thus, the NAD^+/NADH redox couple: (i) operates by a diffusion controlled mechanism; (ii) exhibits poor electrochemical properties at bare electrodes; (iii) requires a large overvoltage because its direct electrochemical reduction/oxidation is kinetically unfavorable [3-5]. So, an effective way to avoid these problems is the mediated electrocatalytic oxidation of NADH.

The phenothiazine derivatives are one of the compounds more frequently used as mediators to design efficient electrocatalytic schemes for NADH recycling. Thus, to develop biosensors based on NAD^+-dependent enzymes it is important to integrate the enzyme-NAD^+ cofactor and the catalyst for NADH oxidation as an assembly that electrically communicates with the amperometric transducer [4,6,7].

Because ethanol is an important compound in medicine, biotechnology and food industry, amperometric methods based on using of either alcohol oxidase (AOX) [7] or alcohol dehydrogenase (ADH) [1,8-12] to an appropriate electrode are employed. The interest in ADH instead of AOX for ethanol detection is due to the fact that in the first enzymatic reaction oxygen is not involved [13].

The alcohol dehydrogenase (ADH) has been immobilized onto the electrode surface by physical entrapment using Nafion membrane [14] or a dialysis membrane [9], into electropolymerised polypyrrole film or *o*-phenylenediamine [13] as well as by cross-linking using glutaraldehyde/albumin [15,16].

Recently [17], it was demonstrated that a graphite electrode modified with 1,1,2,2,3,3,4,6,7,8,9-undecachloro-1,2-dihydro-phenothiazine (G/UDP) shows a significant reduction of the NADH oxidation overpotential and a remarkably stable voltammetric response. In this context, the aim of the present study was to use this new electrochemical interface for NADH detection in order to develop and characterize a G/UDP/ADH amperometric biosensor for the ethanol detection.

EXPERIMENTAL SECTION

Chemicals

β-nicotinamide adenine dinucleotide, NAD^+ was purchased from Merck (Darmstadt, Germany), alcohol dehydrogenase (ADH, alcohol:NAD^+ oxidoreductase; EC 1.1.1.1., from bakers yeast, activity of 340 U mg^{-1}) was obtained from Sigma (St. Louis, MO, USA) and both used as received. Glutaraldehyde (25 % w/v), obtained from Aldrich (Steinheim, Germany), was diluted to 2.5 % (v/v) with distilled water. Dimethylformamide was purchased from Merck (Darmstadt, Germany) and absolute ethanol (96 %) was obtained from Prodvinalco, Cluj-Napoca.

The phenothiazine derivative, 1,1,2,2,3,3,4,6,7,8,9-undecachloro-1,2-dihydro-phenothiazine (UDP, see Scheme 1) was kindly offered by Prof. Silberg (Department of Organic Chemistry, "Babes-Bolyai" University), who synthesized it as described previously [18]. The supporting electrolyte was a 0.1 M phosphate buffer solution (pH 7.0), prepared using appropriate amounts of Na_2HPO_4 and NaH_2PO_4 (Merck, Darmstadt, Germany). All other reagents were of analytical grade and used as received.

All solutions were prepared with distilled water. The ethanol aqueous solution and the ADH stock solution were prepared in phosphate buffer solution (pH 7) and stored at 4^0 C.

Enzymatic activity determination of alcohol dehydrogenase

Before use, the enzymatic activity of ADH was spectrophotometrically tested (Jasco V530, PC connected spectrophotometer). The UV-VIS absorption spectrum of a phosphate buffer solution (pH 7), containing 10^{-3} M ethanol and 10^{-3} M NAD^+, was compared with that of the same solution containing in addition 476 units ADH/ml. In the presence of ADH, a maximum of absorption located at 330 nm proves the enzymatic formation of β-NADH, according to reaction 1:

$$\text{Ethanol} + \beta - \text{NAD}^+ \xleftrightarrow{\text{ADH}} \text{Acetaldehyde} + \beta - \text{NADH} + \text{H}^+ \quad (1)$$

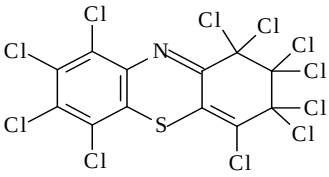

Scheme 1. *Structure of 1,1,2,2,3,3,4,6,7,8,9-undecachloro-1,2-dihydro-phenothiazine (UDP).*

Preparation of the G/UDP-modified electrodes

A spectrographic graphite rod (Ringsdorff-Werke, GmbH, Bonn-Bad Godesberg, Germany), of ~ 3 mm diameter, was wet polished on fine (grit 400 and 600) emery paper (Buehler, Lake Bluff, In., USA). Then, a graphite piece of suitable length was carefully washed with distilled water, dried, and finally press-fitted into a PTFE folder in order to obtain a graphite electrode, having in contact with the solution, a flat circular surface of ~ 0.071 cm^2.

Spreading onto the graphite surface 5 μl of 10 mM UDP dissolved in dimethylformamide, and leaving the graphite for 20 minutes at room temperature to evaporate the solvent the G/UDP-modified electrodes were obtained. Before immersion in a test solution, the G/UDP-modified electrodes were carefully washed with doubly distilled water.

Preparation of the G/UDP/ADH bioelectrodes

In order to immobilize the ADH on the G/UDP-modified electrodes a cross-linking technique with glutaraldehyde (GA) was used. Thus, 3 mg of ADH were dissolved in 100 μl of 0.1 M phosphate buffer solution (pH 7) and was stirred thoroughly with 50 μl glutaraldehyde (2.5 % v/v). Spreading onto the electrode surface 5 μl ADH-GA mixture the G/UDP/ADH bioelectrodes were obtained. This procedure was repeated three times. Before use the resulting bioelectrodes were incubated at 4^0 C, for least 1 h in a phosphate buffer solution (pH 7).

Electrochemical measurements

Electrochemical experiments were carried out using a typical three-electrode electrochemical cell. The modified graphite electrode was used as working electrode, a platinum ring as counter electrode and a saturated calomel electrode (SCE) or Ag|AgCl (KCl_{sat}) as reference electrodes.

Cyclic voltammetry experiments were performed on an electrochemical analyzer (Autolab-PGSTAT 10, EcoChemie, Utrecht, The Netherlands) connected to a PC for potential control and data acquisition.

Amperometric measurements were carried out with the G/UDP/ADH biosensor at an applied potential of +150 mV *vs.* Ag|AgCl (KCl_{sat}) and under constant stirring using a modulated speed rotator (model AMSFRX, Pine, Grove City, Pa., USA). The current-time data were collected using a computer-controlled BAS CV-50W voltammetric analyzer (Bioanalytical Systems, West Lafayette, In., USA). The experiments were performed in phosphate buffer solution (pH 7) containing 1 mM NAD^+. The background current was first allowed to decay to a constant value, and

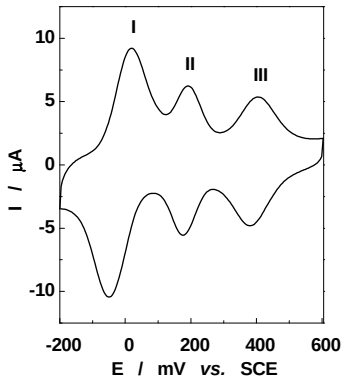

***Fig. 1**. Voltammetric response of UDP adsorbed on spectrographic graphite. Experimental conditions: starting electrode potential, -200 mV vs. SCE; scan rate, 50 mV s^{-1}; supporting electrolyte, 0.1 M phosphate buffer (pH 7.0).*

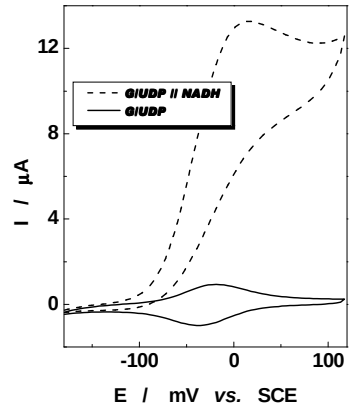

Fig. 2. *NADH electrocatalytic oxidation at G/UDP-modified electrode: voltammetric response in 0.1 M phosphate buffer solution (pH 7.0) (_____) and in the presence of 5 mM NADH (.....). Experimental conditions: scan rate, 5 mV s^{-1}; surface coverage, ~3.0 nmol cm^{-2}; starting potential, -180 mV vs. SCE.*

then the ethanol was added. The steady-state current was measured under constant solution stirring.

Results and discussion

1. Electrochemical behavior of the G/UDP modified electrode

The voltammetric response recorded for G/UDP electrodes (Fig. 1), exhibited three peak pairs placed at following formal standard potentials: $(E^{0'})_I$ = -15; $(E^{0'})_{II}$ = 185; $(E^{0'})_{III}$ = 396 mV *vs.* SCE (pH 7.0). The first peak pair of UDP was attributed to the formation of the 1,2,3,4,6,7,8,9-octachlorophenothiazinyl cation radical [19]. The second and the third peak pairs were supposed to correspond to two different dimers formed during the electrode potential cycling, namely 3,10'-bis(1,1,2,2,3,3,4,6,7,8, 9-undecachloro-1,2-dihydro-phenothiazine) and 10,10'- bis(1,1,2,2,3,3,4,6,7,8,9-undecachloro-1,2-dihydro-phenothiazine) [17]. All further results will refer exclusively to the first peak pair, because its redox formal potential is well placed in the for amperometric detection [20]. The electrochemical analysis of the voltammetric response, corresponding to the formation of the UDP cation radical involves a quasi-reversible, $1e^-/1H^+$ transfer. The UDP formal redox potential was found pH-dependent with a slope of 52 mV/ΔpH [17].

2. Electrocatalytic activity of the G/UDP modified electrode

Starting from the favorable electrochemical behavior of the UDP adsorbed on graphite, its electrocatalytic activity towards NADH oxidation was tested by cyclic voltammetry (Fig. 2).

In the presence of NADH, a remarkable enhancement of the anodic peak current, associated with the progressive diminishing of the cathodic one, proved the electrocatalytic effect of UDP. The electrocatalytic efficiency, estimated as the

$(I_{cat})_{NADH}/(I_{cat})$ ratio, at an applied potential of +15 mV *vs.* SCE, was found equal to 5, when the NADH concentration was 5 mM.

Taking as reference the potential for NADH electro-oxidation at bare graphite electrodes [21,22], an overpotential decrease higher than 400 mV was observed. The calibration curve of G/UDP-modified electrode for NADH (results not shown), recorded at an applied potential of +15 mV *vs.* SCE, exhibited a linear range up to ~1 mM NADH and a sensitivity of 1.0 mA/(M.cm^2).

3. Electrochemical behavior of G/UDP/ADH bioelectrode

3.1. Detection of NADH generated by enzymatic reaction

The above-presented results showed that the G/UDP-modified electrode exhibits a significant catalytic activity toward NADH oxidation. However, it was necessary to check if its sensitivity is enough high to allow the detection of the enzymatically generated NADH resulting from reaction (1). In order to verify this supposition, the G/UDP voltammetric response in a phosphate buffer solution was compared to that corresponding to the same electrode in contact with a buffer solution containing simultaneously dissolved ADH and NAD^+ as well as with that recorded at G/UDP-modified electrode immersed in a buffer solution containing dissolved ADH, NAD^+ and ethanol (Fig. 3). It can be seen that the presence of ethanol in the solution containing NAD^+ and ADH lead to a significant increase of the anodic peak current, proving the ability of the G/UDP-modified electrode to detect the enzymatically generated NADH.

3.2. Analytical performances of G/UDP/ADH bioelectrode

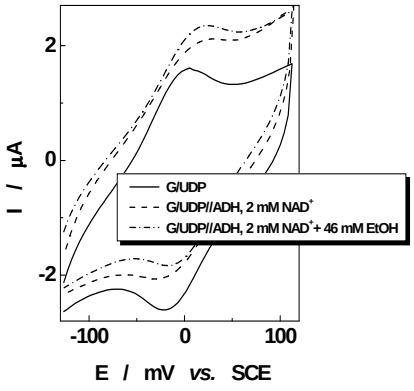

ADH catalyzes the oxidation of ethanol with a simultaneous reduction of an equivalent amount of NAD^+ to NADH (reaction 1) and, subsequently, the generated NADH reduces UDP_{ox} (Scheme 2).

Fig. 3. *Cyclic voltammograms at G/UDP-modified electrode in phosphate buffer solution (pH 7.0) (_____), in the presence of 2 mM NAD^+ and 100 U ml^{-1} ADH (— —) and after addition of 46 mM ethanol (_._._). Experimental conditions: starting electrode potential, -130 mV vs. SCE; scan rate, 5 mV s^{-1}.*

During the anodic scan the reduced mediator (UDP_{red}) will be reoxidized at the electrode and, consequently, the anodic peak current will increase significantly. A catalytic current will be not observed if any component shown in Scheme 2 is absent.

By fixing the NAD^+ concentration in solution, the increase of the peak current should depend only on the ethanol concentration. This is the basis for the ethanol determination via NADH amperometric detection, using the G/UDP/ADH bioelectrode.

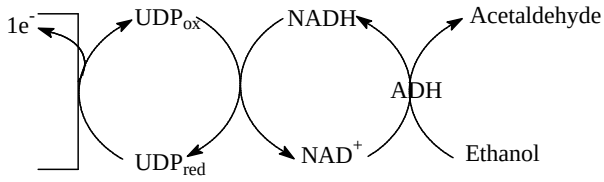

Scheme 2. *Scheme of the electrochemical coupled enzymatic oxidation of ethanol*.

The batch amperometric response of G/UDP/ADH bioelectrode to successive additions of ethanol, observed at an applied potential of +150 mV *vs.* Ag/AgCl (KCl_{sat}) and a fixed (1 mM) NAD^+ concentration [9], corresponds to a typical Michaelis–Menten kinetics (Fig. 4).

A linear response was observed up to 0.6 mM ethanol for G/UDP-modified electrode in the presence of dissolved ADH and up to 2 M ethanol for the G/UDP/ADH bioelectrode. A detection limit of 0.2 mM ethanol was calculated for the G/UDP-modified electrode and 1.5 mM ethanol for the G/UDP/ADH bioelectrode (signal-to-noise ratio of three). The response time necessary to reach 95% of the steady state signal was almost independent on the substrate concentration and, in both cases, its average value was less than 50 s.

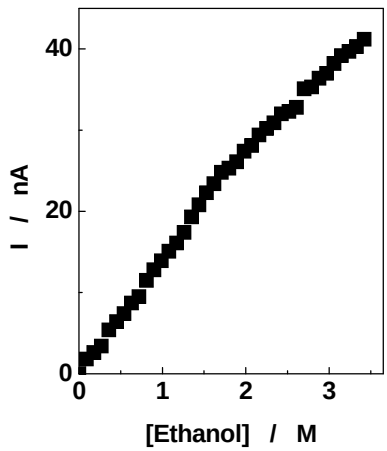

Fig. 4. *Calibration curve for ethanol at G/UDP/ADH modified electrode. Experimental conditions: applied electrode potential, +150 mV vs. Ag|AgCl; electrode rotation speed, 300 rpm; supporting electrolyte, 0.1 M phosphate buffer (pH 7.0).*

The stability of the G/UDP/ADH bioelectrode was evaluated by measuring periodically its response towards ethanol. The response remained at 90% of the initial value for 2 days and decayed to half of its initial value after one week, indicating the G/UDP/ADH bioelectrode displays a relatively stable response for ethanol. *Experimental*

The decrease in the response towards ethanol might be due mainly to the loss of ADH enzyme activity, because it was noticed that the G/UDP electrode exhibited a higher stability (more than a week) for NADH detection [17].

For immobilized enzymes used to obtain amperometric biosensors, the observed electrochemical response may be controlled either kinetically or by sub-

strate transport. For an immobilized enzyme reaction that is kinetically controlled, the steady-state current, I_{SS}, is proportional to the initial rate of the enzymatic process. In order to obtain the kinetic parameters of the biosensor, three different linearization of Michaelis-Menten equation (Lineweaver–Burk, Hanes–Woolf and Eadie–Hoffstee) were used. The kinetic parameters obtained for G/UDP/ADH bioelectrode are presented in Table 1. As expected, the ADH immobilization lead to an increase of K_M^{app} value and a decrease of sensitivity in comparison with the corresponding values obtained when ADH was dissolved in solution (K_M = 3 M and S = 45 nA/M).

A survey of the literature shows that the value of apparent constant Michaelis–Menten, K_M^{app}, for ADH varies between 3.2 mM (for dissolved ADH; Pt rotated disk electrode; using hexacyanoferrate(III) as mediator; at pH 8.8) [23] and 41.7 mM ethanol (for ADH immobilized on a nickel hexacyanoferrate modified microband gold electrode, using glutaraldehyde/bovine serum albumin cross-linking procedure; at pH 7.5) [9]. The difference between the results obtained in this study and those presented above could be due to the restricted substrate access at the electrode surface, as a result of diffusion constraints created by the enzyme layer. This finding confirms the fact that the value of K_M^{app} is not an intrinsic property of a given enzyme, but it is strongly dependent of the microenvironment around the immobilized enzyme and the transductor geometry.

Table 1.

Analytical parameters for G/UDP/ADH bioelectrode.

K_M^{app} (M)	I_{max} (μA)	Sensitivity (nA/M)	R/ no. of exp. points
Lineweaver – Burk linearization			
7.2 ± 0.8	0.12 ± 0.01	17.7 ± 0.5	0.9984 / 22
Hanes – Woolf linearization			
7.5 ± 0.9	0.13 ± 0.01	17.5 ± 0.5	0.9833 / 22
Eadie – Hoffstee linearization			
7.2 ± 1.0	0.12 ± 0.01	17.6 ± 4.2	0.9617 / 20

Conclusions

The results indicate that the new bioelectrode, obtained by ADH cross-linking with glutaraldehyde on the surface of a G/UDP-modified electrode, is a promising detector for ethanol. Its analytical signal is based on the electrocatalytic oxidation of NADH enzymatically generated in the reaction between ethanol and NAD^+, in the presence of ADH. G/UDP/ADH bioelectrode responds rapidly to ethanol with a detection limit of 1.5 mM. The response current increases linearly with ethanol concentration up to 2 M. The bioelectrode maintains its activity for about 2 days.

Acknowledgements

Financial support from CNCSIS (Grant CNCSIS A_T 26/43-2003) and Romanian Academy (GAR 43/2003) is gratefully acknowledged. Authors acknowledge Professor I. A. Silberg, Department of Organic Chemistry, “Babes-Bolyai” University Cluj-Napoca (Romania) for kindly providing UDP.

REFERENCES

[1] L. Gorton, A. Lindgren, T. Larsson, F. D Munteanu, T. Ruzgas, I. Gazaryan, *Anal. Chim. Acta*, **1999**, 91, 400.
[2] L. Gorton, E. Dominguez, Rev. *in Mol. Biotechnol.*, **2002**, 82, 371.
[3] Z. Samec, P. J. Elving, *J. Electroanal. Chem.*, **1983**, 144, 217.
[4] M. Zayats, A. B. Kharitonov, E. Katz, A. F. Buckmann, I. Wilner, *Biosens. & Bioelectron.*, **2000**, 15, 671.
[5] H.-L. Schmidt, W. Schuhmann, *Biosens. & Bioelectron.*, **1996**, 11, 127.
[6] J. Katrlik, J. Svorc, M. Stred'ansky, S. Miertus, *Biosens. & Bioelectron.*, **1998**, 13, 181.
[7] M. Boujtita, J. P. Hart, R. Pittson, *Biosens, & Bioelectron.*, **2000**, 15, 257.
[8] L. T. Kubota, L. Gorton, *Electroanalysis*, **1999**, 11, 719.
[9] C.-X. Cai, K.-H. Xue, Y.-M. Zhou, H. Yang, *Talanta*, **1997**, 44, 339.
[10] W. J. Blaedel, R. C. Engstrom, *Anal. Chem.*, **1980**, 52, 1691.
[11] F. Tobalina, F. Pariente, L. Hernandez, H. D. Abruna, E. Lorenzo, *Anal. Chim. Acta*, **1999**, 395, 17.
[12] A. Karyakin, E. Karyakina, W. Schuhmann, H.-L. Schmidt, *Electroanalysis*, **1994**, 6, 821.
[13] M. J. Lobo Castanon, A. J. Miranda Ordieres, P. Tunon-Blanco, *Biosens. & Bioelectron.*, **1997**, 12, 511.
[14] A. Karyakin, O. A. Bobrova, E. A. Karyakina, *J. Electroanal. Chem.*, **1995**, 399, 179.
[15] M. Somasundrum, J. V. Bannister, J. Chem. Soc., *Chem. Commun.*, **1993**, 1629.
[16] F. Y. Bernadette, R. L. Christopher, *Anal. Chem.*, **1987**, 59, 2111.
[17] D. Gligor, L. Muresan, I. C. Popescu, I. A. Silberg, *Rev. Roum. Chim.*, **2002**, 47(10-11), 953.
[18] C. Bodea, I. Silberg, *Rev. Roumaine Chim.*, **1964**, 9, 425.
[19] G. Cauquis, A. Deronzier, J. -L. Lepage, D. Serve, *Bull. Soc. Chim. France*, **1977**, (3-4), 295.
[20] L. Gorton, *Electroanalysis*, **1995**, 7, 23.
[21] H. Jaegfeldt, T. Kuwana, G. Johansson, *J. Am. Chem. Soc.*, **1983**, 105, 1805.
[22] A. Torstensson, L. Gorton, *J. Electroanal. Chem.*, **1981**, 130, 199.
[23] M. K. Ciolkosz, J. Jordan, *Anal. Chem.*, **1993**, 65, 164.

STUDIA UNIVERSITATIS BABEŞ-BOLYAI, CHEMIA, XLIX, 1, 2004

FLOW GRAPH THEORY, AN ALTERNATIVE TO STEADY STATE APPROXIMATION

MARIUS SOCOL and IOAN BALDEA

Faculty of Chemistry and Chemical Engineering, Babes-Bolyai University of Cluj, 11 Arany Janos Str. Cluj-Napoca 400028 Romania. E-mail: m_socol2000@yahoo.com

ABSTRACT. Flow graphs used in physics and electronics have been applied to chemical kinetics. The expressions of various concentrations of species involved in various mechanisms have been described on the base of the signal flow graphs. Flow graphs were constructed in agreement with the mechanism and differential equations that characterize the time evolution of molecules or radicals involved, and the characteristic determinants for the system. They were applied to substitution, enzyme catalyzed and chain reactions.

INTRODUCTION

Although the steady-state approximation has been used for almost a century[1] in describing complex mechanisms, the condition of constant concentration of the active intermediates is never fulfilled. *The method is said to entail setting to zero the first derivative of the concentration of each intermediates involved in the reaction mechanism.* Even in the well-known mechanism of HBr synthesis, the bromine atom concentration computed by steady-state approximation is in fact the one given by the dissociation of bromine molecule, that is an equilibrium concentration. The less severe condition of very small accumulation rate of intermediate as compared to the one of reactant consumption or product accumulation is in fact the quasi steady state approximation. It has been used for substitution reactions, non-equivalent redox reactions, chain reactions, acid-base catalytic reactions, enzyme catalyzed reactions, or heterogeneous catalyzed reactions. Several examples are discussed in this paper.

To show that, the consecutive reactions with reversible step is being chosen. The reaction sequence for the net transformation of A to C *via* reversible formation of intermediate B is:

$$A \Leftrightarrows B, \quad k_1, k_{-1} \qquad B \longrightarrow C \quad k_2 \tag{1}$$

The differential rate equations are:

$$\begin{aligned} \frac{-d[A]}{dt} &= k_1[A] - k_{-1}[B] \\ \frac{d[B]}{dt} &= k_1[A] - k_{-1}[B] - k_2[B] \\ \frac{d[C]}{dt} &= k_2[B] \end{aligned} \tag{2}$$

In order to integrate them, the system can be simplified in certain circumstances to a far more tractable form. It consist on setting d[B]/dt= 0. A situation is a common one, and method finds wide application in many different chemical systems as enumerated above. As one can see, that is an unduly strict statement of the condition, which must be met to validate the method. Nonetheless, proceeding in this fashion for the moment and equating d[B]/dt to zero, the steady state concentration is:

$$[B]_{ss} = \frac{k_1[A]}{k_{-1} + k_2} \tag{3}$$

It reveals that the concentration of B is not constant but depends on the concentration of starting reactant A. As reaction proceeds, the starting material decays and the steady-state concentration of the intermediate declines. By substituting it to the rate expression of [A] consumption yields:

$$\frac{-d[A]}{dt} = k_1[A] - \frac{k_{-1}k_1[A]}{k_{-1} + k_2} = \frac{k_1k_2[A]}{k_{-1} + k_2} \tag{4}$$

and the accumulation of final product C is:

$$\frac{d[C]}{dt} = k_2[B] = \frac{k_1k_2[A]}{k_{-1} + k_2} \tag{5}$$

It results that the two rates -d[A]/dt and d[C]/dt are equal, as a consequence of setting d[B]/dt = 0. The conservation of mass requires

$$[A] + [B] + [C] = [A]_0$$

Actually, d[B]/dt is not zero. If it were, d[A]/dt would also be zero and no reaction would occur. Thus it seems worthwhile to examine more closely the nature of this approximation, so widely useful. It is necessary and sufficient condition for the validity of the above relations that

$$[B] << [A] + [C]$$

If it is so, from the material balance expressions

$$[A] = [A]_0 - [C] \quad \text{or} \quad [C] = [A]_0 - [A] - [C]$$

results the equality between the rate of consumption of A and accumulation of C. Another approach to exploring the nature of the steady-state approximation is based on the rearrangement of the rate expression of d[B]/dt to

$$[B] = \frac{k_1[A] - d[B]/dt}{k_{-1} + k_2} \tag{6}$$

By using this, the consumption of A is of the form

$$\frac{-d[A]}{dt} = \frac{k_1k_2[A]}{k_{-1} + k_2} + \frac{k_{-1}d[B]/dt}{k_{-1} + k_2} \tag{7}$$

This general equation contains a second term not found in steady-state solution. Another view of the condition needed to reduce this general solution to a simplified one resulting in steady-state approximation is:

$$\frac{d[B]}{dt} << \frac{k_1 k_2 [A]}{k_{-1}} \tag{8}$$

This is a condition[2] far less restrictive than the starting mathematical statement d[B]/dt = 0.

For the system with mixed consecutive and parallel processes

$$A + B \Leftrightarrows C \qquad k_1, k_{-1}; \qquad C + D \rightarrow P \qquad k_{2;}$$

where C is an active intermediate, the condition of steady-state validity is:

$$\frac{d[C]}{dt} << \frac{k_1 k_2}{k_{-1}} [A][B][D] \tag{9}$$

These general rules were applied to various reaction systems as enumerated above. It is often important to compare the form of an experimental rate law with the one derived for the proposed mechanism. The rate law is expressed in terms of the concentrations of reactants, products, and catalysts in the reaction mixture, eliminating the concentrations of the reaction intermediates. The comparison is needed to learn whether each postulated mechanism is consistent with the data. For that reason one must develop some facility with the derivations.

Graphs and diagrams of various types have been used to depict reaction mechanisms in chemistry as chain processes, catalyzed processes, and enzyme-catalyzed processes[3,4]. Temkin[5-7] and Segal[8] have proposed a convenient version of cyclic graphs. These graphs incorporate only intermediate species as vertices and not starting materials and main or secondary products. They were used to deduce - in a quite simple way - the concentration of reactive intermediates and the overall reaction rate[9-14]. Inspired by the flow graphs used in electronics, physics and engineering[15-17], we show in this work how to use flow graphs to associate them with reaction mechanisms in order to obtain some kinetic characteristics of any reaction scheme. Besides the intermediates, these graphs incorporate also the starting chemical species, the main and secondary products. At the same time, we associated determinants to chemical change and constructed graphs on this base. Our approach has the advantage of offering the opportunity to calculate the concentration of any species involved either being in a quasi-steady-state or a transient concentration.

In dealing with complex reaction kinetics we have applied signal flow graph[18]. A flow graph is a diagram that represents a set of simultaneous differential equations connecting the system variables which could be solved by using Cramer method[15,19]. It consists of a network in which vertices or nodes, representing chemical species involved in the mechanism, are connected by edges acting as signal multipliers. These signal flow graphs (SFG) depict the flow of signals from one point of the system to another, give the relationships among signals and yield the determinants of the systems. We consider here the flow graphs for several examples where the steady state has been applied above in order to see how simple is this way to reach the steady-state concentration of intermediates or to find the rate law.

The basic principles of flow graphs, their properties, their algebra along with several applications have been presented previously[18].

APPLICATIONS

Monomolecular nucleophilic substitution. A classical example is the S_N1 mechanism for substitution in organic or inorganic chemistry. The replacement of H_2O from complexes $ML_6(H_2O)^{n+}$ by an anion Y^- has been found to be essentially first-order in both complex and substituting anion over a large range of conditions. Experiments of this kind are not entirely satisfactory with positively charged complexes because of complications brought about by ion-pair formation. To avoid this, anionic complexes were used. The concentration of $Co(CN)_5H_2O^{2-}$ has been found to conform to a S_N1 mechanism[20]:

$$\begin{aligned} &Co(CN)_5H_2O^{2-} \Leftrightarrows Co(CN)_5^{2-} + H_2O \qquad k_1, k_2 \\ &Co(CN)_5^{2-} + Y^- \longrightarrow Co(CN)_5Y^{3-} \qquad k_3 \end{aligned} \tag{10}$$

with Y^- being Br^-, I^-, CN^-, CNO^-, OH^-. The steady-state concentration for pentacoordinate intermediate is:

$$[Co(CN)_5^{2-}]_{ss} = \frac{k_1[Co(CN)_5H_2O]}{k_2 + k_3[Y^-]} \tag{11}$$

and the rate law:

$$\frac{d[Co(CN)_5Y^{3-}]}{dt} = \frac{k_1k_3[Co(CN)_5H_2O][Y^-]}{k_2 + k_3[Y^-]} \tag{12}$$

The apparent first-order rate coefficient expression can be rearranged in a linear form. From various k_{obs} determined under various experimental conditions a various incoming ligands, a value of $k_1=1.6\times10^{-3}$ s^{-1} has been found.

For this system the flow graph is depicted bellow[18]:

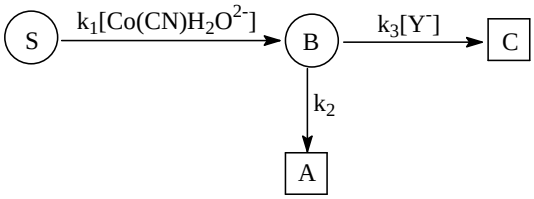

Fig.1. *The global flow graph*

where "S" represents the source of the interested species (B) or the input node, "B" is $Co(CN)_5^{2-}$, "C" is $Co(CN)_5Y^{3-}$ and "A" refers to $Co(CN)_5H_2O^{2-}$. It is observed that the reactant $Co(CN)_5H_2O^{2-}$ take place to the source and in the same time as an output node because it is formed in the first reversible reaction. The transmittances are the pseudo-first-order rate constants with respect to $Co(CN)_5^{2-}$ (B).

$$[Co(CN)_5^{2-}] = \frac{\text{The formation} \quad \text{det er min ant}}{\text{The consumption} \quad \text{det er min ant}} \tag{13}$$

The *formation flow graph* results from the main graph in which the interested species (B) becomes the target (the output node):

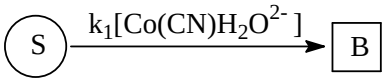

Fig. 2. *The formation flow graph of the species B*

$$\Delta_{formation} = k_1[Co(CN)H_2O^{2-}] \quad (14)$$

From the consumption determinant a graph (*the consumption flow graph*) is derived, which indicates the flowing from the transitional species to the output nodes and is obtained from the main flow graph eliminating the source:

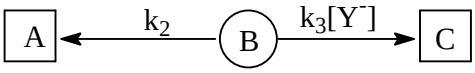

Fig. 3. *The consumption flow graph*

The value of the consumption determinant results from adding the transmittances of the independent ways to obtain a products[15-17]:

$$\Delta_{consumption} = k_2 + k_3[Y^-] \quad . \quad (15)$$

It results that

$$[Co(CN)_5^{-2}] = \frac{k_1[Co(CN)H_2O^{-2}]}{k_2 + k_3[Y^-]} \quad (16)$$

which is the same with that obtained above (11).

Enzymatic reactions. An representative example of enzymatic reaction is:

$$\begin{aligned} S + E &\Leftrightarrow X_1 && k_1, k_{-1} \\ X_1 + S &\rightarrow P + E && k_2 \\ X_1 &\Leftrightarrow X_2 && k_3, k_{-3} \\ X_2 &\rightarrow X_3 + E && k_4 \end{aligned} \quad (17)$$

with the rate law: $r = k_2[S][X_1]$.

By applying the QSSA, we obtain:

$$r = \frac{k_1 k_2 [S]^2 [E]_0}{k_1[S] + k_2[S] + k_{-1} + \frac{k_1 k_3 [S]}{k_{-3} + k_4} + \frac{k_3 k_4}{k_{-3} + k_4}} \quad (18)$$

The same results were obtained by King and Altman[4] using a schematic method of deriving the rate laws for enzyme catalyzed reactions, and also by Segal and co-workers[9,10] using the graph method. In the case of enzymatic reaction, the global signal flow graph is the perfect image of the mechanism:

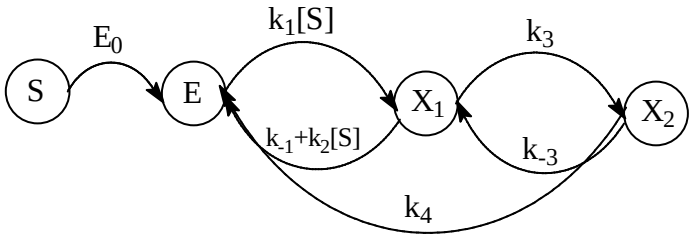

Fig. 4. *The global flow graph for enzymatic reaction*

The enzyme balance is $[E]+[X_1]+[X_2] = [E]_0$. The consumption of each species leads to the formation of the others species, so the consumption determinant could be written as a summation of three determinants[4] resulting from the flow graphs, characterized by the propriety that every species becomes the target species (the output node):

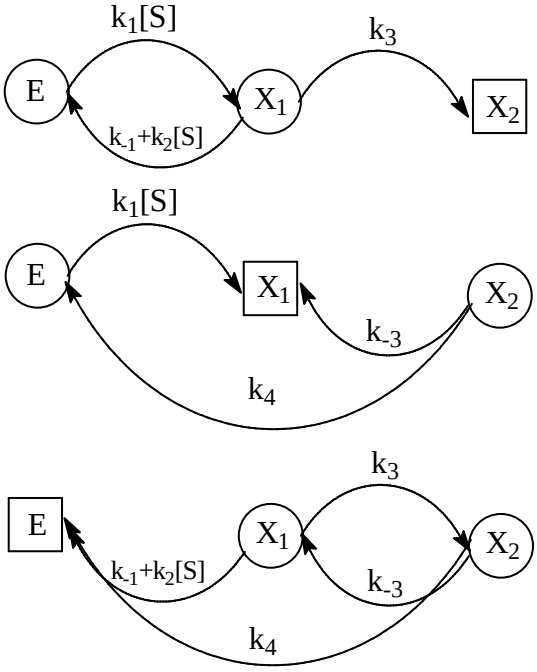

Fig. 5. *The consumption flow graphs of the implied specie*

Using the algebra properties of the flow graph[15-17,21] the consumption is:

$$\Delta_{\text{consumption}} = k_1[S]k_3 + (k_{-3} + k_4)k_1[S] + (k_{-3} + k_4)(k_{-1} + k_2[S]) + k_3k_4 \quad (19)$$

The formation flow graph for the intermediary "X_1" is:

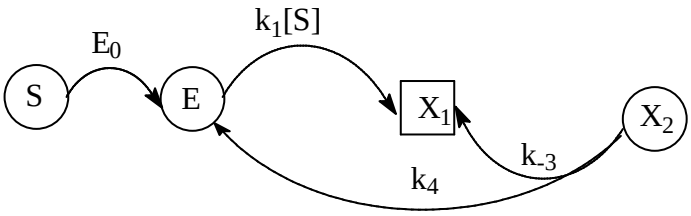

Fig. 6. *The formation flow graph for the species X_1*

"S" is the source or input node and represents, in this case, the initial concentrations of the involved species. The value of the formation determinant is:

$$\Delta_{X1} = E_0k_1[S]k_4 + E_0k_1[S]k_{-3} = E_0k_1[S](k_{-3} + k_4) \quad (20)$$

$$[X_1] = \frac{\Delta_{X1}}{\Delta_{\text{consumption}}} = \frac{E_0k_1[S](k_{-3} + k_4)}{k_1[S]k_3 + (k_{-3} + k_4)k_1[S] + (k_{-3} + k_4)(k_{-1} + k_2[S]) + k_3k_4} \quad (21)$$

Knowing that the rate law is $r = k_2[S][X_1]$ we obtain:

$$r = \frac{k_1k_2[S]^2[E]_0}{k_1[S] + k_2[S] + k_{-1} + \frac{k_1k_3[S]}{k_{-3} + k_4} + \frac{k_3k_4}{k_{-3} + k_4}} \quad (22)$$

which is the same result as that given by King and Altman[4] andE.Segal[9,10].

Chain Reactions. The application refers to gas decomposition of ethanal. The main reaction is:

$$CH_3CHO \rightarrow CH_4 + CO \quad (23)$$

and exhibits a fractional order 1.5 on ethanal. Trace quantities of C_2H_6 and H_2 were also detected in the products. Consider the following chain mechanism[22]:

Initiation	$CH_3CHO \rightarrow CH_3^{\cdot} + CHO^{\cdot}$	k_1
	$CHO^{\cdot} \rightarrow CO + H^{\cdot}$	k_2
	$CH_3CHO + H^{\cdot} \rightarrow H_2 + CH_3CO^{\cdot}$	k_3
Propagation	$CH_3^{\cdot} + CH_3CHO \rightarrow CH_4 + CH_3CO^{\cdot}$	k_4
	$CH_3CO^{\cdot} \rightarrow CH_3^{\cdot} + CO$	k_5
Termination	$2\,CH_3^{\cdot} \rightarrow C_2H_6$	k_6

(24)

The formyl radical produced in the initiation reaction does not enter the chain reaction but gives the rise to secondary products. Making the steady state approximation, in order to eliminate the intermediate concentrations, one can derive the rate law:

$$\frac{d[CH_3]}{dt} = k_1[CH_3CHO] - k_4[CH_3CHO][CH_3] + k_5[CH_3CO] - 2k_6[CH_3]^2 = 0$$

$$\frac{d[CHO]}{dt} = k_1[CH_3CHO] - k_2[CHO] = 0$$

$$\frac{d[H]}{dt} = k_2[CHO] - k_3[H][CH_3CHO] = 0 \qquad (25)$$

$$\frac{d[CH_3CO]}{dt} = k_3[H][CH_3CHO] + k_4[CH_3][CH_3CHO] - k_5[CH_3CO] = 0$$

Addition of the steady-state conditions for the intermediates gives the result:

$$2k_1[CH_3CHO] = 2k_6[CH_3]^2 \quad ; \quad [CH_3]_{ss} = \sqrt{\frac{k_1[CH_3CHO]}{k_6}} \qquad (26)$$

and the rate is:

$$-\frac{d[CH_3CHO]}{dt} = 2k_1[CH_3CHO] + k_4\left(\frac{k_1}{k_6}\right)^{1/2}[CH_3CHO]^{3/2} \qquad (27)$$

This result is in agreement with the experimental rate law, provided the second term is much larger than the first. For long chain approximation, meaning that the substrate is consumed mainly in propagation step, this holds. Therefore, the experimental rate constant is:

$$k_{obsd} = k_4\left(\frac{k_1}{k_6}\right)^{1/2} \qquad (28)$$

The global flow graph of the equation system is a perfect image of the reaction mechanism[18]:

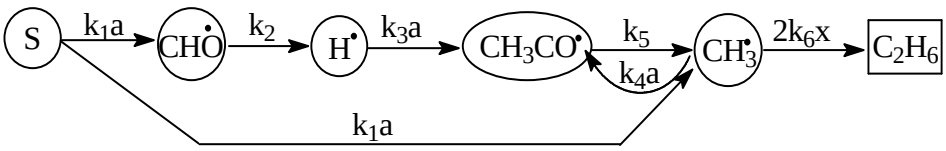

Fig. 7. *The global flow graph of system (24)*

where "S" represents the reactant CH_3CHO. The transmittances are the pseudo-first order rate constants with respect to the intermediate species; "a" means $[CH_3CHO]$ and "x" is $[CH_3]$.

The consumption flow graph is obtained from the system flow graph eliminating the source (input node):

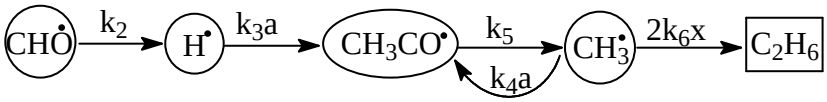

Fig. 8. *The consumption of the radical specie flow graph*

$$\Delta_{consumption} = k_2 \cdot k_3 a \cdot k_5 \cdot 2k_6 x \tag{29}$$

The formation flow graphs are drawn considering the species of interest as target nodes (output nodes). Their values are the product of the transmittances, starting from the source to the target species.

The formation flow graph for $CH_3^{\cdot}$ is:

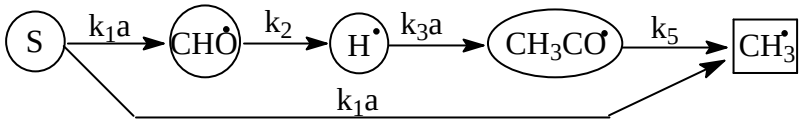

Fig. 9. *The formation of $CH_3^{\cdot}$ radical flow graph*

$$\Delta_{fCH3} = k_1 a \cdot k_2 \cdot k_3 a \cdot k_5 + k_1 a \cdot k_2 \cdot k_3 a \cdot k_5 = 2\, k_1 a \cdot k_2 \cdot k_3 a \cdot k_5 \tag{30}$$

$[CH_3] = x = \Delta_{fCH3} / \Delta_{consumption}$ and results:

$$k_1[CH_3CHO] = k_6[CH_3]^2 \quad ; \quad [CH_3] = \sqrt{\frac{k_1[CH_3CHO]}{k_6}} \tag{31}$$

which is the same result as discussed above.

The formation flow graph for $H^{\cdot}$ is:

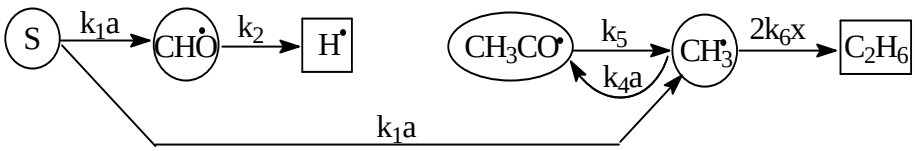

Fig. 10. *The formation of the $H^{\cdot}$ flow graph*

$$\Delta_{fH} = k_1 a \cdot k_2 \cdot k_5 \cdot 2k_6 x \tag{32}$$

Inserting the intermediate concentration obtained from the ratios of determinants into the rate law, gives:

$$-\frac{d[CH_3CHO]}{dt} = 2k_1[CH_3CHO] + k_4\left(\frac{k_1}{k_6}\right)^{1/2}[CH_3CHO]^{3/2} \tag{33}$$

which is identical to that obtained by applying the classical QSSA.

When one becomes accustomed to the flow graph all the formation or consumption determinants can be written directly from the global graph scheme and their concentrations calculated straightforward. The overall rate is immediately deduced. It avoids the need of detailed calculations with QSSA.

Acknowledgement.

The authors greatly acknowledge CNCSIS for financing this work by Grant no.4/164, 2003.

REFERENCES

1. M. Bodenstein, *Z. Physik. Chem*., **1913**, 85, 329.
2. H. S. Johnston *Gas Phase Reaction Rate theory*, Ronald Press, New-York, **1969**, 329-332.; L. Volk, W. Richardson, K. H. Lau, M. Hall. S. H. Lin, *J.Chem. Educ*., **1977**, 54, 95.
3. J. A. Christiansen, *Adv. Catalysis,* **1953**, 5, 311-353.
4. E. L. King, C. Altman, *Phys. Chem.*, **1956**, 60, 1375
5. M. I. Temkin , *Dokl. Akad. Nauk SSSR,* **1963**, 152, 156-159.
6. M. I. Temkin, *Dokl. Akad. Nauk SSSR,* **1965**, 165, 615-618.
7. M. I. Temkin, *Mechanism and Kinetics of Complicated Reactions*, S. Z. Roginski, Moscow, **1970**, p. 57.
8. E. Segal, *Ann. Univ. Bucuresti,* **2003**, 12(1-2), 257.
9. E. Segal, *Progress in Catalysis,* **1997**, *6,* 135-141.
10. E. Segal, *Progress in Catalysis,* **1998**, *7,* 1-4.
11. O. N. Temkin , D. G. Bonchev , *J. Chem. Ed.,* **1992**, 69, 544-550.
12. A. V. Zeigarnik, O. N. Temkin, D. G. Bonchev, A. V Zeigarnik, *J. Chem. Inf .Comput .Sci,* **1995**, 35, 729-737.
13. A. V. Zeigarnik, O. N. Temkin, D. G. Bonchev, *J. Chem. Inf. Comput. Sci,* **1996**, 36, 973-981.
14. A. V. Zeigarnik , *Kinet .Katal.*,**1996***, 37*, 372-385.
15. K. Ogata, *Modern Control Engineering,* Prentice Hall International, New Jersey, **1995**.
16. N. S. Nice, *Control System Engineering,* Addison-Westley Publishing Company, **1995**, p. 240-260, 268-275.
17. R. C. Dorf, R. H. Bihop, *Modern Control System*, Prentice Hall International, New Jersey, **2001**, p. 66-80,118-158.
18. M. Socol, I. Baldea, *Studia Univ. Babes-Bolyai, Chem*. **2003**, 48(1), 109.
19. A. C. Aitken, *Determinants and Matrices,* Oliver and Boyd, Edinburgh, **1939**, Chap. 2.
20. A. Haim, W. K. Wilmarth *, Inorg. Chem*.,**1962**, *89,* 573; R.G. Pearson , F. Basolo, *J. Am. Chem. Soc.*, **1956**, 78, 4878.
21. T. Ionescu, *Grafuri. Aplicatii. Vol 1.* Ed. Didactica si Pedagogica, Bucuresti , **1973**, p. 198- 207.
22. J. W. Moore, R. G. Pearson, *Kinetics and Mechanism*, 3-rd Ed. Willey, New York, **1981**; J. H. Espenson, *Chemical Kinetics and Reaction Mechanisms,* McGraw-Hill Book Co. New-York, **1981**, p. 137.

STUDIA UNIVERSITATIS BABEŞ-BOLYAI, CHEMIA, XLIX, 1, 2004

PROBABILISTIC APPROACH AND SIMULATION METHODS FOR RISK ASSESSMENT

CĂLIN I. ANGHEL[*], RADU IATAN[**]

** Department of Chemical Engineering, Faculty of Chemistry and Chemical Engineering, University "Babeş-Bolyai", 400028 Cluj-Napoca;*
*** Department of Technological Equipment, Faculty of Mechanical Engineering, University "Politehnica" Bucuresti,*

ABSTRACT. The purpose of this paper is to present a probabilistic approximation procedure for the risk assessment, suitable for technological equipments. It is reported like a risk of failure for a tank vessel type during its serviceable life. Simulation technique of a threshold value, named the limit state function (LSF), was prefered. It was conducted under the direct simulation method named *Latin Hypercube Sampling* (LHS). The *LSF* was establishing on the base of the growth of a local admissible flaw of the welding seams until the fracture occurs. A professional analysis package *Cristal Ball 2000-free trial version*, was used to perform the simulation. Finally the study reveals the probabilistic assessment of failure for a chlorine tank under technological loads and design parameters. The study estimates the risk of damage as a measure for the safety. Highly values for *LSF* lead to low values for the risk of failure. This threshold value may be a key factor for engineers to decide when the structure can become unsafe. The method can be used to predict the probability of failure, such as the limit-state in risk and reliability analysis. This type of study is suitable for chemical engineers to work out optimal inspection and mentenance schedules

1. Introduction

The behaviour of any technological equipment for process industries under operating conditions are always affected by variability and uncertainties; for example, variations in service loadings, scatters in material properties, chemical degradation and so one. The level of safety of these structures – often estimated by the load carrying capacity diminish with time and the risk of a major technological accident increase. Many studies were developed in order to maintain an acceptable level of safety and avoid technological incidents, achieving improvements in serviceability assessment. Some of the main issues related are: (a) introduction of qualitatively representation of service loads, (b) more consistent analysis of load effect combination and (c) transition to probabilistic reliability assessment concept.

The aim of this paper is to present a procedure suitable for engineers in the stage of a preliminary risk analyse, to avoid major technological incidents. It focuses on the reliability assessment concept. The development of computer technology allows a transition from deterministic structural reliability assessment methods to 'fully' probabilistic concepts using the full potential of the computer. The need to incorporate variability and uncertainties in an engineering design has long been recognized. One of the traditional approach, the so-called ''deterministic design'', makes use of

safety coeficients in order to prevent unpredicted failures due to the variability of the data. On the other side, a relatively new trend, named "probabilistic design", allowing the estimation of the reliability of the design, considers the full stochastic variability of the data.

Briefly, the reliability of an engineering system can be defined as its ability to fulfill its design purpose for a time period. The fundamental base to measure this ability is provided by the theory of probability. So the reliability of a structure can be viewed as the probability of its satisfactory performance according to some performance functions under specific service conditions within a stated time period. In estimating this probability, system uncertainties are modeled using random variables with probability distribution functions. Many methods have been proposed for structural reliability assessment purposes, such as: first-order reliability method (FORM), first-order second moment method (FOSM), advanced second moment method (ASM) and computer-based simulation methods [6-8].

In this paper only the computer-based probabilistic simulation method for reliability assessment is presented. It is a direct simulation method, named *Latin Hypercube Sampling* (LHS). Latin hypercube sampling is considered to be a development of simple random sampling or *Monte Carlo Simulation*. It is more efficient than simple random sampling *Monte Carlo Simulation* (MCS). It requires fewer simulations to produce the same level of precision. Latin hypercube sampling is generally recommended over simple random sampling when the model is complex or when time and resource constraints are an issue. Like as *Monte Carlo Simulation*, *Latin Hypercube Sampling* is a computer-based method of analysis that uses statistical sampling techniques in order to obtain a probabilistic approximation to the solution of a mathematical equation or model.

The study reported as a probabilistic assessment of failure for a chlorine tank, under the technological loads and design parameters, has two distinct objectives. The first is the crude probabilistical estimation of failure of a tank-type reactor. The second is the preliminary assessment of the safety level or the risk level. Based on the general presumptions of the probabilistic simulation methods the formulation of a performance or limit state function (LSF) it is necessary. This function represents the total performance of the structure and includes the main operating and dimensional parameters. Simulation technique based on a professional risk analysis package Cristal Ball 2000-free trial version are used to estimate the probability of failure under operating parameters. The main stages of this approach are:

- establishing the *LSF* on the base of failure pressure function;
- establishing the probability of failure based on the *LSF;*
- assessing the risk level.

The model and the established *LSF* contain some idealizations and assumptions, which can introduce additional uncertainties. Supplementary a sensitive analysis-according variance reduction of the *LSF* to the basic variables on which depends may be performed. This is necessary to identify the most important variables in failure analysis, so the model could be improved by focusing on the most crtitical parameters.

2. Theoretical considerations

To avoid some cumbersome approaches, unnecessary for the purpose of this paper, only general design standard limitations [1,2] are considered. For simplicity, the main idealisations and assumptions are mentioned:

• basic variables: material properties, design parameters, rate of corrosion-erosion, operating parameters, depth of acceptable defect, etc. are assumed to be random variables;

• any estimator is statistic, hence any estimated parameter is a random variable;

• the random variables were assumed to be statistically independent – just for simplicity;

•it will be considered only two constructive areas of the tank: *"I"* for the collecting bottom closure and *"II"* for pipe connections "R7A , R7B";

There are a lot of methods to establish the failure pressure model. Based on general design standards [4,5,8] the failure pressure model choosen in this paper derived from one deterministic, when the damage is done by a pre-existing initial flaw on welding joints that escaped in non-destructive detection. Then the limit state function (*LSF)* is expressed as a failure pressure mode, reported to fracture mechanics, on the base of the critical energy for propagation the admissible flaws of the welding seams.

2.1 Latin Hypercube Sampling (LHS).

Latin hypercube sampling is a stratified sampling scheme designed to ensure that the upper or lower ends of the distributions used in the analysis are well represented. Because direct *Monte Carlo simulation* is a foundation for *Latin hypercube sampling* technique, some general statements is timely. The direct *Monte Carlo simulation* is a process of approximating the output of a model through repetitive random application of a model's algorithm. In the context of the *cumulative distribution function* of a real-valued random variable *X* the output of the model may be generally defined as $P(x) = \Pr ob\{X \le x\}$.

The corresponding notion for a multidimensional random vector $(X_1, X_2, ...X_n)$ is the *joint cumulative distribution function*

$$P(x_1, x_2, ...x_n) = \Pr ob\{X_i \le x_i \rightarrow for \cdots all \cdots i = 1...n\}.$$

Considering the *joint density function* we have the relationship :

$$\Pr ob\{x \in D\} = \int_D f(x_1, x_2, ...x_n) \cdot dx_1 \cdot dx_2 \cdots dx_n, \quad (1)$$

where $D \subset R^n$ for any Lebesgue measurable subset.

The reliability of a process equipment structure using the computer simulation methods can be estimated based on a performance or limit state function (LSF). In the context of previous statements these functions can be expressed in terms of basic random variables *Xi* for relevant loads and structural strength. Mathematically, the performance function *Z* can be described as

$$Z = Z(X_1, X_2, ...X_n) \quad (2)$$

where *Z* is called the limit state function (LSF) of interest. The unsatisfactory performance limit state of interest can be defined as $Z \le 1$. Accordingly, with $Z < 1$, the structure is in the unsatisfactory performance state and when $Z > 1 \approx D$ it is in the safe state. If the joint probability density function for the basic random variables *Xi* 's is $f_{X_1, X_2, ...X_n}(x_1, x_2, ...x_n)$ then the unsatisfactory performance probability P_U of a structure can be given by the integral:

$$P_u = \iint_D \cdots \int\int f_{X_1, X_2, \ldots X_n}(x_1, x_2, \ldots x_n) \cdot dx_{x_1} \cdot dx_2 \cdot \ldots dx_n \tag{3}$$

where the integration is performed over the domain *D* in which $Z > 1 \approx D$. In general, the joint probability density function is unknown and the integral is a difficult and cumbersome task.

Due to the difficulties in solving this integral Eq. (3) for practical purposes alternate methods of evaluating P_U are required. One of these methods is the direct simulation method named *Latin Hypercube Sampling* (LHS). This sampling method is a stratified sampling scheme designed to ensure that tails of the distributions used in the analysis are well represented. This simple and intuitive method consists in calculating Eq. (2) for a great number of combinations of X_i. The combinations, called ''trials'', are randomly sampled from the probability distribution of each X_i, by means of the standard random-generator functions implemented on any modern computer.

The probability P_U according to the performance function of Eq. (2) is provided by the integral of Eq. (3). The larger the margin of safety *Z* and the smaller its variance, the larger the needed simulation effort to obtain sufficient simulation runs with unsatisfactory performances. In other words, smaller unsatisfactory-performance probabilities require larger numbers of simulation cycles. Assuming N_U to be the number of simulation cycles for which $Z < 0$ in a total *N* simulation cycles, unsatisfactory performance probability P_U of a structure given by the integral Eq. (2) can be expressed as:

$$P_U = N/N_U . \tag{4}$$

2.2 Crack propagation model

To avoid cumbersome approaches only general design standard and several already published papers [1-6] limitations are considered. Based on general design standards settlements, the critical load model used in this paper derived from one deterministic model. Accordingly some scenarios of failure, mentioned in several already published works [3-6,8], the admissible value of a pre-existing initial flaw on welding joints that escaped in non-destructive detection is consider a threshold value for fracture. These flaws are approximated with a curved crack in a plane stress state. Based on the general statements of fracture mechanic, the *LSF* is established on the base of the spreading the local admissible flaws of the welding seams, until the fracture occurs. The flaws increasings are assumed to be linearly directly along the crack direction. The analyze is reported to the welding seam in the two areas of interest, on the base of critical energy of spreading the admissible flaws of the welding seams.

When the amplitude of stress intensity factor reaches the value for the impact ductility $KCV \approx K_{IC,}$ the crack propagation will become unstable. According to some previous papers [3,4] related to fracture for a ductile elastic-plastic steel type R52 STAS 2883/2-80, the *LSF* is reported as the matching of the fracture toughness of the materials K_{IC} and the stress intensity factor K_I. Based on the previous statements, the general form of the *LSF* in this stage is:

$$\mathrm{LSB} = K_{IC} / K_I \geq 1; \tag{5}$$

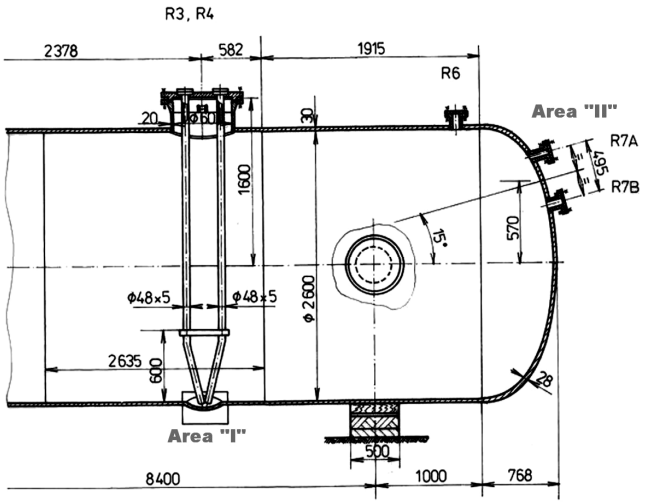

Fig. 1. *The main design and constructive dimensions of the tank*.

On these presumptions, two distinct *LSF* may be defined for the areas of interest:

"Area I"

$$LS1B = \frac{\left[1{,}034 \times E \times KCV\right]^{0,5}}{\left[1{,}77KA1 \times R_{S1}^{0,5}\left[\frac{Pe \times (D + Sp - Vc \times Tu)}{Ks \times (Sp - Vc \times Tu)} + \frac{10Mi \times De}{\left[De^4 - (D - 2Vc \times Tu)^4\right]}\right]\right]} \geq 1 \quad (6)$$

"Area II"

$$LS2B = \left[1{,}034 \times E \times KCV\right]^{0,5} \Big/ \left[1{,}77KA2 \times R_{F1}^{0,5}\left[\frac{Pe \times (D + Sp)}{Ks \times Sp}\right]\right] \geq 1. \quad (7)$$

Table 1.

The main values of design and simulation parameters

Parameters	**Values**	**Statistical distribution**
Elasticity modulus, E[MPa]	210000	N
Corrosion rate, Vc[mm/an]	0.5	N
Working elapsed time, Tu[year]	10	W
Fracture toughness, K_{IC}[N/mm$^{3/2}$]	2115	N
Yielding strength, $\sigma_{0,2}$[MPa]	340	N
Fracture strength, σ_r[MPa]	510	N
Inner diameter, D[mm]	2600	N
Design body thickness, Spc[mm]	25.5	N
Design bottom thickness, Spf[mm]	30	N

Parameters	Values	Statistical distribution
Operating pressure, Pe[Mpa]	1.6	W
Welding seam's radius, Rs1[mm]	200	N
Maximum bending moment, Mi[N*mm]	340000000	N
Hole's pipe diameter, d[mm]	40	N
Bottom's radius, Rif[mm]	1300	N
Welding seam's radius, Rs2[mm]	20	N
Welding factor *Ks*	1.8	N
*** According to technical book of the tank "Ch. 441.437 – 7" and Fig. 1		

The geometrical shape factors of the flaws in the areas of interest ***"I"-"II"*** were defined according related statement [3] by the following form:

$$KA1 = \left[0{,}5\sin\alpha_1 \times (1+\cos\alpha_1)^{0,5}\right] \Big/ \left[1-\sin^2\frac{\alpha_1}{2}\right] \tag{8}$$

$$KA2 = \left[0{,}5\sin\alpha_2 \times (1+\cos\alpha_2)^{0,5}\right] \Big/ \left[1-\sin^2\frac{\alpha_2}{2}\right]. \tag{9}$$

where the angular rates for the spreading of the flaws, α_1 and α_2, may be calculated by an approximate expression :

$$\alpha = \frac{2a}{2R_{C,F}} \times \frac{180}{\pi} \text{ [degree]}, \tag{10}$$

where *"2a"* is the initial or current size of the flaws.

Based on some general assumptions presented in some related papers [4,6,8], the crack propagation model to catastrophic failure is evaluated under the Paris-Erdogan's law,. in the following basic form:

$$\frac{da}{dn} = \frac{C \cdot (\Delta K_I)^m}{(1-R)\cdot[K_{IC} - \Delta K_I]^s} \tag{11}$$

where *da/dn* is the crack propagation rate, ΔK_I is the change in the stress intensity factor K_I at the crack tip for the "*nth"* cycle; *C*, *m*, s, ΔK_I, K_{IC} are material constants and *R* is the cyclic amplitude ratio. Finally the characteristic forms of the *LSF* in the areas of interest is given by the following expressions [4]:

"Area I"

$$N_{CI} = 8{,}17\times10^{12} \times \int_{a_0}^{a_m} \frac{da}{K_{I1}^{2,93}} + 3{,}07 \div 10^{8} \times \int_{a_m}^{a_{critic}} \frac{2115 - K_{I1}}{K_{I1}^{2,61}} da\,; \tag{12}$$

"Area II"

$$N_{CII} = 8{,}17\times10^{12} \times \int_{a_0}^{a_{critic}} \frac{da}{K_{I2}^{2,93}}. \tag{13}$$

The *LSF* defined by the previous Eq.(5-10) state the safety margins during tank's service. Reaches or overfulfilment the limit state values of these is evaluate probabilistic from *Latin Hypercube Sampling*. Thus the probability of *LSF's* values under the limit state range is defined as the safety domain. According to the basic probability statements, the probability of failure will be stated as the reverse. Finally, considering a comparative assessment of these scenarios, risk assessment of failure for the chlorine tank is judged on the base of the values of this limit state functions, yielding the probability of failure.

3. Numerical applications and discussions

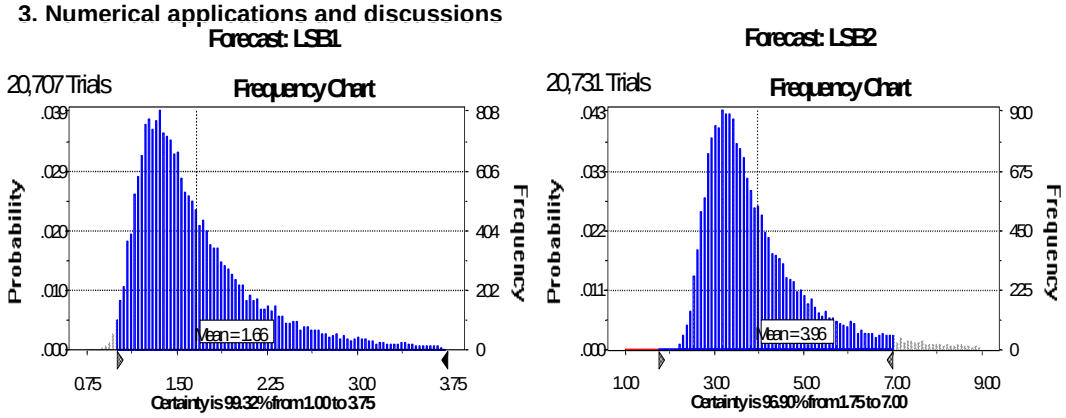

Fig.2. *Probability forecast for LSF on the base of the fracture propagation.*

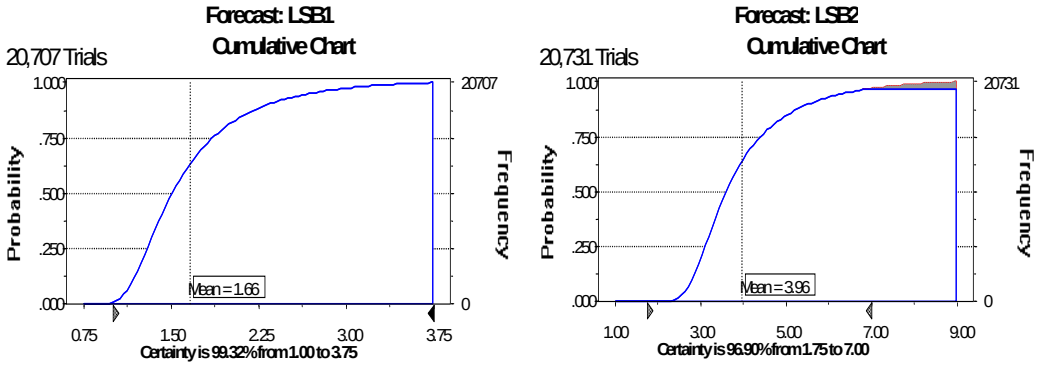

Fig. 3. *Cumulative probability forecast for LSF on the base of the fracture propagation.*

Numerical simulations based on two alternative principles, a maximum number of 100.000 trials or a control of precision defined by the minimum confidence parameters of 95% reported to standard deviation, were conducted under the *Latin Hypercube Sampling*. The probability trends for *LSF* reported as the safety coefficients and the matching of both fracture toughness K_{IC} and stress intensity factor K_I are significant for the *LSB1* in the *"Area I"*(Fig. 4). Thus on the basis of probability histograms (Fig.2-3.) the probability of crack progression to failure is meaningful only in the *"Area I"*, when*:*

Probability of failure = 1- Certainty $\Rightarrow$1 – 0,9932 = 0,0068.

According to Mc.Leods and Plewes's scale, this probability of failure suits on the scale of risk in the range between $10^{-2}…10^{-3}$. This risk is characterized as a reduced one. Due to the variations in service load during service elapsed time, a fatigue damage can occur. Hence, the containment of this damage becomes essential for the safety working life of the tank.

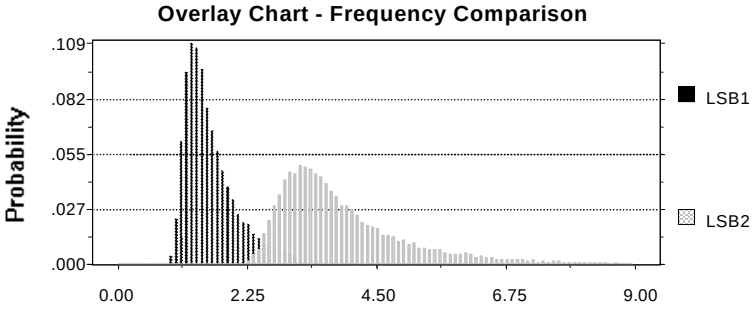

Fig. 4. *Overlay trend probability forecast for LSF*

Based on general crack propagation model, evaluated under the Paris-Erdogan's law Eq. (11-13), when serviceable elapsed lifetime is assimilated to one variable cyclic pressure low rate, numerical simulated values for the crack growth were obtained (Fig.5). Numerical simulated results and the linear crack propagation are in reasonable agreement with probability histograms.

On the base of these simulations, feasible *N* load cycles or the assessment of safety serviceable life may be evaluated (Table 2).

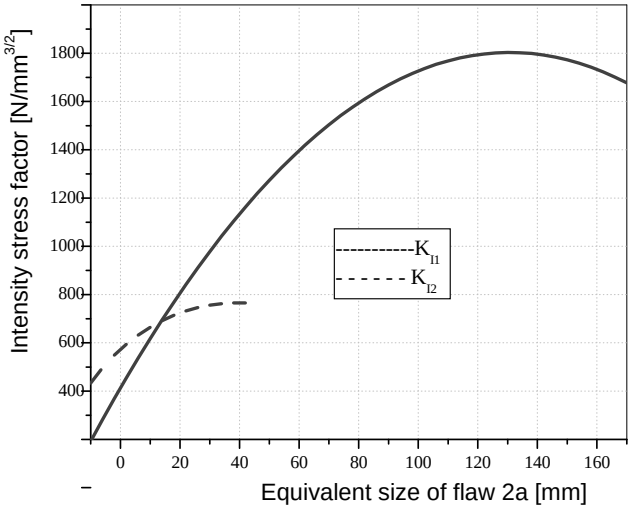

Fig. 5. *Crack growth considering the fracture propagation in the areas of interest.*

Table 2.

Crack propagation scenario for admissible flows

Area "I"		**Area "II"**	
Initial flaw 2a=3mm	Initial stress concentration factor K_{I1} =327[N/mm$^{3/2}$]	Initial flaw 2a=3mm	Initial stress concentration factor K_{I2} =433[N/mm$^{3/2}$]
Final flaw 2a=155mm	Final stress concentration factor K_{I1} =1815[N/mm$^{3/2}$]	Final flaw 2a=16mm	Final stress concentration factor K_{I2} =765[N/mm$^{3/2}$]
Predicted service lifetime cycles N_{CI} = 2.112×10^5 cycles		Predicted service lifetime cycles N_{CI} = 1,89×10^5 cycles	

Additional assumptions:

- the crack propagation will become unstable when $KCV \approx K_{IC,}$ $K_I \approx K_{IC}$.
- $K_{IC} \cong 2115$ [N/mm$^{3/2}$], the impact ductility of material;
- Assuming N≈100 load cycles/day during a serviceable life $T_U \approx 300$ days/year, the safety probabilistically serviceable life in the areas of interest are:
  - In the *"Area-I"* approximate 2,3 years;
  - In the *"Area-II"* approximate 2,1 years

4. Conclusions

The paper introduces a probabilistic approximation procedure for calculating the risk of failure, named the risk assessment for tank vessel during its serviceable life. Numerical results demonstrate a significant dependence on the operational and design state of the tank vessel. These approaches reduce the need for excessive safety margins in design and more cumbersome experimental and analytical approaches. High values for *LSF* lead to low values for the risk of failure. This threshold value may be a key factor suitable for engineers to decide when the structure can become unsafe. The method can be used to predict the probability of failure, such as the limit-state in risk and reliability analysis. This type of study is recommended for engineers, specially for chemical engineers to work out optimal inspection and maintenance schedules.

REFERENCES

1. *** Design Standard C4-90*,* Technical Publishing House Bucharest, 32-70.
2. *** Standard of Chemical Industry, IITPIC-NID-7438-78, 14-29, 105-110.
3. Al. Pavel, *Safe operation of Petrochemical Equipment*, **1987**, Technical Publishing House Bucharest, v.1-2 (In Romanian).
4. M. Teodorescu, Rev. Chim., **1982**, 33, (9), 859-862.

5. W. Shen, A. B. O. Soboyejo, W. O. Soboyejo, *Int. J. Fatig.*, **2001**, 23, 917-925.
6. S. Rahman, G. Chen, R. Firmature, Int. J. Pres. Vessels. Piping, **2000**, 77, 3-16.
7. D. G. Robinson, *A Survey of Probabilistic Methods Used In Reliability, Risk and Uncertainty Analysis: Analytical Techniques I*, Sandia National Laboratories, **1998**, Report SAND98-1189.
8. S. Rahman, G. Chen, Fatigue Fract. Engng. Mater. Struct., **2000**, 23, 879–890.

STUDIA UNIVERSITATIS BABEŞ-BOLYAI, CHEMIA, XLIX, 1, 2004

SYNTHESIS AND STEREOCHEMISTRY OF SOME NEW 1,3-OXATHIANES OBTAINED FROM 1,4-DIMERCAPTOTHREITOL

LUMINITA MUNTEAN, IOANA GEORGETA GROSU, DORA DEMETER, NICULINA BOGDAN, SORIN MAGER

"Babeş-Bolyai" University, Faculty of Chemistry and Chemical Engineering, 11 Arany Janos str., RO-400028, Cluj-Napoca, Romania

ABSTRACT. The synthesis and the stereochemistry of some new 1.3-oxathianes with *cis* decaline skeleton are disscused. The NMR investigations revealed the anancomeric structure of compounds.

INTRODUCTION

In the last years [1-7] the 1,3,5,7-tetraoxadecaline (TOD) system was intensively studied, beeing used as "building-block" in a series of macromolecular host compounds. The TOD system exists in *trans* (rigid, obtained from erythritol) and *cis* (flipping, yielded from threitol) configurations.

The similar tetraaza [8] and dioxadiaza [9] systems were also investigated, similar results being reported.

It was considered of interest to study the stereochemistry of the 1,5-dioxa-3,7-dithiadecaline, containing two 1,3-oxathiane units because of two main resons: our interest in the stereochemistry of 1,3-oxathiane derivatives (including the ring-chain tautomerism) [10-12] and the "construction" of macrocycles using these derivatives as substrates.

RESULTS AND DISCUSSION

The compounds were obtained using the condensation reaction between 1,4-dimercaptothreitol (1) and *p*-nitrobenzaldehyde and *p*-nitroacetophenone, respectively (Scheme 1).

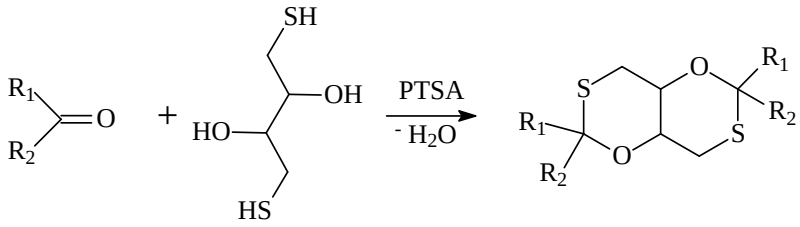

$R_1 = H \quad R_2 = p\text{—}C_6H_4\text{—}NO_2$ **2**

$R_1 = CH_3 \quad R_2 = p\text{—}C_6H_4\text{—}NO_2$ **3**

Scheme 1

The conformational analysis for compounds **2** and **3** shows anancomeric structures. For compound **2,** the conformational equilibrium is shifted towards the conformation A, with the phenyl groups in equatorial position, whereas compound **3** prefers the conformer D with the phenyl groups in axial orientation.

The anancomeric structure of the compounds determines the recording in the NMR spectra of different signals for the axial and equatorial protons of 1,3-oxathiane rings.

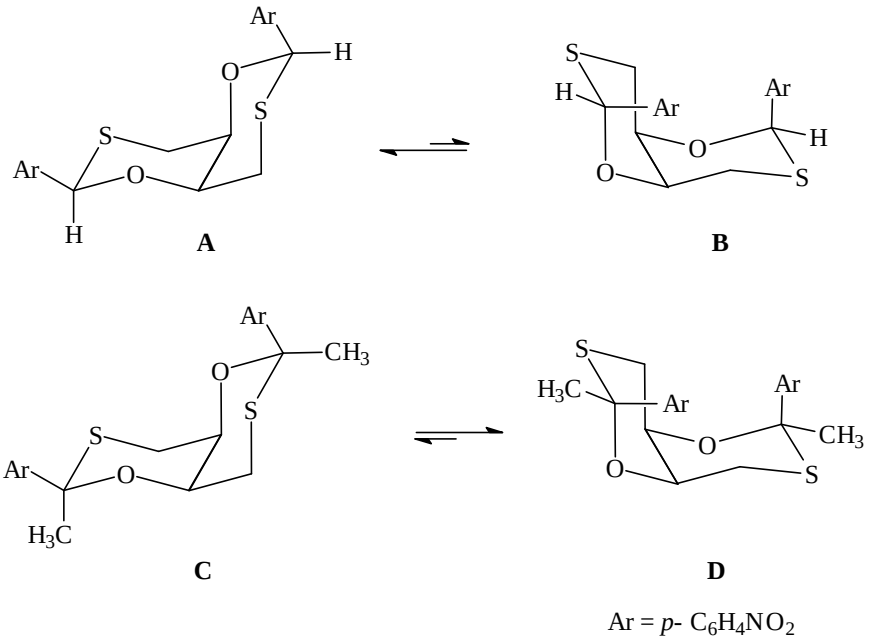

Scheme 2

As an example, the ^{1}H-NMR spectrum of compound **3** (Figure **1**) shows an AB system for the aromatic protons (δ =8.21, δ =7.68 ppm) and a multiplet (δ =4.34 ppm) belonging to the protons 9 and 10. The spectrum also exhibits two doublets of doublets (δ_{ax}=3.18, δ_{eq}=3.07 ppm) associated with the methylene protons of the two CH_2S groups and a singlet (δ =1.94 ppm) for the methyl groups.

CONCLUSIONS

The NMR investigations of compounds **2,3** revealed anancomeric structures due to the presence of different substituents in positions 2 and 6. The aryl groups prefer the equatorial orientation when they are the unique substituents at positions 2 and 6 and the axial position when the second substituent at these positons are methyl groups (compound **3**).

EXPERIMENTAL

^{1}H and ^{13}C spectra were recorded at room temperature, using $CDCl_3$ as solvent, in 5 mm tubes, on a Bruker NMR spectrometer, equipped with a multinuclear head, operating at 300 MHz for protons and at 75 MHz for carbon atoms.

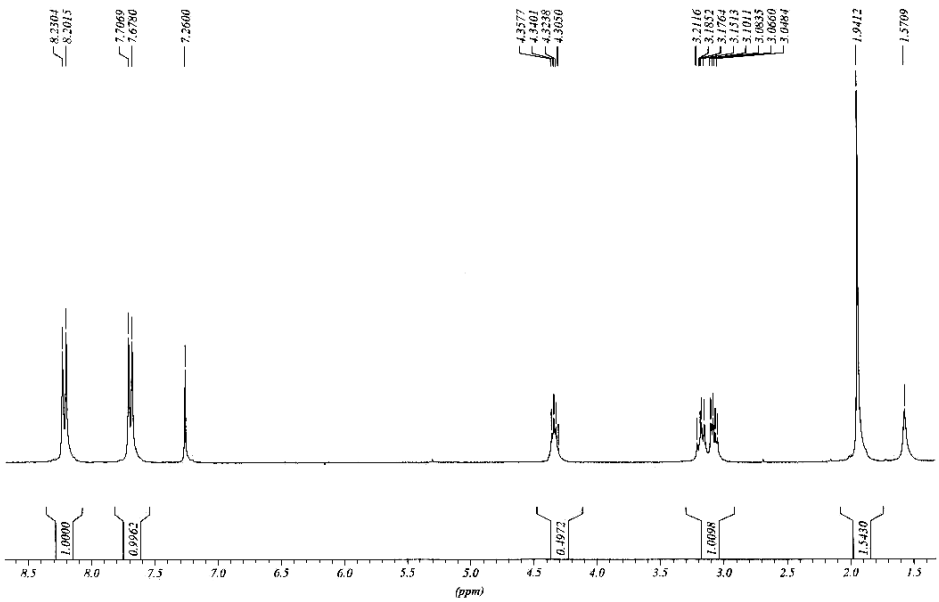

Fig. 1. *^{1}H NMR spectrum of compound **3***

Melting points were measured with Kleinfeld Apotec melting point apparatus and are uncorrected.

New compounds **2,3** general procedure

Stoechiometric amounts of 1,4-dithiathreitol and carbonyl compound (0.05 mol) with catalytic amounts of *p*-toluenesulphonic acid (0.05 g) were solved in 20 ml toluene and refluxed until 80% of the theoretical amount of water was separated by the Dean Stark trap. After cooling at room temperature, the catalyst was neutralized (under stirring 0.5 h) with KOH 0.1 M (20 ml). The organic layer was washed twice with 20 ml water. The toluene was removed and the 1.3-oxathiane compounds were purified by flash chromatography.

2.6-Di(p-nitrophenyl)-1.5-dioxa-3.7-dithia-biciclo[4.4.0]decane (cis, RR, SS) ***2***

White crystals, m.p. 235.1-235.2^{0}C. Yield 27%. $C_{18}H_{16}O_6S_2N_2$ found C 51.20, H 3.53, N 6.81, S 15.08 , required C 51.42, H 3.84, N 6.66, S 15.25

^{1}H NMR ($CDCl_3$, δppm): 3.2-3.4 (4H, dd, overlapped signals, 4, 8-CH_2), 4.50 (2H, m, 9, 10-H), 6.24 (2H, s, 2,6-H), 7.63 (4H, d, J = 8.7 Hz, aromatic protons), 8.21 (4H, d, J = 8.7 Hz, aromatic protons); ^{13}C NMR ($CDCl_3$, ppm): 35.46 ($C^{4,8}$), 84.37 ($C^{9,10}$), 85.73 ($C^{2,6}$), 124.20, 127.79 (tertiary aromatic carbon atoms), 148.59, 159.31 (quaternary aromatic carbon atoms)

2.6-Dimethyl, 2.6-di(p-nitrophenyl)-1.5-dioxa-3.7-dithia-biciclo[4.4.0]decane (cis, RR, SS) ***3***

White crystals, m.p. 119-120^{0}C. Yield 33%. $C_{20}H_{20}O_6S_2N_2$ found C 53.73, H 4.25, N 6.18, S 14.52, required C 53.46, H 4.49, N 6.25, S 14.30

^{1}H NMR ($CDCl_3$, δppm): 1.94(6H, s, 2,6-CH_3), 3.07 (2H, dd, J = 10.5, J'= 5.2 Hz, 4,8-H_{eq}), 3.18 (2H, dd, J = 10.5, J'= 5.2 Hz, 4,8-H_{ax}), 4.34 (2H, m, 9, 10-H), 7.68 (4H, d, J = 8.7 Hz, aromatic protons), 8.21 (4H, d, J = 8.7 Hz, aromatic protons); ^{13}C NMR ($CDCl_3$, ppm): 32.48 (2,6-CH_3) 35.35 ($C^{4,8}$), 83.04 ($C^{9,10}$), 95.48 ($C^{2,6}$), 123.86, 126.15 (tertiary aromatic carbon atoms), 147.33, 154.02 (quaternary aromatic carbon atoms)

REFERENCES

1. H. Senderowitz, A. Linden, L. Golender, S. Abramson, B. Fuchs, *Tetrahedron*, **1994**, 9691
2. H. Senderowitz, L. Golender, B. Fuchs, *Tetrahedron*, **1994**, 9707
3. S. Abramson, E. Ashkenazi ,I. Goldberg, M. Greenwald, H. Jatzke, M. Vardi, S. Weinman, B. Fuchs, *J.Chem.Soc., Chem.Comm.*, **1994**, 1611
4. K. Frische, M. Greenwald, E. Ashkenasi, N. G. Lemcoff, S. Abramson, L. Golender, B. Fuchs, *Tetrahedron Lett.*, **1995**, 36 (50), 9193
5. A. Linden, H.-D. Beckhaus, S. P. Verevkin, C. Rüchardt, B. Ganguly, B. Fuchs, *J.Org.Chem.*, **1998**, 63, 8205
6. B. Ganguly, B. Fuchs, *J.Org.Chem.*, **2000**, 65, 558
7. M. Grabarnik, N. G. Lemcoff, R. Madar, S. Abramson, S. Weinman, B. Fuchs, *J.Org. Chem.*, **2000**, 65, 1636
8. O. Reany, I. Goldberg, S. Abramson, L. Golender, B. Ganguly, B. Fuchs, *J.Org. Chem.*, **1998**, 63, 8850
9. A. Star, I. Goldberg, N. G. Lemcoff, B. Fuchs, *Eur.J.Org.Chem.*, **1999**, 2003
10. A. Terec, I. Grosu, L. Muntean, L. Toupet, G. Plé, C. Socaci, S. Mager, *Tetrahedron,* **2001**, 57, 8751
11. A. Terec, I. Grosu, L. Muntean, S. Mager, *Heterocycles*, **2003**, 60(6), 1477
12. M. Stuparu, I. Grosu, L. Muntean, G. Plé, C. Cismas, A. Terec, A. Nan, *Monatsh. Chem.*, published online October 9, **2003**

STUDIA UNIVERSITATIS BABEŞ-BOLYAI, CHEMIA, XLIX, 1, 2004

APPLICATIONS OF CALIX[4]PYRROLES

SILVIA LOZOVANU, LUMINITA SILAGHI-DUMITRESCU AND IOAN ALEXANDRU SILBERG

Department of Chemistry, "Babeş-Bolyai" University, 1 Mihail Kogalniceanu Street, 400028, Cluj-Napoca, Romania

INTRODUCTION

The self-assembly of complementary fragments occurs throughout nature and plays an essential role in the construction of biological "superstructures" such as nucleic acids, multicomponent enzymes, cell membranes, etc.[1,2]. The structural information required for facile self-assembly is preprogrammed in the topography and functionality of the building block surfaces[3,4].

Calix[4]pyrroles are a class of old[5] but yet new compounds that show interesting anion and neutral substrate binding properties[6]. The anion binding properties of *meso*-octamethylcalix[4]pyrrole **1**, was first mentioned by Jonathan L. Sessler and coworkers[7], and subsequently developed by his group[8].

The discovery that calix[4]pyrroles such as **1** are effective anion binding agents in solution has led to the synthesis of a variety of new calixpyrrole macrocycles that have been used for anion binding, sensing and for new anion separation technologies. The general route for the synthesis of calix[4]pyrroles is the condensation of pyrrole with ketones in the acid catalysis[5,9]

This review is dedicated to some applications of calix[4]pyrroles as anion and neutral binders, chromatic, fluorescent and electrochemical sensors.

THE BINDING AND SEPARARATION OF ANIONS

Anions play essential roles in biological processes; indeed, it is believed that they participate in 70% of all enzymatic reactions[7].

Different research groups, which work in the field of molecular recognition, synthesized receptors that bind anions by using hydrogen bonds alone, or in concert with electrostatic interactions.

The solution binding properties of calix[4]pyrroles **1-5**, were studied by using ^{1}H NMR titration techniques in CD_2Cl_2 and stability constants were determined using the EQNMR least-squares fitting procedure[10]. The data summarized in **Table 1**, revealed that all compounds are not only effective 1:1 anion binding agents in solution but they are also selective. Specifically, they show a marked preference for F^- over other anionic guests (Cl^-, Br^-, I^-,$H_2PO_4^-$ and HSO_4^-).

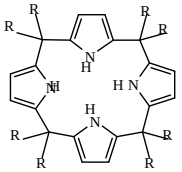

1 R = Me

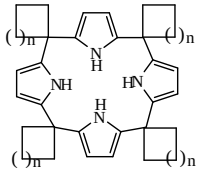

2a n=3 **2b** n=2 **2c** n=1

The stability constants for *spiro*-calix[4]pyrroles **2b** and **2c** in CD_2Cl_2 are lower (fluoride: 3000 and 2300; chloride: 100 and <100, respectively) than for macrocycle **2a** (**Table 1**). All *spiro*-calix[4]pyrroles demonstrate the much lower stability constants than octamethyl **1** does; so the anion binding ability decreases in the order: octamethyl > *spiro*-cyclohexyl > *spiro*-cyclopentyl > *spiro*-cyclobutyl (i. e., **1** > **2a** > **2b** > **2c**)[11].

Table 1

*Stability constants for compounds **1-5** with anionic substrates in CD_2Cl_2 at 298K. " - " – not determined*

anion - "guest"	*Stability constant (M^{-1})*				
	1[7]	**2a**[7]	**3**[12]	**4**[12]	**5**[12]
F^-	17 170(± 900)	3600 (± 395)	170(±20)	1100(±200)	27000(±4000)
Cl^-	350(±5.5)	117(±4.0)	<10	47(±1)	4300(±600)
Br^-	10(±0.5)	-	-	-	-
I^-	<10	-	-	-	-
$H_2PO_4^-$	97(±3.9)	<10	-	-	-
HSO_4^-	<10	-	-	<10	650(±40)

The similar titrations of the monomeric 2,5-dimethylpyrrole using fluoride anion demonstrate that the binding properties of anions are not so pronounced.

The anion binding properties of calix[4]pyrroles are an obvious proof of the capacity of polypyrrolic macrocycles of similar sizes and shapes to form hydrogen bonds[13].

Compound **3** and **4** show lower stability constants with fluoride and chloride than calix[4]pyrroles **1** and **2a**. This is due to the electron-donating ability of eight *C*-rim methoxy groups causing a decrease in the acidity of the pyrrole NH protons in **3** and to unfavourable interactions between the bound anion and the lone pair electrons on the oxygen atoms of the *C*-rim ester group in **4**.

In contradiction to receptors **3** and **4**, compound **5** exhibits higher stability constants for the binding of fluoride, chloride and dihydrogen phosphate anions than does **1** under the same conditions as the substitution with electron–withdrawing bromine atoms increases the acidity of the pyrrole NH protons thus enhancing anion binding ability.

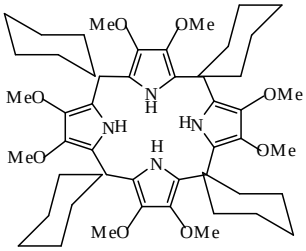

3

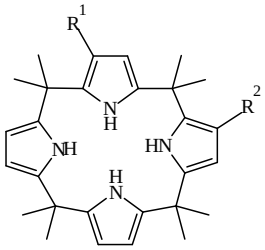

4 $R^1 = CH_2CO_2Et$, $R^2 = H$

These last three examples illustrate that the anion binding property of the calix[4]pyrroles can be tuned by appending different groups to the carbon in *C*-rim of the calixpyrrole. Receptors of increased anion binding ability such as **5** may have potential uses as anion sequestering agents (for example, in removal of

phosphate pollutants from aqueous environments) while those with decreased anion binding ability (compound **3** and **4**) could prove useful in HPLC; in this latter application low affinity constants and fast complexation-decomplexation rates generally lead to efficient separation of substrates.

The introduction of the electron-withdrawing fluorine substituents to the β-pyrrolic positions of calix[4]pyrrole (**5a**) results in a dramatic increase of the affinity this receptor displays toward anionic substrates in solution[14].

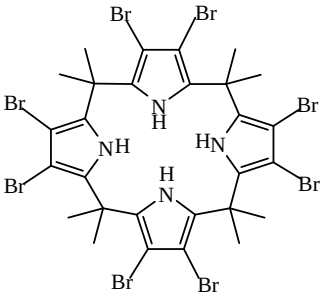

5

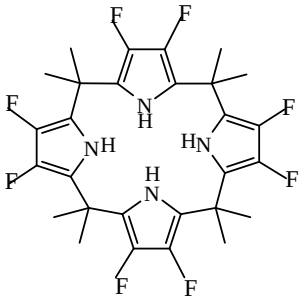

5a

Calix[4]pyrrole **5a** displays not only increased affinity for anions, specifically chloride and dihydrogen phosphate for which accurate K_a values for 1:1 complex formation could be obtained, but also increased selectivities for certain anions as compared to **1** (*Table 1)*. Affinity constants for **5a** (mol^{-1}) for anionic substrates (in the form of their tetrabutylammonium salts) and DMSO-d_6 as neutral substrate recorded in acetonitrile-d_3 (0.5% v/v D_2O) at 22°C are the following: 17100 (F^-), 10700 (Cl^-), 9100 ($H_2PO_4^-$), 20 (DMSO-d_6). The ratio of the binding constants of **5a** and **1** ($R_{5a/1}$) are: for F^- - ≥1.71, for Cl^- - 2.14, for $H_2PO_4^-$ - 7.0 and for DMSO-d_6 - >4.0.

Studies of mono-halogen substituted calix[4]pyrroles reveal that replacement of a single β-pyrrolic hydrogen atom can increase the anion binding ability of calix[4]pyrroles for a variety of anions (*e.g.* Cl^-, Br^-, $H_2PO_4^-$, HSO_4^-) in comparison to normal non-halogen substituted calix[4]pyrrole. The chlorine substituted calix[4]pyrrole was found to display a slightly higher affinity in the case of each anion than the fluorine-bearing derivate[15].

The fact that the substituents of the calix[4]pyrroles (in the *C*-rim or in the *meso*-position) influence the anion binding capacity, led to the synthesis of new functionalized calix[4]pyrroles as illustrated in the examples **6** and **7**. By using NMR spectroscopy to probe the effect of anion binding in solution, it was found that under conditions of strong binding, such as those proved true for fluoride, phosphate, and chloride anions interacting with the $\alpha\alpha\alpha\alpha$ isomers of **6** and **7** and fluoride anions interacting with the $\alpha\alpha\beta\beta$ isomer of **6**, addition of the substrate served to lock the system into the expected cone conformation[16].

In the case of the $\alpha\alpha\alpha\beta$ isomer of **6** and the $\alpha\alpha\beta\beta$ isomer of **7**, high concentrations of fluoride anion served to lock the system into separate, well-defined conformations that, on the basis of symmetry considerations, were assigned as being the two conformationally accessible conelike forms and the cone and partial

cone conformations, respectively. In other systems, where weaker anion binding occurred, the addition of anions did not serve to lock the fluxional calixpyrrole core into a single conformation. Quantitative assessments of anion binding affinity were made using the induced changes in the ^{1}H NMR spectra as a function of anion concentration. From these analyses (**Table 2**) it became clear that the affinities of **6** and **7** for chloride and dihydrogenphosphate anions are actually lower than those of **1**. This, presumably, is due to a combination of electronic effects and steric interactions between the *meso*-aryl groups and the anion.

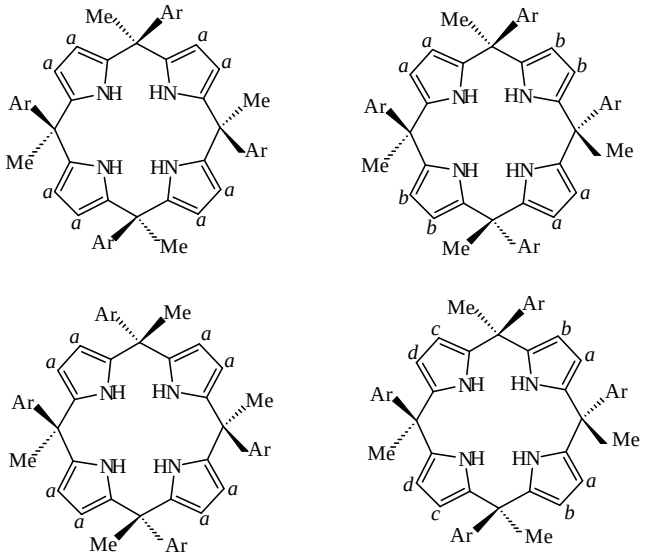

6 Ar = 4-hydroxyphenyl; **7** Ar = 4-methoxyphenyl

Table 2

*Stability constants for compounds **1**, **6** and **7** (M^{-1}) with anionic substrats in acetonitrile-d_3 (0.5% v/v D_2O) at 22 °C*

anion-"guest"	**1**[16]	**6**[16]			**7**[16]		
		αααββ	αααβ	αααα	αααββ	αααβ	αααα
F^-	>10 000	>10 000	5 000	>10 000	4 600	1 100	10 000
Cl^-	>5 000	1 400	260	320	<100	220	300
$H_2PO_4^-$	1 300	520	230	500	<100	<80	<100

It is important to appreciate that isomers in the **6** and **7** do serve to modulate the anion binding affinities. For example, the αααα isomer of **7** has the highest affinity for anions among the three isomers of **7**.

It was observed that the anion binding affinities of **6** are greater than those of **7.** The explanation offered by the analysis is the presence of hydroxy groups in **6** able to serve as secondary hydrogen-bonding recognition elements that stabilize the calix[4]pyrrole-anion complex. In the case of the αααα isomer of **6** this effect

reverses the intrinsic fluoride>chloride>phosphate selectivity that has previously been observed for calix[4]pyrroles[8a].

Not only *p*-hydroxyacetophenone, but also *m*-hydroxyacetophenone can be used as ketone in order to obtain calix[4]pyrroles in three isomeric forms, with the cone conformer displaying topologicaly variabile multi-site or multi-point surfaces for binding anionic or neutral substrates[17].

Tetra-ester (**8**) and tetra-amide (**9**) macrocycles with «super-extended cavities» were noticed to have higher selective anion coordination properties[18].

The adition of 20 equivalents of Cl^-, Br^-, I^-, $H_2PO_4^-$ or HSO_4^- anions (as tetrabutylammonium salts) to deuteriated DMSO solutions of **8** and **9** caused no changes in the NMR spectra of these calix[4]pyrroles. This means that compounds **8** and **9** do not interact with these anionic guests in DMSO solution.

On the other hand, the addition of fluoride anions in the same conditions causes changes in the ^{1}H NMR spectra of compounds **8** and **9**, corresponding to the formation of fluoride complexes with slow complexation/decomplexation kinetics.

The presence of an extended cavity in compound **6** and a super-extended cavity in compounds **8** and **9** serves to decrease (**6**) and switch off (**8** and **9**) the affinity of this class of receptors for anions other than fluoride in DMSO solution[18].

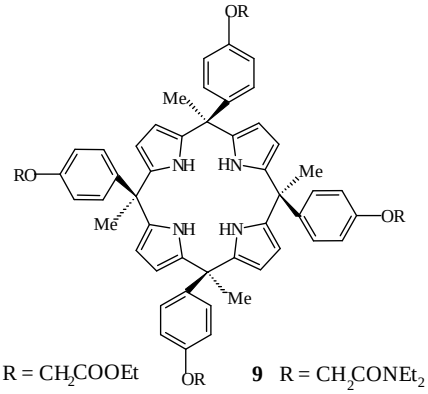

8 R = CH_2COOEt **9** R = CH_2CONEt_2

The binding behavior of the «super-extended cavity» tetraacetylcalix[4]pyrrole[19]. was investigated by NMR titration, and the complex was found to exclusively bind fluoride anions in DMSO-d_6 The binding behavior was investigated by Monte Carlo free energy perturbation simulations and Poisson calculations, and the ion specificity was seen to result from the favorabile electrostatic interactions that the fluoride gains by sitting lower in the phenolic cavity of the receptor[20].

Using different symmetrical or asymmetrical ketones were elaborated diverse calixpyrrole *meso*-substituted systems. It was observed that many of these systems demonstrate basic anion binding characteristics of the calix[4]pyrrole skeleton [21] and these properties are indeed affected by the number and type of substituents present on the *meso*-like bridges and/or β–pyrrolic sites.

An interesting application of functionalised calix[4]pyrroles is the separation of different mixtures using carboxylic acid functionalized calix[4]pyrroles attached to aminopropyl silica gel *via* both the *meso*-position (**10**) and *β*-positions (**11**). The stability

constants (M^{-1}) of **10** and **11** in CD_2Cl_2 solution for different anions are respectively: chloride – 415(±45), 405(±10); dihydrogenphosphate - 62(±6), 80(±15); hydrogensulfate - <10, <10[22].

The calix[4]pyrrole-modified silica provide a new solid support for the HPLC separation of nucleotides, oligonucleotides, N-protected aminoacids and perfluorinated biphenyls. Using **Gel A** and **Gel B** (***Fig.1***) were separated: a) fluoride, chloride, bromide, hydrogensulfate, and dihydrogenphosphate anions; b) phenyl arsenate, phenyl phosphate, phenyl sulfonate; c) N-protected anionic aminoacids (serine, glutamine, alanine, phenylalanine, tryptophan, aspartate, and glutamate).

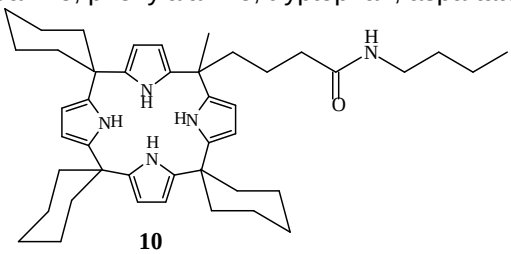

10

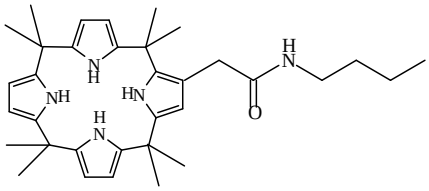

11

The **Gel A** was used for the HPLC separation of 5´-adenosine monophosphate (AMP), 5´-adenosine diphosphate (ADP), and 5´-adenosine triphosphate (ATP)[22].

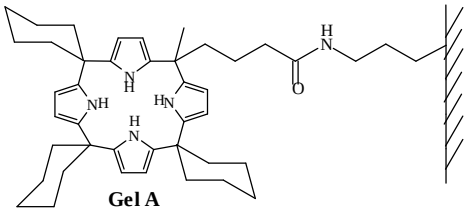

Gel A

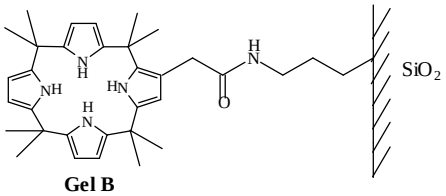

Gel B

Fig.1

These same media also permit the HPLC-based separation of mixtures of neutral species such as polyfluorobiphenyls[8a].

Calix[4]pyrroles containing the ferrocenyl (Fc) moiety attached to one of the *meso*-positions **12** and **13** bind anions in dichlorometane-d_2 solution[23].

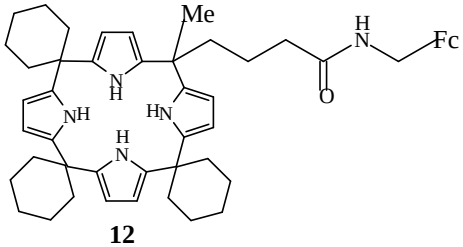

12

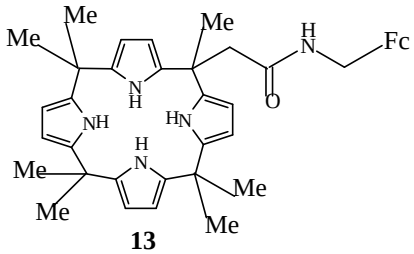

13

It was demonstrated by ^{1}H NMR titration studies in acetonitrile-d_3/ DMSO-d_6 (9:1, v/v) that calix[4]pyrrole **14** coordinates fluoride, chloride and dihydrogen phosphate in this solvent mixture with association constants (M^{-1}): 3375, 3190 and 304[24].

In the **Fig. 2** is designed the schematic representation of the ferrocene CH and calix[4]pyrrole NH hydrogen-bonding interactions, which permit to stabilise the bound anion.

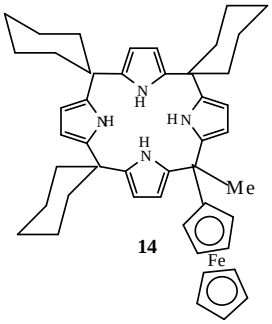

14

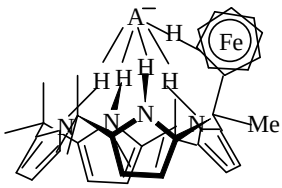

Fig. 2

Supramolecular interaction of calix[4]pyrroles with several inorganic anions was reported by addition of this macrocycle to the background electrolyte in capillary zone electrophoresis (CZE)[25]. It was observed that the retention time of all anions increases with increasing concentration of calix[4]pyrroles and the effect of F^- is most evident.

The analyses via FABMS of calix[4]pyrroles derived from steroidal ketones demonstrate that these macrocycles are reasonable in effecting the enantioselective recognition of appropriate organic anions. Results for antipodal R>S selectivity were obtained in the case of tartaric acid and mandelic acid[26].

Calix[4]pyrrole dimmers **15** [X=bond, *p*-C_6H_4, *m*-C_6H_4] synthesized by palladium (0) catalysed C-C bond formation show an interesting effect of cooperative binding[27]. In the case of **15** [X=bond] authors made a detailed study of carboxyl ate anion binding using ^{1}H NMR spectroscopy. For isophthalate anion it was observed a 1:1 binding stoichiometry and a much higher association constants was found than for the control monomer, octamethylcalix[4]pyrrole. For phthalate and benzoate anions, 1:2 (host:guest) binding stoichiometries and lower association constants were recorded than with isophthalate anion. The controle compound, octamethylcalix[4]pyrrole, showed a 1:1 binding stoichiometry and much lower association constants than **15** [X=bond], not just with isophthalate, but also phthalate and benzoate anions[27].

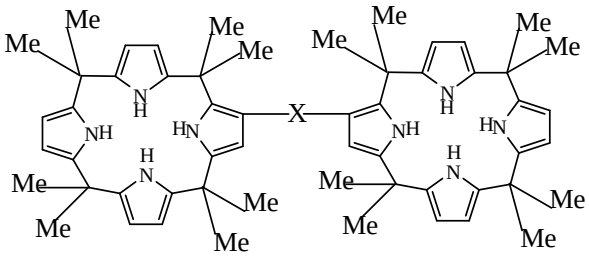

15

The calix[4]pyrroles bearing *m*-orcinol-derived diether straps of different lengths on one side of tetrapyrrolic core **16-18**[28] and the analogous diester **19**[29] display enhanced affinities for chloride and bromide anion.

Schematic representation of strapped calix[4]pyrroles show how the properties of the parent system can be modified (X^- represents an anion and G – an ancillary binding motif) [**Fig.3**].

It was found that the anion binding ability of these systems could be effectively tuned by modifying the length and nature of the bridging straps. In the specific case of the diether systems the largest chloride affinity in acetonitrile and DMSO was seen with the shortest strap, whereas the highest affinity for bromide anion was recorded in the case of the longest strap (**Table 3**).

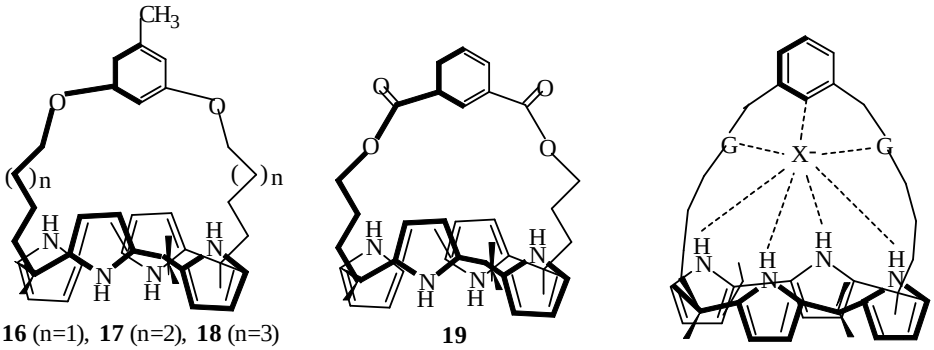

16 (n=1), **17** (n=2), **18** (n=3) **19**

Fig. 3

Table 3

*Association constants for the binding of chloride and bromide by compound **16-19** measured by isothermal titration calorimetry (ITC) at 30°C using the corresponding alkylammonium and cryptand salts.*

TBA=tetrabutylammonium.

calix[4]pyrrole[28]	*TBA-Cl*[28]	*K-cryptand-Cl*[28]	*TBA-Br*[28]	*TBA-Cl*[28]
	CH_3CN			*DMSO*
16	3 630 000	4 270 000	30 000	340 000
17	1 370 000	1 810 000	31 000	11 000
18	1 370 000	1 810 000	120 000	7 400
19	1 380 000	1 620 000	~0	110 000

On the basis of these findings, as well as supporting ^{1}H NMR spectroscopic studies, it was postulated that not only cavity size, but also the ability of the aryl portion of the strap to serve as CH hydrogen bond site are important in tuning the observed anion affinities.

X-Ray crystal analyses of the Bu_4NCl complex of calixpyrrole **1** and the Bu_4NF complex of calixpyrrole **2** revealed that in both cases the calix[4]pyrrole ligand adopts a cone-like conformation in the solid state. In the case of the chloride complex (**Fig.4**) the nitrogen-anion distances are in the range of 3.3264(7)-3.331(7)Å, while for the corresponding fluoride complex they are 2.790(2)Å[8a]. The results demonstrate that in these two complexes the chloride and fluoride anions reside 2.319(3) and 1.499(3) Å above N_4 root mean square planes of calixpyrrole **1** and **2**, respectively. Thus, the fluoride anion appears to be more tightly bound, at least in the solid state.

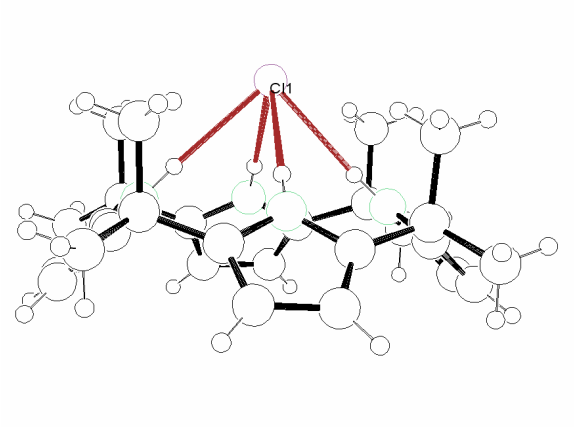

Fig. 4

In order to find the explanation of the conformation of calix[4]pyrroles in the absence of halide anion in comparison with its conformation in the presence of the same anion some theoretical studies were made. The complexation of anions by octamethylcalix[4]pyrrole **1** and 2,5-dimethylpyrrole were investigated by energy minimizations in the gas phase and by Monte Carlo (MC) simulations in dichloromethane using the OPLS force field[30]. It was found that, in agreement with experiment, the 1,3-alternate conformation of **1**, in which adjacent pyrrole rings are pointing in opposite directions, is the most stable conformation in the absence of a halide anion. The cone conformer of **1**, having all pyrrole units in a parallel orientation, is not stable in the absence of halide anion, but it is the most stable conformation upon anion binding due to the formation of four NH-halide hydrogen bonds. The relative free energies of binding of chloride, bromide and iodide with the cone of **1** in dichloromethane were calculated with free energy perturbation (FEP) simulations to be in the excellent agreement with experiment. The calculations predict a far greater affinity for fluoride ion than was measured. Authors explained this fact by the influence of the presence of trace amounts of water.

Later it was examined the influence of different factors on the anion binding properties of calix[4]pyrroles. The binding of different anions to calix[4]pyrrole was studied using molecular dynamics coupled to thermodynamic integration calculations. The effect of diverse apolar solvents, octafluoro substitution, and the change in binding free energy derived from the presence of cosolute and water traces were studied [31]. It was demonstrated that both calix[4]pyrrole **1** and octafluorocalix[4]pyrrole **5a** have preference for F^- in the gas phase and pure aprotic solvents, but the situation can change much in protic solvents or in the presence of the hydrated cation which is used as cosolute of the anion. These results provide interesting clues for a better understanding of the process detected experimentally as «binding».

CALIX[4]PYRROLES – SENSORS FOR ANIONS

The development of chemosensors for specific chemical species is emerging as a research area of considerable importance within the generalized field of supramolecular chemistry.

As shown before the calix[4]pyrroles are very good anion receptors[8a] so they show considerable promise in the area of anion sensing.

In general, such systems contain some combinations of substrate-recognition functionality (receptor) and optical-signaling capacity (cromophore), either directly linked or appropriately associated in a noncovalent manner, and are designed to permit the detection of substrates by binding-induced changes in absorption or emission properties[32]. The use of calix[4]pyrroles as chromatic sensors and fluorescent sensors is presented below.

Chromatic sensors

While the utility of these approaches are becoming increasingly appreciated in terms of both qualitative and quantitative analysis, the number of chromatic sensors available at present for anionic substrates remains quite limited. Only a few chemical systems are known that undergo colour changes of sufficient magnitude that they can be used for the direct «naked-eye» sensing of anions[6].

In the process of the formation of the complex from *meso*-octamethyl-calix[4]pyrrole **1** and the 4-nitrophenolate anion (yellow) **20** in MeCN or CH_2Cl_2 the colour of the complex **1•20** disappears (*Scheme 1*)[6]. Complexation studies were made using ^{1}H NMR titration techniques. Significant downfield shift (from δ 7.0 to 10.6) of the pyrrole NH proton was observed upon the addition of 5 equiv. of tetrabutylammonium 4-nitrophenolate, consistent with the formation of calixpyrrole – phenolate hydrogen bonds. Analysis of titration data using the EQNMR computer program[10] revealed that *meso*-octamethylcalix[4]pyrrole forms a 1:1 complex with 4-nitrophenolate with a stability constant of 290 (±9.7) dm^3 mol^{-1}.

Because this value is much lower than that reported earlier for F^- (17 200 M^{-1}), the substitution of a *p*-nitrophenolate by F^- took place when a CD_2Cl_2 solution of the complex **1•20** was treated with aliquots of tetrabutylammonium fluoride. After an initial addition of 0.2 equiv. of fluoride, the NH proton resonance broadened and could not be located in the NMR spectrum. Only after addition of 1.0 equiv. of fluoride did the NH resonance reappear, further shifted downfield by over 3 ppm as compared to **1•20**, indicating the formation of a calixpyrrole-fluoride complex. As expected from the values of the stability constants, tetrabutylammonium chloride and dihydrogenophosphate produced smaller downfield shifts (0.78 for Cl^- and 0.37 ppm for $H_2PO_4^-$).

The strongest absorbance is observed upon addition of fluoride anions followed by chloride and dihydrogenphosphate anions. This trend reflects the absolute and relative affinities of *meso*-octamethylcalix[4]pyrrole for these anionic guests (**Table 4**)[6].

Table 4

Relative absorbance values for calixpyrrole – 4-nitrophenolate solutions containing equimolar concentrations of various anions.

Anions	**F^-**	**Cl^-**	**$H_2PO_4^-$**	**Br^-**	**HSO_4^-**
Δ Absorbance	0.282	0.193	0.162	0.092	0.015
Relative absorbance	1.0	0.68	0.57	0.33	0.05

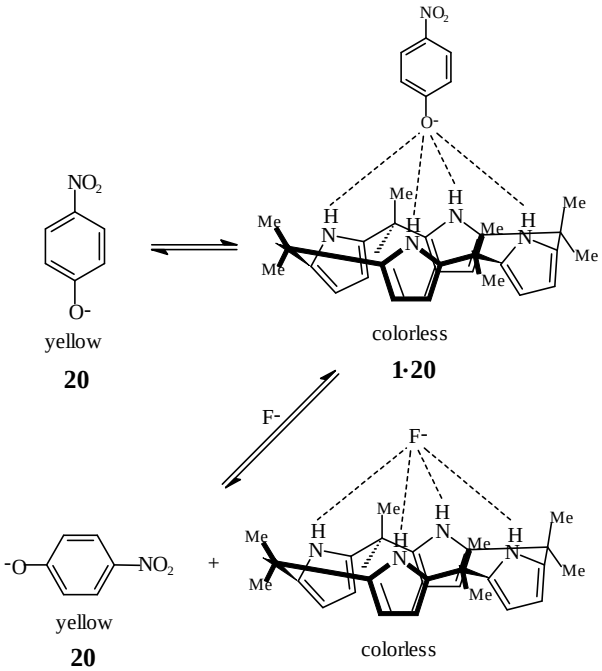

Scheme 1

The calix[4]pyrroles, such as **1**, may be used to produce anion sensors that can report the presence of anions (for example, fluoride anion) by means of a colour change.

Compounds **21-25** with arylalkynyl groups onto one of the *β*-pyrrolic positions of the calix[4]pyrrole skeleton (*Scheme 2)* were prepared by metal-mediated carbon-carbon bond cross coupling reactions, especially the Sonogashira reactions. Compound **21** contains an electron-donating substituent, whereas both calix[4]pyrroles **22** and **23** contain electron-withdrawing aryl subunits. Furthermore, compounds **24** and **25** contain a built-in fluorophore and a built-in chromophore, respectively[33].

It was found[33] that the mono- and dinitrophenyl-functionalized systems **22** and **23** undergo naked eye-detectable spectral changes upon exposure to the tetrabutylammonium salts of fluoride, chloride, and phosphate anions in a dichloromethane solution. The addition of fluoride anion to dichloromethane solutions of **23** (5×10^{-5}M) leads to a significant broadening of the UV – VIS absorption bands while engendering a noticeable red-shift in the position of the absorption maximum (λ_{max} shifts from 441 to 498 nm). As a consequence of these anion-induced spectral changes, the solution undergoes a naked-eye detectable colour change from yellow to red. Addition of 200 equiv. of tetrabutylammonium chloride caused the change of the color from yellow to orange (the absorption maximum, λ_{max}, shifts from 441 to 483 and 478 nm, respectively). Exposure to bromide, iodide and sulfate anions, even in vast excess did not lead to any noticeable changes in either colour or basic spectral properties.

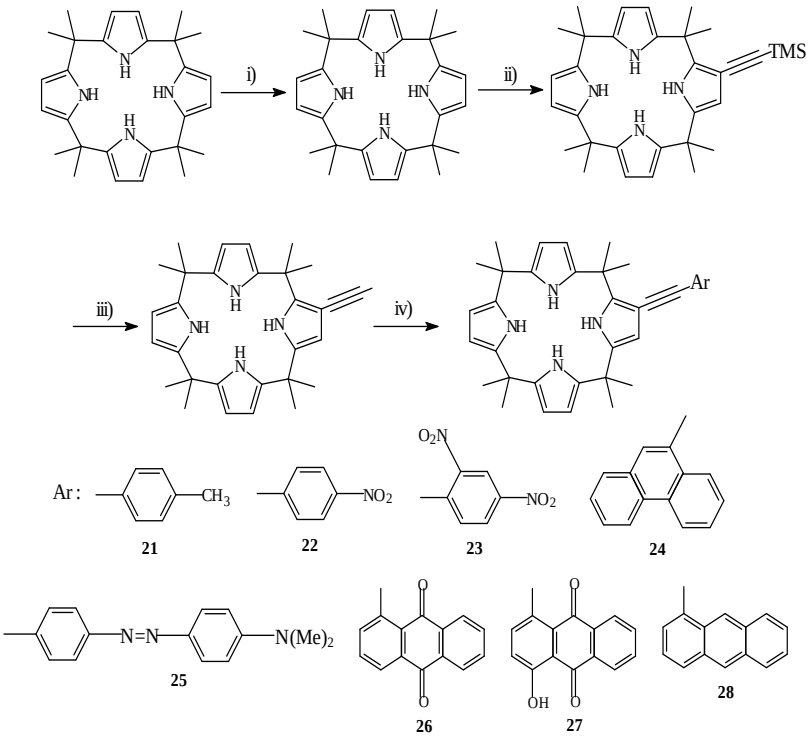

Scheme 2. (i) I_2-$(CF_3CO_2)_2PhI$ (20%); (ii) TMS acetylene, $Pd(PPh_3)_4$ (73%), CuI; (iii) tetrabutylammonium fluoride, then $NaHCO_3$ (89%); (iv) ArI, $Pd(PPh_3)_4$, CuI.

The treatment of the mononitrobenzene conjugated calix[4]pyrrole **22** with 20 equiv. of tetrabutylammonium fluoride changed the colour of the solution from pale yellow to intense yellow related to the shift of the absorption peak from 391 to 433 nm[6]. The presence of chloride and phosphate anions could also be detected from the intense final yellow colour after their exposure to **22**. No discernable change could be noticed when dichloromethane solution of **22** was exposed to 200 equiv. of bromide, iodide and sulfate anions.

No important changes were observed for compound **21** when it was treated with anions. It is thus clear that "attachment" of nitro groups produces a bathochromic shift in the absorption peak (this effect is especially pronounced in the case of dinitrobenzene compound **23**).

The functionalized calix[4]pyrroles of the type described above could emerge as useful anion sensors and the ***Fig. 5*** represents the schematic mechanism of the changes in colour observed when calix[4]pyrrole **23** is exposed to certain anions.

Calix[4]pyrrol-anthraquinones systems **26**, **27** and **28**[32] act as an optically sensitive indicator of anion binding.

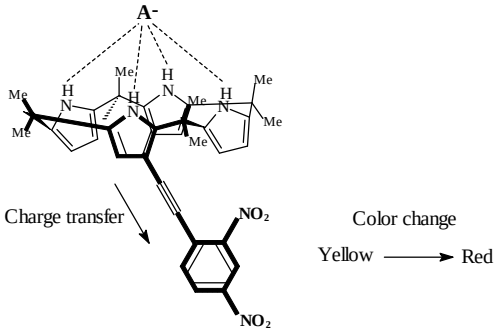

Fig.5

System **26** represents a good sensor for F^-, Cl^- and $H_2SO_4^-$ in dichloromethane and the effect can be detected with "naked-eye". In the absence of anions, the absorption spectrum of receptor **26** is characterized by the presence of two peaks at λ_{max}=357 and 467 nm, (in comparison with anthraquinone itself which has λ_{max}=327 nm). Upon the addition of fluoride anion, the peak at 467 nm decreases while a new peak appears at 518nm, the color of the solution modifies from yellow to red. These changes are complete after the addition of only six equivalents of F^- ions. The addition of either chloride or phosphate ions induced a less impressive colour change (from yellow to reddish-orange) and required greater amounts of anion to effect a commensurate change (the absorption peak shifts to 501 and 497 nm upon the addition of 100 equivalents of tetrabutylammonium chloride and phosphate, respectively).

Exposure to bromide, iodide, and sulfate anions, species that do not bind to calix[4]pyrroles appreciably[32], did not lead to any noticeable change in colour. This combination of anion-specific response/nonresponse makes this system an effective naked-eye-detectable anion sensor.

The addition of 100 equivalents of various anions to dilute (5.0×10^5M) solutions of **27** in dichloromethane is accompanied by the colour change of the system from red to blue or purple, again with the most pronounced effect for fluoride ions.

The above qualitative changes are reflected in more quantifiable terms in the corresponding absorption spectra. Whereas 4-hydroxyanthraquinone itself is pale yellow and displays an absorption maximum at 405 nm in dichloromethane, conjugation to calix[4]pyrrole through an alkyne spacer shifts the absorption maximum to the red region of the spectrum and produces a species with lowest energy absorption maximum at 526 nm. Upon the addition of fluoride ions, the absorption maximum is shifted even further (to 613 nm) and the solution turns blue. Similar, but less pronounced bathochromic shifts are seen upon the addition of excess chloride and dihydrogen phosphate ions, with the lowest energy maxims being observed at 567 and 549 nm, respectively. In these cases the colour of the solution change from red to purple and to dark purple, respectively.

No significant colour changes were observed upon the addition of bromide, iodide, and sulfate ions. These spectral results, as well as the corresponding visual changes, are thus completely consistent with the association constants for **27** with different anions, namely $F^->Cl^->H_2PO_4^->>Br^-\sim I^-\sim HSO_4^-$.

The origins of the dramatic colour changes observed with chemosensors **26** and **27**, was ascribed to charge-transfer interactions between the electron-rich, calix[4]pyrrole-bound anions and the electron-deficient anthraquinone moieties. The anthracene-containing control compound **28**, a calix[4]pyrrole system bearing a more electron-rich appendage, does not act as a naked-eye-detectable anion sensor, while the addition of 100 equivalents of tetrabutylammonium fluoride to a 5.0×10^{5}M solution in CH_2Cl_2 induced only a slight bathochromic shift in the absorption maximum (λ_{max} shifts from 408 to 416 nm) along with a modest reduction in absorption intensity. Detailed ^{1}H NMR spectroscopic and fluorescence analyses revealed, however, that **28** nonetheless acts as an efficient receptor for F^- Cl^-, and $H_2PO_4^-$ ions under these conditions[11].

The non-covalent calix[4]pyrrole-chloranil aggregation has been used as anion sensor for the facile identification of F^- and $H_2PO_4^-$ ions in chloroform and it can be used as a chromatic sensor for effective and selective detection of F^- and $H_2PO_4^-$ anions. The specific phosphate/chloride selectivity is potentially advantageous in biological sensing applications[34].

These systems were investigated using UV-VIS spectroscopic techniques. Chloranil **29** itself displays an absorption maximum at 370 nm in chloroform. In the presence of calix[4]pyrrole **30**, the peak at 370 nm undergoes an obvious increase, while a new absorption peak appears at 622 nm. The colour of mixed system changed from pale yellow to blue, as a result of the formation of 1:1 molecular complex (with the binding constant 5800 M^{-1}), which was confirmed by Job plot analysis.

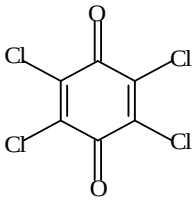

29

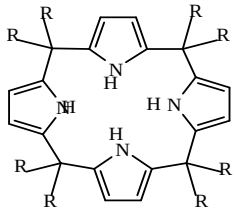

30 R = Et

Similarly, the addition of *meso*-cyclopentylcalix[4]pyrrole **2b** to the solution of chloranil changes the colour from pale yellow to purple (at 550 nm). However, under the same conditions, less impressive changes were observed upon addition of *meso*-octamethylcalix[4]pyrrole **1**, or *meso*-tetracyclohexylcalix[4]pyrrole **2** to the solution of **29**[34].

Fluorescent sensors

Fluorescent anthracene-calix[4]pyrrole conjugates **31-33** are the receptors which can detect the presence of anions by a significant quenching of their fluorescence[35].

Quenching was observed in varying degrees upon addition of other anions to receptors **31-33**; the addition of fluoride anion to **31** causes the highest fluorescence quenching, followed by dihydrogenphosphate and chloride anions.

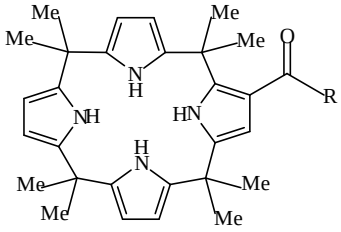

31 R = NH-1-anthryl

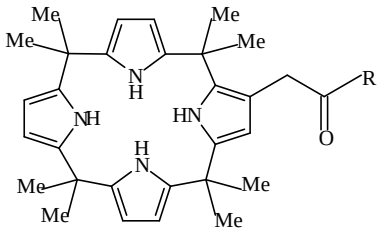

32 R = NH-1-anthryl

33 R = $NHCH_2$-9-anthryl

The same anion can quench the fluorescence of different calix[4]pyrrolic systems with distinct efficiency, as it is shown in **Table 5**.

Table 5

*Stability constants for compounds **31**, **32** and **33** with various anions (as tetrabutylammonium salts) in CH_2Cl_2 and CH_3CN as determined from fluorescence quenching analyses at 25°C.*
"-" - quenching insufficient to provide an accurate stability constant value.

Anions	*Log K (in CH_2Cl_2)*			*Log K (in CH_3CN)*		
	31[35]	**32**[35]	**33**[35]	**31**[35]	**32**[35]	**33**[35]
F^-	4.94	4.52	4.49	5.17	4.69	4.69
Cl^-	3.69	2.96	2.79	4.87	3.81	3.71
Br^-	3.01	-	-	3.98	2.86	-
$H_2PO_4^-$	4.20	3.56	-	4.96	3.90	-

The highest stability constants found for compounds **31** can be explained by the conjugated bond pathway linking the fluorophore and anion-binding site of the calixpyrrole providing an electronic communication pathway between them. Compounds **31-33** represent prototypical calix[4]pyrrole based-fluorescent anion sensing agents.

Calix[4]pyrroles **34-36** represent the second generation of calixpyrrole-based fluorescent anion sensors[36]. These systems bind anions with greater affinity than previous systems while displaying a more efficient fluorescent response. In the design of sensors **34-36**, a rigid aromatic spacer was used so as to fix the distance between the quencher (anion) and the signalling moiety. This spacer element contained either a sulphonamide (compounds **34** and **35**) or thiourea (sensor **36**) group.

These linker moieties were introduced with the expectation that they might provide additional hydrogen bond donor sites that would act in concert with the calixpyrrole NH protons to enhance the overall anion binding affinities. The affinity constants for all three sensors and four anions are listed in **Table 6**[36].

Sensors **34-36** display the highest anion binding affinities so far recorded for calixpyrrole-type receptors. They are also the first to show high phosphate/chloride selectivity (2 orders of magnitude) and, in the case of sensor **36**, the first such systems to operate successfully in the presence of water at physiological pH.

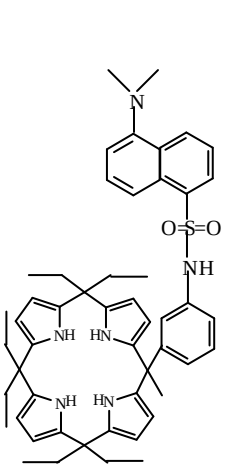

34

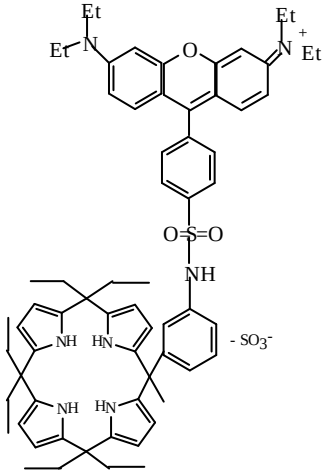

35

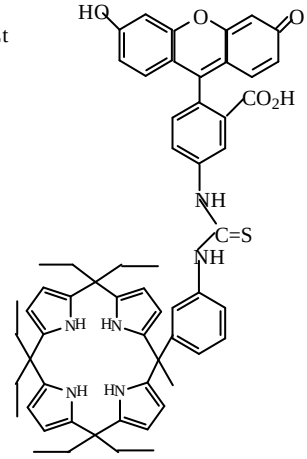

36

Table 6

*Affinity constants for sensors **34-36** and anionic substrates as determined in acetonitrile (0.01% v/v water) for sensors **34** and **35** and acetonitrile-water (96 :4, pH=7.0±0.1) for sensor **36**.*

Anions	*Association constants (mol^{-1}) determined by emission quenching*		
	34 (5×10^{-6}M) [36]	**35** (5×10^{-6}M) [36]	**36** (5×10^{-6}M) [36]
F^-	222 500	>1 000 000	>0 200 000
Cl^-	10 500	18 200	<10 000
$H_2PO_4^-$	168 300	446 000	682 000
$HP_2O_7^{3-}$	131 000	170 000	>2 000 000

Electrochemical sensors

Only a few electrochemically active sensors based on calix[4]pyrroles have been reported[37,38]**.** Electrochemically active sensors, designed to permit the detection of substrates by binding-induced changes in the redox properties, are generally composed of a receptor unit, which works by the covalent association of a substrate-recognition functionality, and an electrochemical-signaling capacity (redox-active unit).

The redox-active tetrathiafulvalene (TTF) unit can exist in three stabile redox states (TTF^0, TTF^+, and TTF^{2+}). This unit was used in the synthesis of the first calix[4]pyrrole incorporating a TTF redox moiety **37** which is an efficient chemosensor and allows the detection of anions by electrochemical means[38].

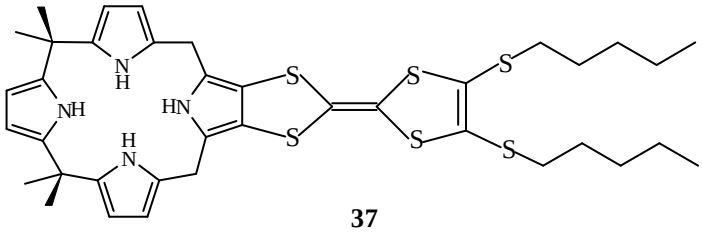

37

This system displays the strongest anion binding affinities yet recorded for calix[4]pyrrole receptors, and the binding constants between **37** and Br^-, Cl^-, and F^- ions are two orders of magnitude higher than those reported for *meso*-octamethylcalix[4]pyrrole **1** under the same conditions[8a] (**Table 7**).

Table 7[38]

*Binding constants between **37** and the Br^-, Cl^-, and F^- ions determined by ^{1}H NMR spectroscopy at 300 K, and first redox potentials $E^1_{1/2}$ of the complexes **37**·X^- (where X is a halide) determined by CV at 298K.*

X^-	K_a [M^{-1}] (CD_3CN/0.5% v/v D_2O)	$E^1_{1/2}$ [mV](MeCN)[a]	ΔE[mV](MeCN)[b]
Br^-	7 600[c]	+467	-34
Cl^-	120 000[d]	+462	-43
F^-	2 100 000[e]	-	-

[a] – values obtained from 1:1 mixtures of **37** and nBu$_4$NX; [b] – maximum (ΔE_{max}) were obtained from 1:2 mixtures of **37** and nBu$_4$NX; [c] – a CD_3CN (0.5% v/v D_2O) solution of nBu$_4$NBr which also contained receptor **37** at the initial concentration to account for dilution effects; [d] – determined from competitive binding experiments. An average K_{rel} of 16.8 for the ions Cl^-/Br^- was obtained by analyzing a CD_3CN (0.5% v/v D_2O) solution of **37** (3.9 mM) containing Br^- (3.9 equiv.) and Cl^- (either 1.6 or 2.1 equiv.), estimated error was <15%; [e] – determined from competitive binding experiments. An average K_{rel} of 16.9 for F^-/Cl^- was obtained by analyzing a CD_3CN (0.5% v/v D_2O) solution of **37** (3.9 mM) containing Cl^- (7.4 equiv.) and F^- (either 2.0 or 2.2 equiv.), estimated error was <15%.

The stronger affinity of **37** towards anions is presumably a direct consequence of the pyrrolo-TTF-NH proton being more acidic than the other NH protons of **37**. This fact implies that the pyrrolo-TTF-NH proton is able to form a stronger hydrogen bond with anions upon complexation, as compared to NH protons in the parent calix[4]pyrrole.

Calix[4]pyrroles were used as anion binding agents in liquid polymeric membrane ion-selective electrodes. Poly(vinyl chloride)-derived ion-selective electrodes prepared from *meso*-octamethylcalix[4]pyrrole **1** display at lower pH values (*i.e.*, 3.5 and 5.5) strong anionic responses toward Br^-, Cl^-, and $H_2PO_4^-$ and, to a much lesser extent in the case of F^-. By contrast, at high pH (*i.e.*, 9.0) ion-selective electrodes not only display cationic responses toward chloride and bromide anions but also selectivities (*i.e.*, $Br^- < Cl^- < OH^- \approx F^- < H_2PO_4^-$)[39]. This fact was considered consistent with the poly(vinyl chloride)-supported receptor behaving as a direct anion binding agent at low pH but acting as a hydroxide-complexing receptor at higher pH.

Using cyclic voltammetry were studied the electrochemical properties of ferrocenyl including calix[4]pyrroles **12** and **13** and it was demonstrated that these systems bind anions in dichloromethane-d_2 solution[23]. Electrochemical studies using cyclic voltammetric and square-wave voltammetric techniques of calix[4]pyrroles **14** containing a ferrocene moiety attached to one of the *meso*-position show cathodic shifts of up to 100 mV with dihydrogenphosphate anions[24].

BINDING OF NEUTRAL SUBSTRATES

Molecular recognition of neutral compounds presents a challenge in the area of supramolecular chemistry. Binding of substrates such as short-chain alcohols and simple monoamides is particulary difficult because these molecules have few

functionalized sites available for hydrogen bonding, and they lack the large hydrocarbon surface necessary to participate in efficient hydrophobic or π - π stacking interactions. Association constants for neutral substrate/synthetic receptor complexes are thus generally modest, even though the architectural complexity of the receptors is often high[1].

It was found that the molecular recognition chemistry of the calix[4]pyrroles is not limited to anionic substrates. The coordination of neutral species was achieved using *meso*-octamethylcalix[4]pyrrole **1**. The ^{1}H NMR titration experiments in C_6D_6, revealed that this calix[4]pyrrole forms complexes with neutral species, including short chain alcohols, amides and other oxygen-containing neutral species[10]. Although the binding constants are modest, a clear trend is evident within the alcohol and amide series. Specifically, it was found that the relevant stability constants decrease as the steric bulk around the oxygen atom is increased (**Table8**)[8a].

The structure of **1** coordinated to two molecules of MeOH was determined by X-ray diffraction analysis. The calixpyrrole in this neutral substrate adopts a 1,3-alternate conformation in the solid state. In the case of DMF molecules, each of the two DMF molecules was found to be coordinated to a single calix[4]pyrrole macrocycle *via* two hydrogen bonds and this complex adopts a 1,2-alternate conformation [8a].

Similarly, using X-ray analysis it was found that calix[4]pyrrole **2a** also acts as a receptor by H-bond interactions to an EtOH solvent. The pyrrole groups are arranged in a 1,3-alternate conformation that gives rise to disorder in the EtOH guest, due to its ability to coordinate both above and below the plane of the macrocycle[40].

Table 8

*Association constants for **1** with neutral substrates*

Neutral substrate	$K_a(M^{-1})$	*Neutral substrate*	$K_a(M^{-1})$
MeOH	12.7±1.0	*N,N*-dimethylacetamide	9.0±0.9
EtOH	10.7±0.7	1,1,3,3-tetramethylurea	2.2±0.1
BnOH	9.7±0.7	DMSO	16.2±1.1
Pr^{i}OH	7.0±0.4	1,2-dimethylimidazole	5.4±0.3
Bu^{s}OH	6.2±0.4	acetone	2.2±0.2
N-formylglycine ethyl ester	13.3±1.0	nitromethane	-
DMF	11.3±0.8		

Meso-octaethylcalix[4]pyrrole **30** inclusion crystals with lower alcohols undergo reversible guest-responsive structural changes, for much a long-range cooperative effect with a Hill coefficient of 40 was observed[41].

According to the X-ray analysis, the conformation of octabenzylcalix[4]pyrrole **38** in **38**·2(acetone)·acetone$_{lattice}$ is 1,3-alternate (as in **1**·2(MeOH)), but the two acetone guests are both located on the *same* face of the ligand, held in place by single H-bonds.

The molecular structure of **38**·2(acetone)·acetone$_{lattice}$ demonstrates that the NH groups of bulky calixpyrrole 38 can access the carbonyl portion of acetone**,** thus, the weak solution binding of acetone by unhindered **1** (K_a = 2.2±0.2 M^{-1}) cannot be explained on steric grounds. In this case, water could not be completely removed from the solution used in the titrations, and the presence of this competing H-bonding material could account for the low apparent K_a.

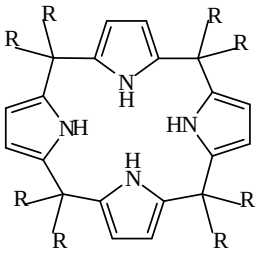

38 R = CH_2Ph

These results confirm that the calixpyrroles can be used to bind neutral species both in solution and in the solid state.

Calix[4]pyrroles **6** and **7** containing deep cavities and fixed walls show binding properties not only for anions, but also for neutral species. For example, in the specific case of the αααα isomer of **6**, a deep cavity structure was observed in the solid state, wherein the calixpyrrole core is in a so-called cone conformation (***Fig.6***). Structures of lower symmetry are seen in the case of the other isomers, with conformations other than pure cone (*e.g.*, 1,3-alternate, partial cone) being observed in certain instances (*e.g.*, the αααβ isomer of **7**; **Fig.6**)[16].

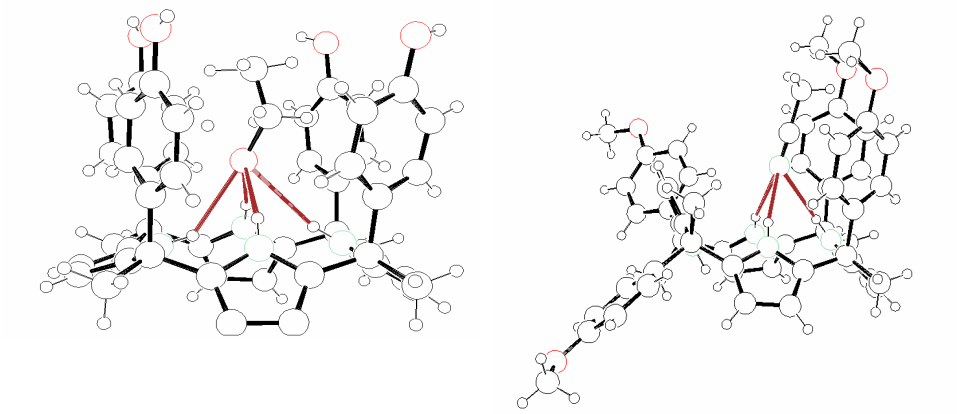

Fig. 6. *View of the molecular structures of the ethanol adducts of the αααα isomer of **6** in the cone conformation (left) and the acetonitrile adduct of the αααβ isomer of **7** in the partial cone conformation (right). Dashed lines are indicative of a hydrogen-bonding interaction.*

Some calix[4]pyrroles with extended or superextended cavities play an important role in multi-point or multi-site host-guest interactions. For instance, compound **6** in its cone conformation **a** is associated into dimmers or trimmers, the molecular complexity being determined by the guest molecule. In the presence of hydrogen-binding substrates such as DMF or acetic acid, the isomer **6a** is assembled into closed two-basket cavity dimmers, **6a**·DMF, or into cyclic turmeric units **6a**·$AcOH^3$.

The trimeric cavity hosts nine molecules of AcOH, three of them being associated to the calix[4]pyrrole moieties while the other six establish an intermolecular hydrogen bonding network with other trimmers.

It was observed that not only the attached moiety, but also its position influences the selectivity of the calix[4]pyrroles. Systems containing cytosine-substituted calix[4]pyrrole conjugates, bearing the appended cytosine attached at either a β- or *meso*-pyrrolic position, were tested as nucleotide-selective carriers and as active components of nucleotide-sensing ion-selective electrodes at pH 6.6[42]. Studies of carrier selectivity were made using a Pressman-type model membrane system consisting of an initial pH 6.0 aqueous phase, an intervening dichloromethane barrier containing the calix[4]pyrrole conjugate, and a receiving basic aqueous phase. Good selectivity was found for the Watson-Crick complementary nucleotide, 5'-guanosine monophosphate (5'-GMP), in the case of the *meso*-linked conjugate with the relative rates of through-membrane transport being 7.7:4.1:1 for 5'-GMP, 5'-AMP, and 5'-CMP, respectively. By contrast, the β-substituted conjugate, while showing a selectivity for 5'-GMP that was enhanced relative to unsubstituted calix[4]pyrrole, was found to transport 5'-CMP roughly 4.5 times more quickly than 5'-GMP. Higher selectivities were also determined for 5'-CMP when both the β-and *meso*-substituted conjugates were incorporated into polyvinyl chloride membranes and tested as ion selective electrodes at pH 6.6, whereas near-equal selectivities were observed for 5'-CMP and 5'-GMP in the case of unsubstituted calix[4]pyrroles. These seemingly disparate results are consistent with a picture wherein the *meso*-substituted cytosine calix[4]pyrrole conjugate, but not its β- linked congener, is capable of acting as a ditopic receptor, binding concurrently both the phosphate anion and nucleobase portions of 5'-GMP to the calixpyrrole core and cytosine "tails" of the molecule, respectively, with the effect of this binding being most apparent under the conditions of the transport experiments[42].

Another use of calix[4]pyrroles is the investigation of thin films of *meso*-tetra(methyloctyl) calix[4]pyrrole, which were transferred onto hydrophobized quartz and silicon oxide sheets by using the Langmuir-Schaefer (LS) method (horizontal lifting). Scanning force microscopy investigation show that the LS films are almost homogeneous and are consistent with the X-type configuration with the hydrophobic tails of the calix[4]pyrrole disposed almost perpendicularly with respect to the substrate. Induced circular dichroism (ICD) measurements were performed in the presence of chiral alcohol vapors, such as (-)-(R)-2-butanol, (-)-(R)-2-pentanol, and (-)-(R)-2-hexanol. The results show that although not chiral by themselves this kind of calix[4]pyrrole molecules within the film exhibit chirality induced by binding with the chiral guests. The reversibility of the binding event, coupled with the differentiated response observed towards the investigated alcohols, makes the LS films promising active layers for the chemical recognition of short-chain polar neutral molecules[43].

Silver surfaces covered with Langmuir-Blodgett (LB) films of *meso*-octaethyl-calix[4]pyrrole **30** were investigated as sensing material for alcohol vapors recognition by Surface Plasmon Resonance (SPR) transduction methodology[44,45,46] In particular, SPR tests were performed by exposure of calix[4]pyrrole **30** films at fast sequential alcohol insets in the optical cell. The results demonstrate that this calix[4]pyrrole provides a clear recognition of alcohol species used in the inset sequences.

The same calix[4]pyrrole films were inspected by Atomic Force Microscopy (AFM). The films deposited onto silver were also tested for recognition of alcohol vapors by the SPR technique. The results reveal an increased sensitivity in the series isopropanol > ethanol > methanol[47].

CALIX[4]PYRROLES – POTENTIOMETRIC SENSORS FOR NEUTRAL SPECIES

Calix[4]pyrroles were applied as a new class of ligands of potentiometric sensors for neutral nitrophenol isomers. Lipophilic macrocyclic and acyclic derivatives of pyrrole were applied as sensory elements of liquid membrane potentiometric sensors destined for the recognition of neutral form of nitrophenol isomers. It was determined that the potential of liquid membranes containing pyrrole derivatives strongly depend on the pH of the solution. Their potentiometric responses generated in the presence of nitrophenol derivatives were studied at three different pH: 4.0, 6.0 and 8.0. It was found that all studied membranes respond towards the neutral form of nitrophenol isomers and do not respond to their anionic forms. It was determined that the symmetry of the macrocyclic cavity of calix[4]pyrroles has a very mild effect on the molecular recognition of nitrophenol guests and the membrane incorporating macrocycle pyrrole derivatives generate a higher potentiometric signal in the presence of neutral nitrophenol in comparison to membranes containing acyclic pyrrole derivatives. It was noticed that these sensors display higher selectivity for *para*-nitrophenol[48].

Using the same manner and calix[4]pyrrole **2a** and **39** as ligands authors[49] show a very high affinity of calix[4]pyrrole-containing liquid membrane electrodes to uptake of protons and very high selectivity toward *para*-nitrophenol, in his neutral form in the presence of other nitrophenols and dihydroxybenzene isomers.

They also demonstrate the mechanism of the potentiometric signal generation of these sensors, generally, consisting on the reversible interaction of protonated calix[4]pyrrole membrane surface with the neutral nitrophenol guest, and subsequent proton transfer from the interface to the aqueous solution.

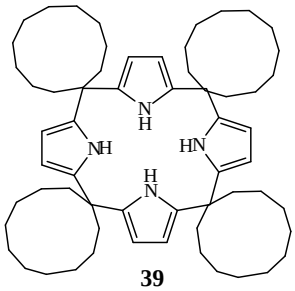

39

Potentiometric discrimination of fluoro- and chlorophenols isomers based on the host functionality of calix[4]pyrolle at liquid membrane interfaces was also reported by the same group of authors[50].

OTHER APPLICATIONS OF CALIX[4]PYRROLES

Tl(I) selective electrodes based on *meso*-octamethylcalix[4]pyrrole **1**, *meso*-octaethylcalix[4]pyrrole **30** and *meso*-tetraspirocyclohexylcalix[4]pyrrole **2** as sensor molecules were tested. This electrode exhibit a fast response time of 30 s and high selectivity over Na^+, K^+ and other metal ions with only Ag^+ interfering. It was demonstrated

that this electrode works well in the pH range 2.0-11.0 and can be successfully employed for the determination of Tl^+. The presented electrode was also used as an indicator electrode in potentiometric titration of Tl^+ [51].

The electropolymerization properties of calix[4]pyrroles containing pendant N-substituted pyrrole moieties **40** and **41** were studied and it was found that electrochemical copolymerisation with pyrrole was successful. By contrast, attempts to polymerise the calix[4]pyrroles alone failed[52].

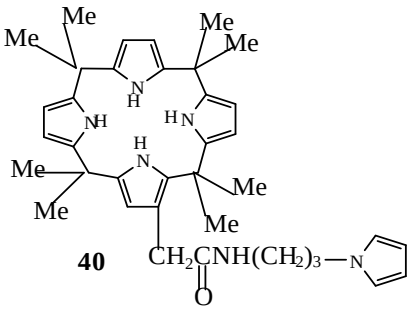

40

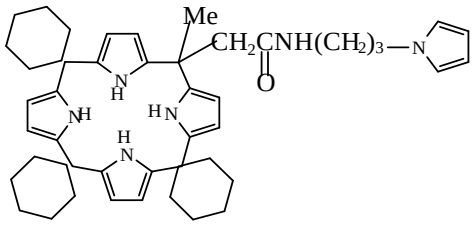

41

The examples presented in this review suggest that there could be a rich molecular recognition chemistry associated with calix[4]pyrroles. Not only the introduction of *meso*-, but also the β- substituents allow the anion and neutral binding and selectivity of the calix[4]pyrrole skeleton. Facile fictionalisation of calix[4]pyrrole systems opens the possibility of producing calixpyrroles with an endless variety of secondary binding sites that may allow for the optimised recognition of cationic, anionic, and neutral guests[16]. On the other hand, calix[4]pyrroles exhibit very interesting chromatic, fluorescent and electrochemical sensing properties, which can be used in different area.

REFERENCES

1 William E. Allen, Philip A. Gale, Christopher T. Brown, Vincent M. Lynch, and Jonathan L. Sessler, *J. Am. Chem. Soc*., 1996, **118**, 12471.

2 Lehn, J. M., *Supramolecular Chemistry*; VCH Press: Weinheim, Germany, 1995.

3 Lucia Bonomo, Euro Solari, Gülsen Toraman, Rosario Scopelliti, Mario Latronico and Carlo Floriani, *Chem. Commun*., 1999, 2413.

4 Jonathan L. Sessler, Andrei Andrievsky, Philip A. Gale and Vincent M. Lynch, *Angew. Chem. Int. Ed. Engl.*, 1996, **35**, 2782.

5 a) A. Baeyer, *Ber. Dtsch. Chem. Ges.*, 1872, **5**, 1094; b) A. Baeyer, *Ber. Dtsch. Chem. Ges.*, 1886, **19**, 2184; c) M.Dennstedt and J. Zimmermann, *Chem. Ber.*, 1886, **19**, 2189; d) M.Dennstedt and J. Zimmermann, *Chem. Ber.*, 1887, **20**, 850; e) M.Dennstedt, *D. Chem. Ber.*, 1890, **23**, 1370; f) V. V. Chelintzev and B. V. Tronov, *J.Russ. Phys. Chem. Soc.*, 1916, **48**, 105; g) V. V. Chelintzev and B. V. Tronov, *J.Russ. Phys. Chem. Soc.*, 1916, **48**, 1197;h) P. Rothemund and C. L. Gage, *J. Am. Chem. Soc.*, 1955, **77**, 3340.

6 Philip A. Gale, Lance J. Twyman, Cristin I.Handlin and Jonathan L. Sessler, *Chem. Commun.*, 1999, 1851.

7 Philip A. Gale, Jonathan L. Sessler, Vladimír Král, and Vincent Lynch, *J. Am. Chem. Soc.*, 1996, **118**, 5140.

8 a)Philip A. Gale, Jonathan L. Sessler and Vladimír Král, *Chem. Commun*., 1998, 1; b) Gale, P.A.; Anzenbacher Jr. P.; Sessler J. L.: *Coordination Chemistry Reviews*, 2001, **222**, 57.

9 W.H. Brown, B. J. Hutchinson and M. H. MacKinnon, *Can. J. Chem*., 1971, **49**, 4017.

10 Hynes, M. J., *J. Chem. Soc. Dalton Trans*., 1993, 311.

11 Jonathan L. Sessler, Pavel Azenbacher,Jr., Hidekazu Miyaji, Karolina Jursíková, Ellen R. Bleasdale, and Philip A. Gale, *Ind. Eng.Chem. Res.,* 2000, **39**, 3471.

12 Philip A. Gale, Jonathan L. Sessler, William E. Allen, Nicolai A. Tvermoes and Vincent Lynch, *Chem. Commun*., 1997, 665.

13 Shao, Shi Jun; Yu, Xian Da; Cao, Shu Qin, *Chinese Chemical Letters,* 1999, **10(3)**, 193.

14 Pavel Azenbacher,Jr., Andrew C. Try, Hidekazu Miyaji, Karolina Jursíková, Vincent M. Lynch, Manuel Marquez, and Jonathan L. Sessler, *J. Am. Chem. Soc*., 2000, **122**, 10268.

15 Miyaji, Hidekazu; An, Deqiang; Sessler, Jonathan L., *Supramolecular Chemistry*, 2001, **13(6)**, 661.

16 Pavel Azenbacher,Jr., Karolina Jursíková, Vincent M. Lynch, Philip A. Gale, and Jonathan L. Sessler, *J. Am. Chem. Soc*., 1999, **121**, 11020.

17 Bonomo, Lucia; Solari, Euro; Toraman, Gulsen; Scopelliti, Rosario; Floriani, Carlo; Latronico, Mario, *Chem. Commun.(Cambridge)*, 1999, **23**, 2413.

18 Salvatore Camiolo and Philip A. Gale, *Chem. Commun*., 2000, 1129.

19 Camiolo, Salvatore; Coles, Simon J.; Gale, Philip A.; Hursthouse, Michael B.; Sessler, Jonathan L., *Acta Crystallographica, Section E*: Structure Reports Online, 2001, **E57(9)**, 0816-0818.

20 Woods, Christopher J.; Camiolo, Salvatore; Light, Mark E.; Coles, Simon J.; Hursthouse, Michael B.; King, Michael A.; Gale, Philip A.; Essex, Jonathan W., *J. Am. Chem. Soc*., 2002, **124 (29)**, 8644.

21 Jonathan L. Sessler, Pavel Azenbacher,Jr., Karolina Jursíková, Hidekazu Miyaji, John W. Genge, Nicolai A. Tvermoes, William E. Allen, and James A. Shriver, *Pure & Appl. Chem.,* 1998, **70**, 2401.

22 Jonathan L. Sessler, Philip A. Gale, and John W.Genge, *Chem. Eur. J*., 1998, **4**, 1095.

23 Sessler, Jonathan L.; Gebauer, Andreas; Gale, Philip A., *Gazzetta Chimica Italiana*, 1998, Volume Date 1997, *127(11)*, 723.

24 Philip A. Gale, Michael B. Hursthouse, Mark E.Light, Jonathan L. Sessler, Colin N. Warriner and Rebecca S. Zimmerman, *Tetrahedron Letters*, 2001, **42**, 6759.

25 He, li Jun; Cai, Qing Song; Shao, Shi Jun; Jiang, Sheng Xiang, *Chinese Chemical Letters,* 2001, **12(6)**, 511.

26 Dukh, Mykhaylo; Drasar, Pavel; Cerny, Ivan; Pouzar, Vladimir; Shriver, James A.; Král, Vladimír; Sessler, Jonathan L., *Supramolecular Chemistry*, 2002, **14(2-3)**, 237.

27 Sato, W.; Miyaji, H.; Sessler, J. L., *Tetrahedron Letters*, 2000, **41(35)**, 6731.

28 Chang-Hee Lee, Hee-Kyung Na, Dae-Wi Yoon, Dong-Hoon Won, Won-Seob Cho, Vincent M. Lynch, Sergey V. Shevchuk, and Jonathan L. Sessler, *J. Am. Chem. Soc*., 2003, **125**, 7301.

29 Dae-Wi Yoon, Hoon Hwang, and Chang-Hee Lee, *Angew. Chem. Int. Ed.*, 2002, **41**, 1757.

30 Willen P. van Hoorn and William L. Jorgensen, *J. Org. Chem.,* 1999, **64**, 7439.

31 J. Ramón Blas, Manuel Márquez, Jonathan L. Sessler, F. Javier Luque, and Modesto Orozco, *J. Am. Chem. Soc*., 2002, **124**, 12796.

32 Hidekazu Miyaji, Wataru Sato, and Jonathan L. Sessler, *Angew.Chem. Int. Ed*., 2000, **39**, 1777.

33 Hidekazu Miyaji, Wataru Sato, Jonathan L. Sessler and Vincent M. Lynch, *Tetrahedron Letters*, 2000, **41**, 1369.

34 Shijun Shao, Yong Guo, Lijun He, Shengxiang Jiang and Xianda Yu, *Tetrahedron Letters*, 2003, **44**, 2175.

35 Hidekazu Miyaji, Pavel Azenbacher,Jr., Jonathan L. Sessler, Ellen R. Bleasdale and Philip A. Gale, *Chem. Commun*., 1999, 1723.

36 Pavel Azenbacher, Jr., Karolina Jursíková, and Jonathan L. Sessler, *J. Am. Chem. Soc.*, 2000, **122**, 9350.

37 P.A. Gale, M.B. Hursthouse, M.E. Light, J. L. Sessler, C. N. Warriner, R. S. Zimmerman, *Tetrahedron Lett*., 2001, **42**, 6759.

38 Kent A. Nielsen, Jan O. Jeppensen, Eric Levillain, and Jan Becher, *Angew.Chem. Int. Ed.*, 2003, **42**, 187.

39 Král, Vladimír; Sessler, Jonathan L.; Shishkanova, Tatiana V.; Gale, Philip A.; Volf, Radko, *J. Am. Chem. Soc.*, 1999, **121(38)**, 8771.

40 Camiolo, Salvatore; Coles, Simon J.; Gale, Philip A.; Hursthouse, Michael B.; Paver, Michael A., *Acta Crystallographica, Section E*: Structure Reports Online, 2001, **E57(3)**, 0258-0260.

41 Furusho, Yoshio; Aida, Takuzo, *Chem. Commun*. (Cambridge), 1997, **22**, 2205.

42 Sessler, Jonathan L.; Král, Vladimír; Shishkanova, Tatiana V.; Gale, Philip A., *Proceedings of the National Academy of Sciences of the United States of America,* 2002, **99(8)**, 4848.

43 a) Sortino, Salvatore; Petralia, Salvatore; Pignataro, Bruno; Marletta, Giovanni; Conoci, Sabrina; Valli Ludovico, *New Journal of Chemistry,* 2003, **27(3)**, 615. b) Sortino, S.; Petralia, S.; Condorelli, G.; Conoci, S.; Valli L.; Rella R., *Sensors for Environmental Control, Proceedings of the International Workshop on New Developments on Sensors for Environmental Control,* Lecce, Italy, May 27-29, 2002 (2003), 79.

44 Conoci, S.; Valli L.; Rella R.; Palumbo, M.; *Sensors for Environmental Control, Proceedings of the International Workshop on New Developments on Sensors for Environmental Control,* Lecce, Italy, May 27-29, 2002 (2003), 74.

45 Conoci, S.; Palumbo, M.; Pignataro, B.; Rella R.; Valli L.; Vasapolo, G., *Colloids and Surfaces, A: Physicochemical and Engineering Aspects,* 2002, 198-200 869-873.

46 Conoci, S.; Palumbo, M.; Valli L.; Vasapolo, G.; Rella R.; Siciliano, P., *Sensors and Microsystems, Proceedings of the Italian Conference: Extended to Mediterranean Countries*, 5th, Lecce, Italy, Feb. 12-16, 2000 (2000), 112.

47 Conoci, S.; Valli L.; Pignataro, B.; Marletta, G.; Rella R., *Sensors and Microsystems, Proceedings of the Italian Conference*, 6th, Pisa, Italy, Feb. 5-7, 2001 (2002), 81.

48 Piotrowski, Tomasz; Radecka, Hanna; Radecki, Jerzy; Depraetere, Stefaan; Dehaen, Wim, *Material Science & Engineering, C: Biomimetic and Supramolecular Systems,* 2001, **C18(1-2)**, 223.

49 Tomasz Piotrowski, Hanna Radecka, Jerzy Radecki, Stefaan Depraetere, Wim Dehaen, *Electroanalysis*, 2001, **13**, 342.

50 T. Piotrowski, H. Radecka, J. Radecki, S. Depraetere, W. Dehaen, *Analytical Letters,* 2002, **35***,* 12.

51 Park, Kyeong Soon; Jung, Sung Ouk; Lee, Shim Sung; Kim, Jae Sang, *Bulletin of the Korean Chemical Society,* 2000, **21(9)**, 909.

52 Gale, Philip A.; Bleasdale, Ellen R.; Chen, George Z., *Supramolecular Chemistry*, 2001, **13(4)**, 557.

STUDIA UNIVERSITATIS BABEŞ-BOLYAI, CHEMIA, XLIX, 1, 2004

SCANNING ELECTRON MICROSCOPY STUDY OF UNDOPED AND METAL DOPED ANODIC POROUS ALUMINA MEMBRANES

ZOFIA VÉRTESY[1*], ERZSÉBET VERESS[2], GHEORGHE MIHĂILESCU[3], STELA PRUNEANU[3], LÁSZLÓ P. BIRÓ[1]

[1] Research Institute for Technical Physics and Materials Science, Hungarian Academy of Sciences, H-1525 Budapest, PO Box 49, Hungary;
[2] Babeş-Bolyai University, Faculty of Chemistry, Department of Inorganic Chemistry, Str. Arany János Nr. 11 Cluj, 400028, România;
[3] National Institute for Isotopic and Molecular Technology, Str. Donath Nr. 65-103 Cluj, 400290, România.

[*]Corresponding author. E-mail address: vertesyz@mfa.kfki.hu

ABSTRACT. Porous Al_2O_3 membranes were prepared by low-temperature anodic oxidation in aqueous electrolyte solution of Al foils with and without thermal pretreatment. Some of membranes were doped with Co and Ni by a.c. electrolysis. Scanning electron microscopy of the membranes confirms the existence of strain field regions, thus providing an experimental evidence of the earlier proposed mechanism for the development of the porous structure. The Co doped membranes were found as being very effective substrates for catalytic growth of carbon nanotubes.

Keywords: Porous Al_2O_3; Scanning Electron Microscopy; Carbon Nanotubes

1. INTRODUCTION

The obtaining of well-ordered nanostructured patterns with good accuracy over large areas is important task of the modern microelectronics. Utilization of substrates of naturally self-organized meso- or nanostructure can spectacularly reduce the processing times in comparison with conventional and electron beam lithography. Porous alumina prepared by anodic oxidation of aluminum has been recently studied and applied to produce nanowires, nanodots from different metals [1-3]. In this paper we report some of our results about the influence of the preparation conditions on the morphology of such alumina membranes, as well as some results obtained in the study carried out on electrochemically metallized membranes (doped by a.c. deposition of Ni or Co) in order to establish the dopant localization and structure. Alumina membranes doped with Co were tested as substrates for low-temperature catalytic growth of carbon nanotubes.

2. EXPERIMENTAL

Porous Al_2O_3 membranes were prepared from pre-annealed as well as thermally untreated 0.1 mm thick Al foils. Heat treatment was performed at 250^0C or 300^0C, and for 30 or 50 min, respectively. Low-temperature anodic oxidation was carried out in a two-compartment electrochemical cell, one compartment of which contained the aqueous electrolyte solution and the other distilled water. The Al foils were placed vertically between the two compartments providing their hermetic separation.

The exposed area of the Al foils was of 6 cm^2. An Al disk of 15 cm^2 area was used as counter electrode. In order to avoid the dissolution of the porous layer formed, during the oxidation the electrolysis compartment was cooled by circulating through a glass coil water chilled in a cryostat. However, the temperature slowly raised in time, from 4.0 ± 0.2^0C at the start to 6.0 ± 0.5^0C when the anodization was finished.

The preparation of the membranes was preceded by electrochemical cleaning ("polishing") of the Al foils, by anodic oxidation carried out for 2 min at 85^0C and current density of 100 mA/cm^2 (used electrolyte: 70 % HNO_3 + H_3PO_4). Then, the foils were rinsed in distilled water, immersed for 5 min in 1 M NaOH, and carefully washed with bidistilled water.

Preparation of membranes by anodic oxidation was carried out in several steps as follows:

(i) Oxidation at constant potential (10 V) for 10 min;
(ii) Oxidation at constant current in 17 % sulfuric acid at current density of 15 mA/cm^2; the time of oxidation was 90 and respectively 120 min for the different specimens;
(iii) Oxidation at constant potential (20 V) for 15 min in 15 % sulfosalicylic acid;
(iv) Finally, the samples were treated with 5 % H_3PO_4 in order to enlarge the pores and avoid their sealing.

The remained Al substrate was removed in a 0.1 M $CuCl_2$ solution prepared in 20 % HCl.

On some of the obtained Al_2O_3 membranes, Co or Ni was deposited by a.c. electrolysis. The deposition was carried out at 13 V and 40^0C for 20 min using a metallization bath which contained 30 g/l $CoSO_4$, 40 g/l H_3BO_3 and 20 g/l $(NH_4)_2SO_4$ in case of Co deposition, and respectively 30 g/l $NiCl_2$, 40 g/l H_3BO_3 and 20 g/l $(NH_4)_2SO_4$ in case of Ni doping.

Carbon nanotubes were synthesized by low-temperature catalytic decomposition of a hydrocarbon over the Co doped alumina membranes. In this purpose, N_2 diluted acetylene was passed over the metallized sample for 10 min, the temperature ranging from 600^0C to 700^0C. The flows of the carrier gas (N_2) and of the reacting gas (acetylene) were set to 300 and 30 ml/min, respectively [4].

The surface morphology and cross-sectional structure of the samples were observed by means of SEM using a JEOL JSM 840 microscope. Microanalysis of metal doped membranes was carried out using ORTEC EDS equipment.

3. RESULTS

We have observed membranes in cross-sectional and in plan view. Micrographs in cross-sectional view show that oxidation produced columnar pores in all samples. In plan view all samples also show some common morphologic elements (plateaus, cracks, bulges). The size and number of morphologic elements is different in case of different preparation conditions. The formation of porous Al_2O_3 is accompanied by generation of strain fields at the interfaces between the substrate Al and the barrier layer of Al_2O_3 as well as between the Al_2O_3 and the electrolyte solution. This process is described in ref. [3]. Bulges find by us can be regarded as material evidence for the existence of such fields (see Fig. 1.). This supposition is confirmed by the finding of especially large number of bulges presented by non-annealed samples.

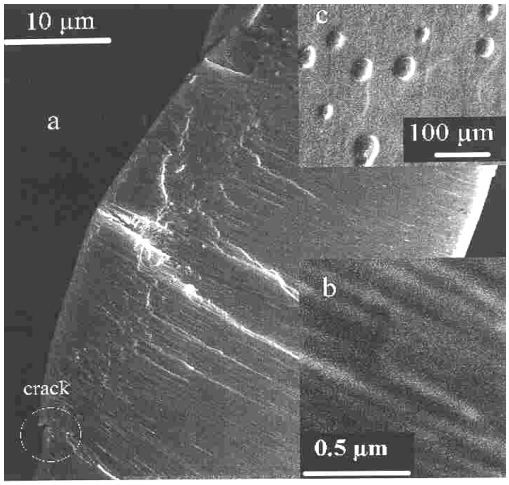

Fig. 1. *Membrane morphology in case of non-annealed sample obtained by two-step anodic oxidation. Cross-sectional view: (a) bulge accompanied by cracks; (b) pores in higher magnification. Plan view: (c) bulges as they appear on the membrane surface.*

Thermal treating of the Al foils influences the size of the formed pores: the average pore diameter in case of pre-annealed samples was of only 35 – 45 nm vs. 50 nm as measured in non-annealed samples (Fig. 2.).

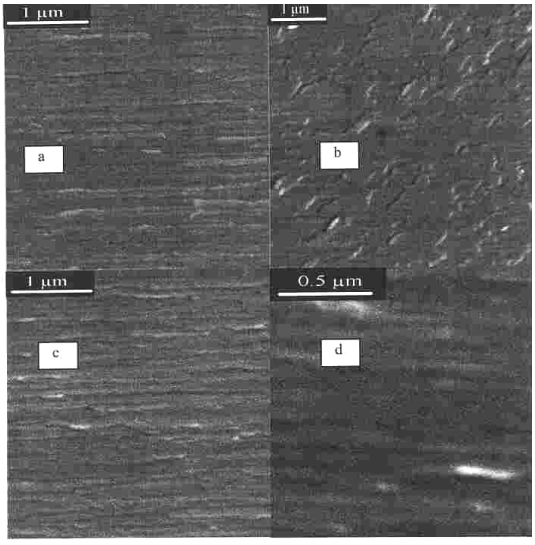

Fig. 2. *Pores size in different samples. (a) Sample pre-annealed at 250^{0}C for 50 min; (b) and (c) samples pre-annealed at 300^{0}C for 30 min; (d) non-annealed samples.*

The morphology of the examined samples was very "rich" and non-regular indicating a non-regular underlying porous structure: the columnar pores are not arranged in symmetrical hexagonal cells. However, as can be seen on Fig. 3., in some pre-annealed samples the plateaus observed form joint angles of approximately 120^0 in evidence of the "hidden" hexagonal symmetry. Open self-organized pores have been found exclusively in non-annealed samples (Fig. 4.).

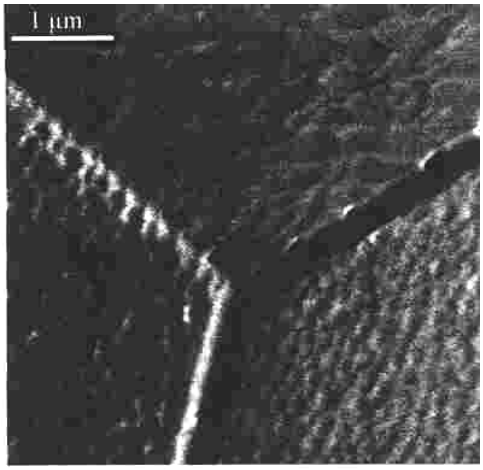

Fig. 3. *plateaus formed on the surface of a sample pre-annealed at 300^{0}C for 30 min, indicating a "hidden" hexagonal ordonation of the membrane structure.*

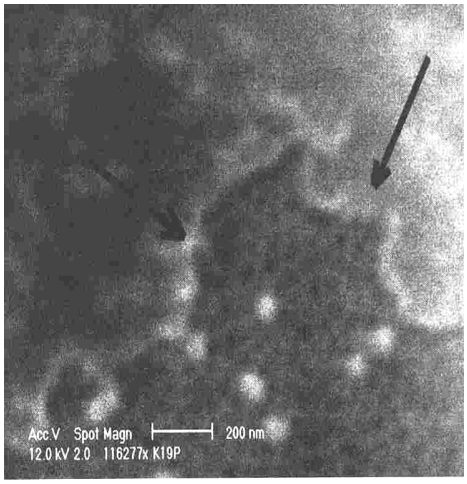

Fig. 4. *Open pores domain on the surface of a non-annealed alumina membane*

A well-defined closure layer (the so called barrier layer) appears at the Al/Al_2O_3 interface (Fig. 5a.).

A similar continuous closure layer at the top of membrane (at the Al_2O_3/electrolyte interface) can be observed in case of pre-annealed samples only (Fig. 5b.).

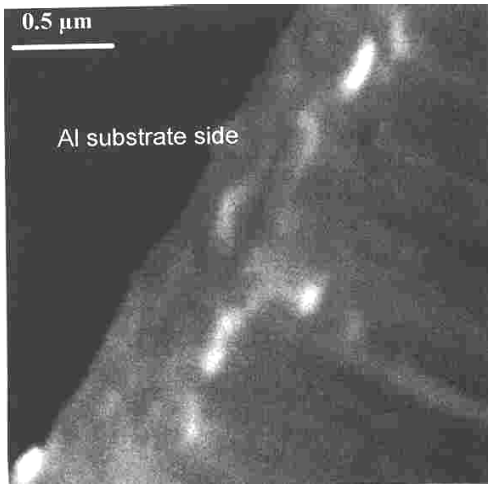

Fig. 5.a. *Closure layer at the Al/Al_2O_3 interface in case of a non-annealed sample.*

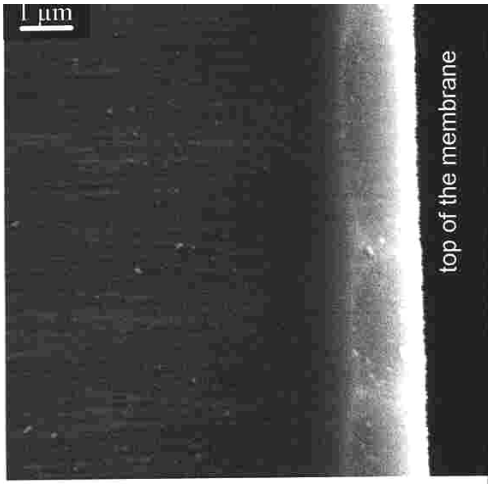

Fig. 5.b. *Closure layer at the Al_2O_3/electrolyte interface (at the top of the alumina membrane) formed in case of a pre-annealed sample.*

The metal penetration depth was determined by microanalysis on metallized samples. In non-annealed samples the presence of metal was detected in depth until approximately 4 μm. In case of pre-annealed samples, the deposited metal quantity was under the detection limit of the measuring apparatus: despite the visible presence of the metal, we were not able to evidence it.

The Co doped membranes were experimented, and proved to be suitable, as substrates for the purpose of catalytic growth of carbon nanotubes. As the catalytic activity was higher as expected, it was impossible to control the carbon nanotubes growing process even in the mildest experimental condition used (Fig.6).

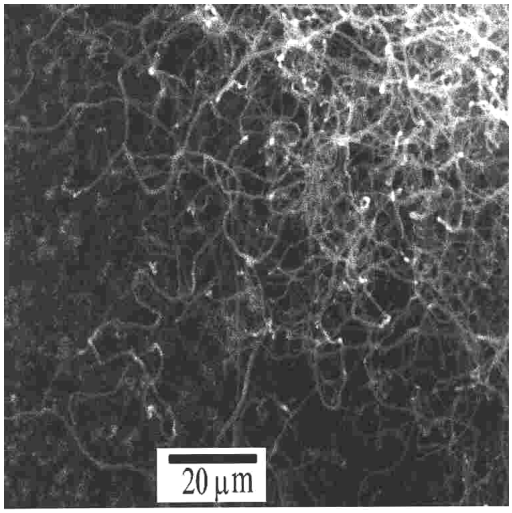

Fig. 6. *Carbon nanotubes "scrub" grown on a Co doped non-annealed anodic alumina membrane.*

4. CONCLUSIONS

The presented results can be summarized as follows:

(i) the electrochemical oxidation procedure applied leads to formation of columnar pores even at low potential and short exposition time;

(ii) pre-annealing seems to decreasing the strain field caused by the complex pore development process;

(iii) the diameter of the formed pores can be influenced by the pre-annealing conditions (time and temperature of Al foils thermal treatment);

(iv) carbon nanotubes can be grown in low-temperature conditions on similarly prepared Co doped samples in non-controlled way only.

ACKNOWLEDGEMENTS

This work was partially supported by the T 030435 Grant of the Hungarian Scientific Research Fund and the research grant awarded to Veress Erzsébet by the Hungarian Ministry of Education.

REFERENCES

1. Masuda, H., Fukuda, K.; Science, 268 (1995), 1466;
2. Masuda, H., Satoh, M.; J. Appl. Phys., 35 (1996), L126;
3. Shingubara, S., Okino, O., Sayama, Y., Sakue, H., Takahagi, T.; Jpn. Appl. Phys., 36 (1997), 7791;
4. Willems, I., Kónya, Z., Colomer, J-F., van Tendeloo, G., Nagaraju, N., Fonseca, A., Nagy, J. B.; Chem. Phys. Letters, 317 (2000), 71.

STUDIA UNIVERSITATIS BABEŞ-BOLYAI, CHEMIA, XLIX, 1, 2004

THE INFLUENCE OF THE OXIDIZING AGENTS ON THE KINETICS OF COPPER LEACHING FROM CHALCOPYRITE CONCENTRATE WITH SULPHURIC ACID

CAMELIA LUMINITA VARGA[1], I. BALDEA[2], ANCA MIHALY-COZMUTA[1]

[1] Department of Chemistry, North University of Baia Mare, 4800 Baia Mare, Romania
[2]Department of Physical Chemistry, "Babes-Bolyai" University, 400028 Cluj-Napoca, Romania

ABSTRACT. The leaching rate constant and the apparent activation energy of chalcopyrite concentrate were investigated in sulphate media. The chemical composition (weight percent) of concentrate was: 30.38% Cu, 4.20% Zn, 1.92% Pb, 28.89% Fe and 34.49% S, respectively. The leaching time, the leaching temperature and the quantity of ferric sulphate and of oxygen as oxidizing agents were modified during the experiments. From the shape of the leaching curves, three stages of the process were observed. The apparent activation energy depends on the period of leaching as well as on the presence of ferric ion and oxygen as oxidizing agents in the leaching medium. The study intends to establish the rate controlling reaction step, according to both the activation energies, and the analytical expressions for each period.

INTRODUCTION

The most common hydrometallurgical processes for copper recovery are based on the solubilization in sulphuric medium. The sulphate-based process exhibits some potential advantages over the other systems. The sulphate leaching chemistry is generally simpler and better understood than other media leaching chemistry, and copper recovery by solvent extraction and electrowinning from sulphate medium is easier.

The dissolution of copper from chalcopyrite concentrate involves a complex mechanism. The most studied copper mineral is chalcopyrite, which leaches in sulphate medium by a parabolic kinetic [1-3], caused by the progressive formation of a sulphur layer or other products at the external surface. It behaves as a passivation layer.

From kinetic and surface science studies, the following reaction sequence has been proposed to describe the oxidative leaching and passivation of chalcopyrite in sulphate medium [3]:

$$CuFeS_2 \longrightarrow Cu_{1-x}Fe_{1-y}S_2 + x\,Cu^{2+} + y\,Fe^{2+} + 2(x+y)\,e^- \quad \text{(fast), (1)}$$

$y >> x,\ x + y \approx 1$

$$Cu_{1-x}Fe_{1-y}S_2 \longrightarrow Cu_{1-x-z}S_2 + z\,Cu^{2+} + (1-y)\,Fe^{2+} + 2(z+1-y)\,e^- \quad \text{(slow), (2)}$$

$$Cu_{1-x-z}S_2 \longrightarrow (1-x-z)z\,Cu^{2+} + 2\,S^{2+} + 2(1-x-zy)\,e^- \quad \text{(the slowest). (3)}$$

Within the fast initial period, the iron leaches preferentially as compared to copper. An intermediate disulphide phase is formed, $Cu_{1-x}Fe_{1-y}S_2$, where $y >> x$ and $x + y \approx 1$. In the second slow stage, the disulphide phase is further oxidized to form

copper polysulphide, $Cu_{1-x-z}S_2$, alternatively expressed as CuS_n where n=2/(1-x-z). The copper polysulphide acts on chalcopyrite as a passive layer.

The rate controlling reaction step is the slow decomposition of the copper polysulphide to cupric ions and elemental sulphur, with the polysulphide chains restructuring to form S_8 rings. The elemental sulphur is porous enough, so that the rate is not limited by reactant/product diffusion through sulphur unless the sulphur melts during leaching when higher temperatures are used.

EXPERIMENTAL

The leaching tests were carried out on chalcopyrite concentrate obtained by flotation of ores from mines around Baia Mare. The chemical and mineralogical composition of the investigated concentrate is shown in table 1.

Table 1.

The chemical and mineralogical composition of concentrate.

Chemical composition					
Element	Cu	Zn	Pb	Fe	S
% (weight percent)	30.38	4.2	1.93	28.89	34.49
Mineralogical composition					
Mineral	Chalcopyrite ($CuFeS_2$)	Pyrite (FeS_2)	Sphalerite (ZnS)	Galena (PbS)	
% (weight percent)	85.5-86.5	5-6	6-7	2-3	

The particle size of chalcopyrite concentrate ranged between 0.071 and 0.1 mm. A solution of 8.0 N H_2SO_4 was used as leaching medium. Each leaching experiment was performed with 2 g chalcopyrite concentrate and 15 ml leaching solution therefore, with a solid/liquid ratio of 1/7.5. The leaching experiments were carried out between 20 and 60°C.

To increase the copper dissolution, ferric sulphate was added to the leaching solution, as oxidizing agent. The tested concentration of ferric sulphate in 8.0 N H_2SO_4 was of 10, 20 and 30 g/l. Also, the leaching pulp was stirred by air bubbling at 200 l/hour in a volume of 210 ml leaching agent, at the same ratio of solid/liquid. The leaching experiments were carried out at a temperature of 40 and 60°C when the oxidizing agents (Fe^{3+} and/or O_2) were used. The leaching pulp was filtrated and the copper concentration of the solution was analyzed spectrophotometrically by using cuprizon as complexing agent.

RESULTS AND DISCUSSIONS

The leaching curves, presented in figure 1, indicates three periods of leaching [4-6]. From the shape of the leaching curve, it is obvious that the leached copper pecent present a sharply increse in the initial period followed by a tendency of leveling of in the third period of the solubilization.

Similary to the shrinking-core model for gas-solid noncatalytic reactions [7], three rates are observed:

I - diffusion of reagents through the boundary layer;
II - diffusion through the layer of products;
III - reaction at the interface of the unreacted core.

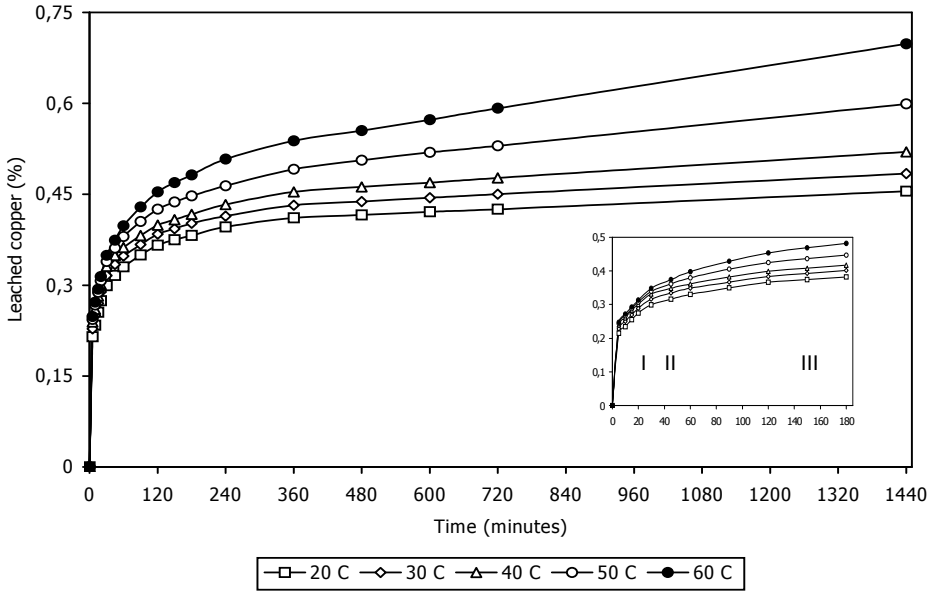

Fig. 1. *The chalcopyrite concentrate's leaching curves as a function of time at different temperatures.*

We were encouraged to use this shrinking-core model by the fact that the particle size did not vary after the leaching process. By drying the remaining solid material and separation by screening, the same size (between 0.071 and 0.1 mm) has been obtained.

It is obvious that the initial stage of solubilization is characterized by linear kinetics. Within this stage, the rate controlling reaction step is the external diffusion (the diffusion of reagents from the bulk solution to the particle surfaces).

The second period of solubilization could be described by a power function. For this leaching period, the rate controlling reaction step is the internal diffusion through the product layer adherent to the original material.

Within the third stage of solubilization, the rate controlling reaction step seems to be the chemical reaction.

The change of the leached copper percent in first, second and third period, respectively, could be described by the analytical expressions presented in table 2, where t is the leaching time, t_∞ represents the time for complete copper conversion if the process would follow the same mechanism throughout, and x is the converted fraction of copper. The ratio $\frac{1}{t_\infty}$ represents the rate constant (time^{-1}).

From the graphic representation of the functions $t/t_\infty=f(t)$, could be observed a near-linear dependences with a good enough correlation coefficients, as seen in figure 2 (a, b and c). Thus, the assumed model seems to be satisfactory.

The values of the apparent rate constants were estimated from the slopes of the straight lines obtained by using the experimental data for all three periods of chalcopyrite concentrate leaching, with sulphuric acid at 20°C.

Table 2.

The analytical expressions which describes the change of the leached copper percent in first, second and third period, respectively.

Period	*Analytical expressions*	*Time elapse* (minutes)
I	$\frac{t}{t_\infty} = 1 - (1 - x) = k_1 t$ (1)	0÷30
II	$\frac{t}{t_\infty} = 1 - 3(1 - x)^{\frac{2}{3}} + 2(1 - x) = k_2 t$ (2)	30÷180
III	$\frac{t}{t_\infty} = 1 - (1 - x)^{\frac{1}{3}} = k_3 t$ (3)	180÷1440

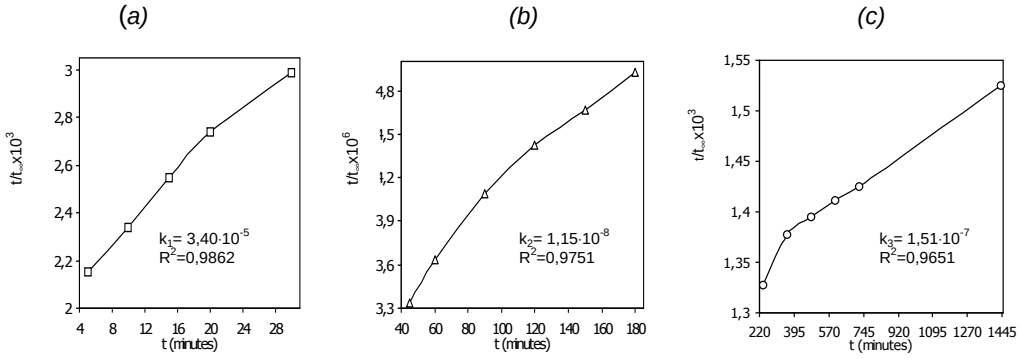

Fig.2. *The near-linear dependences t/t∞=f(t) for all three periods of chalcopyrite concentrate leaching with sulphuric acid at 20°C.*

The values of the rate constants, obtained as function of leaching temperature, for chalcopyrite concentrate solubilization curves, are listed in table 3. As seen, important enhancement of rate constant is obtained within the third and second stage, and only small enhancement within the first stage when the leaching temperature is risen. Also, it could be observed a differences between the first period rate constant value and the other two periods rate constant values. We atributed the differences to the formation of the adherent product layer to the original material, which produces the decrease of the leaching rate.

Table 3.

The values of the rate constants.

Temperature (°C)	10^5 k_1 (min^{-1})	10^8 k_2 (min^{-1})	10^7 k_3 (min^{-1})
20	3.40	1.15	1.51
30	3.56	1.23	2.00
40	3.73	1.25	2.50
50	3.84	1.67	3.33
60	4.04	2.50	5.00

The quantitative expression of the temperature influence can be obtained by the Arrhenius relation. The values of the apparent activation energies are presented in table 4.

Table 4.

The apparent activation energy.

Period	I	II	III
E_a (kJ/mol)	3.14 ± 0.002	18.76 ± 0.028	24.21 ± 0.001

To increase more the copper dissolution from chalcopyrite concentrate with sulphuric acid, oxidizing agents were added into the leaching solution. Therefore, the influence of the ferric sulphate and/or oxygen addition, as oxidizing agent, on the rate of chalcopyrite concentrate was studied. Figure 3 presents the chalcopyrite concentrate leaching curves, with sulphuric acid when using the oxidizing agent.

The rate constants and apparent activation energies, within the temperature range 40-60°C, for all of three period in the presence of oxidizing agents, are presented in table 5.

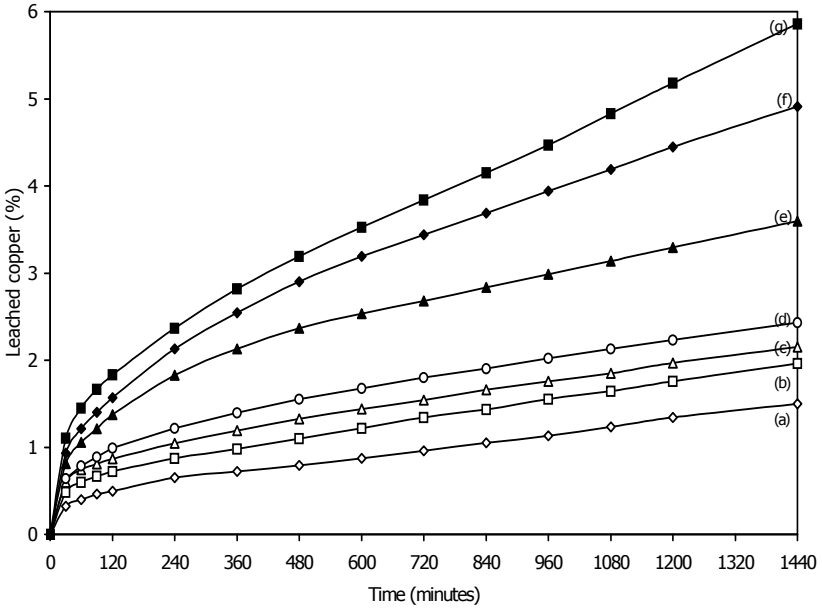

Fig. 3. *The chalcopyrite concentrate leaching curves, when using oxidizing agents, as function of time.*

(a) the addition of oxygen at 40°C; (b) the addition of oxygen at 60°C; (c) the addition of oxygen and ferric sulphate (30 g/l) at 40°C; (d) the addition of ferric sulphate (10 g/l) at 60°C; (e) the addition of ferric sulphate (20 g/l) at 60°C; (f) the addition of ferric sulphate (30 g/l) at 60°C; and (g) the addition of oxygen and ferric sulphate (30 g/l) at 60°C.

Table 5.

The rate constants and apparent activation energies, for all of three oxidizing leaching period of the chalcopyrite concentrate.

Oxidizing agents	Period	Temperature (°C)	k (min^{-1})	E_a (kJ/mol)
O_2	I	40	8.64×10^{-5}	17.2
		60	12.86×10^{-5}	
	II	40	1.58×10^{-4}	33.6
		60	3.43×10^{-4}	
	III	40	3.33×10^{-8}	47.6
		60	10.00×10^{-8}	
O_2 and Fe^{3+}	I	40	1.11×10^{-7}	65.2
		60	5.00×10^{-7}	
	II	40	1.28×10^{-8}	38.2
		60	3.09×10^{-8}	
	III	40	3.04×10^{-8}	52.1
		60	10.11×10^{-8}	

CONCLUSIONS

The obtained apparent activation energies are comparable with those found in literature: about 69 kJ/mol for ferric chloride chalcopyrite leaching, in the range of 40-100°C [8]. Also, the small leached copper percent obtained for ferric sulphate chalcopyrite (about 6% in 24 hours) can be compared with the literature values. At ferric chloride chalcopyriteleaching, in similar conditions, the leached copper percent are at about 7% [8]. The ferric chloride chalcopyrite leaching conditions was:

- the fraction of concentrate sample between 0.071 and 0.1 mm;
- the chemical composition of fraction: 32.3% Cu, 28.4% Fe, 31.9% S;
- the solid/liquid ratio of 1/25;
- the leaching agent concentration: 1.0 M $FeCl_3$ in 0.2 M HCl;
- the leaching time: 240 minutes;
- the temperature: 60°C;
- the stirring speed: 300 rpm.

The slightly increased percent for ferric chloride chalcopyrite leaching, can be explained by the fact that the ferric chloride is much more aggressive than sulphate, due to the ability to accelerate dissolution of the mineral, owing to the formation of complexes, as well as due to the fact that a high stirring speed was applied to the pulp.

The examination of the obtained rate constants and apparent activation energies leads to the following conclusions:

According to the apparent activation energy (~3 kJ/mol) in the range 20-60°C, the rate controlling reaction step within the first period of leaching is the diffusion of leaching agent from the bulk to the grain surface (external diffusion);

Within the initial stage of dissolution, fast leaching rates have been observed due to dissolution of the fine portions of chalcopyrite concentrate, the high concentration gradients at the interface, as well as the fact that the start of the process is not retarded by layers of elemental sulphur or other weak reactive products, formed on the leached surface;

The second period of leaching is much longer than the first one and the values of the apparent activation energy (~18 kJ/mol) indicate that the diffusion of reactants and products over the passivating layer (internal diffusion), as the rate controlling reaction step;

For the third period of leaching the values of the apparent activation energy (~24 kJ/mol) indicate the same rate controlling reaction step, as in second period;

The increase of the apparent activation energy (up to 50 kJ/mol), when the oxidizing agents were used, can be assigned to the change of mechanism. It is highly probable that the copper polysulphide layer can release copper (see reaction (3)) in the interaction with the oxidizing agents, and the chemical control is installed.

The same conclusions were driven when the same oxidizing agents were used for leaching of low-grade chalcocite-covellite-chalcopyrite ore in sulphuric acid media [5].

REFERENCES

1. R. L e H o u l l i e r, E. G h a l i, *Hydrometallurgy*, **1982**, *9*, 169;
2. J.E. D u t r i z a c, *Can. Metall. Q.*, **1989**, *28*(4), 337;
3. R.P. H a c k l, D.P. D r e i s i n g e r, E. P e t e r s, J.A. K i n g, *Hydrometallurgy*, **1995**, *39*, 25;
4. C.L. V a r g a, L. O n i c i u, *Studia* Universitatis *Babeş-Bolyai*, **1999**, *44*(1-2), 193;
5. C.L. V a r g a, L. O n i c i u, I. B a l d e a, *Studia Universitatis Babeş-Bolyai*, **1999**, *44*(1-2), 249;
6. C.L. V a r g a, *PhD Thesis,* Babeş-Bolyai University of Cluj-Napoca, **2000**;
7. J.M. S m i t h, *Chemical Engineering Kinetics*, Mc.Graw-Hill, Kagacusha Ltd, Tokyo, 2nd Ed., **1970**, p. 571-596;
8. T. H a v l i k, R. K a m m e l, *Minerals Engineering*, **1995**, *8*(10), 1125.

STUDIA UNIVERSITATIS BABEŞ-BOLYAI, CHEMIA, XLIX, 1, 2004

STUDY ABOUT THE AFFINITY FOR HEAVY METALS OF SPONTANEOUS VEGETATION THAT GROWS UP ON THE WALLS OF THE TAILING PONDS

LEONARD MIHALY COZMUȚĂ[1], ANCA MIHALY COZMUȚĂ[2], CAMELIA VARGA[1], ANCA PETER[1]

[1] *Chemical Department of North University of Baia Mare, 76 Victoriei Str, 4800*

ABSTRACT. The paper present aspects concerning accumulation of heavy metals (Pb, Cu, Zn) in the walls of a tailing pond and in the spontaneously vegetation species who grow up on that. 10 soil samples and 8 vegetation species samples have been analyzed. Based on two parameters, namely concentration degree and selectively coefficient, the preferentially accumulation series has been established for studied heavy metals.

INTRODUCTION

Processing ores activity, an important branch of mining industry, presents a major impact on environment because of wastewaters and solid wastes resulted from different applied technologies. Considering that in every year thousands tones of ores are processed, it is obviously that the amount of wastewaters is very important. The wastewaters coming from non-ferrous and golden ores processing plants, that applied flotation technology, contain flotation reagents (xanthates, phenols, simple and complex cyanides), soluble salts of heavy metals (Pb, Cu, Zn, Fe) and solid suspensions. Solid suspensions are represented by the raw processing particles, contained in range 50 – 96% in the ores processed. For the most processing plants, the only solution to store and clean up the wastewaters is a tailing pond. Those take place a decanting of suspensions, the clear waters resulted cannot be spilled in running waters because they still contain dissolved pollutant agents. That is why, the mentioned waters should be advanced cleared. Because the cleaning process takes a long time, an important problem shows up, concerning the strong pollutant impact of tailings ponds on the environment. Theirs integration in environment is a major problem. The solid wastes, where the chemical analysis show high concentrations of heavy metals, are made by low granularity particles. They are easily transported by the wind and pollute the environment on a wide area. The stability of the tailing ponds is improved by the vegetation that grows up spontaneously on the walls.

COLLECTING AND PROCESSING THE SAMPLES

Our study has chosen the tailing pond exploited by REMIN SA Company – Baia Mare – Romania, spreads on 120 hectares. The profile of the company is obtaining of the heavy metals (Pb, Cu, Zn) concentrates by using flotation technology. The wastes resulted from the processes are spilled in the mentioned tailing pond.

Also, in the same tailing pond are spilled the wastewaters coming from golden ores cyanidation process and acid mine waters resulting from the non-ferrous mines that surrounded the area.

On the areas where the flotation waters are spilled, with a basic pH, the vegetation grows up better than the areas were acid mine waters are evacuated. Also, as we claim to the top of the tailing pond, the vegetation is less and on the last level, the newest one, none vegetation species have been present.

Development of the vegetation on the walls of tailing pond is stopped by the high concentration of heavy metals and acidity of the soil and by the bacterial leaching processes that occur inside of solid layers of the walls.

For the study, have been collected 10 soil samples from surface and 30 cm depth and 8 vegetation species samples that grower-up on that soil [1].

These samples were air-dried at room temperature prior to grinding in agate mortars, sieving (at –500 microns) and dissolution. In this purpose, 10 mL of 1:1 (v/v) HCl was added to 0.2 g sample in a 150 mL beaker and the sample heated to near dryness. After cooling, 10 mL of 3:1 (v/v) HNO_3 + HCl Lunge mixture, was added, and again the acid was evaporated to near dryness. The residue was dissolved in 25 mL HCl 1:4 (v/v) and heated for approximately 15 minutes in open air. The sample was then transferred into a 100 mL volumetric flask and diluted to the mark with distilled water. The sample was filtered to remove suspended particulate matter and the solution has been chemical measured using an AAS-IN spectrometer. The concentrations of heavy metals contained were analyzed by nebulization of the solution in the acetylene-air flame and measuring the light absorption of lead, zinc and copper atoms, at 283.3 nm, 213.9 nm and 324.7 nm wave lengths [2, 3, 4].

The heavy metal concentrations were calculated as follows:

$$C = \frac{C_0 \cdot V}{m} \tag{1}$$

where:

C_0 – the metal concentration read from calibration curve, mg/l

V – the total volume of solution, ml

m – the weight of dried sample taken for analysis, g

In Figure 1÷ 3 are presented the calibration curves used.

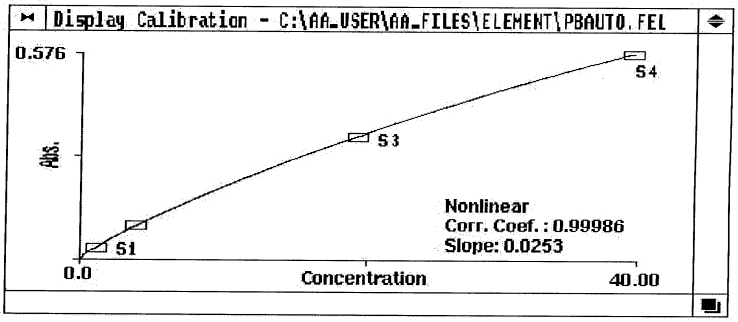

Figure 1. *Calibration curve for Pb*

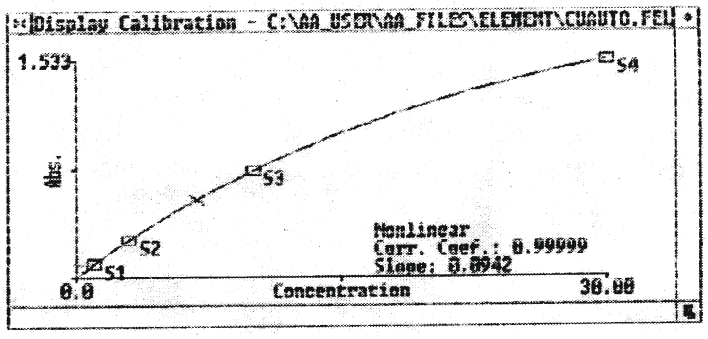

Figure 2. *Calibration curve for Cu*

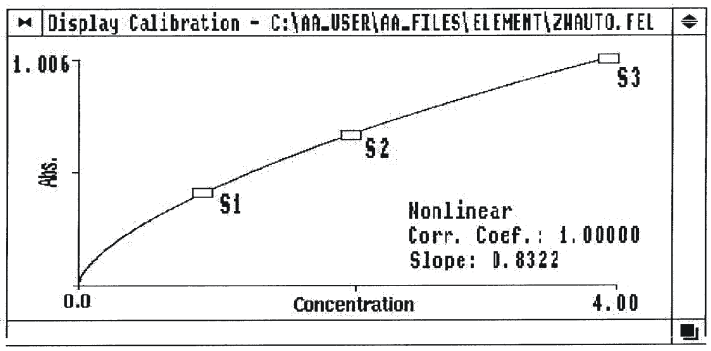

Figure 3. *Calibration curve for Zn*

EXPERIMENTAL RESULTS

In Tables 1 and 2 presents the amounts of heavy metals in soil and vegetation samples collected.

Table 1.

The amount of heavy metals in soils samples

General symbols of the sample	Soil samples				
	Collecting depth	Symbols of the soil sample	Concentration of heavy metals, C_1 (%)		
			Cu	Pb	Zn
1	Surface	1A	0.07	0.17	0.22
	At 30 cm depth	1B	0.03	0.14	0.11
2	Surface	2A	0.01	0.12	0.07
	At 30 cm depth	2B	0.01	0.10	0.08
3	Surface	3A	0.04	0.19	0.15
	At 30 cm depth	3B	0.03	0.14	0.11
4	Surface	4A	0.07	0.2	0.21
	At 30 cm depth	4B	0.05	0.19	0.18
5	Surface	5A	0.07	0.11	0.46
	At 30 cm depth	5B	0.07	0.12	0.24

Table 2

The amount of heavy metals in vegetation samples

Vegetation samples			Concentrations of heavy metals C_2, (%)		
Names of plants	Symbols of the soil samples from where the plants have been collected	Symbols of plants samples	Cu	Pb	Zn
1	2	3	4	5	6
Reinoutria japonica	1	1C	0.0020	0.0059	0.0185
Arctium lappa	1	1D	0.0043	0.0080	0.0194
Robinia pseudaccacia	2	2C	0.0024	0.0005	0.0187
Typha latifolia (rush)	3	3C	0.0022	0.0033	0.0059
Festuca pratensis (grass)	4	4C	0.0032	0.0065	0.0107
Vegetation samples			Concentrations of heavy metals C_2, (%)		
Robinia pseudaccacia (acacia – pods)	4	4D	0.0054	0.0191	0.0196
Chamomilla millefolium (chamomile)	4	4E	0.0312	0.0295	0.2053
Alchemilla millefolium	5	5C	0.0138	0.0175	0.1277

DISCUSSION OF THE RESULTS

For an objective appreciation of the results, we calculated two parameters: *concentration degree (CD, %)* and *selectively coefficient (SC, %)* for each heavy metal from plants.

Concentration degree (CD, %) is defined as follow:

$$CD(\%) = \frac{C_2}{C_1} 100 \tag{2}$$

where C_1 and C_2 are the parameters from the Tables 1 and 2.

The resulted values are presented in Table 3.

Selectively coefficient (SC, %) indicate the affinity of each vegetation specie for a heavy metal and he has been calculated as follow:

$$SC(\%) = \frac{CD}{\sum_{i=1}^{n} CD} = 100 \tag{3}$$

where:

Σ CD – the sum of concentration degrees of all heavy metals analyzed, [%];
n – the number of vegetative species analyzed, [adimensional].

Table 3

The values of concentration degree (CD, %) for analyzed metals

Symbols of plants samples	Vegetation species	Concentration degree, CD (%)		
		Cu	Pb	Zn
1	2	3	4	5
1C	*Reinouttria japonica*	2.86	3.47	8.41
2C	*Robinia pseudaccacia*	24.00	0.5	23.38
3C	*Typha latifolia* (rush)	5.50	1.74	3.93
4C	*Festuca pratensis* (grass)	4.57	3.25	5.09
5C	*Achilea millefolium*	19.71	14.58	53.21
1D	*Arctium lappa*	6.14	4.70	8.82
4D	Robinia pseudaccacia (acacia – pods)	10.80	10.05	10.89
4E	Matricaria chamomile (chamomile)	44.57	24.58	85.54

In Table 4 are presented the calculated values of SC (%) for studied species. Base on these, we express the preference of each studied species for each analyzed heavy metals.

Table 4

The calculated values of selectively coefficient, SC (%),
for each studied species and heavy metals

Name	Selectively coefficient SC (%)			Preference for heavy metals		
	Cu	Pb	Zn	Maximum	Middle	Low
Reinoutria japonica	19.29	23.57	57.14	Zn	Pb	Cu
Arctium lappa	31.23	23.90	44.87	Zn	Cu	Pb
Robinia pseudaccacia (acacia – leafs)	50.12	1.04	48.84	Cu	Zn	Pb
Festuca pratensis (grass)	35.39	25.17	39.44	Zn	Cu	Pb
Robinia pseudaccacia (acacia – pods)	34.02	31.66	34.32	Zn	Cu	Pb
Matricaria chamomilla (chamomille)	28.81	15.88	55.31	Zn	Cu	Pb
Achilea millefolium	22.52	16.67	60.81	Zn	Cu	Pb
Typha latifolia (rush)	49.24	15.58	35.18	Cu	Zn	Pb

CONCLUSIONS

Based on the experimental data, we can draw the following conclusions:

1. All analyzed species accumulate heavy metals from the soils that they develop;

2. With the exceptions of *Typha latifolia* (rush) and *Robinia pseudaccacia* (acacia-leafs), Zn is the heavy metal present the higher concentration degrees. These are in range 85.54%, for *Matricaria chamomille* (chamomile) and 3.93 for *Typha latifolia* (Table 3). The explanation is connected to the high level of Zn in the solid wastes where the mentioned species grows. The species *Typha latifolia* (rush) and *Robinia pseudaccacia* (acacia – leafs) have a particular behavior. Thus they were collected from a soil containing 0.15 % Zn and 0.04% Cu (*Typha latifolia)* and 0.07% Zn and 0.01% Cu (*Robinia pseudaccacia)* (Table 1), the analyses of plants show a higher concentration degree for Cu than Zn (Table 2).

3. Most of vegetative species accumulate a low led amount (Table 3). The maximum concentration degree was realized by *Matricaria chamomilla* (chamomile), 24.58%, and the lower, by *Robinia pseudaccacia* (acacia -leafs), 0.5%.

4. Between the studied heavy metals, copper presents the lower concentration in solid wastes, in range 0.01 ÷ 0.07% (Table 1), but vegetative species assimilate copper rather than led, although the concentrations of led in soil samples are almost ten times higher (Table 1).

5. We can observe that, as the others authors indicate [5-10], the plants adapted on these conditions, act according to a buffer system. They accumulate in a high quantity the metals with lowest concentrations in soil and in a low quantity the metals with the highest concentrations in soil.

Starting from the presented data, we can conclude that, for the analyzed vegetation species, the preferentially accumulation series of studied heavy metals is:

$$Zn > Cu > Pb.$$

REFFERENCES

1. STAS 6922(1)/1990 – Collection of samples;
2. Study Protocol, ICIA Cluj Napoca - *Methodology for determination of heavy metals (Cd, Pb, Cu, Zn,) in soils*;
3. Study Protocol, ICIA Cluj Napoca - *Methodology for determination of heavy metals (Cd, Pb, Cu, Zn,) in sediments;*
4. N i s k a v a a r a, H. - *A comprehensive scheme of analysis for soils, sediments, humus and plant samples using inductively coupled plasma atomic emission spectrometry (ICP-AES)*, Geological Survey of Finland, Special Paper, 20, p. 167-175, 1995.
5. Š p i r o c h o v á, I. - *Accumulation of heavy metals in plants*, Institute of Chemical Technology Prague, 2000
6. H r n c í r o v á, M. -*Use of plants removing of heavy metals*. - Institute of Chemical Technology Prague, 2002
7. K a l e t o v á, M. - *Removing of heavy metals by phytoremediation*, Institute of Chemical Technology Prague, 2002;
8. W e t y e l, A., W e r n e r, D. – *Ecotoxicological evaluation of contaminated soil using the legume root nodule symbiosis as effect parameter*, Environ. Toxicol. Water Qual., 1995, 10, p. 127 – 134;
9. K o t r b a P., R u m l, T. – *Bioremediation of heavy metals pollution constituents metabolites and metabolic pathways of living*, Collect. Czech. Chem. Commun., 2000, *8*, p. 1205 – 1247;
10. K o t r b a, P., R u m l, T. – *Heavy metals finding peptides and proteins in plants*, Collect. Czech. Chem. Commun., 1999, 7, p. 1057 – 1086.